Neurotrophic Factor Signaling Mechanisms Underlying the Development of Peripheral Neural Circuits

By

Christopher R. Donnelly

A dissertation submitted in partial fulfillment
of the requirements for the degree of
Doctor of Philosophy
(Oral Health Sciences)
in the University of Michigan
2018

Doctoral Committee:

Associate Professor Brian A. Pierchala, Chair
Professor Robert M. Bradley
Professor Roman J. Giger
Professor Vesa M. Kaartinen
Professor Charlotte M. Mistretta

“Success is the ability to go from one failure to another with no loss of enthusiasm.”

&

“Personally I’m always ready to learn, although I do not always like being taught.”

Sir Winston Churchill

Christopher R. Donnelly

chdonnel@umich.edu

ORCID ID: 0000-0003-2487-8881

ACKNOWLEDGEMENTS

First, I would like to thank my advisor Dr. Brian Pierchala for your mentorship and support throughout this process. I am infinitely grateful for the advice, time, resources, and space you gave me to enable me to begin my transition into becoming a competent independent scientist. Your laboratory has prepared me to enter my postdoctoral fellowship with all the tools necessary to succeed.

I would also like to thank the members of the Pierchala laboratory that I have worked alongside over the years. In particular, thank you to the many undergraduate students I have had the opportunity of mentoring and supervising throughout my time, especially Alan Halim, Esther Suh, and Amol Shah. Your help was invaluable over the years, and it was my pleasure to work with such hard-working, talented, and clever students. Additionally, I would like to thank my fellow graduate students in the Pierchala lab: Amanda Wehner, Nicole Gabreski, and a special thanks to Jen Shadrach. Your scientific advice and sanity during times of borderline insanity made all the difference over the years.

To the members of my thesis committee: I sincerely appreciate your advice, guidance, and willingness to serve as mentors. I would like to thank Dr. Robert Bradley and Dr. Charlotte Mistretta in particular: you were mentors to me even before I officially began the program, and I greatly enjoyed having the opportunity to collaborate scientifically with your laboratories. Beyond our collaboration, I am grateful for the relationship that I have with you, and appreciate that you never stopped encouraging and guiding my development as a neuroscientist.

To the many faculty, residents, and fellow students who have supported me in the support of my clinical education, I thank you. In particular, Dr. Theodora Danciu for our discussions and the career guidance you have given me as I have deliberated the ideal career path over the last few years.

Thank you to the many people in the Oral Health Sciences PhD program who supported me in the pursuit of this dissertation, all of whom I cannot possibly name here. For guidance, wisdom, and career advice, I thank Dr. Dave Kohn, Dr. Peter Polverini, Dr. Paul Krebsbach, Dr. Jacques Nor, and Dr. Yu Lei in particular. To Pat Schultz and Manette London: the OHS PhD student group could not possibly have had a better Office of Research support staff, and I truly appreciate your help throughout the years. To my program director, Dr. Jan Hu: I cannot express to you enough how thankful I am to have had your unwavering your support over the last seven years; I truly value our relationship and your mentorship. Lastly, I would like to thank my fellow OHS PhD students: in particular, Dr. Shih-Kai Wang and Joe Nguyen, for your friendship and willingness to engage in meaningful scientific and philosophical discussions.

I would like to thank my family and friends, for their love and support in this process. I am grateful to my mother, for sacrificing anything and everything necessary to ensure my betterment and happiness. Lastly, thank you to my wife, Lorenza, for being there through thick and thin, and for always pushing me to strive to be the best I can be in all aspects. I could not have done this without you.

TABLE OF CONTENTS

LIST OF FIGURES

ABSTRACT

The first discovery of a growth-regulating signaling molecule was more than 65 years ago, when the work of Rita Levi-Montalcini, Viktor Hamburger, and Stanley Cohen led to the identification and purification of nerve growth factor (NGF). As the prototypical growth factor, the identification of NGF was a milestone in developmental biology, leading to the subsequent discovery of hundreds of additional secreted growth factors. Many decades later, NGF is now recognized as one of many neurotrophic factors (NTFs) and the founding member of the neurotrophin family, which includes NGF, brain-derived neurotrophic factor (BDNF), neurotrophin-4 (NT-4), and neurotrophin-3 (NT-3). The physiologic functions of these factors are mediated by the tropomyosin-related kinase (Trk) receptor family as well as the p75 neurotrophin receptor (p75). A more recently identified family of neurotrophic factors is the the glial cell line-derived neurotrophic factor (GDNF) family ligands (GFLs), which are potent growth factors that promote the survival of numerous populations of neurons in both the peripheral nervous system (PNS) and central nervous system (CNS). The GFLs consist of four homologous ligands: GDNF, neurturin , artemin (ARTN) and persephin (PSPN), and signal by first binding to one of four GDNF family co-receptors (GFRαs) to initiate their signaling. GFRαs are glycerophosphtidylinositol (GPI) linked proteins and, after binding to GFLs, they bind to and activate the tyrosine kinase Ret and initiate downstream signaling.

This thesis work collectively sought to understand the functions of Ret signaling in peripheral nervous system development. In the first investigation (Chapter 2), we explored the function of a newly identified p75-Ret receptor complex in the development of nociceptive sensory neurons of the dorsal root ganglion (DRG), known to be

dependent on GFL-Ret signaling for their survival and maintenance. In our investigation we found that p75 is required for cell surface localization of Ret. In the absence of p75, GFL-dependent, but not NGF-dependent, nociceptors are specifically reduced, with sensory populations that normally express lower levels of Ret being most greatly affected by p75 deletion. Based on these data, we conclude that p75 has a surprising role in augmenting GFL signaling, and collectively serves to promote the establishment of postnatal sensory neuron diversity.

In the second study (Chapter 3), we investigated the function of this p75-Ret receptor complex in developing sympathetic neurons of the superior cervical ganglion (SCG). Interestingly, p75 signaling regulates programmed cell death (PCD) during perinatal development. In this investigation, we found that Ret expression is restricted to a subpopulation of apoptotic neurons that are rapidly eliminated. Ret and p75 form a complex induced by pro-apoptotic stimuli both *in vitro* and *in vivo*. Importantly, p75 deletion specifically within Ret-expressing neurons, and Ret deletion specifically during PCD, result in a significant abrogation in apoptosis. These studies collectively revealed a surprising non-canonical function of Ret in augmenting apoptotic signaling through p75 during PCD *in vivo*.

In the last study (Chapter 4), we explored the function of Ret in the development of the peripheral taste system, focusing our studies on the geniculate ganglion (GG) which afferently innervates taste buds within fungiform papillae on the anterior 2/3 of the dorsal tongue. We identified a novel, biphasic function for GDNF-Ret signaling in the peripheral taste system, initially acting to promote the chemosensory phenotype of all GG neurons, while acting postnatally to define a unique subpopulation of lingual

mechanoreceptors. These findings collectively broaden our understanding of the cues responsible for taste neuron development, and bring to light new information regarding taste neuron heterogeneity.

CHAPTER 1: INTRODUCTION

The Initial Neurotrophic Factor Hypothesis

Viktor Hamburger's experimental findings using the chick embryo transplantation model were the first to demonstrate that neuronal populations are affected by the population size of their target tissue. In these experiments, the addition of ectopic limb buds could increase the neuronal population while removal of a limb bud eliminated the neurons that normally innervate this target (Hamburger, 1934). These observations gave rise to the idea that neurons are initially generated in excess during organogenesis, and that these neuronal populations depend on a trophic supply produced by the target tissue these neurons innervate. These observations led to the pioneering work of Rita Levi-Montalcini and Stanley Cohen in the 1950s who discovered that mouse sarcomas secrete a factor that was able to elicit neurite outgrowth from peripheral sensory or sympathetic ganglia (Hamburger and Levi-Montalcini, 1949; Levi-Montalcini and Hamburger, 1951; Levi-Montalcini and Hamburger, 1953). These data gave rise to the idea that a soluble, diffusible "neurotrophic factor" is present, exerting cellular effects resulting in growth and survival of neurons. These findings formed the basis of the collaborative work of Rita Levi-Montalcini and Stanley Cohen, which led to the identification and purification of the first growth factor, which they named nerve growth factor (NGF) (Cohen and Levi-Montalcini, 1956; Levi-Montalcini and Angeletti, 1968). Importantly, based on these experimental observations, Levi-Montalcini and Hamburger proposed the "Neurotrophic Factor Hypothesis," which posited that neurons are initially born in excess and extend an overabundance of axons towards their target

tissues where they compete for a limited supply of neurotrophic factors. Neurons that fail to receive sufficient neurotrophic factor support undergo programmed cell death (PCD), thereby directly matching the size of neuronal populations with that of their target tissues (Levi-Montalcini, 1987).

The Neurotrophins and Trk Receptors

During the initial discovery of nerve growth factor, it was observed that although NGF could produce robust neurite extension from sensory and autonomic ganglia, it was insufficient to support the survival or growth of other cranial ganglia, leading Levi-Montalcini and colleagues to postulate that additional growth factors may exist (Levi-Montalcini and Angeletti, 1968). Nearly 30 years after the identification of NGF, brain-derived neurotrophic factor (BDNF) was isolated from pig brain and shown to share sequence homology with NGF (Hohn et al., 1990; Leibrock L. et al., 1989). Today, there are four recognized members of the neurotrophin family of neurotrophic factors: NGF, BDNF, neurotrophin-3 (NT-3)(Maisonpierre P. C. et al., 1990), and neurotrophin-4 (NT-4; also known as NT-4/5)(Eide et al., 1993; Klein, 1994; Lo, 1992). Collectively, the neurotrophins are synthesized as proneurotrophins, which undergo intracellular proteolytic processing to produce dimeric mature proteins capable of initiating signal transduction cascades (Kaplan and Stephens, 1994).

High affinity neurotrophin signaling is mediated by the tropomyosin-related kinase (Trk) family of receptor tyrosine kinases. Each neurotrophin binds with greatest affinity to its cognate Trk receptor: NGF binds preferentially to TrkA (Barker and Shooter, 1994; Ehlers et al., 1995), BDNF and NT-4 to TrkB (Klein et al., 1990; Klein et

al., 1993a), and NT-3 to TrkC (Klein et al., 1994; Lamballe et al., 1993), although NT-3 can also bind with reduced affinity and efficacy to TrkA (Wyatt, 1997). In addition, all four neurotrophins can bind to the p75 neurotrophin receptor (p75) with reduced affinity (Chao, 1994; Lee et al., 1992a), the functions of which are more complex and described in detail later in this chapter. The Trk receptors are type-1 transmembrane receptors with large, heavily glycosylated extracellular domains (ECDs), a single pass transmembrane domain, and an intracellular tyrosine kinase domain with enzymatic activity (Greene, 1995). Neurotrophin binding and subsequent activation occur as a result of engagement of a dimeric neurotrophin complex with the immunoglobulin C2 domain, resulting in homodimerization (Chao, 2003). Upon ligand-mediated activation, Trk receptors undergo internalization followed by subsequent recycling or degradation, or the formation of signaling endosomes that are retrogradely transported from axons to cell bodies (Ehlers et al., 1995; Grimes et al., 1996; Riccio et al., 1997; Tsui-Pierchala and Ginty, 1999).

Neurotrophin binding initiates dimerization and subsequent autophosphorylation of the Trk receptors, leading to the activation of three predominant downstream signaling pathways: (1) Ras activation controls the activation of the MAP kinase (MAPK) signaling cascade, controlling neurite outgrowth and differentiation (Nakamura et al., 1996); (2) activation of phosphoinositide 3-kinase (PI3K) via Ras or Gab1 promotes neuronal survival and growth (Crowder and Freeman, 1998); and (3) activation of PLC-γ results in activation of Ca^{2+} and protein kinase C (PKC)-dependent pathways, controlling synaptic plasticity and differentiation (Obermeier et al., 1994; Stephens et al.,

1994). All three pathways can lead to changes in gene transcription resulting in short and long-term phenotypic changes.

For peripheral neurons, PI3K-dependent pathways are the key regulators of target-derived neurotrophic factor-mediated survival, through several distinct effectors. First, activation of PI3K leads to activation of the serine/threonine protein kinase AKT, which in turn regulates phosphorylation of substrates that govern regulation of the caspase death cascade such as Bcl-2 associated death promoter (BAD)(Datta et al., 1997; Kennedy et al., 1997). Phosphorylation of BAD (which promotes apoptosis by binding to Bcl-xl thus preventing it from inhibiting the apoptotic activity of Bax) leads to inhibition through cytoplasmic sequestration by phospho-protein interacting 14-3-3 proteins (Ito et al., 1997; Putcha et al., 1999). In addition, PI3K pathways inhibit the activity of several transcription factors whose gene products promote apoptosis (Franke et al., 1997).

Functions of the Neurotrophins in the Peripheral Nervous System

Neurotrophins have wide-ranging roles in peripheral and central nervous system development, regulating neuron survival, differentiation, axon outgrowth, synaptic plasticity, and many other cellular functions (Chao, 2003; Snider, 1994). Beyond the nervous system, the neurotrophins have key developmental roles on several non-neuronal tissues, including muscle, cochlea, and pancreas. The specificity in neurotrophin function is achieved primarily by tissue-specific regulation of neurotrophin and Trk receptor expression. With a small number of examples to the contrary (Gatto et al.), the Trk receptors are expressed in a mutually exclusive pattern. While TrkA and

TrkC are found primarily in distinct subsets of peripheral neurons (Eide et al., 1993; Kaplan and Stephens, 1994; Lamballe et al., 1993; Tessarollo et al., 1993), TrkB is primarily expressed in neurons and glial cells of the central nervous system (Klein et al., 1990). Studies utilizing NGF and TrkA germline knockout animals indicated that NGF-TrkA signaling is critical for the developmental survival of sympathetic neurons, as well as distinct subsets of nociceptive sensory neurons in the dorsal root ganglion (DRG) and trigeminal ganglion (TG)(Silos-Santiago et al., 1995; Smeyne et al., 1994a). These studies are well-mirrored by human patients with mutations in NTRK1, the human gene encoding TrkA, which results in hereditary sensory and autonomic neuropathy (HSAN type IV) characterized by an inability to sweat and feel pain (Pezet and McMahon, 2006). In contrast, germline knockout studies analyzing *TrkC*$^{-/-}$ or *NT-3*$^{-/-}$ mice have found only modest effects on sympathetic neuron survival, with more pronounced deficits in placodally-derived cranial sensory ganglia as well as proprioceptive DRG neurons (Klein et al., 1994; Tessarollo et al., 1997). Within the central nervous system, *Ngf*$^{-/-}$ and *TrkA*$^{-/-}$ mice have modest deficits in hippocampal development (Chen et al., 1997), while *TrkB*$^{-/-}$ mutant mice have much more severe deficits in hippocampal, cortical, striatal, and thalamic neurons, among others, and *TrkB*$^{-/-}$ mice rarely survive beyond three weeks of age (Gupta et al., 2013; Klein et al., 1993a).

Trk Receptor Trafficking and Processing

Trk receptor synthesis occurs in the endoplasmic reticulum and undergoes post-translational glycosylation of the extracellular domain in the Golgi apparatus. Trk receptors are transported to the cell surface by microtubule-dependent kinesins, often

traveling long distances beyond the cell body for localization in dendrites or axonal growth cones (Kuruvilla et al., 2004). Activation and signaling is in part governed by membrane localization, where sphingolipid and cholesterol-rich domains known as lipid rafts, rich with RTK adaptor proteins and other signaling regulators (Brown and London, 1998), form important signaling hubs for Trk receptors. TrkA is concentrated in caveolae-containing lipid rafts prior to ligand engagement (Spencer et al., 2017), while TrkB translocates to lipid rafts in response to BDNF-mediated activation (Pereira and Chao, 2007).

Following activation by neurotrophins, the internalization of Trk receptors is accomplished by either a clathrin and dynamin-dependent pathway, or an actin-dependent process (Beattie et al., 2000; Kirkham and Parton, 2005; Nichols and Lippincott-Schwartz, 2001). Following internalization of the activated neurotrophin-Trk receptor complex, Trk receptors continue active signaling from early endosomes. While some endosomes are preferentially recycled and shuttled back to the cell surface to escape lysosomal or proteasomal degradation, others undergo degradation (Grimes et al., 1996; Ye et al., 2003). TrkA, for example, contains a recycling signal in its juxtamembrane domain that allows for preferential sorting towards the recycling pathway, while TrkB and TrkC are more frequently shuttled towards the degradative pathway (Chen et al., 2005b). When neurotrophin receptors are localized in the distal axons, the internalization of the ligand-receptor complex can give rise to a signaling endosome which is retrogradely transported to convey trophic signals to the cell body, activating PI3K and MAPK pathways while in transit from axons to cell soma and dendrites (Ginty and Segal, 2002).

p75 Neurotrophin Receptor

p75, initially identified as a low-affinity receptor for NGF, is a member of the tumor necrosis factor (TNF) superfamily of death receptors, and is now recognized to bind all neurotrophins with similar affinity (Chao, 1994). Structurally, p75 is composed of four cysteine-rich domains comprising the extracellular domain, a transmembrane domain, and an intracellular domain containing two distinct regions: (1) the Chopper domain in the juxtamembrane region capable of inducing cell death; and (2) a C-terminal region that shares homology with the death domains present in other TNF receptor family members, which also mediate apoptotic signal transduction (Bamji et al., 1998; Charalampopoulos et al., 2012; Vilar et al., 2009b). Binding of the neurotrophins to p75 occurs via the cysteine-rich domains in its extracellular domain (He and Garcia, 2004). p75 has been demonstrated to exist on the cell surface as a monomer, a dimer, and a trimer, depending on the mode of activation (Anastasia et al., 2015). Additionally, trafficking of p75 shares similarities with the Trk receptors, as p75 has been shown to concentrate to lipid rafts in response to neurotrophin binding, and upon activation, can be sorted into endosomal compartments that may be recycled or targeted for degradation (Hibbert et al., 2006; Spencer et al., 2017). Some evidence supports the notion that following its internalization, p75 also can form signaling endosomes that are retrogradely transported from distal axons to somal and dendritic compartments, prolonging its signaling (Curtis et al., 1995; Hibbert et al., 2006).

While the functions of the Trk receptors are generally trophic in nature, the functions of p75 signaling are more complicated. While p75 is widely expressed

throughout neuronal and glial populations in both the PNS and CNS (Ibanez and Simi, 2012), the requirement and specific functions of the enigmatic receptor depend heavily on the cellular context of activation (e.g. which other neurotrophic factor receptors are present), the co-receptors it complexes with, and the specific ligand promoting its activation. In some instances, p75 modulates neuronal survival (Barker and Shooter, 1994; Wehner et al., 2016b), while in other contexts its activation leads to death receptor signaling culminating in apoptosis (Frade and Barde, 1999; Frade et al., 1996).

The survival functions of p75 depend on its co-expression with the Trk receptors, where p75 can enhance the binding affinity between the neurotrophin ligands and their cognate Trk receptors, thereby promoting their pro-survival and growth functions (Hantzopoulos et al., 1994), although there is still debate about whether p75 does so by directly associating with the Trk receptors. The most striking phenotype observed in *p75*$^{-/-}$ mice is the deficit in sensory neuron survival (Lee et al., 1992a), reminiscent of the phenotype observed in TrkA and NGF germline knockout mice, further substantiating the role of p75 in augmenting Trk signaling. p75 is also known to complex with the Lingo-1 and Nogo receptors to regulate growth cone collapse, neurite retraction, and spine density in response to the myelin-derived ligands Nogo, MAG, and MOG (Kraemer et al., 2014; Vilar et al., 2009a).

More recently p75 has come to be appreciated as the high affinity receptor for the unprocessed neurotrophins, or proneurotrophins, along with the proneurotrophin co-receptors Sortilin or SorCS2 (Lee et al., 2001; Volosin et al., 2008). In the PNS and in cholinergic basal forebrain neurons, activation of p75 in by proneurotrophins, or by neurotrophins in the absence of the cognate Trk receptor, results in the activation of the

nuclear factor-κB (NF-κB) and c-Jun N-terminal kinase (JNK) pathways, resulting in cell death (Bamji et al., 1998; Kenchappa et al., 2010; Volosin et al., 2006). Neurotrophin or proneurotrophin binding initially leads to the recruitment of cytosolic adaptors such as NRAGE to the p75 intraceullar domain (ICD), resulting in the activation of JNK and a subsequent upregulation of p75 cleavage by the α-secretase TACE. TACE cleavage results in extracellular shedding of the ECD, thereby beginning the receptor intramembrane proteolysis process (Bertrand et al., 2008). Cleavage of the ECD allows for binding and further cleavage by the presenilin-dependent γ-secretase, liberating the intracellular domain (ICD) of p75 into the cytosol for signaling. In the cytosol, the p75 ICD forms a bridging complex with neurotrophin receptor-interacting factor (NRIF) and the E3 ubiquitin ligase TRAF6, where TRAF6 ubiquitinates NRIF causing nuclear translocation and transcriptional activation and expression of pro-apoptotic mediators (Geetha et al., 2005; Kanning et al., 2003; Kenchappa et al., 2010)(Summarized in Figure 1.2). In support of this signaling model, the analysis of p75, TRAF6, NRIF, and JNK3 knockout mice have all revealed deficits in sympathetic neuron programmed cell death at birth. Interestingly, these deficits are eventually corrected by adulthood (Bamji et al., 1998; Kenchappa et al., 2006; Kraemer et al., 2014).

The Neurotrophic Factor Hypothesis Revisited

The neurotrophic factor hypothesis posits that neurons are generated in excess during neural development, setting the stage for a competition between neurons for a limited supply of target-derived neurotrophic factor. Neurons receiving an adequate supply of trophic factor activate PI3K and MAPK-dependent pathways, and concurrently

downregulate pro-apoptotic pathways, ultimately leading to neuronal survival (Dudek et al., 1997; Yuen et al., 1996). Neurons failing to receive adequate trophic support undergo apoptosis and are subsequently eliminated. Despite a plethora of studies demonstrating the existence of active death receptor signaling mechanisms, such as that regulated by p75, the neurotrophic factor hypothesis remained unchallenged for nearly half a century. More recently Deppmann et al. (2010) drew from models of competition between axons at the neuromuscular junction and employed computational modeling approaches to demonstrate the likely existence of “competition factors” that were found to be neurotrophin ligands activating p75 in sympathetic neurons. In this model, in line with the neurotrophic factor hypothesis, “winning” sympathetic neurons – those receiving adequate quantities of NGF – upregulate TrkA through a positive feedback loop, while also upregulating the expression of BDNF for release from distal axon terminals. “Losing neurons” – those that fail to achieve adequate quantities of NGF fail to receive a survival signal, and are also not protected from activation of pro-apoptotic signaling cascades. The local release of BDNF from “winning neurons” binds to p75 on distal axon terminals of the “losing neurons”, initiating an active death receptor signaling cascade, thereby accelerating the process of programmed cell death and shortening the window of nervous system refinement (Deppmann et al., 2008). Several additional competition factors have been subsequently proposed to mediate this process, including Semaphorin3A (Wehner et al., 2016a), amyloid precursor protein (APP) signaling through death receptor-6 (Nikolaev et al., 2009), TNFα (Barker et al., 2001), and the proneurotrophins (Lee et al., 2001).

The GDNF family ligands

The glial cell line-derived neurotrophic factor (GDNF) family ligands (GFLs) are a second family of neurotrophic factors, distantly related to the TGF-β superfamily, consisting of four homologous growth factors: GDNF, neurturin, artemin, and persephin. The GFLs exert their functions by first binding as homodimers to glycerophosphtidylinositol (GPI)-linked co-receptors known as GDNF family receptor-αs (GFRαs), which then engages the receptor tyrosine kinase Ret (Airaksinen and Saarma, 2002). Each GFL has a preferred GFRα co-receptor, with GDNF preferentially binding to GFRα1 (Cacalano et al., 1998), neurturin to GFRα2 (Buj-Bello et al., 1997), artemin to GFRα3 (Baloh et al., 1998), and persephin to GFRα4 (Enokido et al., 1998)(Figure 1.3), although some cross binding has been observed at high concentrations of ligand in *in vitro* systems (Creedon et al., 1997). Additionally, while the physiologic effects of the GFLs in the PNS and in non-neuronal tissues are mediated through GFRα-Ret signaling, some populations within the CNS such as the neocortex and hippocampus abundantly express the GFRα receptors but not Ret (Pozas and Ibanez, 2005), suggesting the existence of additional signal-transducing GFL receptors. In concordance with this hypothesis, alternative receptors such as neuronal cell adhesion molecule (NCAM) and syndecan-3 have been identified (Bespalov et al., 2011; Paratcha et al., 2003) and mediate some of the functions of the GFLs in the CNS.

As the founding member of the GFLs, GDNF was initially identified as a survival factor for rat embryonic midbrain dopaminergic neurons (Lin et al., 1993). Since its discovery, the functions of GDNF have been greatly expanded to include roles in kidney organogenesis, spermatogenesis, enteric nervous system development, sensory

neuron survival and differentiation, parasympathetic neuron migration and proliferation, and motor axon guidance (Buj-Bello et al., 1995; Enomoto et al., 2000; Golden et al., 2010; Gould et al., 2008; Meng et al., 2000; Molliver et al., 1997a; Moore et al., 1996; Pichel et al., 1996; Sanchez et al., 1996). Despite the many roles in nervous system development, GDNF and GFRα1-deficient mice die at birth primarily due to kidney agenesis and the complete lack of the enteric nervous system.

In the central nervous system, GDNF is expressed in neurons of the hypothalamus, hippocampus, cerebellum, and dopaminergic midbrain neurons (Golden et al., 1998), although substantial CNS deficits are not observed in animals lacking GDNF or GFRα1 despite the origins of its discovery (Tomac et al., 1995; Trupp et al., 1997). While GDNF signaling may be dispensable for developmental survival of these neurons, reports suggest that the maintenance of adult midbrain dopaminergic neurons is dependent on GDNF, which has been demonstrated to modulate striatal dopamine homeostasis (Kopra et al., 2017; Kumar et al., 2015). Additionally, GDNF has been reported to protect dopaminergic neurons of the ventral tegmental area (VTA) against drugs of abuse (Barak et al., 2011). These studies have led to the development of therapeutic strategies employing GDNF for use in treating neuropsychiatric and neurodegenerative disorders. Several clinical trials involving GDNF protein infusion in patients with Parkinson’s Disease have been completed (Gill et al., 2003; Kordower, 2003), with only modest benefits observed thus far.

As the second member of the GFL family to be identified, neurturin (NRTN) was first identified as a survival factor for cultured sympathetic neurons (Kotzbauer et al., 1996). NRTN is widely expressed in many neuronal and non-neuronal cell types in both

embryos and adults (Golden et al., 1998), and has been shown to have several distinct functions compared to GDNF. *Nrtn*$^{-/-}$ mice have deficits in developing parasympathetic, dorsal root, trigeminal, and nodose sensory ganglia, and like GDNF, plays an important role in the development of enteric neurons of the gut (Enomoto et al., 2000; Ernsberger, 2008; Sasselli et al., 2012). In addition to its roles as a survival factor for neurons, NRTN has also been observed to regulate liver bud migration (Tatsumi et al., 2007), erythropoiesis, airway inflammation (Mauffray et al., 2015), and psoriasis (Sakai et al., 2017). In the CNS, NRTN also protects midbrain dopaminergic neurons from degeneration in animal models of Parkinson's Disease (PD)(Horger et al., 1998). Like GDNF, phase I and phase II clinical trials were performed utilizing NRTN as a treatment for PD, and in this case NRTN was introduced into the striatum using an adeno-associated viral delivery scheme (Marks et al., 2016; Ramaswamy et al., 2009; Warren Olanow et al., 2015). To date, these trials have been inconclusive, but with promising early results suggestive of therapeutic efficacy in early stage PD patients (Bartus and Johnson, 2017). Current approaches are underway to improve NRTN expression and bioavailability following AAV-neurturin delivery.

Artemin (ARTN), the third GFL to be identified through a database homology search, is expressed at relatively low levels in both the CNS and in peripheral tissues (Baloh et al., 1997). Ablating ARTN or GFRα3 in mice results in deficits in postganglionic sympathetic neurons due to a loss of sympathetic ganglion coalescence and migration, as well as reduced survival of nociceptive sensory neurons of the dorsal root ganglion (Baloh et al., 1998; Nishino et al., 1999). In adult mice, Fontana et. al. (2012) discovered Schwann cell-derived ARTN mediated a c-Jun-dependent increase in

axon regeneration and motoneuron survival (Fontana et al., 2012). Additionally, ARTN has been proposed to have both pro- and anti-nociceptive effects, depending on the model of pain utilized and the location of delivery. In the spinal nerve ligation (SNL) model of nerve injury, systemic delivery of ARTN was effective in reducing the injury-induced decrease in paw withdrawal thresholds in response to both inflammatory and thermal stimuli, and also reduced capsaicin-dependent release of inflammatory nociceptive mediators (Gardell et al., 2003), leading the authors to propose that ARTN has antinociceptive roles *in vivo*. Interestingly, Cayhan et. al. found that ARTN was dramatically increased in human cancer cells and promoted cancer cell invasion in pancreatic ductal adenocarcinoma, although these changes were not correlated with increased pain (Ceyhan et al., 2010). Additional studies are necessary to determine the therapeutic efficacy of ARTN in pain pathologies.

As the final member of the GFL family to be identified through homology cloning (Milbrandt et al., 1998), the physiological roles known for persephin (PSPN) are more limited. PSPN is expressed at very low levels in both the PNS and CNS of both rodents and primates (Golden et al., 1999). PSPN is the only GFL with no binding affinity for syndecan-3 (Bespalov et al., 2011). Like other GFLs, PSPN is neuroprotective to midbrain dopaminergic neurons in OHDA models of PD (Sidorova et al., 2010). Mice lacking PSPN have no known developmental or adult abnormalities, but are particularly sensitive to cerebral ischemia (Tomac et al., 2002). In sharp contrast to the other GFLs, PSPN does not promote migration, differentiation, or survival of peripheral ganglia, nor do PSPN-deficient mice display any overt phenotypic changes in the enteric nervous system development or in kidney morphogenesis (Milbrandt et al., 1998).

Biology of the GDNF Family Receptors

GFL-mediated signal transduction occurs through a receptor complex consisting of two GFRα molecules and two Ret receptors (Durbec et al., 1996; Jing et al., 1996; Trupp et al., 1996). While each GFL ligand binds preferentially to a cognate GFRα receptor (as described in previous sections), some crosstalk exists wherein GDNF can also bind to GFRα2 to activate Ret, and NRTN can bind to GFRα1 (Baloh et al., 1997). Each GFRα co-receptor shares 30%-45% sequence identity, with many common structural features between them. All of the GFRαs have three cysteine-rich domains (CRD1, CRD2, and CRD3) with the exception of GFRα4 which lacks CRD1 (Enokido et al., 1998). Mutational analysis of each CRD has suggested that CRD2 and CRD3 are required for ligand interaction, while CRD1 acts only to stabilize the complex (Anders et al., 2001; Ibanez, 2013; Kjaer and Ibanez, 2003). Comparison of the crystal structures of complexed GDNF-GFRα1 and ARTN-GFRα3 reveals that the ligand-receptor binding site is highly conserved between GFL-GFRαs, while a hinge region linking CRD1 and CRD2 is more variable, likely explaining at least some of the observed preferential ligand-receptor pairing (Parkash and Goldman, 2009).

The GFRα receptors are linked to the cell surface through a GPI-anchor, which selectively isolates these receptors to lipid raft domains, thereby facilitating signaling with nearby acylated and palmitoylated signaling effectors also localized to lipid rafts. Engagement of GFRα by the preferred GFL causes subsequent recruitment of Ret to lipid rafts, where signaling occurs (Tansey et al., 2000). Interestingly, when GFRα1 is excluded from lipid rafts through the creation of a knockin mouse wherein the GPI-

anchor of GFRα1 was replaced with a transmembrane domain known to be excluded from lipid rafts, disruptions occur in kidney morphogenesis, motor axon guidance, and enteric nervous system development, thus mimicking the phenotypes observed in GFRα1 knockout mice (Tsui et al., 2015). Additionally, the creation of soluble GFRα receptors through phosphoinositide-specific phospholipase C (PI-PLC) cleavage, or the addition of recombinant soluble GFRα, can activate Ret *in trans* (Paratcha et al., 2001). However, transgenic mice expressing GFRα1 from the *ret* locus (in a GFRα1$^{-/-}$ background) had no observable phenotypes (Enomoto et al., 2004), making the physiological relevance of *trans* activation of Ret by GFRα1 uncertain. Both the expression pattern of the GFRα co-receptor and the observed phenotype of the null mice are generally similar to that of their cognate ligands (Airaksinen and Saarma, 2002).

In addition to the GFRα receptors, two related receptors exist: GDNF family receptor α-like (GFRAL) and growth arrest specific-1 (GAS-1) (Cabrera et al., 2006). A recent report demonstrated that GFRAL does not bind GDNF family members, but instead mediates the effects of growth differentiation factor-15 (GDF15) through activation of Ret to control food intake and animal body weight (Emmerson et al., 2017; Hsu et al., 2017; Mullican et al., 2017; Yang et al., 2017).

To date, Ret is the only receptor tyrosine kinase that does not bind its ligands directly, but instead requires a co-receptor for activation. Ret is a single-pass, type 1 transmembrane RTK that is conserved from humans to *Drosophila melanogaster* (Anders et al., 2001). The gene encoding Ret (Rearranged during Transfection) was initially described as a gene product activated by DNA rearrangement in a T cell

lymphoma (Iwamoto et al., 1993). The *Ret* gene consists of 20 exons and undergoes alternative splicing to generate to several unique splice variants (Ivanchuk et al., 1997; Tahira et al., 1990). Alternative splicing of intron 19 gives rise to three unique isoforms, Ret9, Ret51, and Ret43 (not present in rodents), which are identical except for their C-terminal amino acid sequence. Surprisingly, this modest change in the C-terminal residues confers isoform-specific differences in their subcellular trafficking, signaling, and function (Lorenzo et al., 1995; Tsui-Pierchala et al., 2002a) (discussed later). Additionally, exon skipping in the 5' region of the *Ret* gene gives rise to at least two isoforms of Ret, $Ret^{\Delta 3}$ and $Ret^{\Delta 345}$, the physiologic function of which is unknown (Le Hir et al., 2002, Gabreski et al. 2016).

The structure of Ret differs from other RTKs in many key respects. First, while the ECDs of most RTKs are composed primarily of leucine-rich repeats, immunoglobulin domains, or fibronectin-like domains, the ECD of Ret is composed of 4 cadherin-like domains, with a calcium-binding site located between CLD2 and CLD3, as well as a cysteine-rich domain proximal to the membrane which is required for ligand binding (Anders et al., 2001). The presence of calcium is required for proper folding and cell surface localization of Ret (Knowles et al., 2006), while the unusual CLD motifs are thought to stabilize Ret dimers (Kjaer and Ibanez, 2003). The transmembrane domain of Ret is required for dimerization, although how this region promotes dimerization remains unclear (Ibanez, 2013). The intracellular aspect of Ret is composed of a long juxtamembrane domain, a highly conserved tyrosine kinase domain, and a C-terminal tail with multiple tyrosines (Tyr) capable of becoming phosphorylated upon dimerization and autophosphorylation of Ret. Phosphorylation of these tyrosines allow for the

interaction and docking of signaling molecules, promoting the subsequent activation of downstream signaling cascades (Airaksinen and Saarma, 2002).

Ret is initially translated with a signal sequence targeting it to the endoplasmic reticulum, where it undergoes rapid glycosylation to produce an immature 150 kDa protein (Tsui-Pierchala et al., 2002b). Ret then undergoes further post-translational modification within the trans-Golgi network, resulting in a mature, fully glycosylated 170 kDa membrane-localized protein. Unlike the neurotrophin receptors, inactive plasma-membrane localized Ret is found outside lipid raft domains, and Ret is only recruited to rafts by the formation of the GFL-GFRα complex, thereby enabling association of Ret and raft-localized Src (Pierchala, 2006; Tansey et al., 2000). Activation of Ret results in clathrin-dependent internalization (Richardson et al., 2006), and important isoform-specific differences exist in Ret degradation. While Ret51 is internalized more rapidly than Ret9, a greater proportion of Ret51 escapes degradation and undergoes Rab11+ recycling, while Ret9 is primarily targeted for degradation (Richardson et al., 2012; Tsui and Pierchala, 2010). The observed isoform-specific differences in Ret degradation at least partially explain why GDNF can promote retrograde survival of DRG sensory neurons, but not sympathetic neurons, as sensory neurons preferentially express Ret51 (Tsui and Pierchala, 2010).

The three major signaling pathways downstream of Ret activation are similar to those described for the Trk receptors: (1) the Ras-MAPK pathway, chiefly regulating neurite outgrowth and differentiation of neurons (Grimm et al., 2001); (2) the PI3K-AKT pathway, essential for neuronal survival (Hemmings, 1997); and (3) the PKC pathway, regulating proliferation, differentiation, and neurite outgrowth (Battaini, 2001). Each

pathway is controlled by the phosphorylation of specific Tyr residues, each recognized by different docking proteins with different binding affinities.

The C-terminal splicing of Ret creating distinct Ret9 and Ret51 isoforms results in important differences in the intracellular domain of Ret, and thus, confers isoform-specific differences in signaling properties. While Ret51 contains 18 tyrosine residues equipped for downstream signaling, the shorter Ret9 isoform only contains 16 residues (Tsui-Pierchala et al., 2002a). Of these, adaptor proteins have been identified for at least eight of these tyrosine residues: Tyr^{687}, Tyr^{752}, Tyr^{905}, Tyr^{928}, Tyr^{981}, Tyr^{1015}, Tyr^{1062}, and Tyr^{1096}, the last of which is present only in the longer Ret51 isoform (Encinas et al., 2004; Grimm et al., 2001; Ishiguro et al., 1999; Jain et al., 2006; Kurokawa et al., 2001; Melillo et al., 2001; Salvatore et al., 2000; Taraviras et al., 1999). Transgenic mice with a phenylalanine substitution for Tyr^{1062} have deficits in kidney morphogenesis. Interestingly, in monoisoformic mice selectively expressing either Ret9 or Ret51, the phenotype resulting from Tyr^{1062} substitution was much more severe in Ret9-only mice, presumably because Ret51-only mice were able to compensate through signal transduction from Tyr^{1096} (Jain et al., 2006).

With a few notable exceptions of GFL functions in the CNS mediated by NCAM or syndecan-3, the physiologic functions of Ret can be described as the collective addition of the functions of each GFL or GFRα co-receptor. In short, Ret is required for early induction, branching, and morphogenesis of the ureteric bud in the developing kidney (Schuchardt et al., 1994; Schuchardt et al., 1996), and mediates maintenance and self-renewal of spermatogonial stem cells in the testis (Meng et al., 2000).

In the nervous system, Ret signaling is critical for the development of sympathetic (Enomoto et al., 2001), motor (Gould et al., 2008), sensory (Golden et al., 2010; Luo et al., 2009; Luo et al., 2007), and enteric nervous system development (Schuchardt et al., 1994; Schuchardt et al., 1996), as well as the postnatal maintenance of dopaminergic midbrain neurons (Kramer et al., 2007). In humans, loss-of-function mutations in *ret* are strongly associated with Hirschsprung's disease, characterized by severe deficits in enteric neuron development, as well as patients with congenital abnormalities of the kidney and urinary tract (CAKUT) (Eng, 1996; Jain et al., 2004; Pan and Li, 2012). Gain of function mutations, on the other hand, lead to endocrine cancers, including multiple endocrine neoplasia type 2A and 2B (MEN2A and MEN2B), differentiated from one another by the presence of orofacial mucosal neuromas and gastrointestinal symptoms present in MEN2B (Eng, 1996). Patients with gain of function Ret mutations are also particular at risk for developing familial medullary thyroid carcinomas (Ball, 2011; Santoro et al., 1990).

Summary

In this work, we utilize several peripheral nervous system populations to expand upon our knowledge of the molecular mechanisms governing Ret signal transduction, and the physiological functions of Ret. In chapter two, we identify a novel function for p75 in augmenting GFL-Ret signaling in nociceptive sensory neurons of the DRG, revealing a highly specific and surprising new function for p75 in postnatal sensory neuron differentiation (Chen et al., 2017). In chapter three, we again investigate the functions of this p75-Ret receptor complex, and discover a highly unusual, non-

canonical Ret signaling pathway promoting p75-dependent programmed cell death of perinatal sympathetic neurons. Finally, in chapter four, we identify a novel biphasic role for GDNF-Ret signaling in geniculate ganglion neurons: the prenatal determination of chemosensory cell fate, and the postnatal specification of a unique population of lingual mechanoreceptors (Donnelly et al., 2018). Collectively, these studies broaden our knowledge of the physiological roles of Ret, and bring forth new concepts with important implications for the design of therapeutic regimens harnessing Ret signal transduction.

Figures:

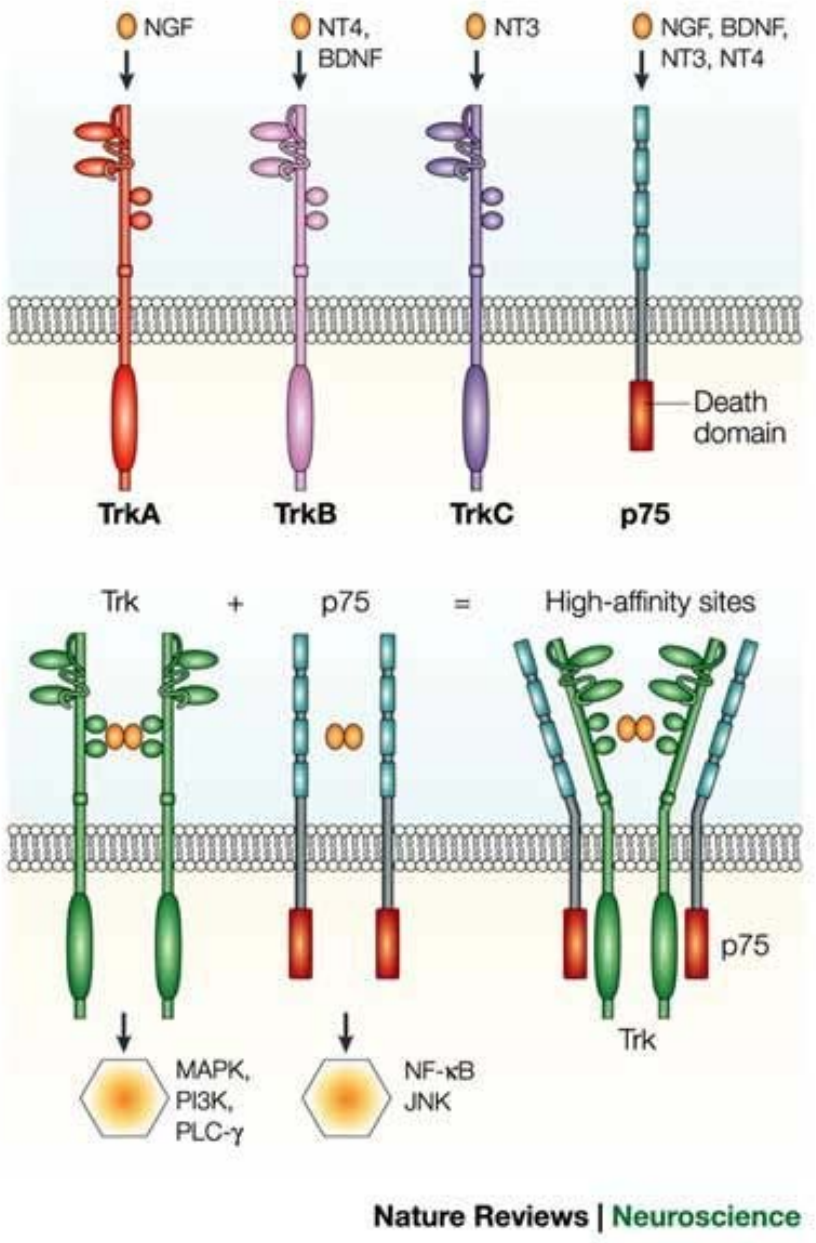

Figure 1.1: Neurotrophin signaling through the Trk and p75 receptors.
All four neurotrophins, nerve growth factor (NGF), brain-derived neurotrophic factor (BDNF), neurotrophin-4 (NT-4), and neurotrophin-3 (NT-3) exert their trophic functions through the tropomyosine-related kinase (Trk) receptors, with NGF binding to TrkA, BDNF and NT-4 binding to TrkB, and NT-3 binding preferentially to TrkC. In addition, in the absence of the cognate Trk receptor, all four neurotrophins can also activate p75, a member of the tumor necrosis family of death receptors, to promote apoptosis (top). When both Trk and p75 receptors are present, p75 can enhance neurotrophin signaling

through the Trk receptor, enhancing survival (bottom). This figure was adopted from (Chao, 2004)

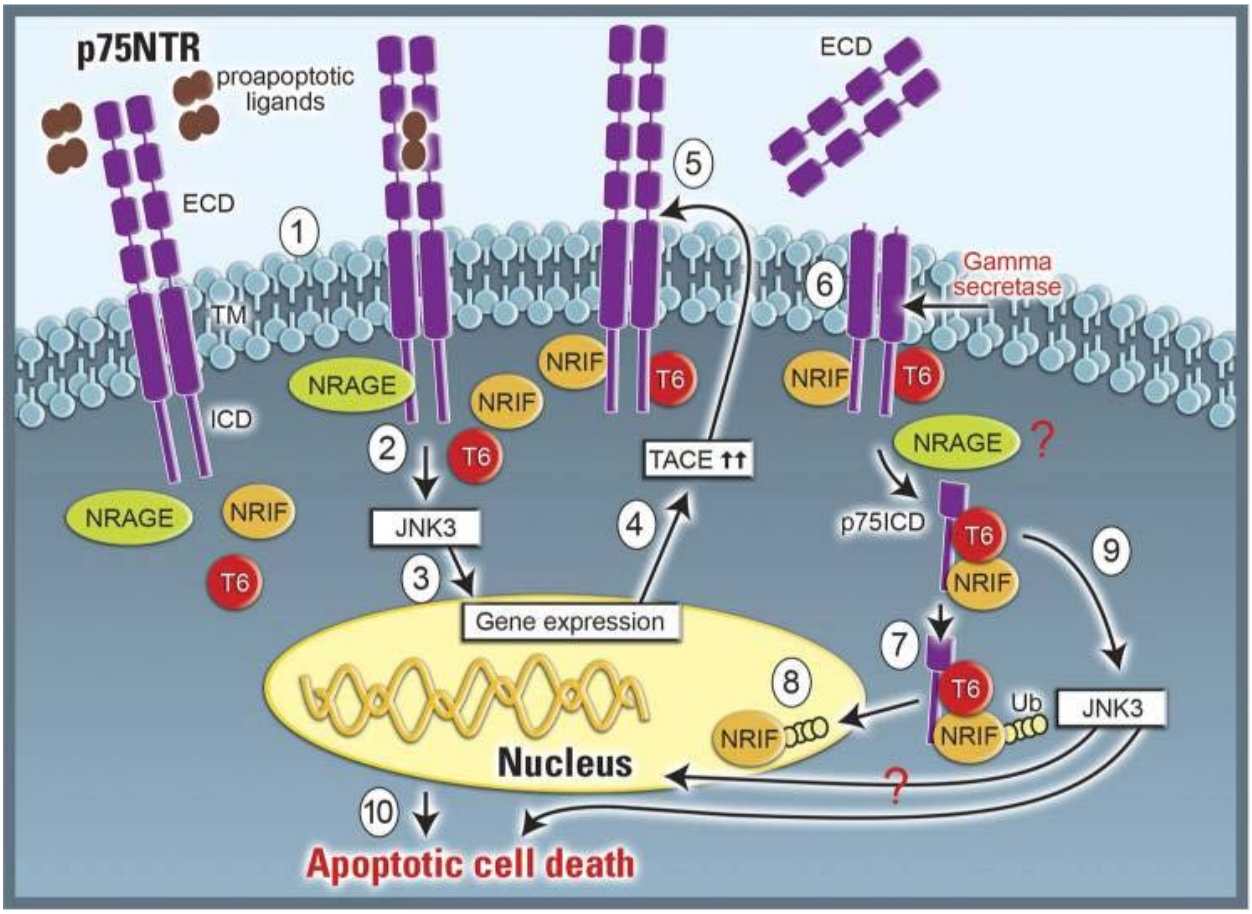

Figure 1.2: Mechanism of p75-mediated apoptosis in sympathetic neurons. Activation of p75 by proapoptotic ligands such as neurotrophins, proneurotrophins, or trophic factor withdrawal (1) initially leads to the recruitment of cytosolic adaptors such as NRAGE to the p75 ICD (2), resulting in the activation of JNK (3) and a subsequent upregulation of p75 cleavage by the α-secretase TACE (4). TACE cleavage (5) results in extracellular shedding of the ECD, thereby beginning the receptor intramembrane proteolysis process (Bertrand et al., 2008). Cleavage of the ECD allows for binding and further cleavage by the presenilin-dependent γ-secretase (6), liberating the intracellular domain (ICD) of p75 into the cytosol for signaling. In the cytosol, the p75 ICD forms a bridging complex with neurotrophin receptor-interacting factor (NRIF) and the E3 ubiquitin ligase TRAF6, where TRAF6 ubiquitinates NRIF (7) causing nuclear translocation (8) and transcriptional activation and expression of pro-apoptotic mediators, ultimately leading to apoptotic cell death. This figure was adopted from Kenchappa et al. (2010).

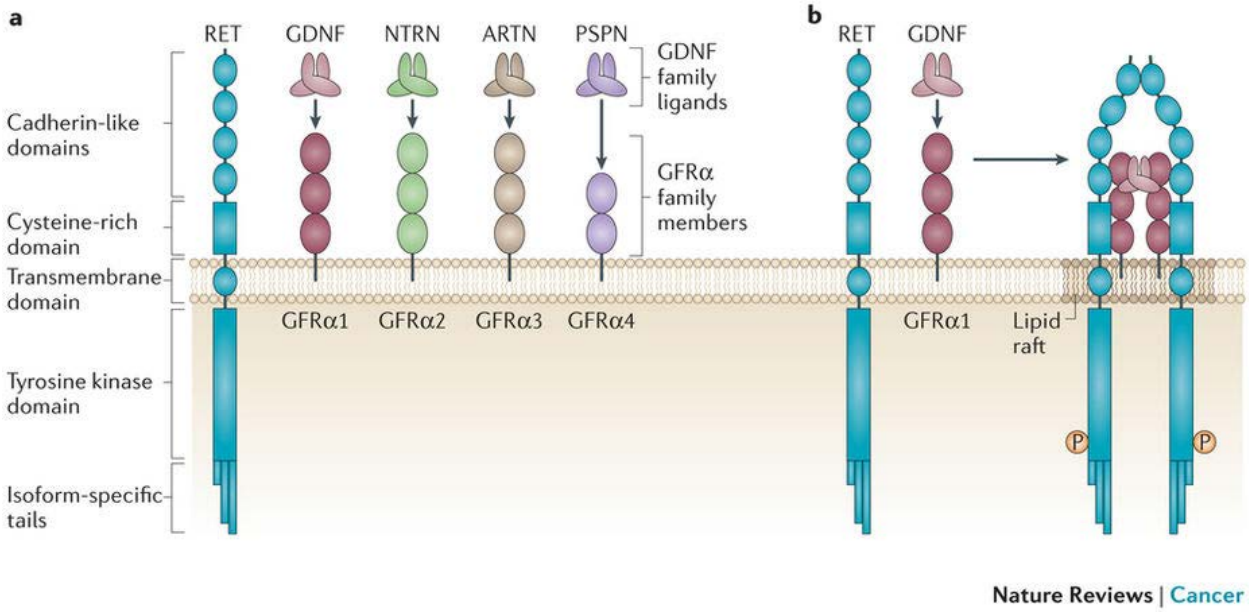

Figure 1.3: The glial cell line-derived neurotrophic factor family ligands exert their trophic functions through the receptor tyrosine kinase Ret.
(A) The GFLs, consisting of GDNF, neurturin (NRTN), artemin (ARTN), and persephin (PSPN) act as dimers, first binding to their respective GPI-anchored GDNF family Receptor-α co-receptor (GFRα1-4). **(B)** Formation of the GFL-GFRα complex leads to recruitment of Ret into lipid raft domains and formation of a GFL-GFRα-Ret complex, leading to Ret dimerization and autophosphorylation of the intracellular tyrosine kinase domain, allowing subsequent recruitment of phospho-specific signaling adapters. Importantly, Ret has several C-terminal splice variants, conferring isoform-specific signaling properties described in greater detail in Chapter 1. This figure was adopted from (Mulligan, 2014).

Chapter 1 References

Airaksinen, M.S., and M. Saarma. 2002. The GDNF family: signalling, biological functions and therapeutic value. *Nat. Rev. Neurosci.* 3:383-394.

Anastasia, A., P.A. Barker, M.V. Chao, and B.L. Hempstead. 2015. Detection of p75NTR Trimers: Implications for Receptor Stoichiometry and Activation. *The Journal of neuroscience : the official journal of the Society for Neuroscience*. 35:11911-11920.

Anders, J., S. Kjar, and C.F. Ibanez. 2001. Molecular modeling of the extracellular domain of the RET receptor tyrosine kinase reveals multiple cadherin-like domains and a calcium-binding site. *The Journal of biological chemistry*. 276:35808-35817.

Ball, D.W. 2011. Management of medullary thyroid cancer. *Minerva Endocrinol.* 36:87-98.

Baloh, R.H., M.G. Tansey, J.P. Golden, D.J. Creedon, R.O. Heuckeroth, C.L. Keck, D.B. Zimonjic, N.C. Popescu, E.M. Johnson, Jr., and J. Milbrandt. 1997. TrnR2, a novel receptor that mediates neurturin and GDNF signaling through Ret. *Neuron*. 18:793-802.

Baloh, R.H., M.G. Tansey, P.A. Lampe, T.J. Fahrner, H. Enomoto, K.S. Simburger, M.L. Leitner, T. Araki, E.M. Johnson, Jr., and J. Milbrandt. 1998. Artemin, a novel member of the GDNF ligand family, supports peripheral and central neurons and signals through the GFRalpha3-RET receptor complex. *Neuron*. 21:1291-1302.

Bamji, S.X., M. Majdan, C.D. Pozniak, D.J. Belliveau, R. Aloyz, J. Kohn, C.G. Causing, and F.D. Miller. 1998. The p75 neurotrophin receptor mediates neuronal

apoptosis and is essential for naturally occurring sympathetic neuron death. *The Journal of cell biology*. 140:911-923.

Barak, S., S. Ahmadiantehrani, V. Kharazia, and D. Ron. 2011. Positive autoregulation of GDNF levels in the ventral tegmental area mediates long-lasting inhibition of excessive alcohol consumption. *Translational psychiatry*. 1.

Barker, P.A., and E.M. Shooter. 1994. Disruption of NGF binding to the low affinity neurotrophin receptor p75LNTR reduces NGF binding to TrkA on PC12 cells.

Barker, V., G. Middleton, F. Davey, and A.M. Davies. 2001. TNFalpha contributes to the death of NGF-dependent neurons during development. *Nature neuroscience*. 4:1194-1198.

Bartus, R.T., and E.M. Johnson, Jr. 2017. Clinical tests of neurotrophic factors for human neurodegenerative diseases, part 2: Where do we stand and where must we go next? *Neurobiology of disease*. 97:169-178.

Battaini, F. 2001. Protein kinase C isoforms as therapeutic targets in nervous system disease states. *Pharm. Res.* 44:353-361.

Beattie, E.C., C.L. Howe, A. Wilde, F.M. Brodsky, and W.C. Mobley. 2000. NGF signals through TrkA to increase clathrin at the plasma membrane and enhance clathrin-mediated membrane trafficking. *J. Neurosci.* 20:7325-7333.

Bertrand, M.J., R.S. Kenchappa, D. Andrieu, M. Leclercq-Smekens, H.N. Nguyen, B.D. Carter, F. Muscatelli, P.A. Barker, and O. De Backer. 2008. NRAGE, a p75NTR adaptor protein, is required for developmental apoptosis in vivo. *Cell Death Differ*. 15:1921-1929.

Bespalov, M.M., Y.A. Sidorova, S. Tumova, A. Ahonen-Bishopp, A.C. Magalhaes, E. Kulesskiy, M. Paveliev, C. Rivera, H. Rauvala, and M. Saarma. 2011. Heparan sulfate proteoglycan syndecan-3 is a novel receptor for GDNF, neurturin, and artemin. *The Journal of cell biology*. 192:153-169.

Brown, D.A., and E. London. 1998. Functions of lipid rafts in biological membranes. *Annu Rev Cell Dev Biol*. 14:111-136.

Buj-Bello, A., J. Adu, L.G. Pinon, A. Horton, J. Thompson, A. Rosenthal, M. Chinchetru, V.L. Buchman, and A.M. Davies. 1997. Neurturin responsiveness requires a GPI-linked receptor and the Ret receptor tyrosine kinase. *Nature*. 387:721-724.

Buj-Bello, A., V.L. Buchman, A. Horton, A. Rosenthal, and A.M. Davies. 1995. GDNF is an age-specific survival factor for sensory and autonomic neurons. *Neuron*. 15:821-828.

Cabrera, J.R., L. Sanchez-Pulido, A.M. Rojas, A. Valencia, S. Manes, J.R. Naranjo, and B. Mellstrom. 2006. Gas1 is related to the glial cell-derived neurotrophic factor family receptors alpha and regulates Ret signaling. *J. Biol. Chem*. 281:14330-14339.

Cacalano, G., I. Farinas, L.C. Wang, K. Hagler, A. Forgie, M. Moore, M. Armanini, H. Phillips, A.M. Ryan, L.F. Reichardt, M. Hynes, A. Davies, and A. Rosenthal. 1998. GFRalpha1 is an essential receptor component for GDNF in the developing nervous system and kidney. *Neuron*. 21:53-62.

Ceyhan, G.O., K.H. Schafer, A.G. Kerscher, U. Rauch, I.E. Demir, M. Kadihasanoglu, C. Bohm, M.W. Muller, M.W. Buchler, N.A. Giese, M. Erkan, and H. Friess. 2010.

Nerve growth factor and artemin are paracrine mediators of pancreatic neuropathy in pancreatic adenocarcinoma. *Annals of surgery*. 251:923-931.

Chao, M.V. 1994. The p75 Neurotrophin Receptor. *J. Neuroboil.* 25:1373-1385.

Chao, M.V. 2003. Neurotrophins and their receptors: a convergence point for many signalling pathways. *Nature reviews. Neuroscience*. 4:299-309.

Charalampopoulos, I., A. Vicario, I. Pediaditakis, A. Gravanis, A. Simi, and C.F. Ibanez. 2012. Genetic dissection of neurotrophin signaling through the p75 neurotrophin receptor. *Cell reports*. 2:1563-1570.

Chen, K.S., M.C. Nishimura, M.P. Armanini, C. Crowley, S.D. Spencer, and H.S. Phillips. 1997. Disruption of a single allele of the nerve growth factor gene results in atrophy of basal forebrain cholinergic neurons and memory deficits. *The Journal of neuroscience : the official journal of the Society for Neuroscience*. 17:7288-7296.

Chen, Z., C.R. Donnelly, B. Dominguez, Y. Harada, W. Lin, A.S. Halim, T.G. Bengoechea, B.A. Pierchala, and K.F. Lee. 2017. p75 Is Required for the Establishment of Postnatal Sensory Neuron Diversity by Potentiating Ret Signaling. *Cell reports*. 21:707-720.

Chen, Z.Y., A. Ieraci, M. Tanowitz, and F.S. Lee. 2005. A novel endocytic recycling signal distinguishes biological responses of Trk neurotrophin receptors. *Molecular biology of the cell*. 16:5761-5772.

Cohen, S., and R. Levi-Montalcini. 1956. A nerve growth stimulating factor isolated from snake venom. *Proc. Natl. Acad. Sci.* 42:571-574.

Creedon, D.J., M.G. Tansey, R.H. Baloh, P.A. Osborne, P.A. Lampe, T.J. Fahrner, R.O. Heuckeroth, J. Milbrandt, and E.M. Johnson, Jr. 1997. Neurturin shares receptors and signal transduction pathways with glial cell line-derived neurotrophic factor in sympathetic neurons. *Proceedings of the National Academy of Sciences of the United States of America*. 94:7018-7023.

Crowder, R.J., and R.S. Freeman. 1998. Phosphatidylinositol 3-kinase and Akt protein kinase are necessary and sufficient for the survival of Nerve Growth Factor-dependent sympathetic neurons. *J. Neurosci.* 18:2933-2943.

Curtis, R., K.M. Adryan, J.L. Stark, J.S. Park, D.L. Compton, G. Weskamp, L.J. Huber, M.V. Chao, R. Jaenisch, K.-F. Lee, R.M. Lindsay, and P.S. DiStefano. 1995. Differential role of the low affinity neurotrophin receptor (p75) in retrograde axonal transport of the neurotrophins. *Neuron*. 14:1201-1211.

Datta, S.R., H. Dudek, X. Tao, S. Masters, H. Fu, Y. Gotoh, and M.E. Greenberg. 1997. Akt phosphorylation of BAD couples survival signals to the cell-intrinsic death machinery. *Cell*. 91:231-241.

Deppmann, C.D., S. Mihalas, N. Sharma, B.E. Lonze, E. Niebur, and D.D. Ginty. 2008. A model for neuronal competition during development. *Science (New York, N.Y.)*. 320:369-373.

Donnelly, C.R., A.A. Shah, C.M. Mistretta, R.M. Bradley, and B.A. Pierchala. 2018. Biphasic functions for the GDNF-Ret signaling pathway in chemosensory neuron development and diversification. *Proceedings of the National Academy of Sciences of the United States of America*. 115:E516-e525.

Dudek, H., S.A. Datta, T.F. Franke, M.J. Birnbaum, R. Yao, G.M. Cooper, R.A. Segal, D.R. Kaplan, and M.E. Greenberg. 1997. Regulation of neuronal survival by the serine-threonine protein kinase Akt. *Science (New York, N.Y.)*. 275:628-830.

Durbec, P., C.V. Marcos-Gutierrez, C. Kilkenny, M. Grigoriou, K. Wartiowaara, P. Suvanto, D. Smith, B. Ponder, F. Costantini, M. Saarma, and et al. 1996. GDNF signalling through the Ret receptor tyrosine kinase [see comments]. *Nature*. 381:789-793.

Ehlers, M.D., D.R. Kaplan, D.L. Price, and V.E. Koliatsos. 1995. NGF-stimulated retrograde transport of TrkA in the Mammalian Nervous System. *J. Cell Bio.* 130:149-156.

Eide, F.F., D.H. Lowenstein, and L.F. Reichardt. 1993. Neurotrophins and their receptors- current concepts and implications for neurologic diseases. *Exp. Neurol.* 121:200-214.

Emmerson, P.J., F. Wang, Y. Du, Q. Liu, R.T. Pickard, M.D. Gonciarz, T. Coskun, M.J. Hamang, D.K. Sindelar, K.K. Ballman, L.A. Foltz, A. Muppidi, J. Alsina-Fernandez, G.C. Barnard, J.X. Tang, X. Liu, X. Mao, R. Siegel, J.H. Sloan, P.J. Mitchell, B.B. Zhang, R.E. Gimeno, B. Shan, and X. Wu. 2017. The metabolic effects of GDF15 are mediated by the orphan receptor GFRAL. *Nature medicine*. 23:1215-1219.

Encinas, M., R.J. Crowder, J. Milbrandt, and E.M. Johnson, Jr. 2004. Tyrosine 981, a novel Ret autophosphorylation site, binds c-Src to mediate neuronal survival. *J. Biol. Chem.* 279:18262-18269.

Eng, C. 1996. Seminars in medicine of the Beth Israel Hospital, Boston. The RET proto-oncogene in multiple endocrine neoplasia type 2 and Hirschsprung's disease. *N Engl J Med*. 335:943-951.

Enokido, Y., F. de Sauvage, J.A. Hongo, N. Ninkina, A. Rosenthal, V.L. Buchman, and A.M. Davies. 1998. GFR alpha-4 and the tyrosine kinase Ret form a functional receptor complex for persephin. *Curr Biol*. 8:1019-1022.

Enomoto, H., P.A. Crawford, A. Gorodinsky, R.O. Heuckeroth, E.M. Johnson, Jr., and J. Milbrandt. 2001. RET signaling is essential for migration, axonal growth and axon guidance of developing sympathetic neurons. *Development 128, 3963-3974*. 128:3963-3974.

Enomoto, H., R.O. Heuckeroth, J.P. Golden, E.M. Johnson, Jr., and J. Milbrandt. 2000. Development of cranial parasympathetic ganglia requires sequential actions of GDNF and neurturin. *Development (Cambridge, England)*. 127:4877-4889.

Enomoto, H., I. Hughes, J. Golden, R.H. Baloh, S. Yonemura, R.O. Heuckeroth, E.M.J. Johnson, and J. Milbrandt. 2004. GFRalpha1 expression in cells lacking RET is dispensable for organogenesis and nerve regeneration. *Neuron*. 44:623-636.

Ernsberger, U. 2008. The role of GDNF family ligand signalling in the differentiation of sympathetic and dorsal root ganglion neurons. *Cell Tissue Res*. 333:353-371.

Fontana, X., M. Hristova, C. Da Costa, S. Patodia, L. Thei, M. Makwana, B. Spencer-Dene, M. Latouche, R. Mirsky, K.R. Jessen, R. Klein, G. Raivich, and A. Behrens. 2012. c-Jun in Schwann cells promotes axonal regeneration and motoneuron survival via paracrine signaling. *The Journal of cell biology*. 198:127-141.

Frade, J.M., and Y.A. Barde. 1999. Genetic evidence for cell death mediated by nerve growth factor and the neurotrophin receptor p75 in the developing mouse retina and spinal cord. *Development (Cambridge, England)*. 126:683-690.

Frade, J.M., A. Rodriguez-Tebar, and Y.-A. Barde. 1996. Induction of cell death by endogenous nerve growth factor through its p75 receptor. *Nature*. 383:166-168.

Franke, T.F., D.R. Kaplan, and L.C. Cantley. 1997. PI3K: Downstream AKTion blocks apoptosis. *Cell*. 88:435-437.

Gardell, L.R., R. Wang, C. Ehrenfels, M.H. Ossipov, A.J. Rossomando, S. Miller, C. Buckley, A.K. Cai, A. Tse, S.F. Foley, B. Gong, L. Walus, P. Carmillo, D. Worley, C. Huang, T. Engber, B. Pepinsky, R.L. Cate, T.W. Vanderah, J. Lai, D.W. Sah, and F. Porreca. 2003. Multiple actions of systemic artemin in experimental neuropathy. *Nature medicine*. 9:1383-1389.

Gatto, G., I. Dudanova, P. Suetterlin, A.M. Davies, U. Drescher, J.L. Bixby, and R. Klein. Protein tyrosine phosphatase receptor type O inhibits trigeminal axon growth and branching by repressing TrkB and Ret signaling. *The Journal of neuroscience : the official journal of the Society for Neuroscience*. 33:5399-5410.

Geetha, T., R.S. Kenchappa, M.W. Wooten, and B.D. Carter. 2005. TRAF6-mediated ubiquitination regulates nuclear translocation of NRIF, the p75 receptor interactor. *The EMBO journal*. 24:3859-3868.

Gill, S.S., N.K. Patel, G.R. Hotton, K. O'Sullivan, R. McCarter, M. Bunnage, D.J. Brooks, C.N. Svendsen, and P. Heywood. 2003. Direct brain infusion of glial cell line-derived neurotrophic factor in Parkinson disease. *Nat. Medicine*.

Ginty, D.D., and R.A. Segal. 2002. Retrograde neurotrophin signaling: Trk-ing along the axon. *Current opinion in neurobiology*. 12:268-274.

Golden, J.P., R.H. Baloh, P.T. Kotzbauer, P.A. Lampe, P.A. Osborne, J. Milbrandt, and E.M. Johnson, Jr. 1998. Expression of neurturin, GDNF, and their receptors in the adult mouse CNS. *The Journal of comparative neurology*. 398:139-150.

Golden, J.P., J.A. DeMaro, P.A. Osborne, J. Milbrandt, and E.M. Johnson, Jr. 1999. Expression of neurturin, GDNF, and GDNF family-receptor mRNA in the developing and mature mouse. *Experimental neurology*. 158:504-528.

Golden, J.P., M. Hoshi, M.A. Nassar, H. Enomoto, J.N. Wood, J. Milbrandt, R.W.t. Gereau, E.M. Johnson, Jr., and S. Jain. 2010. RET signaling is required for survival and normal function of nonpeptidergic nociceptors. *The Journal of neuroscience : the official journal of the Society for Neuroscience*. 30:3983-3994.

Gould, T.W., S. Yonemura, R.W. Oppenheim, S. Ohmori, and H. Enomoto. 2008. The neurotrophic effects of glial cell line-derived neurotrophic factor on spinal motoneurons are restricted to fusimotor subtypes. *j. Neurosci.* 28:2131-2146.

Greene, L.A., Kaplan, D. R. 1995. Early events in neurotrophin signalling via Trk and p75. *Curr. Opin. Neurobiol.* 5:579-587.

Grimes, M.L., J. Zhou, E.C. Beattle, E.C. Yuen, D.E. Hall, J.S. Valletta, K.S. Topp, J.H. LaVail, N.W. Bunnett, and W.C. Mobley. 1996. Endocytosis of activated TrkA: evidence that nerve growth factor induces formation of signaling endosomes. *Journal of neuroscience*. 16 (24):7950-7964.

Grimm, J., M. Sachs, S. Britsch, S. Di Cesare, T. Schwarz-Romond, K. Alitalo, and W. Birchmeier. 2001. Novel p62dok family members, dok-4 and dok-5, are

substrates of the c-Ret receptor tyrosine kinase and mediate neuronal differentiation. *J. Cell Biol.* 154:345-354.

Gupta, V.K., Y. You, A. Klistorner, and S.L. Graham. 2013. TrkB receptor signalling: implications in neurodegenerative, psychiatric and proliferative disorders. *Int. J. Mol. Sci.* 14:10122-10142.

Hamburger, V. 1934. The effets wing bud extirpation on the development of the central nervous system in chick embryos. *J. Exp. Zool.* 68:449-494.

Hamburger, V., and R. Levi-Montalcini. 1949. Proliferation, differentiation and degeneration in the spinal ganglia of the chick embryo under normal and experimental conditions. *J. Exp. Zool.* 111:457-501.

Hantzopoulos, P.A., C. Suri, D.J. Glass, M.P. Goldfarb, and G.D. Yancopoulos. 1994. The low affinity NGF receptor, p75, can collaborate with each of the trks to potentiate functional responses to the neurotrophins. *Neuron*. 13:187-201.

He, X.L., and K.C. Garcia. 2004. Structure of nerve growth factor complexed with the shared neurotrophin receptor p75. *Science (New York, N.Y.)*. 304:870-875.

Hemmings, B.A. 1997. Akt signaling: linking membrane events to life and death decisions. *Science (New York, N.Y.)*. 275:628-630.

Hibbert, A.P., B.M. Kramer, F.D. Miller, and D.R. Kaplan. 2006. The localization, trafficking and retrograde transport of BDNF bound to p75NTR in sympathetic neurons. *Mol Cell Neurosci*. 32:387-402.

Hohn, A., J. Leibrock, K. Bailey, and Y.-A. Barde. 1990. Identification and characterization of a novel member of the nerve growth factor/brain derived neurotrophic factor family. *Nature*. 344:339-341.

Horger, B.A., M.C. Nishimura, M.P. Armanini, L.C. Wang, K.T. Poulsen, C. Rosenblad, D. Kirik, B. Moffat, L. Simmons, J. Johnson, E.M., J. Milbrandt, A. Rosenthal, A. Bjorklund, R.A. Vandlen, M.A. Hynes, and H.S. Phillips. 1998. Neurturin exerts potent actions on survival and function of midbrain dopaminergic neurons. *J. Neurosci.* 18:4929-4937.

Hsu, J.Y., S. Crawley, M. Chen, D.A. Ayupova, D.A. Lindhout, J. Higbee, A. Kutach, W. Joo, Z. Gao, D. Fu, C. To, K. Mondal, B. Li, A. Kekatpure, M. Wang, T. Laird, G. Horner, J. Chan, M. McEntee, M. Lopez, D. Lakshminarasimhan, A. White, S.P. Wang, J. Yao, J. Yie, H. Matern, M. Solloway, R. Haldankar, T. Parsons, J. Tang, W.D. Shen, Y. Alice Chen, H. Tian, and B.B. Allan. 2017. Non-homeostatic body weight regulation through a brainstem-restricted receptor for GDF15. *Nature*. 550:255-259.

Ibanez, C.F. 2013. Structure and physiology of the RET receptor tyrosine kinase. *Cold Spring Harbor perspectives in biology*. 5.

Ibanez, C.F., and A. Simi. 2012. p75 neurotrophin receptor signaling in nervous system injury and degeneration: paradox and opportunity. *Trends Neurosci*. 35:431-440.

Ishiguro, Y., T. Iwashita, H. Murakami, N. Asai, K.-I. Iida, H. Goto, T. Hayakawa, and M. Takahashi. 1999. The role of amino acids surrounding tyrosine 1062 in Ret in specific binding of the Shc phosphotyrosine-binding domain. *Endocrinology*. 140:3992-3998.

Ito, T., X. Deng, B.K. Carr, and W.S. May. 1997. Bcl-2 phosphorylation required for anti-apoptosis function. *J. Biol. Chem.* 272:11671-11673.

Ivanchuk, S.M., C. Eng, W.K. Cavenee, and L.M. Mulligan. 1997. The expression of RET and its multiple splice forms in developing human kidney. *Oncogene*. 14:1811-1818.

Iwamoto, T., M. Taniguchi, N. Asai, K. Ohkusu, I. Nakashima, and M. Takahashi. 1993. cDNA cloning of mouse ret proto-oncogene and its sequence similarity to the cadherin superfamily. *Oncogene*. 8:1087-1091.

Jain, S., M. Encinas, E.M. Johnson, Jr., and J. Milbrandt. 2006. Critical and distinct roles for key RET tyrosine docking sites in renal development. *Genes Dev.* 20:321-333.

Jain, S., C.K. Naughton, M. Yang, A. Strickland, K. Vij, M. Encinas, J. Golden, A. Gupta, R. Heuckeroth, E.M. Johnson, Jr., and J. Milbrandt. 2004. Mice expressing a dominant-negative Ret mutation phenocopy human Hirschsprung disease and delineate a direct role of Ret in spermatogenesis. *Development (Cambridge, England)*. 131:5503-5513.

Jing, S., D. Wen, Y. Yu, P.L. Holst, Y. Luo, M. Fang, R. Tamir, L. Antonio, Z. Hu, R. Cupples, J.C. Louis, S. Hu, B.W. Altrock, and G.M. Fox. 1996. GDNF-induced activation of the ret protein tyrosine kinase is mediated by GDNFR-alpha, a novel receptor for GDNF. *Cell*. 85:1113-1124.

Kanning, K.C., M. Hudson, P.S. Amieux, J.C. Wiley, M. Bothwell, and L.C. Schecterson. 2003. Proteolytic processing of the p75 neurotrophin receptor and two homologs generates C-terminal fragments with signaling capability. *The Journal of neuroscience : the official journal of the Society for Neuroscience*. 23:5425-5436.

Kaplan, D.R., and R.M. Stephens. 1994. Neurotrophin signal transduction by the trk receptor. *J. Neurobiol.* 25:1404-1417.

Kenchappa, R.S., C. Tep, Z. Korade, S. Urra, F.C. Bronfman, S.O. Yoon, and B.D. Carter. 2010. p75 neurotrophin receptor-mediated apoptosis in sympathetic neurons involves a biphasic activation of JNK and up-regulation of tumor necrosis factor-alpha-converting enzyme/ADAM17. *The Journal of biological chemistry*. 285:20358-20368.

Kenchappa, R.S., N. Zampieri, M.V. Chao, P.A. Barker, H.K. Teng, B.L. Hempstead, and B.D. Carter. 2006. Ligand-dependent cleavage of the P75 neurotrophin receptor is necessary for NRIF nuclear translocation and apoptosis in sympathetic neurons. *Neuron*. 50:219-232.

Kennedy, S.G., A.J. Wagner, S.D. Conzen, J. Jordan, A. Bellacosa, P.M. Tsichlis, and N. hay. 1997. The PI-3 kinase/AKT signaling pathway delivers an anti-apoptotic signal. *Genes & Development*. 11:701-713.

Kirkham, M., and R.G. Parton. 2005. Clathrin-independent endocytosis: new insights into caveolae and non-caveolar lipid raft carriers. *Biochim. Biophys. Acta*. 1746:349-363.

Kjaer, S., and C.F. Ibanez. 2003. Identification of a surface for binding to the GDNF-GFR alpha 1 complex in the first cadherin-like domain of RET. *The Journal of biological chemistry*. 278:47898-47904.

Klein, R. 1994. Role for neurotrophins in mouse neuronal development. *FASEB*. 8:738-744.

Klein, R., D. Martin-Zanca, M. Barbacid, and L.F. Parada. 1990. Expression of the tyrosine kinase receptor gene trkB is confined to the murine embryonic and adult nervous system. *Development (Cambridge, England)*. 109:845-850.

Klein, R., I. Silos-Santiago, R.J. Smeyne, S.A. Lira, R. Brambilla, S. Bryant, L. Zhang, W.D. Snider, and M. Barbacid. 1994. Disruption of the neurotrophin-3 receptor gene trkC eliminates Ia muscle afferents and results in abnormal movements. *Nature*. 368:249-251.

Klein, R., R.J. Smeyne, W. Wurst, L.K. Long, B.A. Auerbach, A.L. Joyner, and M. Barbacid. 1993. Targeted disruption of the trkB neurotrophin receptor gene results in nervous system lesions and neonatal death. *Cell*. 75:113-122.

Knowles, P.P., J. Murray-Rust, S. Kjaer, R.P. Scott, S. Hanrahan, M. Santoro, C.F. Ibanez, and N.Q. McDonald. 2006. Structure and chemical inhibition of the RET tyrosine kinase domain. *The Journal of biological chemistry*. 281:33577-33587.

Kopra, J.J., A. Panhelainen, S. Af Bjerken, L.L. Porokuokka, K. Varendi, S. Olfat, H. Montonen, T.P. Piepponen, M. Saarma, and J.O. Andressoo. 2017. Dampened Amphetamine-Stimulated Behavior and Altered Dopamine Transporter Function in the Absence of Brain GDNF. *The Journal of neuroscience : the official journal of the Society for Neuroscience*. 37:1581-1590.

Kordower, J.H. 2003. In vivo gene delivery of glial cell line--derived neurotrophic factor for Parkinson's disease. *Ann. Neurol.* 53:S120-S132.

Kotzbauer, P.T., P.A. Lampe, R.O. Heuckeroth, J.P. Golden, D.J. Creedon, E.M. Johnson, Jr., and J. Milbrandt. 1996. Neurturin, a relative of glial-cell-line-derived neurotrophic factor. *Nature*. 384:467-470.

Kraemer, B.R., S.O. Yoon, and B.D. Carter. 2014. The biological functions and signaling mechanisms of the p75 neurotrophin receptor. *Handbook of experimental pharmacology*. 220:121-164.

Kramer, E.R., L. Aron, G.M.J. Ramakers, S. Seitz, X. Zhuang, K. Beyer, M.P. Smidt, and R. Klein. 2007. Absence of Ret signaling in mice causes progressive and late degeneration of the nigrostriatal system. *PLOS Biology*. 5:e39.

Kumar, A., J. Kopra, K. Varendi, L.L. Porokuokka, A. Panhelainen, S. Kuure, P. Marshall, N. Karalija, M.A. Harma, C. Vilenius, K. Lillevali, T. Tekko, J. Mijatovic, N. Pulkkinen, M. Jakobson, M. Jakobson, R. Ola, E. Palm, M. Lindahl, I. Stromberg, V. Voikar, T.P. Piepponen, M. Saarma, and J.O. Andressoo. 2015. GDNF Overexpression from the Native Locus Reveals its Role in the Nigrostriatal Dopaminergic System Function. *PLoS genetics*. 11:e1005710.

Kurokawa, K., T. Iwashita, H. Murakami, H. Hayashi, K. Kawai, and M. Takahashi. 2001. Identification of SNT/FRS2 docking site on RET receptor tyrosine kinase and its role for signal transduction. *Oncogene*. 20:1929-1938.

Kuruvilla, R., L.S. Zweifel, N.O. Glebova, B.E. Lonze, G. Valdez, H. Ye, and D.D. Ginty. 2004. A neurotrophin signaling cascade coordinates sympathetic neuron development through differential control of TrkA trafficking and retrograde signaling. *Cell*. 118:243-255.

Lamballe, F., P. Tapley, and M. Barbacid. 1993. trkC encodes multiple neurotrophin-3 receptors with distinct biological properties and substrate specificities. *EMBO*. 12:3083-3094.

Le Hir, H., N. Charlet-Berguerand, V. de Franciscis, and C. Thermes. 2002. 5'-End RET splicing: absence of variants in normal tissues and intron retention in pheochromocytomas. *Oncology*. 63:84-91.

Lee, K.-F., E. Li, J. Huber, S.C. Landis, A.H. Sharpe, M.V. Chao, and R. Jaenisch. 1992. Targeted mutation of the gene encoding the low affinity NGF receptor p75 leads to deficits in the peripheral sensory nervous system. *Cell*. 69:737-749.

Lee, R., P. Kermani, K.K. Teng, and B.L. Hempstead. 2001. Regulation of cell survival by secreted proneurotrophins. *Science (New York, N.Y.)*. 294:1945-1948.

Leibrock L., Lottspeich F., Hohn A., Hofer M., Hengerer B., Masiakowski P., Thoenen H., and a.B. Y-A. 1989. Molecular cloning and expression of brain-derived neurotrophic factor. *Nature*. 341:149-152.

Levi-Montalcini, R. 1987. The nerve growth factor 35 years later. *Science (New York, N.Y.)*. 237:1154-1162.

Levi-Montalcini, R., and P.U. Angeletti. 1968. Nerve growth factor. *Physiol Rev*. 48:534-569.

Levi-Montalcini, R., and V. Hamburger. 1951. Selective growth-stimulating effets of mouse sarcoma on the sensory and sympathetic nervous system of the chick embryo. *J. Exp. Zool.* 116:321-361.

Levi-Montalcini, R., and V. Hamburger. 1953. A diffusible agent of mouse saroma, producing hyperplasia of sympathetic ganglia and hyperneurotization of viscera in the chick embryo. *J. Exp. Zool.* 1123:233-287.

Lin, L.F., D.H. Doherty, J.D. Lile, S. Bektesh, and F. Collins. 1993. GDNF: a glial cell line-derived neurotrophic factor for midbrain dopaminergic neurons. *Science (New York, N.Y.)*. 260:1130-1132.

Lo, D.C. 1992. Signal transduction and regulation of neurotrophins. *Curr. Opin. Neurobiol.* 2:336-340.

Lorenzo, M.J., C. Eng, L.M. Mulligan, T.J. Stonehouse, C.S. Healey, B.A. Ponder, and D.P. Smith. 1995. Multiple mRNA isoforms of the human RET proto-oncogene generated by alternate splicing. *Oncogene*. 10:1377-1383.

Luo, W., H. Enomoto, F.L. Rice, J. Milbrandt, and D.D. Ginty. 2009. Molecular identification of rapidly adapting mechanoreceptors and their developmental dependence on ret signaling. *Neuron*. 64:841-856.

Luo, W., S.R. Wickramasinghe, J.M. Savitt, J.W. Griffin, T.M. Dawson, and D.D. Ginty. 2007. A hierarchical NGF signaling cascade controls Ret-dependent and Ret-independent events during development of nonpeptidergic DRG neurons. *Neuron*. 54:739-754.

Maisonpierre P. C., Belluscio L., Squinto S., Ip N., Furth M. E., Lindsay R. M., and G.D. and Yancopoulos. 1990. Neurotrophin-3: a neurotrophic factor related to NGF and BDNF. *Science (New York, N.Y.)*. 247:1446-1451.

Marks, W.J., Jr., T.L. Baumann, and R.T. Bartus. 2016. Long-Term Safety of Patients with Parkinson's Disease Receiving rAAV2-Neurturin (CERE-120) Gene Transfer. *Human gene therapy*. 27:522-527.

Mauffray, M., O. Domingues, F. Hentges, J. Zimmer, D. Hanau, and T. Michel. 2015. Neurturin influences inflammatory responses and airway remodeling in different

mouse asthma models. *Journal of immunology (Baltimore, Md. : 1950)*. 194:1423-1433.

Melillo, R.M., M. Santoro, S.H. Ong, M. Billaud, F. A., Y.R. Hadari, J. Schlessinger, and I. Lax. 2001. Docking protein FRS2 links the protein tyrosine kinase RET and its oncogenic forms with the mitogen-activated protein kinase signaling cascade. *Mol. Cell. Biol.* 21:4177-4187.

Meng, X., M. Lindahl, M.E. Hyvonen, M. Parvinen, D.G. de Rooij, M.W. Hess, A. Raatikainen-Ahokas, K. Sainio, H. Rauvala, M. Lakso, J.G. Pichel, H. Westphal, M. Saarma, and H. Sariola. 2000. Regulation of cell fate decision of undifferentiated spermatogonia by GDNF. *Science (New York, N.Y.)*. 287:1489-1493.

Milbrandt, J., F.J. de Sauvage, T.J. Fahrner, R.H. Baloh, M.L. Leitner, M.G. Tansey, P.A. Lampe, R.O. Heuckeroth, P.T. Kotzbauer, K.S. Simburger, J.P. Golden, J.A. Davies, R. Vejsada, A.C. Kato, M. Hynes, D. Sherman, M. Nishimura, L.C. Wang, R. Vandlen, B. Moffat, R.D. Klein, K. Poulsen, C. Gray, A. Garces, E.M. Johnson, Jr., and et al. 1998. Persephin, a novel neurotrophic factor related to GDNF and neurturin. *Neuron*. 20:245-253.

Molliver, D.C., D.E. Wright, M.L. Leitner, A.S. Parsadanian, K. Doster, D. Wen, Q. Yan, and W.D. Snider. 1997. IB4-binding DRG neurons switch from NGF to GDNF dependence in early postnatal life. *Neuron*. 19:849-861.

Moore, M.W., R.D. Klein, I. Farinas, H. Sauer, M. Armanini, H. Phillips, L.F. Reichardt, A.M. Ryan, K. Carver-Moore, and A. Rosenthal. 1996. Renal and neuronal abnormalities in mice lacking GDNF. *Nature*. 382:76-79.

Mullican, S.E., X. Lin-Schmidt, C.N. Chin, J.A. Chavez, J.L. Furman, A.A. Armstrong, S.C. Beck, V.J. South, T.Q. Dinh, T.D. Cash-Mason, C.R. Cavanaugh, S. Nelson, C. Huang, M.J. Hunter, and S.M. Rangwala. 2017. GFRAL is the receptor for GDF15 and the ligand promotes weight loss in mice and nonhuman primates. *Nature medicine*. 23:1150-1157.

Nakamura, T., R. Sanokawa, Y. Sasaki, D. Ayusawa, M. Oishi, and M. Nozomu. 1996. N-Shc: a neural-specific adapter molecule that mediates signaling from neurotrophin/Trk to Ras/MAPK pathway. *Oncogene*. 13:1111-1121.

Nichols, B.J., and J. Lippincott-Schwartz. 2001. Endocytosis without clathrin coats. *Trends Cell Biol.* 11:406-412.

Nikolaev, A., T. McLaughlin, D.D. O'Leary, and M. Tessier-Lavigne. 2009. APP binds DR6 to trigger axon pruning and neuron death via distinct caspases. *Nature*. 457:981-989.

Nishino, J., K. Mochida, Y. Ohfuji, T. Shimazaki, C. Meno, S. Ohishi, Y. Matsuda, H. Fujii, Y. Saijoh, and H. Hamada. 1999. GFR alpha3, a component of the artemin receptor, is required for migration and survival of the superior cervical ganglion. *Neuron*. 23:725-736.

Obermeier, A., R.A. Bradshaw, K. Seedorf, A. Choidas, J. Schlessinger, and A. Ullrich. 1994. Neuronal differentiation signals are controlled by nerve growth factor receptor/Trk binding sites for SHC and PLC gamma. *EMBO J.* 13:1585-1590.

Pan, Z.W., and J.C. Li. 2012. Advances in molecular genetics of Hirschsprung's disease. *Anat. Rec.* 295:1628-1638.

Paratcha, G., F. Ledda, L. Baars, M. Coulpier, V. Besset, J. Anders, R. Scott, and F. Ibanez. 2001. Released GFRa1 potentiates downstream signaling, neuronal survival, and differentiation via a novel mechanism of recruitment of c-Ret to lipid rafts. *Neuron*. 29:171-184.

Paratcha, G., F. Ledda, and C.F. Ibanez. 2003. The neural cell adhesion molecule NCAM is an alternative signaling receptor for GDNF family ligands. *Cell*. 113:867-879.

Parkash, V., and A. Goldman. 2009. Comparison of GFL-GFRalpha complexes: further evidence relating GFL bend angle to RET signalling. *Acta crystallographica. Section F, Structural biology and crystallization communications*. 65:551-558.

Pereira, D.B., and M.V. Chao. 2007. The tyrosine kinase Fyn determines the localization of TrkB receptors in lipid rafts. *The Journal of neuroscience : the official journal of the Society for Neuroscience*. 27:4859-4869.

Pezet, S., and S.B. McMahon. 2006. Neurotrophins: mediators and modulators of pain. *Annu Rev Neurosci*. 29:507-538.

Pichel, J.G., L. Shen, H.Z. Sheng, A.C. Granholm, J. Drago, A. Grinberg, E.J. Lee, S.P. Huang, M. Saarma, B.J. Hoffer, H. Sariola, and H. Westphal. 1996. Defects in enteric innervation and kidney development in mice lacking GDNF. *Nature*. 382:73-76.

Pierchala, B.A., J. Milbrandt, and E.M. Johnson, Jr. 2006. Glial cell line-derived neurotrophic factor-dependent recruitment of Ret into lipid rafts enhances signaling by partitioning Ret from proteasome-dependent degradation. *J. Neurosci.* 26:2777-2787.

Pozas, E., and C.F. Ibanez. 2005. GDNF and GFRalpha1 promote differentiation and tangential migration of cortical GABAergic neurons. *Neuron*. 45:701-713.

Putcha, G.V., M. Deshmukh, and J. Johnson, E.M. 1999. Bax translocation is a critical event in neuronal apoptosis: regulation by neuroprotectants, BCL-2, and caspases. *J. Neurosci.* 19:7476-7485.

Ramaswamy, S., J.L. McBride, I. Han, E.M. Berry-Kravis, L. Zhou, C.D. Herzog, M. Gasmi, R.T. Bartus, and J.H. Kordower. 2009. Intrastriatal CERE-120 (AAV-Neurturin) protects striatal and cortical neurons and delays motor deficits in a transgenic mouse model of Huntington's disease. *Neurobiology of disease*. 34:40-50.

Riccio, A., B. Pierchala, C. Ciarallo, and D. Ginty. 1997. An NGF-TrkA-Mediated retrograde signal to transcription factor CREB in sympathetic neurons. *Science (New York, N.Y.)*. 227:1097-1100.

Richardson, D.S., A.Z. Lai, and L.M. Mulligan. 2006. RET ligand-induced internalization and its consequences for downstream signaling. *Oncogene*. 25:3206-3211.

Richardson, D.S., D.M. Rodrigues, B.D. Hyndman, M.J.F. Crupi, A.C. Nicolescu, and L.M. Mulligan. 2012. Alternative splicing results in RET isoforms with distinct trafficking properties. *Mol. Biol. Cell*. 23:3838-3850.

Sakai, K., K.M. Sanders, M.R. Youssef, K.M. Yanushefski, L.E. Jensen, G. Yosipovitch, and T. Akiyama. 2017. Role of neurturin in spontaneous itch and increased nonpeptidergic intraepidermal fiber density in a mouse model of psoriasis. *Pain*. 158:2196-2202.

Salvatore, D., M.V. Barone, G. Salvatore, R.M. Melillo, G. Chiappetta, A. Mineo, G. Fenzi, G. Vecchio, A. Fusco, and M. Santoro. 2000. Tyrosines 1015 and 1062 are *in vivo* autophosphorylation sites in Ret and Ret-derived oncoproteins. *J. Clin. Endo. Metab.* 85:3898-3907.

Sanchez, M.P., I. Silos-Santiago, J. Frisen, B. He, S.A. Lira, and M. Barbacid. 1996. Renal agenesis and the absence of enteric neurons in mice lacking GDNF. *Nature*. 382:70-73.

Santoro, M., R. Rosati, M. Grieco, M.T. Berlingieri, G.L. D'Amato, V. de Franciscis, and A. Fusco. 1990. The ret proto-oncogene is consistently expressed in human pheochromocytomas and thyroid medullary carcinomas. *Oncogene*. 5:1595-1598.

Sasselli, V., V. Pachnis, and A.J. Burns. 2012. The enteric nervous system. *Developmental biology*. 366:64-73.

Schuchardt, A., V. D'Agati, L. Larsson-Blomberg, F. Constantini, and V. Pachnis. 1994. Defects in the kidney and enteric nervous system of mice lacking the tyrosine kinase receptor Ret. *Nature*. 367:380-383.

Schuchardt, A., V. D'Agati, V. Pachnis, and F. Costantini. 1996. Renal agenesis and hypodysplasia in ret-k^- mutant mice result from defects in ureteric bud development. *Development (Cambridge, England)*. 122.

Sidorova, Y.A., K. Matlik, M. Paveliev, M. Lindahl, E. Piranen, J. Milbrandt, U. Arumae, M. Saarma, and M.M. Bespalov. 2010. Persephin signaling through GFRalpha1: the potential for the treatment of Parkinson's disease. *Mol Cell Neurosci*. 44:223-232.

Silos-Santiago, I., D.C. Molliver, S. Ozaki, R.J. Smeyne, A.M. Fagan, M. Barbacid, and W.D. Snider. 1995. Non-TrkA-expressing small DRG neurons are lost in TrkA deficient mice. *The Journal of neuroscience : the official journal of the Society for Neuroscience*. 15:5929-5942.

Smeyne, R.J., R. Klein, A. Schnapp, L.K. Long, S. Bryant, A. Lewin, S.A. Lira, and M. Barbacid. 1994. Severe sensory and sympathetic neuropathies in mice carrying a disrupted Trk/NGF receptor gene. *Nature*. 368:246-248.

Snider, W.D. 1994. Functions of the Neurotrophins during Nervous System Development: what the knockouts are teaching us. *Cell*. 77:627-638.

Spencer, A., L. Yu, V. Guili, F. Reynaud, Y. Ding, J. Ma, J. Jullien, D. Koubi, E. Gauthier, D. Cluet, J. Falk, V. Castellani, C. Yuan, and B.B. Rudkin. 2017. Nerve Growth Factor Signaling from Membrane Microdomains to the Nucleus: Differential Regulation by Caveolins. *International journal of molecular sciences*. 18.

Stephens, R.M., D.M. Loeb, T.D. Copeland, T. Pawson, L.A. Greene, and D.R. Kaplan. 1994. Trk receptors use redundant signal transduction pathways involving SHC and PLC-gamma 1 to mediate NGF responses. *Neuron*. 12:691-705.

Tahira, T., Y. Ishizaka, F. Itoh, T. Sugimura, and M. Nagao. 1990. Characterization of ret proto-oncogene mRNAs encoding two isoforms of the protein product in a human neuroblastoma cell line. *Oncogene*. 5:97-102.

Tansey, M.G., R.H. Baloh, J. Milbrandt, and E.M. Johnson, Jr. 2000. GFRa-mediated localization of RET to lipid rafts is required for effective downstream signaling, differentiation, and neuronal survival. *Neuron*. 25:611-623.

Taraviras, S., C.V. Marcos-Gutierrez, P. Durbec, H. Jani, M. Grigoriou, M. Sukumaran, L.C. Wang, M. Hynes, G. Raisman, and V. Pachnis. 1999. Signalling by the RET receptor tyrosine kinase and its role in the development of the mammalian enteric nervous system. *Development (Cambridge, England)*. 126:2785-2797.

Tatsumi, N., R. Miki, K. Katsu, and Y. Yokouchi. 2007. Neurturin-GFRalpha2 signaling controls liver bud migration along the ductus venosus in the chick embryo. *Developmental biology*. 307:14-28.

Tessarollo, L., P. Tsoulfas, M.J. Donovan, M.E. Palko, J. Blair-Flynn, B.L. Hempstead, and L.F. Parada. 1997. Targeted deletion of all isoforms of the trkC gene suggests the use of alternate receptors by its ligand neurotrophin-3 in neuronal development and implicates trkC in normal cardiogenesis. *Proceedings of the National Academy of Sciences of the United States of America*. 94:14776-14781.

Tessarollo, L., P. Tsoulfas, D. Martin-Zanca, D.J. Gilbert, N.A. Jenkins, N.G. Copeland, and L. Parada. 1993. trkC, a receptor for neurtophin-3, is widely expressed in the developing nervous system and in non-neuronal tissues. *Development (Cambridge, England)*. 118:463-475.

Tomac, A., E. Lindqvist, L.F. Lin, S.O. Ogren, D. Young, B.J. Hoffer, and L. Olson. 1995. Protection and repair of the nigrostriatal dopaminergic system by GDNF in vivo. *Nature*. 373:335-339.

Tomac, A.C., A.D. Agulnick, N. Haughey, C.F. Chang, Y. Zhang, C. Backman, M. Morales, M.P. Mattson, Y. Wang, H. Westphal, and B.J. Hoffer. 2002. Effects of cerebral ischemia in mice deficient in Persephin. *Proc. Natl. Acad. Sci. USA*. 99:9521-9526.

Trupp, M., E. Arenas, M. Fainzilber, A.S. Nilsson, B.A. Sieber, M. Grigoriou, C. Kilkenny, E. Salazar-Grueso, V. Pachnis, and U. Arumae. 1996. Functional receptor for GDNF encoded by the c-ret proto-oncogene. *Nature*. 381:785-789.

Trupp, M., N. Belluardo, H. Funakoshi, and C.F. Ibanez. 1997. Complementary and overlapping expression of glial cell line-derived neurotrophic factor (GDNF), c-ret proto-oncogene, and GDNF receptor- alpha indicates multiple mechanisms of trophic actions in the adult rat CNS. *The Journal of neuroscience : the official journal of the Society for Neuroscience*. 17:3554-3567.

Tsui-Pierchala, B.A., R.C. Ahrens, R.J. Crowder, J. Milbrandt, and J. Johnson, E.M. 2002a. The long and short isoforms of Ret function as independent signaling complexes. *J. Biol. Chem.* 277:34618-34625.

Tsui-Pierchala, B.A., M. Encinas, J. Milbrandt, and J. Johnson, E.M. 2002b. Lipid rafts in neuronal signaling and function. *TINS*. 25:412-417.

Tsui-Pierchala, B.A., and D.D. Ginty. 1999. Characterization of an NGF-P-TrkA retrograde-signaling complex and age-dependent regulation of TrkA phosphorylation in sympathetic neurons. *J. Neurosci.* 19:8207-8218.

Tsui, C.C., N.A. Gabreski, S.J. Hein, and B.A. Pierchala. 2015. Lipid rafts are physiologic membrane microdomains necessary for the morphogenic and developmental functions of glial cell line-derived neurotrophic factor in vivo. *J. Neurosci.* 35:13233-13243.

Tsui, C.C., and B.A. Pierchala. 2010. The differential axonal degradation of Ret accounts for cell-type-specific function of glial cell line-derived neurotrophic factor

as a retrograde survival factor. *The Journal of neuroscience : the official journal of the Society for Neuroscience*. 30:5149-5158.

Vilar, M., I. Charalampopoulos, R.S. Kenchappa, A. Reversi, J.M. Klos-Applequist, E. Karaca, A. Simi, C. Spuch, S. Choi, W.J. Friedman, J. Ericson, G. Schiavo, B.D. Carter, and C.F. Ibanez. 2009a. Ligand-independent signaling by disulfide-crosslinked dimers of the p75 neurotrophin receptor. *J Cell Sci*. 122:3351-3357.

Vilar, M., I. Charalampopoulos, R.S. Kenchappa, A. Simi, E. Karaca, A. Reversi, S. Choi, M. Bothwell, I. Mingarro, W.J. Friedman, G. Schiavo, P.I. Bastiaens, P.J. Verveer, B.D. Carter, and C.F. Ibanez. 2009b. Activation of the p75 neurotrophin receptor through conformational rearrangement of disulphide-linked receptor dimers. *Neuron*. 62:72-83.

Volosin, M., W. Song, R.D. Almeida, D.R. Kaplan, B.L. Hempstead, and W.J. Friedman. 2006. Interaction of survival and death signaling in basal forebrain neurons: roles of neurotrophins and proneurotrophins. *The Journal of neuroscience : the official journal of the Society for Neuroscience*. 26:7756-7766.

Volosin, M., C. Trotter, A. Cragnolini, R.S. Kenchappa, M. Light, B.L. Hempstead, B.D. Carter, and W.J. Friedman. 2008. Induction of proneurotrophins and activation of p75NTR-mediated apoptosis via neurotrophin receptor-interacting factor in hippocampal neurons after seizures. *The Journal of neuroscience : the official journal of the Society for Neuroscience*. 28:9870-9879.

Warren Olanow, C., R.T. Bartus, T.L. Baumann, S. Factor, N. Boulis, M. Stacy, D.A. Turner, W. Marks, P. Larson, P.A. Starr, J. Jankovic, R. Simpson, R. Watts, B. Guthrie, K. Poston, J.M. Henderson, M. Stern, G. Baltuch, C.G. Goetz, C.

Herzog, J.H. Kordower, R. Alterman, A.M. Lozano, and A.E. Lang. 2015. Gene delivery of neurturin to putamen and substantia nigra in Parkinson disease: A double-blind, randomized, controlled trial. *Annals of neurology*. 78:248-257.

Wehner, A.B., H. Abdesselem, T.L. Dickendesher, F. Imai, Y. Yoshida, R.J. Giger, and B.A. Pierchala. 2016a. Semaphorin 3A is a retrograde cell death signal in developing sympathetic neurons. *Development (Cambridge, England)*. 143:1560-1570.

Wehner, A.B., A.M. Milen, R.L. Albin, and B.A. Pierchala. 2016b. The p75 neurotrophin receptor augments survival signaling in the striatum of pre-symptomatic Q175(WT/HD) mice. *Neuroscience*. 324:297-306.

Yang, L., C.C. Chang, Z. Sun, D. Madsen, H. Zhu, S.B. Padkjaer, X. Wu, T. Huang, K. Hultman, S.J. Paulsen, J. Wang, A. Bugge, J.B. Frantzen, P. Norgaard, J.F. Jeppesen, Z. Yang, A. Secher, H. Chen, X. Li, L.M. John, B. Shan, Z. He, X. Gao, J. Su, K.T. Hansen, W. Yang, and S.B. Jorgensen. 2017. GFRAL is the receptor for GDF15 and is required for the anti-obesity effects of the ligand. *Nature medicine*. 23:1158-1166.

Ye, H., R. Kuruvilla, L.S. Zweifel, and D.D. Ginty. 2003. Evidence in support of signaling endosome-based retrograde survival of sympathetic neurons. *Neuron*. 39:57-68.

Yuen, E.C., Y. Li, R.E. Mischel, C.L. Howe, D.M. Holtzman, and W.C. Mobley. 1996. Neurotrophins and the Neurotrophic Factor Hypothesis. *Neural Notes*. 1:3-7.

CHAPTER 2: A P75-RET SIGNALING COMPLEX REGULATES THE ESTABLISHMENT OF POSTNATAL SENSORY NEURON DIVERSITY

Summary

Producing the neuronal diversity required to adequately discriminate all elements of somatosensation is a complex task during organogenesis. The mechanisms guiding this process during dorsal root ganglion (DRG) sensory neuron specification remain poorly understood. Here we show that the p75 neurotrophin receptor interacts with Ret and its GFRα co-receptor upon stimulation with glial cell line-derived neurotrophic factor (GDNF). Furthermore, we demonstrate that p75 is required for GDNF-mediated Ret activation, survival, and cell surface localization of Ret in DRG neurons. In mice in which p75 is deleted specifically within sensory neurons beginning at E12.5, we observe that approximately 20% of neurons are lost between P14 and adulthood, and these losses selectively occur within a subpopulation of Ret+ nonpeptidergic nociceptors, with neurons expressing low levels of Ret impacted most heavily. These results suggest that p75 is required for the development of the nonpeptidergic nociceptor lineage by fine-tuning Ret-mediated trophic support.

Introduction

The generation of the diverse array of sensory neurons necessary for discriminating all aspects of somatosensation is critical for animals to interact and respond to their environment. Sensory neurons in the dorsal root ganglia (DRG)

innervate the peripheral tissues of the body below the neck and communicate sensory information to higher order neurons within the central nervous system. DRG neurons are greatly diversified with respect to their sensory functions, which is mirrored by their unique morphological, physiological, and molecular characteristics. Large, medium, and small diameter neurons carry proprioceptive stimuli (proprioceptors), tactile stimuli (mechanoreceptors) and nociceptive stimuli (nociceptors), respectively. Each of these morphologically distinct groups can be further subdivided based on their expression of different neurotrophic factor receptors, G protein coupled receptors, ion channels and transcription factors. Using these morphological and molecular properties, combined together with electrophysiological properties as well as distinctive central and peripheral innervation patterns, sensory neurons have been categorized into multiple subpopulations (Liu and Ma, 2011).

In adult mice, nociceptors can be divided into two major populations. One population, the peptidergic nociceptors, expresses neuropeptides such as calcitonin gene-related peptide (CGRP) and substance P (SP), and the nerve growth factor (NGF) receptor, TrkA. CGRP- or SP-negative nonpeptidergic nociceptors, in contrast, express the tyrosine kinase Ret and the GFRα co-receptors for the GDNF family ligands. Interestingly, the Ret^{+} nociceptive population of neurons emerges from TrkA-expressing neurons in early postnatal development, and the deletion of TrkA results in the complete loss of Ret-expressing unmyelinated neurons (Molliver et al., 1997b; Silos-Santiago et al., 1995). This Ret-expressing population of nociceptors further differentiates into three subclasses of neurons that express specific Mas-related G protein-coupled receptors (Mrgpr), namely, neurons that express MrgprA3, MrgprB4 or MrgprD (Dong et al., 2001;

Liu et al., 2008). Recent physiologic studies suggest that these three classes of neurons are responsive to pruritogens, the gentle stroking of hair, and noxious mechanical stimulation, respectively (Han et al., 2013; Liu et al., 2012; Liu et al., 2007; Zylka et al., 2005). One central question in developmental biology is how such neuronal diversity is developed and maintained throughout life.

The development of sensory neurons in the DRG is regulated by the interplay between neurotrophic factors and various transcription factors (Marmigere and Ernfors, 2007). Recent studies indicate that the expression of transcription factors such as Runx1, Runx3, Er81, Shox2, and MafA play significant roles in the diversification of DRG neurons (Bourane et al., 2009; Chen et al., 2006; Inoue et al., 2007; Kramer et al., 2006; Scott et al., 2011). Neurotrophin family members have been shown to support the survival of various types of DRG neurons during development. Previous loss–of–function studies of neurotrophin family members Nerve Growth Factor (NGF), Brain Derived Neurotrophic Factor (BDNF), Neurotrophin 3 (NT3) and their respective high-affinity receptors TrkA, TrkB and TrkC, demonstrated that different sensory neuron subtypes require different neurotrophins for their survival. For example, in *Ngf*$^{-/-}$ and *TrkA*$^{-/-}$ mice, nociceptors are lost (Crowley et al., 1994; Smeyne et al., 1994b), while *Nt3*$^{-/-}$ and *TrkC*$^{-/-}$ mice lose proprioceptors (Ernfors et al., 1994; Tessarollo et al., 1994), and *TrkB*$^{-/-}$ and *Bdnf*$^{-/-}$ mice lose mechanoreceptors (Jones et al., 1994; Klein et al., 1993b).

In vitro studies have demonstrated that the GFLs promote the survival and axonal growth of various DRG neurons including nociceptive neurons (Molliver et al., 1997b). *In vivo* loss–of–function studies on GFLs and GFRαs have shown that they are

necessary for the survival of DRG neurons, their proper peripheral projections and cell body size (Ernsberger, 2008; Lindfors et al., 2006). The analysis of three different conditional Ret mutant mice demonstrated that Ret signaling is important for several aspects of DRG neuron development such as cell survival, central and peripheral neuronal projection and expression of phenotypical markers (Franck et al., 2011; Golden et al., 2010; Luo et al., 2007).

The p75 neurotrophin receptor (p75) is a member of the tumor necrosis receptor superfamily. p75 binds members of the Trk receptor family and modulates the cell survival functions of neurotrophins (Ceni et al., 2014). p75 is highly expressed in migrating neural crest cells and most sensory neurons during development. p75 null mice lose approximately 50% of DRG neurons across different sensory neuron subtypes, but the mechanism of these deficits is unclear in part due to expression of p75 in multiple cell types in the peripheral sensory system including neurons, Schwann cells and targets (Lee et al., 1992b). One hypothesis is that neuronal loss is due to an impairment in neurotrophin signaling. Indeed, *in vitro* experiments have shown that sensory neurons isolated from p75 null mutant mice are 2-3 fold less sensitive to the survival promoting effect of NGF treatment (Davies et al., 1993b; Lee et al., 1994). In addition, *in vitro* experiments suggest that p75 prolongs the activation of TrkA receptors by preventing poly-ubiquitination and degradation of TrkA (Makkerh et al., 2005a). These results argue that p75 can serve as a modulator of the neuronal response to neurotrophins. Although the role of p75 for modulating neurotrophin signaling is clearly established, whether the DRG neuron loss in p75 null mutant mice is due to a lack of neurotrophin signaling still remains to be determined.

Here we show that p75 is co-localized with GFRα1, GFRα2 and Ret in a subset of DRG neurons. p75 forms a complex with GFRα1, GFRα2 and Ret *in vitro* and *in vivo*. Removal of p75 from neurons reduced the survival effect of GDNF *in vitro* and impacted a subset of nonpeptidergic nociceptors *in vivo*, especially those that express low levels of Ret. Surprisingly, p75 deletion did not affect TrkA+ or TrkB+ populations of DRG neurons. p75, therefore, serves to augment GFL signaling and maintains the balance of cell specification and diversity during DRG neuron development.

Results

p75 is expressed in a subset of Ret expressing nociceptive neurons

Ret expressing cells in the DRG encompass several neuronal populations mediating different sensory modalities. Previous studies have shown that small diameter nonpeptidergic nociceptors which mediate pain sensation up-regulate Ret expression and down-regulate TrkA expression postnatally. This process is not complete until 2-3 weeks after birth (Molliver et al., 1997b). p75 is expressed in a variety of DRG neuron subclasses, and germline deletion of p75 results in a 50% loss of DRG neurons across different neuronal types (Murray et al., 1999). To determine whether Ret-expressing nonpeptidergic nociceptive neurons express p75, immunostaining was performed on postnatal day 14 (P14) L4 DRG sections with antibodies against p75, Ret, GFRα1 and GFRα2. As shown in Figure 2.1B, 2.1E and 2.1H, small diameter nonpeptidergic nociceptors are Ret^{+} and most of them are also immunopositive for GFRα1 or GFRα2. p75 expression overlapped with some small diameter neurons that are immunopositive for Ret, GFRα1 or GFRα2 (Figures 2.1C, 2.1F, and 2.1I). When we counted neurons that were immunopositive for both p75 and Ret, we found that ~23.8% of small diameter Ret^{+} cells are also $p75^{+}$ (Figure 2.1J). Previous studies have also shown that Ret^{+} nociceptive neurons have different levels of Ret expression and can be divided into groups that express a high level of Ret (Ret^{high} neurons) and a low level of Ret (Ret^{low} neurons), each group with their own characteristic markers (Zylka et al., 2003). When we investigated the co-localization of p75 with Ret in small diameter Ret^{high} (as indicated by arrows in Figure 2.1A-C) and Ret^{low} neurons (as indicated by arrowheads in Figure 2.1A-C), we found that among Ret^{high} neurons, only 22.1% co-

express p75, while 67.6% of Ret^{low} neurons express p75 (Figure 2.1J). The specificity of Ret staining was confirmed by staining sensory neurons taken from tamoxifen (TMX)-labeled *Rosa26*$^{LSL\text{-}tdTomato/+}$*; Ret*-Cre/ER^{T2} mice (Figure 2.2). These results suggest that p75 is in position to regulate the development of a subset of Ret^{+} nociceptive neurons, and its role may be more significant in Ret^{low} sensory neurons.

p75 is a component of the GFRα/Ret receptor complex

To investigate potential interactions between p75 and the components of the GDNF receptor complex, namely GFRα1 and Ret, we stained primary cultures of dissociated DRG neurons with antibodies against p75 and GFRα1. As shown in Figure 2.3A, punctate staining of p75 is often co-localized with GFRα1, although non-overlapping labeling exists. Based on these findings, we next explored whether a functional interaction exists between p75 and GFRα1 and Ret. p75 was co-expressed with GFRα1 or Ret in HEK-293 cells and a co-immunoprecipitation assay was performed. As shown in Figures 2.3B and 2.3C, p75 co-immunoprecipitates with GFRα1 and Ret. GDNF treatment enhanced the association of p75 with GFRα1. On the other hand, GDNF had no effect on the association of p75 with Ret when myc-tagged p75 was co-expressed with Ret alone in HEK293 cells. Quantification of the western blot signals from 3 independent experiments showed that no statistically significant changes in the amount of normalized Ret in the immuoprecipitates in the presence of GDNF as compared to no GDNF pulled down by an anti-myc antibody (fold change +GDNF/-GDNF=1.17, p=0.19) or an anti-p75 antibody (fold change +GDNF/-GDNF=1.08, p=0.58). The amount of normalized p75 in the immuoprecipitates pulled down by an

anti-Ret antibody is also unchanged with GDNF treatment (fold change +GDNF/-GDNF = 0.86, p=0.43). This is likely due to the lack of GFRα1 expression. To determine whether p75 forms a complex with GFRα1 under physiological conditions *in vivo*, co-immunoprecipitation assays were performed using lysates from superior cervical ganglia (SCG). We found that p75 and GFRα1 were able to be co-immunoprecipitated regardless of which protein was isolated by IP (Figure 2.3D). To determine the time course of the interaction between p75 and Ret, primary DRG neuron cultures were generated from P0 rats and maintained in culture for 7-10 days. Importantly, DRG neurons cultured under similar conditions were previously shown to develop in a manner comparable to their *in vivo* development regarding the expression of ion channels and neurotrophic factor receptors (Molliver et al., 1997). 7-10 DIV DRG neurons were stimulated with GDNF for the indicated times, followed by immunoprecipitation of Ret and immunoblotting for p75 and Ret. Interestingly, we observed that GDNF led to a statistically significant increase in p75-Ret association at 15 minutes, 1 hour, and 6 hours (Figure 2.3E-F) after stimulation. These results suggest that p75 forms a complex with GFL receptor components that mediate GFL signaling.

p75 augments GDNF-mediated Ret activation by increasing cell surface localization of Ret

To determine whether p75 modulates GDNF-induced Ret autophosphorylation, primary DRG neuron cultures were generated from p75 conditional knockout mice ($p75^{F/F}$), followed by infection with HSV-expressing Cre to knockdown their expression

of p75, or with HSV-expressing GFP alone as a control. The cultures were then treated with GDNF, followed by immunoprecipitation to assess the level of phosphorylated Ret using an anti-phosphotyrosine antibody. As shown in Figure 2.4A, GDNF induces a rapid phosphorylation of Ret, which is sustained above baseline for at least 60 minutes. Transduction of primary DRG neurons with HSV-GFP-Cre resulted in successful knockdown of approximately 80% of p75 compared to HSV-GFP-transduced neurons (Figure 2.4A-B). Following knockdown of p75, GDNF-induced Ret phosphorylation is dramatically reduced at both 15 minutes and 60 minutes following GDNF treatment (Figure 2.4A, 3C). These results suggest that p75 augments GDNF-mediated Ret activation.

Given the striking loss of GDNF-mediated Ret activation, we hypothesized that loss of p75 may result in changes of cell surface localization of Ret. To explore this possibility, we first transfected NIH/3T3 cells with Ret9 or Ret51, with or without p75 co-transfection. Cell surface proteins were biotinylated using NHS-LC-Biotin and precipitated using neutravidin. Interestingly, we observed that co-transfection of p75 with Ret9 and Ret51 significantly enhanced cell surface levels of both isoforms (Figure 2.4D). To test whether p75 plays a similar role in DRG neurons, we performed cell surface biotinylation experiments in HSV-treated *p75*$^{F/F}$ DRG neurons. We observed a striking reduction in the amount of total cell surface Ret using an antibody that detects both isoforms, as well as a reduction of both individual Ret9 and Ret51 isoforms in HSV-Cre treated neurons compared to HSV-GFP controls (Figure 2.4E, quantifications in 2.4F, 2.4G).

p75 is required for GFL-mediated survival of Ret+ nonpeptidergic nociceptors *in vitro*

Given that p75 is required for GDNF-mediated Ret activation, we sought to determine whether the loss of p75 impacted GFL-mediated DRG neuron survival. Further, because $TrkA^+$ peptidergic nociceptors selectively depend on NGF, while Ret^+ nonpeptidergic nociceptors depend on GDNF and NRTN (Molliver et al., 1997b; Snider and Silos-Santiago, 1996), we hypothesized that p75 deletion would selectively impair GFL-mediated survival within the nonpeptidergic nociceptor population. To this end, we crossed *p75*$^{F/F}$ mice with *UBC*-Cre/ER^{T2} mice, in which a tamoxifen (TMX)-inducible Cre is driven by the ubiquitin C promoter expressed in all cells (generating p75-WT and p75-cKO neurons) (Ruzankina et al., 2007), or *Ret*-Cre/ER^{T2} mice, in which TMX induces recombination selectively within Ret^+ neurons (generating p75-WT and p75-RC neurons) (Luo et al., 2009). DRG neurons were cultured in the presence of NGF and 4-hydroxy-TMX to induce recombination. Importantly, we observed a substantial knockdown of p75 in p75-cKO neurons compared to p75-WT ($p < 0.0001$; greater than 98% reduction; Figures 2.5A-B). No changes were observed in the total amount of TrkA (Figure 2.5A, 2.5C) or Ret (Figure 2.5A, 2.5D) protein levels, further validating this system. Due to the difficulty of detecting GFRα1 and GFRα2 protein levels by western blotting in cultured DRG neurons, we performed immunostaining to determine whether loss of p75 alters the proportion of GFRα1 or GFRα2 neurons. While we observed no difference in the proportion of GFRα1$^+$ neurons ($p = 0.2723$), a small but statistically significant reduction in the proportion of GFRα2$^+$ neurons was observed ($p = 0.0103$; p75-WT: 80.12 ± 1.32 and p75-cKO: 66.76 ± 4.34%; Figure 2.6C-D).

To fully characterize how p75 deletion alters Ret and TrkA expression, we next treated 7-10 DIV, TMX-maintained p75-WT and p75-cKO DRG neurons with NGF, a NGF blocking antibody (αNGF), αNGF and GDNF, or αNGF and NRTN. 48 hours later, p75-WT and p75-cKO DRG neurons were fixed and immunostained for DAPI, TuJ1 (a pan-neuronal marker), Ret, and TrkA. The number of $TrkA^+/Ret^-$ and $Ret^+/TrkA^-$ neurons were quantified in each condition. As expected, we observed no genotype-dependent differences in the number of $TrkA^+$ neurons regardless of treatment condition (Figure 2.6A), although we did observe a significant reduction of $TrkA^+$ neurons following NGF deprivation, as expected (Snider and Silos-Santiago, 1996). Interestingly, the proportion of Ret^+ neurons was increased in p75-cKO compared to p75-WT neurons treated with αNGF, αNGF and GDNF, and αNGF and NRTN, but not in NGF-maintained neurons. Additionally, as expected, we observed a drastic increase in Ret^+ neurons following NGF-deprivation regardless of genotype ($p < 0.0001$ for all genotypes) (Figure 2.6B). Collectively, these data indicate that removal of p75 does not substantially alter levels of TrkA, but enhances upregulation of Ret following NGF deprivation.

To determine whether loss of p75 altered GFL-mediated survival of $TrkA^+$ peptidergic or Ret^+ nonpeptidergic neurons, p75-WT and p75-cKO neurons were treated as described above and the number of apoptotic Ret^+ (Figure 2.5E) and $TrkA^+$ (Figure 2.5F) neurons was quantified by counting pyknotic nuclei. As expected, NGF deprivation led to an increase in the number of apoptotic neurons (Figures 2.5E-F) regardless of genotype. GDNF and NRTN treatments were able to partially rescue Ret^+ neurons from apoptosis (Figure 2.5E; $p < 0.001$ for each), and this rescue affect was substantially diminished in p75-cKO ($p < 0.0001$ for each). As expected, GDNF and

NRTN were not able to rescue TrkA^{+} neurons and loss of p75 had no effect (Figure 4F). To further substantiate these findings, these experiments were repeated using DRG neurons cultured from p75-RC, or p75-WT littermate mice. Interestingly, we observed that GDNF and NRTN were each able to rescue Ret^{+} neurons from apoptosis in p75-WT ($p < 0.0001$), but not p75-RC neurons, with a corresponding increase in apoptosis observed in p75-RC neurons treated with αNGF and GDNF ($p < 0.01$), and αNGF and NRTN ($p < 0.001$) compared to p75-WT neurons (Figure 2.5G). Additionally, as expected, GFL treatment did not rescue TrkA^{+} neurons from apoptosis, and no genotype-dependent effects were observed in TrkA^{+} neurons (Figure 2.5H). Collectively, these results indicate that p75 functions specifically to augment the GFL-mediated survival of Ret^{+} DRG neurons.

Removal of neuronal p75 expression induces a loss of 20% of adult DRG neurons

Based on our findings that p75 is necessary for GFL-mediated survival of DRG neurons *in vitro*, we asked whether it plays similar roles *in vivo*. Previous studies analyzing p75 germline knockout mice have demonstrated that 50% of DRG neurons are lost, and these losses occur across sensory modalities (Lee et al. 1992). It is unclear, however, whether this drastic phenotype reflects a cell-autonomous requirement for p75 within sensory neurons themselves. Thus, we generated *p75*$^{F/F}$ mice (described in Experimental Procedures, Figure 2.7) and crossed them with an *Islet1*-Cre driver that expresses Cre in spinal motor and sensory neurons at later stages (Srinivas et al., 2001). Grossly, *Isl1*-Cre$^{+/-}$; *p75*$^{F/F}$ mice are indistinguishable from their

littermates. To determine at what age p75 is deleted in these animals, p75 immunostaining was performed on E10.5, E12.5, and adult *Isl1*-Cre$^{+/-}$; *p75*$^{F/F}$ mice (compared to *p75*$^{F/F}$ controls). We observed no reduction of p75 immunolabeling at E10.5 (Figure 2.8A, 2.8D), but a drastic loss of p75 by E12.5 (Figure 2.8B, 2.8E). At both E12.5 and adulthood (Figure 2.8C, 2.8F), the vast majority of neurons have lost p75 immunolabeling, with primarily non-neuronal cells expressing the residual p75. Therefore, *Isl1-Cre*$^{+/-}$; *p75*$^{F/F}$ mice lose neuronal p75 expression between E10.5 and E12.5. To determine whether neuronal survival is altered in the *Isl1-Cre*$^{+/-}$; *p75*$^{F/F}$ mice, we performed Nissl staining and counted total cell numbers in L4 DRGs from *Isl1-Cre*$^{+/-}$; *p75*$^{F/F}$ (and *p75*$^{F/F}$ control) mice at P1, P14 or adulthood. As a control, we also analyzed L4 DRG counts in p75 germline knockout mice. As expected, we observed a 50% reduction in P1 *p75*$^{-/-}$ DRGs compared to *p75*$^{+/+}$ controls (Figure 2.8G). Strikingly, given the drastic results observed in P1 *p75*$^{-/-}$ mice, we observed no difference in total L4 DRG neuron numbers at P1 or P14 in *Isl1-Cre*$^{+/-}$; *p75*$^{F/F}$ mice (Figure 2.8G). We did, however, observe that approximately 20% of DRG neurons were lost in adult *Isl1-Cre*$^{+/-}$; *p75*$^{F/F}$ mice compared to *p75*$^{F/F}$ controls (Figure 2.8G). Collectively, these results indicate that neuron-specific deletion of p75 by E12.5 is insufficient to impact neuronal survival during embryogenesis, and suggest neuronal p75 functions postnatally in sensory neuron diversification.

Removal of p75 does not alter the generation of Ret$^+$ or Runx1$^+$ neurons

Loss of NGF-TrkA signaling in a *Bax*$^{-/-}$ background (thereby preventing apoptosis) results in significantly reduced levels of Ret, as well as reduced levels of the

transcription factor Runx1 (Luo et al., 2007). Given that p75 has also been shown to enhance NGF signaling through TrkA, we tested whether the generation of Ret^{+} or Runx1^{+} neurons is affected in *Isl1-Cre*$^{+/-}$; *p75*$^{F/F}$ mice. Upon immunostaining P14 DRG neurons for Ret or Runx1, we observed no differences in the intensity of immunostaining (Figure 2.8H-I, 2.8K-L) or in the total number of Runx1^{+} and Ret^{+} neurons in *Isl1*-Cre$^{+/-}$; *p75*$^{F/F}$ compared to *p75*$^{F/F}$ control mice (Figure 2.8J, 2.8M), suggesting that the removal of p75 does not impact the NGF-TrkA-Runx1 signaling axis, thereby not altering subsequent Ret expression. We further characterized the expression level of TrkA, TrkB, GFRα1 and GFRα2 at P0, P14 and adult DRGs. There is no obvious difference in any of these markers between *Isl1-Cre*$^{+/-}$; *p75*$^{F/F}$ mice and controls at P0 and P14 (Figures 2.9 and 2.10). These results suggest that loss of p75 in the *Isl1-Cre*$^{+/-}$; *p75*$^{F/F}$ mice does not impact the expression level of TrkA, TrkB, or the relevant GFL co-receptors while Ret^{+} nonpeptidergic nociceptors are being generated.

p75 is required for survival of a subset of nonpeptidergic nociceptors

Given that we observed losses of approximately 20% of DRG neurons, and our *in vitro* findings linking p75 to GFL-Ret signaling, we hypothesized that nonpeptidergic nociceptors were selectively lost in adult *Isl1*-Cre$^{+/-}$; *p75*$^{F/F}$ mice. To answer this question, adult *p75*$^{F/F}$ and *Isl1*-Cre$^{+/-}$; *p75*$^{F/F}$ L4 DRG neurons were immunostained for NF200 (mechanoreceptors and proprioceptors), CGRP (peptidergic nociceptors), paravalbumin (proprioceptors), and IB4 (nonpeptidergic nociceptors). Interestingly, we observed no difference in the number of CGRP^{+} (Figure 2.11A, E), Parvalbumin^{+} (Figure 2.11B, F), or NF200^{+} (Figure 2.11D, H) neurons between *Isl1-Cre*$^{+/-}$; *p75*$^{F/F}$ and

p75$^{F/F}$ mice (Figure 2.11O). In contrast, we observed a 35% decrease in IB4^{+} neurons (Figure 2.11C, 2.11G, 2.11O), indicating that p75 is selectively required for the survival of a subset of nonpeptidergic nociceptors. Given that the IB4^{+} immunolabeling may not sufficiently label all nonpeptidergic nociceptors, we sought to corroborate these results by performing co-immunostaining for peripherin and Ret to count the number of small diameter Ret+ nociceptors (Figure 2.11I-N). As shown in Figure 2.11-O, we observed a 25% decrease in the total number of peripherin^{+}/Ret^{+} neurons. We also observed ~30% decrease in the GFRα2^{+} population (Figure 2.10C, F and G) and ~50% decrease in small diameter GFRα1^{+} population (Figure 2.9J, M and N). Collectively, these results indicate that p75 is selectively required to promote the survival of nonpeptidergic Ret^{+} neurons, although we cannot rule out the possibility that p75 has additional functions in other unexplored subpopulations.

To further characterize the neuron loss within the IB4^{+} population, we performed *in situ* hybridization using probes against MrgA, MrgB, and MrgD on adult (6 month old) L4 DRG sections (Dong et al., 2001). Importantly, MrgA^{+} and MrgB^{+} neurons are known to express Ret weakly (Ret^{low}), while MrgD^{+} neurons express Ret more strongly (Ret^{high}) (Zylka et al., 2003). Interestingly, compared to *p75*$^{F/F}$ mice, we observed that *Isl1*-Cre$^{+/-}$; *p75*$^{F/F}$ DRGs had a greater than 50% reduction in MrgA^{+} (Figure 2.12A, D and G) and MrgB^{+} neurons (Figure 2.12B, E and H), while only 27% of MrgD^{+} neurons were lost (Figure 2.12C, F and I). We cannot rule out the possibility that the loss of p75 in DRG neurons causes downregulation of Mrg family gene expression, as previous studies have shown a dependence on Ret signaling (Luo et al., 2007). Nonetheless, these data

are consistent with the model that the p75-dependence of Ret^{+} neurons is correlated with the level of p75 expression in the Ret^{low} and Ret^{high} neurons.

Discussion

In this study, we demonstrate that p75 forms a GDNF-activated receptor complex with GFRα1 and Ret. Furthermore, knockdown of p75 levels within DRG neurons resulted in a drastic impairment in GDNF-mediated Ret activation, and a subsequent loss of cell surface localization of Ret, suggesting that p75 potentiates GDNF-Ret signal transduction through enhancing receptor availability to ligand, or by enhancing recycling. Correspondingly, p75 deletion results in a substantial reduction in GDNF and NRTN-mediated survival of Ret^{+} nonpeptidergic neurons, but not $TrkA^{+}$ peptidergic neurons. Strikingly, especially when considering the 50% loss of DRG neurons during embryonic development in p75 germline null mutants, neuron-specific deletion of p75 by E12.5 resulted in no embryonic deficits. In these animals, 20% of neurons were lost postnatally, with losses occurring selectively within the $IB4^{+}$/$peripherin^{+}$/Ret^{+} class of nonpeptidergic nociceptors during the transition from P14 to adulthood. $MrgA^{+}$ and $MrgB^{+}$ neurons expressing the lowest levels of Ret had the highest degree of p75 expression, and were more significantly affected than Ret^{low} $MrgD^{+}$ neurons. In light of these findings, we propose the following model to explain the role of p75 modulation of Ret signaling in the survival of adult DRG neurons (Figure 2.12J). The expression of p75 increases the level of Ret on the cell surface in $p75^{F/F}$ mice, increasing sensitivity of these neurons to GDNF, thereby potentiating GFL-induced Ret activation and downstream survival. Upon loss of p75 expression in *Isl1*-$Cre^{+/-}$; $p75^{F/F}$ mice, the level of Ret on the cell surface is reduced. Ret^{high} MrgD+ neurons may be better able to compensate for the loss of p75, resulting in lower neuron losses. However, in Ret^{low} $MrgA^{+}$ or $MrgB^{+}$ neurons, the loss of cell surface Ret cannot be adequately buffered,

leading to more substantial losses within the MrgA^{+} and MrgB^{+} neuron population. This model highlights the ability of p75 to fine-tune Ret signaling and maintain the balance of different types of DRG neurons in postnatal development. Our findings further expand the repertoire of receptor complexes that p75 modulates and the developmental processes that p75 impacts.

The developmental diversification of DRG neurons is an intricate process regulated by transcription factors and growth factors. Different types of sensory neurons rely on specific neurotrophic factors for their survival as they differentiate and mature. The p75 receptor can modulate both neurotrophin and GFL signaling pathways, playing a significant role in the development and maintenance of DRG neuron diversity. In p75 knockout mice, 50% of lumbar DRG neurons are lost by the first week of postnatal life (Figure 5G) (Murray et al., 1999). This loss is across all DRG neuronal types and occurs early during embryonic DRG development. In *Isl1-Cre*$^{+/-}$; *p75*$^{F/F}$ mice, p75 expression is removed at E12.5 specifically within nearly all sensory neurons, yet no neuronal deficits are observed before P14, and only 20% of the total neurons are lost in adult *Isl1-Cre*$^{+/-}$; *p75*$^{F/F}$ mice. The striking disparity between neuronal losses in germline p75 knockout mice compared to *Isl1-Cre*$^{+/-}$; *p75*$^{F/F}$ mice suggests that the early deficits in p75 knockout mice may be due to its function in non-neuronal cells. For example, previous studies have indicated that p75 is expressed in neural crest stem cells, which give rise to DRG neurons, satellite cells in the DRG, and Schwann cells. Given that germline p75 knockout animals lack p75 expression in all cell types from the onset of development, the previously observed loss of 50% of neurons across DRG subtypes may be due to defects in neural crest progenitors. Another possibility is that removing p75 from satellite

cells and Schwann cells may create a less supportive environment for the survival of DRG neurons. While we cannot rule out the possibility that the small amount of p75 remaining following *Islet1*-Cre mediated deletion is responsible for the differences observed between germline p75 knockout mice and *Isl1-Cre*$^{+/-}$; *p75*$^{F/F}$ mice, previous studies have also suggested a non-neuronal role for p75 early in sensory neuron development. For example, migration of p75-deficient Schwann cells is impaired and may thereby contribute to a reduced ability of developing sensory neurons to reach their proper target cells (Bentley and Lee, 2000). Nevertheless, the results reported here indicate that p75 has a postnatal function specifically serving to augment Ret signaling in nonpeptidergic nociceptors.

Another unexpected finding of this study is that p75 expression is required for the survival of nonpeptidergic nociceptors, but not other neuronal populations. In our analysis of *Isl1-Cre*$^{+/-}$; *p75*$^{F/F}$ mice, we observed no deficits in the number of CGRP^{+} peptidergic nociceptive neurons, nor is their survival impaired *in vitro*, despite the fact that p75 is expressed in the majority of CGRP^{+} neurons and p75 expression is removed in most CGRP^{+} neurons in *Isl1-Cre*$^{+/-}$; *p75*$^{F/F}$ mice at a developmental period during which these neurons are highly dependent on NGF/TrkA signaling (Figure 2.13). In addition, we observed no deficits in numbers of TrkA^{+}, Runx1^{+}, Ret^{+}, GFRα1^{+}, or GFRα2^{+} neurons at P14. These results are surprising because p75 has been shown in many studies to enhance NGF signaling via TrkA through increased NGF binding affinity (Esposito et al., 2001; Hempstead et al., 1991), as well as through reduced ubiquitination and subsequent degradation of TrkA (Makkerh et al., 2005a). The pro-survival function of p75 in sensory neurons has been proposed by many (Davies et al.,

1993b; Lee et al., 1994) to be through modulation of NGF/TrkA signaling. Based on these results, we conclude that the intrinsic level of NGF signaling is sufficient to maintain their survival and, therefore, p75 is dispensable for NGF/TrkA-dependent survival of peptidergic neurons, although the trophic status of these neurons may still be impacted.

In conclusion, we have found that p75 physically associates with receptors in the GDNF family and plays a novel role in mediating the survival-promoting effects of the GFLs by enhancing cell surface localization of Ret, thereby augmenting GFL/GFRα/Ret signaling. Surprisingly, *in vivo*, deletion of p75 specifically within neurons resulted in no deficits until after P14, suggesting a potential early, non-neuronal role for p75 followed by a postnatal, neuron-specific function in nonpeptidergic nociceptors. Within the nonpeptidergic nociceptor population, neurons of the $MrgA^+$ and $MrgB^+$ subclasses demonstrate a greater dependence on p75 to potentiate Ret signaling compared to $MrgD^+$ neurons. Thus, our data clarify the function of this enigmatic receptor in sensory neurons and identify a unique mechanism by which neurotrophic factor support can be fine-tuned to allow the selective survival of discrete subpopulations, ultimately expanding sensory neuron diversity.

Experimental Procedures

Animals

All experiments were carried out in compliance with the guidelines of the Association for Assessment and Accreditation of Laboratory Animal Care (AAALAC).

For the generation and characterization of *p75*$^{F/F}$ mice, one loxP site was inserted into the intron region between exon II and exon III of the p75 gene while the other loxP site was inserted into the intron region between exon III and exon IV, and is detailed further below (Figure 2.7). Detailed biochemical and anatomical analyses showed that *p75*$^{F/F}$ mice are a good model to study p75 function. For the *in vitro* studies investigating the role of p75 in Ret signaling in primary DRG neuron cultures, *p75*$^{F/F}$ mice generated and described by Bogenmann *et al*. were utilized. Characterization of these mice (Bogenmann et al., 2011a) indicates that they exhibit the same phenotypes as the *p75*$^{F/F}$ mice described above. *Islet1*-Cre mice were previously described and shown to induce Cre mediated recombination at around E12.5 (Srinivas et al., 2001). Ret-Cre/ER^{T2} and UBC-Cre/ER^{T2} mice were previously characterized (Luo et al., 2007; Ruzankina et al., 2007).

Staining of Sensory Neurons from Adult *Rosa26*$^{LSL\text{-}tdTomato}$; *Ret*$^{+/+}$ and Rosa26$^{LSL\text{-}tdTomato}$; *Ret*-Cre/ER^{T2} mice

For the experiments demonstrating the specificity of Ret immunostaining, tamoxifen (TMX; T5648, Sigma Aldrich, St. Louis, MO) was dissolved in corn oil and administered via intraperitoneal injection to adult mice of the indicated genotypes at a dose of 0.25 mg/g body weight for five consecutive days. Mice were then euthanized, perfused with 4% PFA, and trigeminal ganglia were collected, post fixed in 4% PFA for 1 hour and cryoprotected with 30% sucrose overnight. 10µm cryosections were obtained and stained with a goat-anti-Ret (R&D, 1:50), rabbit anti-RFP (Rockland, 1:200), and Tuj1 (Sigma, 1:200). As an additional control, staining using goat anti-Ret was conducted in the presence of a blocking peptide to ensure specificity (Alomone

Labs, 1:50). Donkey anti-mouse 488, donkey anti-rabbit 543, and donkey anti-goat 633 secondary antibodies (Biotium, 1:200) were used.

In situ Hybridization and Immunohistochemistry

In situ probes for *MrgA1*, *MrgA3*, *MrgB4*, *MrgD* and *Ret* were kindly provided by Dr. Xinzhong Dong (Johns Hopkins University). The *in situ* probe for p75 was provided by Mark Bothwell (University of Washington). Digoxigenin (DIG) and fluorescence-labeled *cRNA* probes were used for in situ hybridization. For immunohistochemistry on cell culture and frozen DRG sections, the following antibodies were used: rabbit anti-p75 (a gift from Dr. Moses Chao, 1:500), goat anti-GFRα1 (R&D, 1:100), goat anti-GFRα2 (R&D, 1:100), Goat anti-Ret (R&D, 1:50), rabbit anti-Ret (Santa Cruz, 1:100), rabbit anti-Runx1 (1:1000, a gift from Dr. Tom Jessell), rabbit anti-CGRP (Immunostar, 1:500), rabbit anti-parvalbumin (Swant, 1:1000), chicken anti-TrkB (1:500), rabbit anti-peripherin (Novusbio 1:1000) and Rabbit anti-NF200 (Millipore, 1:500). Alexafluor-546 and Alexafluor-488 conjugated secondary (Molecular Probes, 1:500) antibodies were used. For IB4 staining, FITC conjugated IB4 (Invitrogen, 1:100) was used.

Generation of p75 Conditional Mutant Mice

The p75 floxed ($p75^{F/F}$) mice were generated using standard methods. A targeting vector was constructed by introducing a loxP site into an EcoRV site in intron 2 and a neomycin resistance marker (neo) flanked by loxP sites into an XbaI site in intron 3. The targeting construct was electroporated into ES cells and G418 resistant ES clones were screened by Southern Blotting analysis. When the DNA was digested with

EcoRI, the probe hybridized to a 5kb band for the targeting allele (T) and a 14kb band for the wild type allele (+). ES cell clones containing the targeted (T) allele were isolated and transfected with plasmids expressing Cre recombinase under the control of the CMV promoter. ES cell clones in which the neo^r-cassette was removed but maintained two LoxP sites were isolated. This is called the floxed (F) allele. In the recombined allele (R), the neo^r-cassette and the third exon are removed and only one LoxP site is retained. P75 floxed animals were crossed with a line of nestin-Cre transgenic mice. Brain DNA was isolated from P0 mice, digested with EcoR I and hybridized with the probe. Nearly complete recombination occurred in mice containing floxed alleles and the nestin-Cre transgene (F/R; Cre +). Because the nestin-Cre transgenic mice used in this experiment have leaky Cre expression in the germ cells, germline recombination of the floxed allele can occur. Germline recombination only one allele (R) occurs in mice whose parents carry a floxed allele and the nestin-Cre transgene, even if they no longer express Cre (F/R; Cre -). No recombination of the floxed allele occurs in the absence of Cre expression (F/F; Cre -). Immunofluorescence staining of coronal sections of the septum with anti-p75 antibodies revealed that no p75 proteins are detected in mice containing the floxed allele and the nestin-Cre transgene (F/F, Cre +). To test if p75-s transcripts (spliced product of exon II to exon IV) described by von Shack *et al*. (von Schack et al., 2001) are present in the conditional mutant animals, reverse transcription coupled-PCR (RT-PCR) was used to assay the mRNA isolated from mice containing recombined alleles (R/R), alleles with neo-cassette insertions into exon III of original p75 mutants (-/-) (Lee et al., 1992b), floxed alleles (F/F) or wild type alleles (+/+). No p75-s transcripts were detected using primers and PCR conditions previously described

by von Shack *et al.* (von Schack et al., 2001). Because the 5' primer used by von Shack *et al*. is consisted of two 10-neucleotides complimentary to the end of exon II and the beginning of exon IV, respectively, the primer presumably only detected the spliced product of exon II to exon IV. However, we found that the primer set used by von Shack *et al*. was able to detect any transcripts containing axon IV, including the full-length cDNA. Although we do not know the basis for the lack of specificity, we noticed that the primer set is highly GC-rich. It is worth mentioning that Paul *et al*. recently demonstrated that the mutated p75 allele created by von Shack *et al.* gave rise to an alternatively spiced transcript (Paul et al., 2004), but not in the p75 mutants we generated previously. Over-expression of this spliced product increases cell death (Paul et al., 2004) and may contribute to the phenotype observed in that line of mutant mice. Isl1-Cre mice were a generous gift from Dr. Thomas Jessell.

Cell Counts

Animals at the indicated ages were perfused with 4% PFA and L4 DRGs were isolated, postfixed in 4% PFA for 1 hour and then followed by cryprotection in 30% sucrose overnight. 10μm serial cryosections were made through the entire DRG. For total neuron counts, sections were stained with 0.5% cresyl violet and cells with visible nucleoli were counted as neurons.

Cell Culture and Transfection of Immortalized Cell Lines

NIH/3T3 cells were maintained in DMEM supplemented with 10% fetal bovine serum (FBS), 2 mM glutamine, and 1% penicillin-streptomycin (Invitrogen, Carlsbad, CA). HEK293 cells were maintained in DMEM supplemented with 10% FBS and 1% penicillin-streptomycin (Cellgro). For all biochemistry experiments, cells were plated onto 6-well tissue culture plates and allowed to proliferate to a density of 50% confluence prior to transfection. Transfections of NIH/3T3 cells were performed using Lipofectamine 2000 according to the manufacturer's instructions (Invitrogen). In all NIH/3T3 transfection experiments, a total of 5 µg plasmid DNA was added per well, using a plasmid encoding GFP to keep the total amount of DNA constant between treatments. In all HEK293 transfection experiments, a total of 2µg of DNA was added per well, using a plasmid encoding GFP to keep the total amount of DNA constant. The mammalian expression plasmid encoding p75 was generously provided by Phil Barker.

Production of Dorsal Root Ganglion Neuron Cultures and Neuron Survival Assays

Primary cultures of DRG neurons were produced as described previously (Tsui and Pierchala, 2010). Briefly, DRG neurons were isolated from E19-P1 Sprague-Dawley rats (Charles River, Portage, MI) and P0 *p75*$^{F/F}$ mice (Bogenmann et al., 2011a) crossed to the Cre strains described throughout. DRGs were enzymatically dissociated via incubation with collagenase (Worthington) followed by TrypLE (Invitrogen). Neurons were plated on gas-plasma treated 35 mm^2 dishes (Harrick Plasma; Ithaca, NY) coated with 20% growth factor-reduced matrigel in DMEM (BD Biosciences, San Jose, CA). For all biochemical experiments, neurons were plated as mass cultures at a density of 40-50 ganglia per plate. For death assays, neurons were plated as a droplet at a density of

10-15 ganglia per plate. Neurons were maintained in minimum essential medium (MEM) containing 50 ng/ml NGF (Harlan), 10% (FBS), the antimitotic agents 3.3 μg/ml aphidicolin and 5-fluoro-2-deoxyuridine (20 μM; Sigma, St. Louis, MO), 2 mM glutamine, and 1% penicillin-streptomycin (Invitrogen, Carlsbad, CA). For death assays, neurons were treated as described in the figure legends, fixed 48 hours post-treatment in 4% paraformaldehyde, and coverslipped with DAPI-fluoromount-G. GFP^+ neurons were analyzed to identify pyknotic nuclei, a known morphological feature of apoptotic cell death. For the experiments utilizing TMX-dependent Cre drivers, both control and Cre+ neurons were maintained in the presence of 0.5 μg/ml 4-OH-TMX (Sigma).

Immunoprecipitation and Quantitative Immunoblotting

Cells were treated as indicated in the figure legends. Following treatment, the dishes were placed on ice, gently washed with PBS, pH 7.4, and lysed with immunoprecipitation buffer (Tris-buffered saline (TBS), pH 7.4, 1% Nonidet P-40, 10% glycerol, 500 μM sodium vanadate, and protease inhibitors) as described previously (Tsui and Pierchala, 2010). Anti-Ret51 and/or anti-Ret9 antibodies were added (8 μL; C-20 and C-19-G, respectively; Santa Cruz Biotechnology) to cleared extracts along with protein A and protein G (Invitrogen, Carlsbad, CA) and incubated overnight at 4°C with gentle agitation. Immunoprecipitates were then washed three times with IP buffer and the complexes were prepared for sodium dodecyl sulfate-polyacrylate gel electrophoresis (SDS-PAGE) by adding 2X sample buffer (TBS, pH 6.8, 10% glycerol, 4% SDS, 10% □-mercaptoethanol and 0.02% bromophenol blue) and boiling the

samples for 10 minutes. Immunoblotting was performed as described in the Supplementary Experimental Procedures.

Cell Surface Biotinylation Assays

Cell surface biotin labeling was used to distinguish cell surface proteins from intracellular proteins. Cells were treated as described in the figure legends and then cooled to 4°C to stop membrane traffic. Cells were washed thrice with ice-cold PBS and labeled with 2 mM EZ-Link NHS-LC-Biotin (in PBS; Pierce, Rockville, IL) for 20 minutes, followed by a second 20 minute incubation with fresh biotinylation reagent. The cells were then washed, and any remaining NHS-LC-Biotin was inactivated with two 20-minute incubations in TBS. Cells were then washed again with PBS and detergent extracted using a modified RIPA buffer (Tris, pH 7.4, 100 mM NaCl, 10% glycerol, 1% Triton X-100, 0.1% SDS, protease inhibitors, and 500 µmol/L sodium vanadate). Biotinylated proteins were precipitated with immobilized Neutravidin (Pierce) in an identical manner as the immunoprecipitations described above, and immunoprecipitates and supernatants (containing intracellular proteins) were then prepared for SDS-PAGE and immunoblotting.

Statistics:

Statistical tests were carried out by using GraphPad Prism (GraphPad Software); statistical tests used are indicated throughout the results section. A student's t-test was used to assessing statistical significance between two conditions, while one-way

ANOVA was utilized when multiple variables were compared. All data are reported as the mean ± s.e.m. *$p < 0.05$, **$p < 0.01$, ***$p < 0.001$, ****$p < 0.0001$.

Cell Counts on Immunofluorescently Stained DRGs

For neurons expressing various markers, sections were immunofluorescently stained with various antibodies and double stained with DAPI. Immunopositive cells with intact nuclei were counted. To count Ret^{high} and Ret^{low} neurons, images of Ret immunofluorescence staining of DRG sections were taken using the same camera parameters and batch processed using Photoshop. Then the fluorescence intensity of Ret staining was surveyed by looking at the brightness reading of the cell bodies using Photoshop and compared with the Ret negative cells in the same section. After the survey of all the pictures, we found the fluorescence signal for Ret negative cells in the same section was around 100. Thus, a criterion was set to classify any cells with brightness reading higher than 150 (Maximum is 256) in any part of the cell body as Ret^{high} neurons; brightness reading between 100 and 150 as Ret^{low} neurons; and brightness reading below 100 as no expression. To count small and large diameter $GFR\alpha1^{+}$ neurons, the size of $GFR\alpha1^{+}$ neurons was measured using ImageJ by manually tracing the cell body and measure the area of the selection. By comparing the size of $GFRa1^{+}$ neurons and the $GFRa2^{+}$ neuronal populations and assuming small diameter $GFRa1^{+}$ neurons should have similar size as the majority of $GFRa2^{+}$ neurons (as they both belong to the nonpeptidergic nociceptors), a criteria was set to classify any neurons with area less than 4400 $pixel^2$ as small diameter neurons.

Co-localization Staining of DRG Neurons

P14 DRG neurons were cultured as previously described. Briefly, DRG neurons were dissected from P14 mice and digested with collagenase and trypsin. They were then dissociated with fire polished Pasteur pipettes. The dissociated DRG neurons were cultured on acid-washed glass coverslips coated with laminin for 36 hours before being stained with an anti-p75 and an anti-GFRα1 antibody. The cells were incubated in primary antibodies for 1 hour at 4°C in HEPES-buffered DMEM and then incubated in secondary antibodies for 30 minutes in 4°C. Afterward, the cells were fixed with ice cold 95% ethanol.

Transduction of Dorsal Root Ganglion Neurons

Neurons were infected with herpes simplex viruses encoding either GFP (HSV-GFP; GFP was driven by the CMV reporter), or GFP and Cre (HSV-GFP-Cre; GFP was driven by the CMV reporter and Cre was driven by the IE4/5 promoter) 24 hours after plating. The recombinant viruses (MIT Viral Core Facility, McGovern Institute, Boston, MA) were used at a MOI of approximately 8-10. In all experiments, 48 hours post-transduction the neurons were visualized for GFP fluorescence, which was observed in greater than 90% of neurons, to confirm efficient transduction and, thus, co-expression of Cre recombinase.

Quantitative Immunoblotting

Protein samples were subjected to SDS-PAGE followed by electroblotting onto PVDF membranes (Immobilin P; Millipore). Blots were blocked in 3-5% BSA in Tris-buffered saline containing 0.1% Tween-20, and Western blot analysis was performed using the following antibodies at the indicated concentrations: Ret51 (C-20, Santa Cruz, 1:500-1:1000), Ret9 (C19R, Santa Cruz, 1:1000), phospho-tyrosine (4G10, Millipore, 1:2000-1:3000), p75 (Promega, 1:3000), actin (JLA-20, Iowa Hybridoma Bank, 1:2000), TrkA (C-14, Santa Cruz, 1:1000), and transferrin (T2027, Sigma, 1:2000). Blots were developed using a chemiluminescent substrate (Supersignal, Pierce, Rockford, IL). For quantifications, scanned images of X-ray films were imported into ImageJ (National Institutes of Health) and processed using the gel analysis tool. Integrated density values obtained from immunoblotting were reported as mean values ± SEM, with arbitrary units on the vertical axis. All immunoblot quantifications were normalized to the appropriate control: for co-immunoprecipitation studies, values were normalized to the precipitated protein; for phospho-specific signaling effectors, values were normalized to total levels of these effectors; and values were normalized to actin (used as a loading control) for all other samples. All biochemical experiments were performed independently at least 3 times with similar results, with sample sizes for individual experiments indicated in the figure legends.

Acknowledgments

This research was supported by grants from the NIH (HD034534, NS060833, NS072031, NS089585, AG010435, CA014195, AG042985, AG047669, and

DE023479), the Clayton Foundation, the Schlink Foundation, the Gemcon Family Foundation and the Joe W. and Dorothy Dorsett Brown Foundation. The funders had no role in study design, data collection and analysis, decision to publish, or preparation of the manuscript.

Author contribution

Z.C., C.R.D., B.A.P., and K.F.L. designed experiments, interpreted the data, and wrote the manuscript. Z.C., C.R.D., A.S.H. and B.D. performed the experiments. Y. H. and W.L. generated p75 floxed mice. B.A.P. and K.F.L. were responsible for the overall direction and communication of the experiments.

Figures:

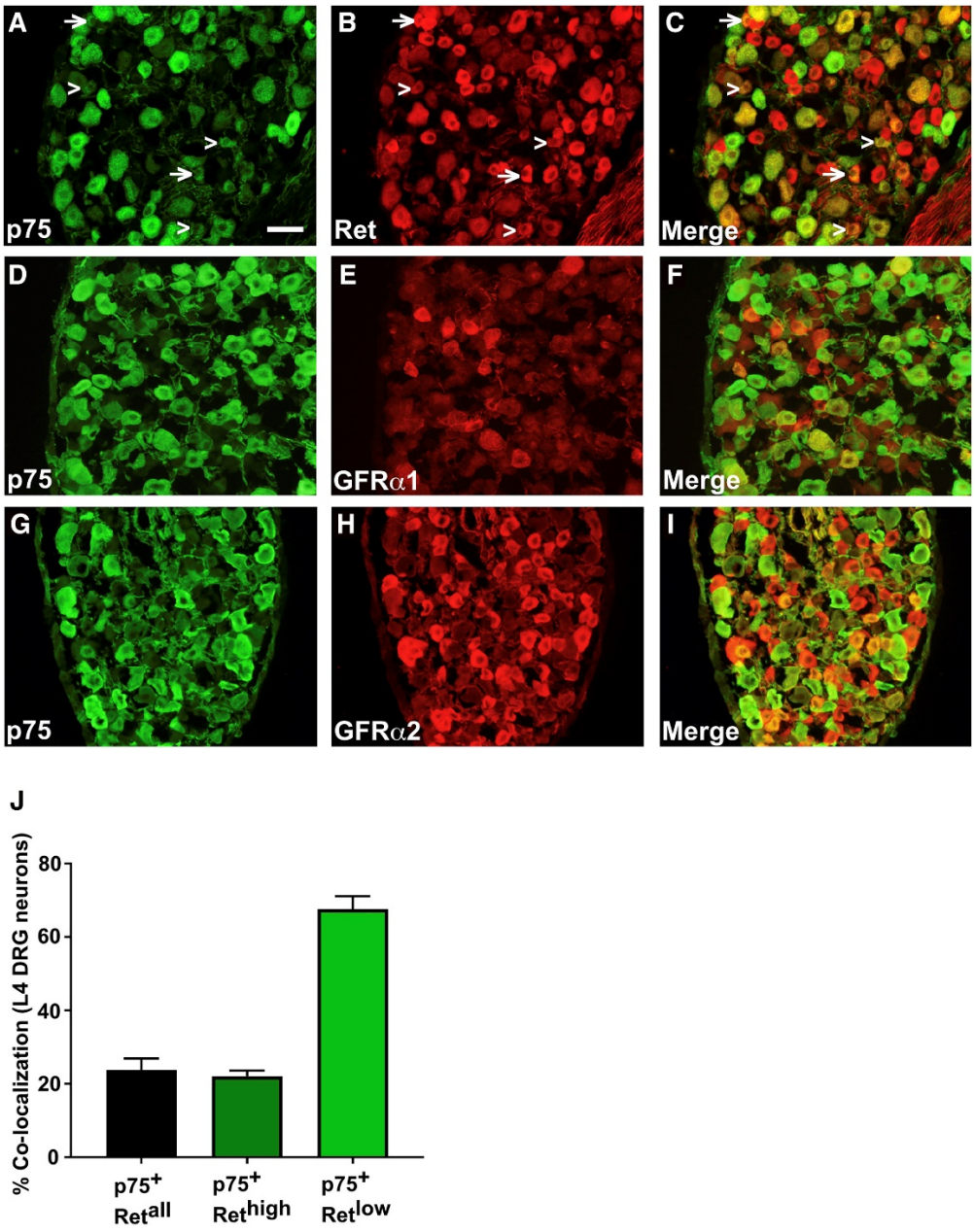

Figure 2.1. **p75 is co-expressed with GFRα1, GFRα2 and Ret in DRG neurons**.
Immunofluorescence staining of p14 DRG sections with anti-p75 (panel A, D, G), anti-Ret (panel B), anti-GFRα1 (panel E), or anti-GFRα2 (panel H) antibodies. The quantitation of co-localization is presented in panel J. Arrows in panel A-C indicate examples of Ret^{high} cells and arrowheads indicate examples of Ret^{low} cells. Scale bar, 100μm

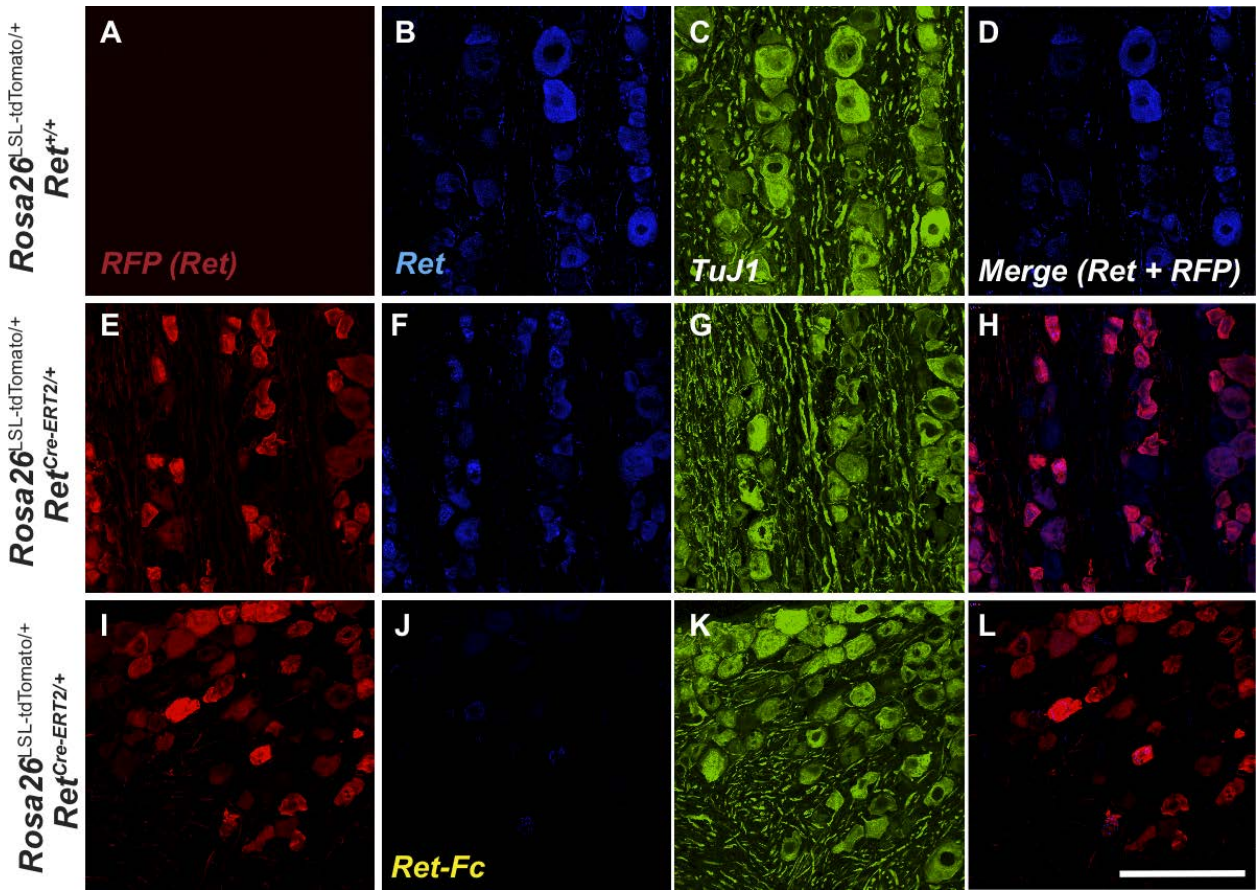

Figure 2.2. Staining of sensory neurons from adult *Rosa26*$^{LSL\text{-}tdTomato}$; *Ret*$^{+/+}$ and *Rosa26*$^{LSL\text{-}tdTomato}$; *Ret*-Cre/ER^{T2} mice

Rosa26$^{LSL\text{-}tdTomato}$; *Ret*$^{+/+}$ mice (A-D) or *Rosa26*$^{LSL\text{-}tdTomato}$; *Ret*$^{Cre\text{-}ERT2/+}$ mice were treated with tamoxifin (TMX) for 5 days (E-L). Trigeminal ganglia were stained with an antibody to detect RFP (A, E, I), Ret (B, F), TuJ1(C, G, K), or the Ret antibody in the presence of the antibody blocking peptide (J). We observed *Ret*-Cre/ER^{T2} induced tdTomato fluorescent protein expression in Ret^{+} trigeminal neurons (E, I). The tdTomato labeling was absent without Ret-Cre/ER^{T2} (A). The goat anti-Ret antibody staining co-localized with Tuj1 staining (D, H, L) and with tdTomato fluorescent protein expression (H). In the presence of a blocking peptide for the goat anti-Ret antibody, the Ret staining was greatly diminished (J, L). These results demonstrate that the anti-Ret antibody selectively and specifically labels Ret^{+} neurons. Scale bar = 100μm.

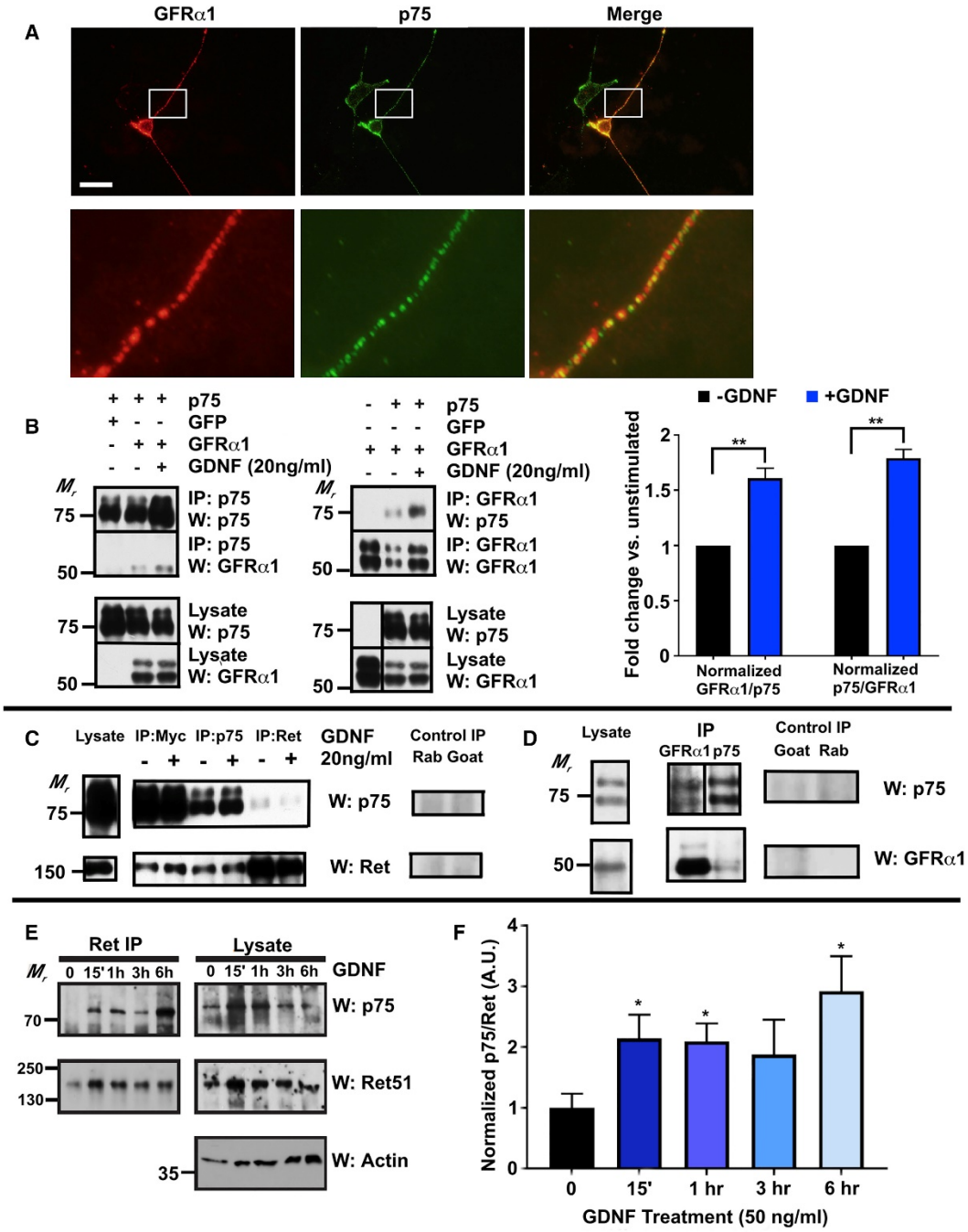

Figure 2.3. p75 forms a receptor complex with GFRα1 and Ret.

(A) Primary DRG neurons were cultured from P14 mice and immunostained with anti-GFRα1 and anti-p75 antibodies without fixation. Images in the second row are magnified regions from the rectangles from images in the first row. Scale bar, 100μm (only for the top panels). (B) Immunoprecipitation assay of HEK293 cells co-transfected with GFRα1 and p75. When GFRα1 and p75 are co-expressed in HEK293 cells, they can be co-immunoprecipitated with an anti-GFRα1 antibody or an anti-p75 antibody.

Quantification of the GFR□1 and p75 signals in co-IP experiments indicates GFR□1 and p75 association increased with GDNF treatments. (C) Immunoprecipitation assay of HEK-293 cells co-transfected with Ret and a myc tagged p75. Ret and p75 can be co-immunoprecipitated with a myc antibody, a rabbit p75 antibody or a goat Ret antibody. Treating the cells with GDNF did not increase the association between p75 and Ret. Normal rabbit (rab) or goat IgG was used as a negative control. (D) Immunoprecipitation assay of P1-2 SCG. GFRα1 can be co-immunoprecipitated with p75 using a rabbit anti-p75 antibody or a goat anti-GFRα1 antibody. Normal rabbit (rab) or goat IgG was used as control. (E) Primary DRG neurons were cultured from E18-P0 rats in the presence of 50 ng/ml NGF. After 7-10 DIV, the neurons were stimulated with medium alone or with GDNF for the indicated times. Ret receptor complexes were immunoprecipitated and immunoblotted for p75 (top panel; left), followed by Ret51 (middle; left). Lysates were immunoblotted for p75, Ret, and for actin (as a loading control). (F) Quantification of p75 co-immunoprecipitating with Ret at each timepoint.

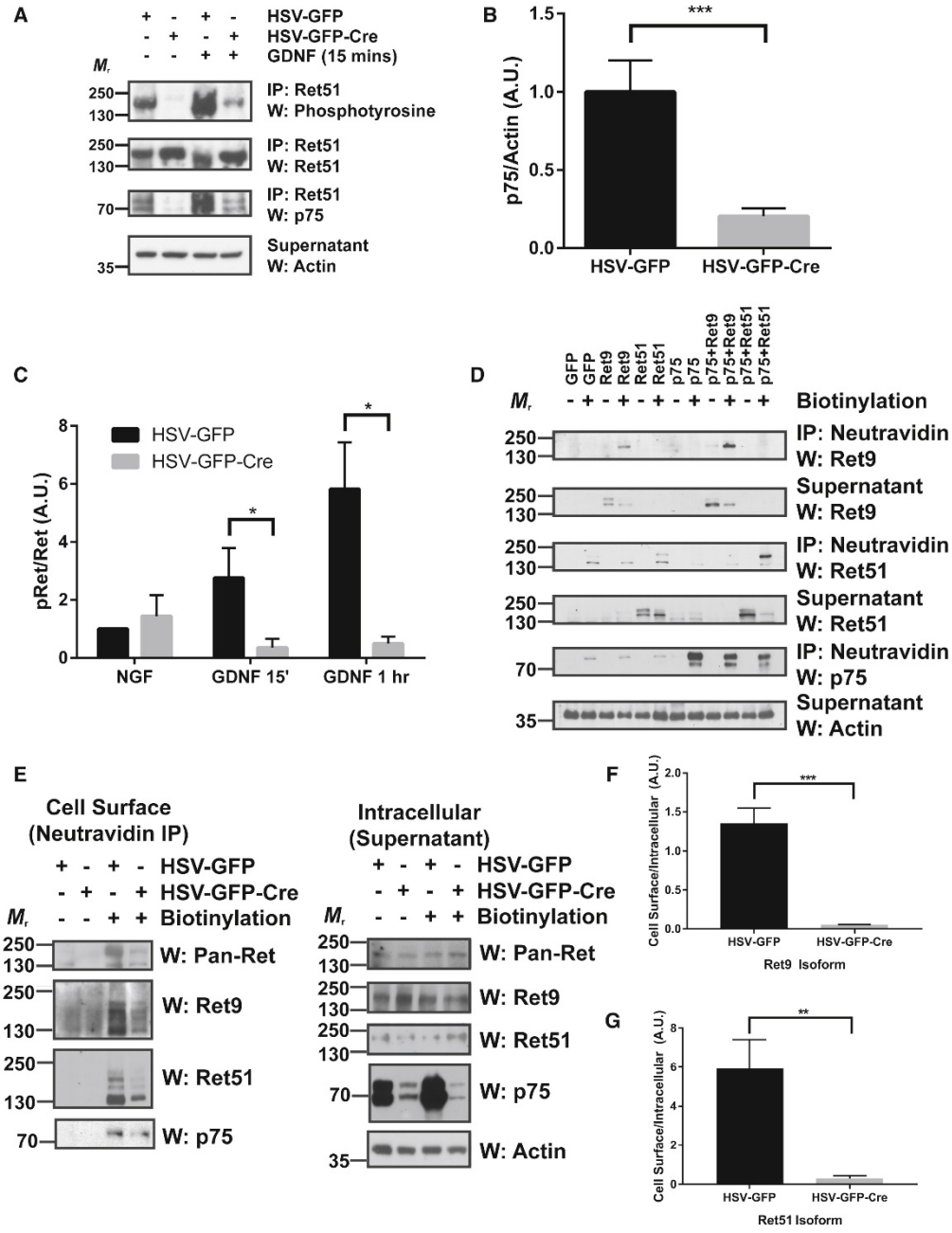

Figure 2.4. p75 augments GDNF-Ret signaling by increasing the cell surface localization of Ret

(A) DRG neurons were cultured from P0 *p75*$^{F/F}$ mice in the presence of 50 ng/ml NGF. After two days, neurons were exposed to HSV-GFP or HSV-GFP-Cre viruses overnight (indicated above the blots). Neurons were maintained in culture until 7 DIV, followed by stimulation with medium alone or with 50 ng/ml GDNF for 15 minutes or 1 hour. Ret was immunoprecipitated and its level of activation was determined by phosphotyrosine immunoblotting. p75 immunoblotting confirmed that p75 protein levels were substantially reduced upon Cre expression. Actin immunoblotting of the supernatants

served as a loading control. (B) Quantifications of p75 levels in 10 separate experiments demonstrate that approximately 80% of p75 is removed following treatment with HSV-GFP-Cre compared to HSV-GFP alone (*** $p < 0.001$). (C) Quantification of the mean proportion of phospho-Ret (pRet) over total Ret ± the standard error (5 experiments were quantified; * $p < 0.05$). (D) NIH/3T3 cells were transfected with GFP, Ret9, Ret51, p75, p75 and Ret9, or p75 and Ret51. After 24-36 hours, the cells were surface biotinylated using NHS-LC-Biotin in PBS (or treated with PBS alone as a control). The cells were then subjected to neutravidin precipitation. Precipitated cell surface proteins and supernatants (containing intracellular proteins) were then immunoblotted for Ret9, Ret51, and p75. Actin immunoblotting served as a loading control. (E) DRG neurons were cultured from P0 *p75*$^{F/F}$ mice and treated as described in A. Neurons were subsequently surface biotinylated as in D followed by neutravidin immunoprecipitation. Precipitated cell surface proteins (left) and supernatants (right; containing intracellular proteins) were analyzed by immunoblotting for pan-Ret (upper), Ret9 (2nd panel), and Ret51 (3rd panel). Actin immunoblotting served as a loading control. p75 immunoblotting confirmed efficient knockdown of greater than 70% of p75. (F) Quantifications of the cell surface levels of Ret9 (*** $p < 0.001$) and (G) Ret51 (** $p < 0.01$) indicate a highly significant difference in HSV-GFP-Cre treated neurons compared to HSV-GFP controls. *IP*, immunoprecipitation; *W*, western blot.

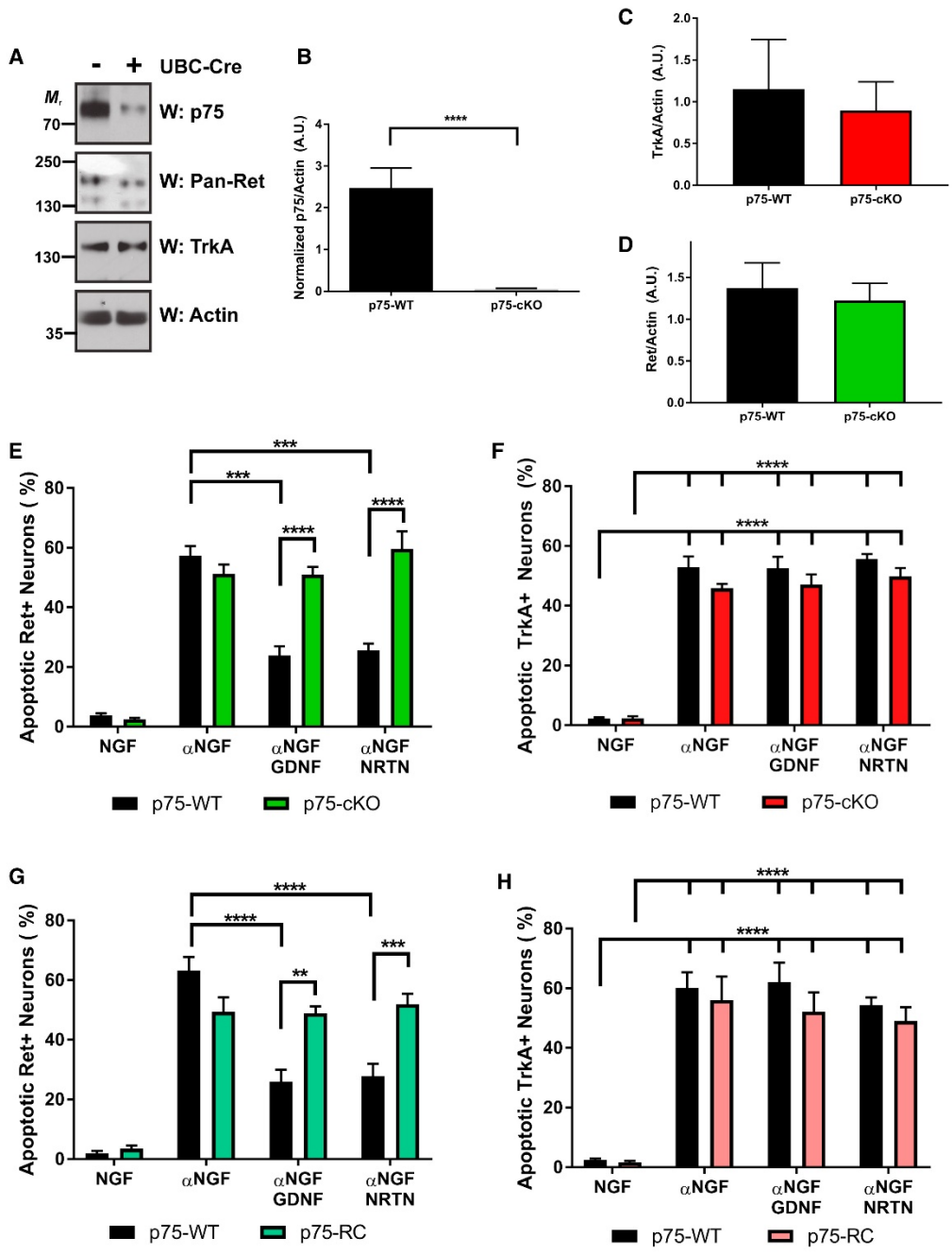

Figure 2.5. p75 mediated Ret-mediated survival of nonpeptidergic nociceptors *in vitro*

(A) Primary DRG neuron cultures were generated from P0 *p75*$^{F/F}$; UBC-Cre/ER^{T2} (p75-cKO) or *p75*$^{F/F}$ control mice (p75-WT) and maintained in the presence of 50 ng/ml NGF and 4-OH-TMX. 7 DIV neurons were lysed and immunoblotted for p75 (top panel) to confirm efficacy of deletion, pan-Ret, TrkA, and actin (as a loading control). (B) Quantification of normalized p75 levels indicated a highly significant reduction of p75 levels in p75-cKO neurons (n=10) compared to p75-WT neurons (n=8; **** $p < 0.0001$).

(C) No difference was observed in total levels of TrkA (n=5 p75-WT and n=7 p75-cKO; p = 0.6982) or (D) Ret protein levels (p=0.6737). (E, F) 7 DIV neurons were treated as described in A and subsequently treated with NGF, an anti-NGF blocking antibody (αNGF), αNGF with GDNF, or αNGF with NRTN (as indicated on the horizontal axis). 48 hours post-treatment, neurons were fixed and stained with Ret, TrkA, and DAPI (to determine nuclear pyknosis, indicating apoptosis) The number of apoptotic $Ret^{+}/TrkA^{-}$ (E) or $Ret^{-}/TrkA^{+}$ neurons (F) was quantified for each treatment group (n=5 for p75-WT and n=3 for p75-cKO for each condition), with all statistical differences noted. GDNF and NRTN treatment was sufficient to recue Ret^{+}, but not $TrkA^{+}$ neurons from apoptosis in p75-WT, but not p75-cKO neurons. (G, H) DRG neuron cultures were generated from P0 *p75*$^{F/F}$ (p75-WT) and *p75*$^{F/F}$; *Ret*-Cre/ER^{T2} (p75-RC) mice and treated, immunostained, and quantified as in E and F (treatments indicated on the horizontal axis). The number of apoptotic $Ret^{+}/TrkA^{-}$ (G) or $Ret^{-}/TrkA^{+}$ neurons (H) was quantified for each treatment group (n=6 for p75-WT and n=5 for p75-RC for each condition). Similar results were noted as in E and F, with GFL treatment able to selectively rescue Ret^{+} neurons from apoptosis in p75-WT, but not p75-RC neurons.

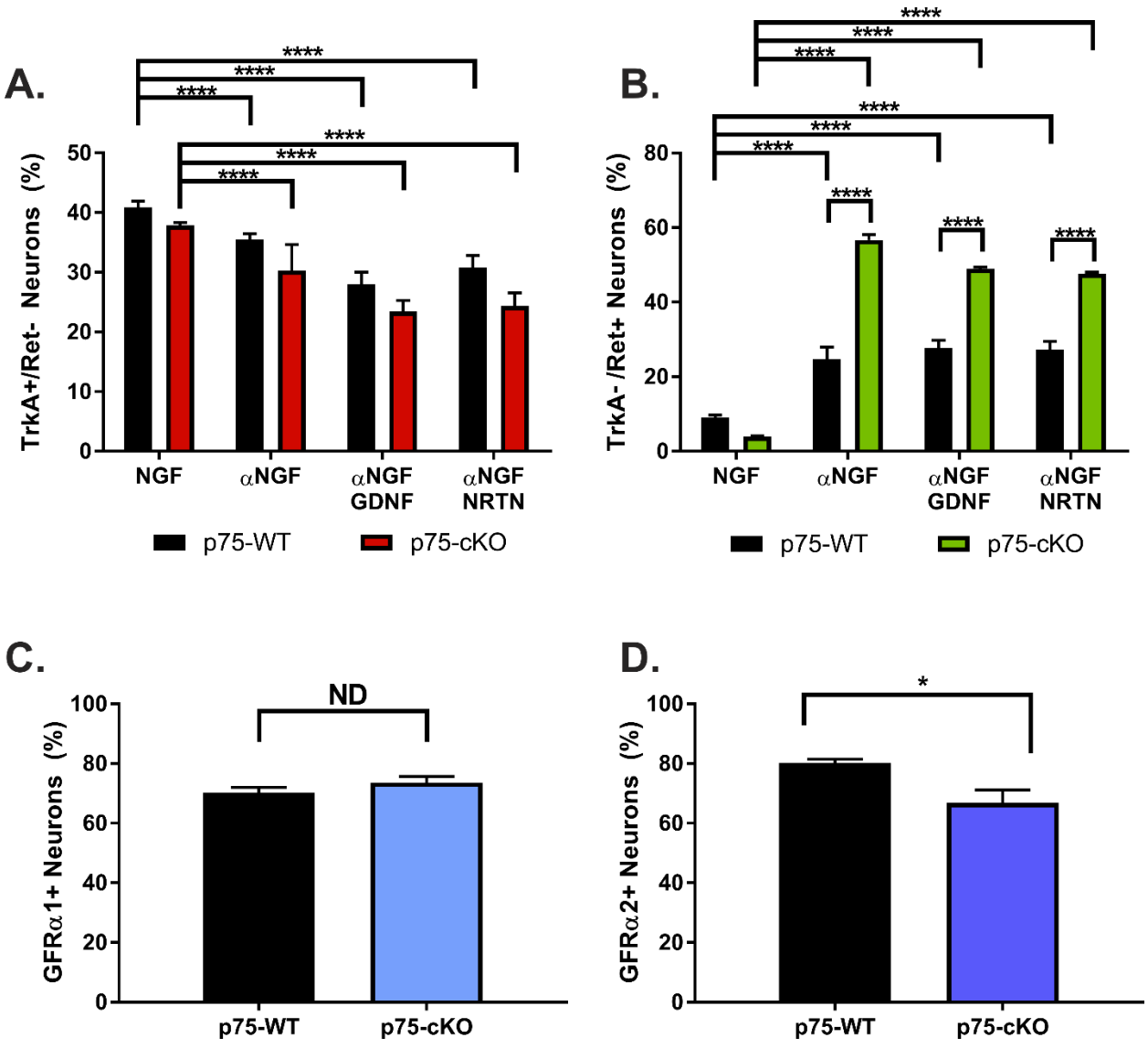

Figure 2.6. Characterization of neurotrophic factor receptor expression in p75-deleted DRG neurons *in vitro*.

(A, B) Primary DRG neuron cultures were generated from P0 *p75*$^{F/F}$ (p75-WT; n=5) and *p75*$^{F/F}$; UBC-Cre/ER^{T2} (p75-cKO; n=3) mice and subsequently maintained in the presence of 50 ng/ml NGF and 0.5 µg/ml 4-OH-TMX. To fully characterize how p75 deletion, NGF deprivation, and GFL treatments impacted TrkA and Ret expression, 7 DIV neurons were treated with NGF, an anti-NGF blocking antibody (αNGF), αNGF with GDNF, or αNGF with NRTN (as indicated on the horizontal axis). 48 hours post-treatment, neurons were fixed and stained with anti-Ret, anti-TrkA, and DAPI (to determine nuclear pyknosis, indicating apoptosis). (A) We observed a significant reduction in TrkA expression following NGF deprivation regardless of genotype. (B) NGF deprivation (regardless of GFL treatment) led to a significant increase in Ret expression. p75-cKO neurons had a significantly larger increase in Ret upregulation

compared to p75-WT neurons following NGF deprivation. (C, D) 7 DIV p75-WT and p75-cKO DRG neurons maintained in NGF and 4-OH-TMX (as described in A) were fixed, immunostained for TuJ1 and GFRα1 or GFRα2, and the number of $GFR\alpha1^{+}$ (C) or $GFR\alpha2^{+}$ (D) neurons was quantified. While no significant differences were observed for GFRα1 ($p = 0.2723$), a small but statistically significant reduction in the number of $GFR\alpha2^{+}$ neurons ($p = 0.103$) was observed in p75-cKO neurons compared to p75-WT neurons.

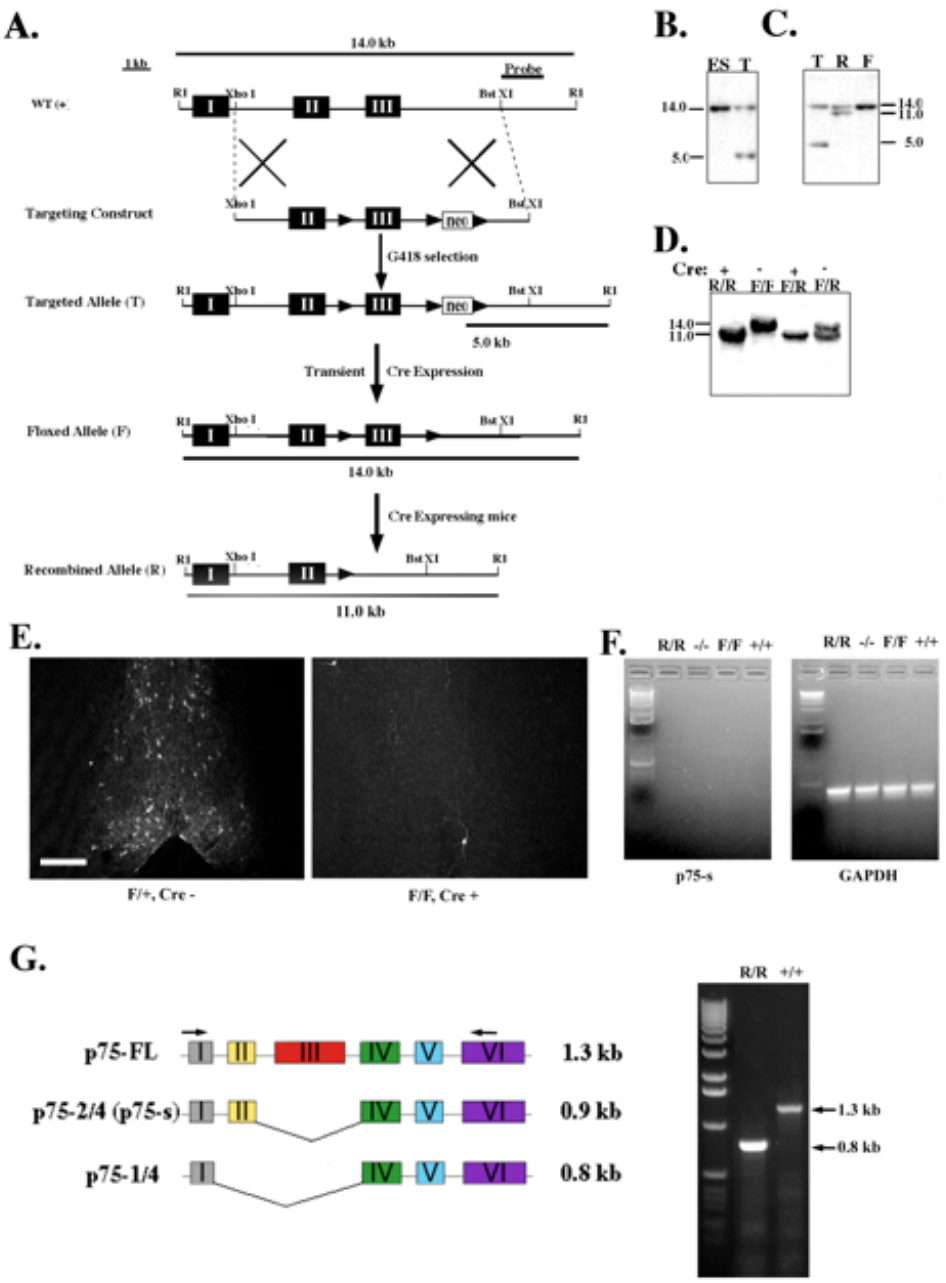

Figure 2.7. Generation of the p75 floxed (*p75*$^{F/F}$) mice

(A) Diagram of the strategy in generating the floxed p75 allele. The targeting vector was constructed by introducing a lox P site into an EcoR V site in intron 2 and a neomycin resistance marker (neo) flanked by loxP sites was introduced into an Xba I site in intron 3. The targeting construct was electroporated into ES cells and selected with antibiotic G418. G418 resistant ES cell clones were screened by Southern blotting analysis. When the DNA was digested with EcoR I, the probe hybridized to a 5.0 kb band for the T allele and a 14.0 kb band for the wild type allele (+) (Panel B). ES cell clones

containing the targeted (T) allele were isolated and transfected with plasmids expressing Cre recombinase under the control of the CMV promoter. ES cell clones in which the neo^r-cassette was removed but maintained two LoxP sites were isolated. This is called the floxed (F) allele. In the recombined allele (R), the neo^r-cassette and the third exon are removed and only one LoxP site is retained (Panel C). (D) P75 floxed animals were crossed with a line of nestin-Cre transgenic mice. Brain DNA was isolated from P0 mice, digested with EcoR I and hybridized with the probe. Nearly complete recombination occurred in mice containing floxed alleles and the nestin-Cre transgene (F/R; Cre +). Because the nestin-Cre transgenic mice used in this experiment have leaky Cre expression in the germ cells, germline recombination of the floxed allele can occur. Germline recombination only one allele (R) occurs in mice whose parents carry a floxed allele and the nestin-Cre transgene, even if they no longer express Cre (F/R; Cre -). No recombination of the floxed allele occurs in the absence of Cre expression (F/F; Cre -). (E) Immunofluorescence staining of coronal sections of the septum with anti-p75 antibodies revealed that no p75 proteins are detected in mice containing the floxed allele and the nestin-Cre transgene (F/F, Cre +). (F) To test if p75-s transcripts (spliced product of exon II to exon IV) described by von Schack *et al*. (von Schack et al., 2001) are present in the conditional mutant animals, reverse transcription coupled-PCR (RT-PCR) was used to assay the mRNA isolated from mice containing recombined alleles (R/R), alleles with neo-casset insertions into exon III of original p75 mutants (-/-) (Lee et al., 1992b), floxed alleles (F/F) or wild type alleles (+/+). No p75-s transcripts were detected using primers and PCR conditions previously described by von Shack *et al.* (von Schack et al., 2001). Because the 5' primer used by von Shack *et al*. is consisted of two 10-neucleotides complimentary to the end of exon II and the beginning of exon IV, respectively, the primer presumably only detected the spliced product of exon II to exon IV. However, we found that the primer set used by von Shack *et al*. was able to detect any transcripts containing axon IV, including the full-length cDNA. Although we do not know the basis for the lack of specificity, we noticed that the primer set is highly GC-rich. It is worth mentioning that Paul *et al*. demonstrated that the mutated p75 allele created by von Shack *et al.* gave rise to an alternatively spiced transcript (Paul et al., 2004), but not in the p75 mutants we generated previously. Over-expression of this spliced product increases cell death (Paul et al., 2004) and may contribute to the phenotype observed in that line of mutant mice. **(G)** To further test if p75-s splice variant exists in the conditional p75 mutation animals, RT-PCR was used to analyze mRNA isolated from controls (+/+) and the mice with recombinant alleles (R/R) using primers from exons I and VI that encompass the full-length mRNA sequence. The full-length p75 transcript (p75-FL) will give rise to PCR products with the size of 1.3 kb. The p75-s transcript (p75-s, p75-2/4) will yield PCR products with the size of 0.9 kb. No 0.9 kb product was detectable. Instead, a 0.8 kb alternative splice variant was present. DNA sequencing of this 0.8 kb product revealed that this variant is a result of RNA splicing from exon I to exon IV (p75-1/4). Importantly, this splice variant is out of reading frame and thus will not produce functional proteins. Taken together, these results indicate that the recombined allele (R) does not generate transcripts that produce functional p75 proteins.

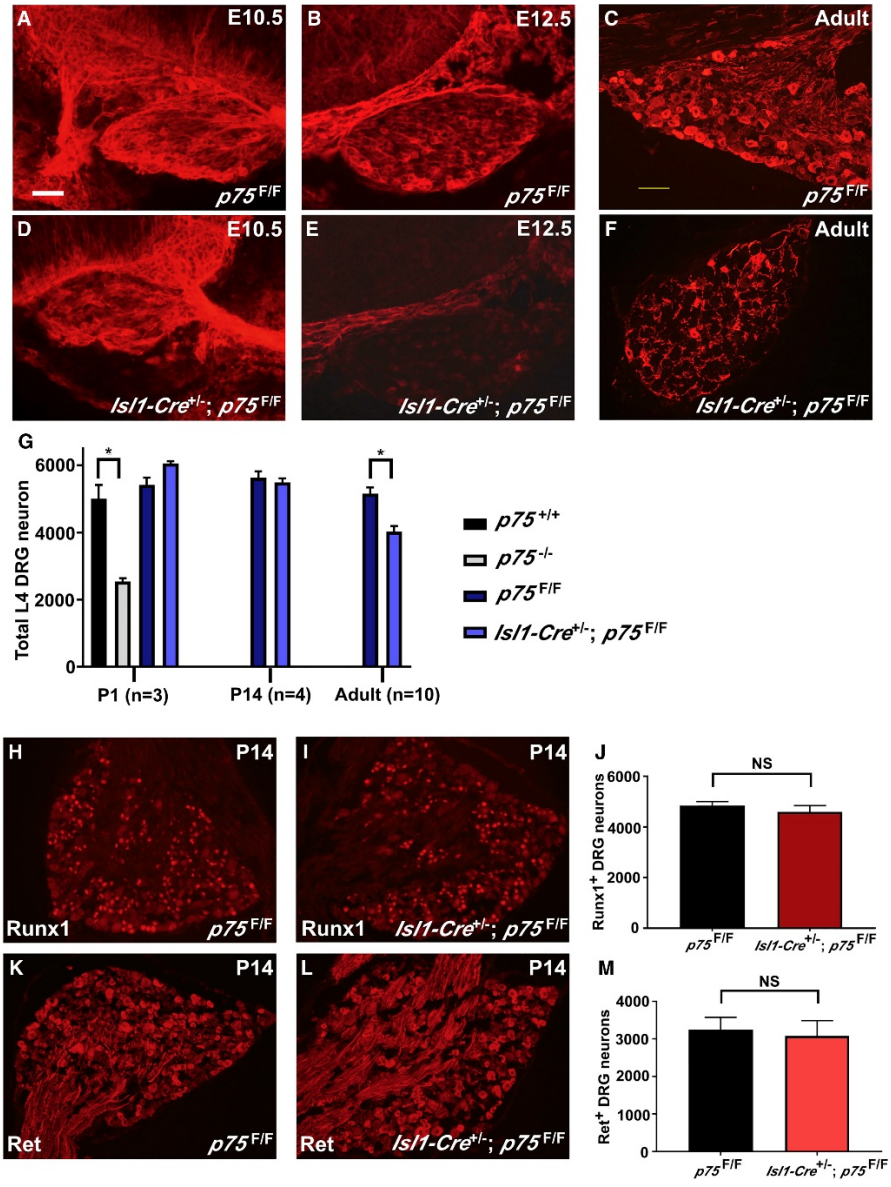

Figure 2.8. *Isl1-Cre*$^{+/-}$; *p75*$^{F/F}$ mice lose 20% of DRG neurons

(A-F) p75 immunofluorescence staining of DRG sections from E10.5, E12.5 and adult *p75*$^{F/F}$ and *Isl1-Cre*$^{+/-}$; *p75*$^{F/F}$ mice is shown in A-F. As shown in panel D, p75 immunoreactivity in DRG sensory neurons is not reduced at E10.5 in *Isl1-Cre*$^{+/-}$; *p75*$^{F/F}$ mice. However, the number of p75-immunoreactive neurons is markedly reduced in E12.5 (panel E) and adult animals (panel F). The immunoreactivity observed in adult DRG is likely coming predominantly from satellite cells, which normally express p75. Scale bar, 100μm. (G) Total neuron numbers in L4 DRGs from *p75*$^{F/F}$ mice were

compared to *Isl1-Cre*$^{+/-}$; *p75*$^{F/F}$ mice at different postnatal ages. Adult *Isl1-Cre*$^{+/-}$; *p75*$^{F/F}$ mice lose approximately 20% of DRG neurons. In contrast, p75$^{-/-}$ mice lose 50% of DRG neurons at P1 (* $p < 0.05$). At p14, Runx1 expression in *p75*$^{F/F}$ mice (H) is similar to *Isl1-Cre*$^{+/-}$; *p75*$^{F/F}$ mice (I). The Ret expression level is also not changed between *p75*$^{F/F}$ (K) and *Isl1-Cre*$^{+/-}$; *p75*$^{F/F}$ (L) mice. There is no change in the number of Runx1^{+} neurons (J) or Ret^{+} neurons (M) at p14 in *Isl1-cre*$^{+/-}$; *p75*$^{F/F}$ mice compared to *p75*$^{F/F}$ mice (n=3).

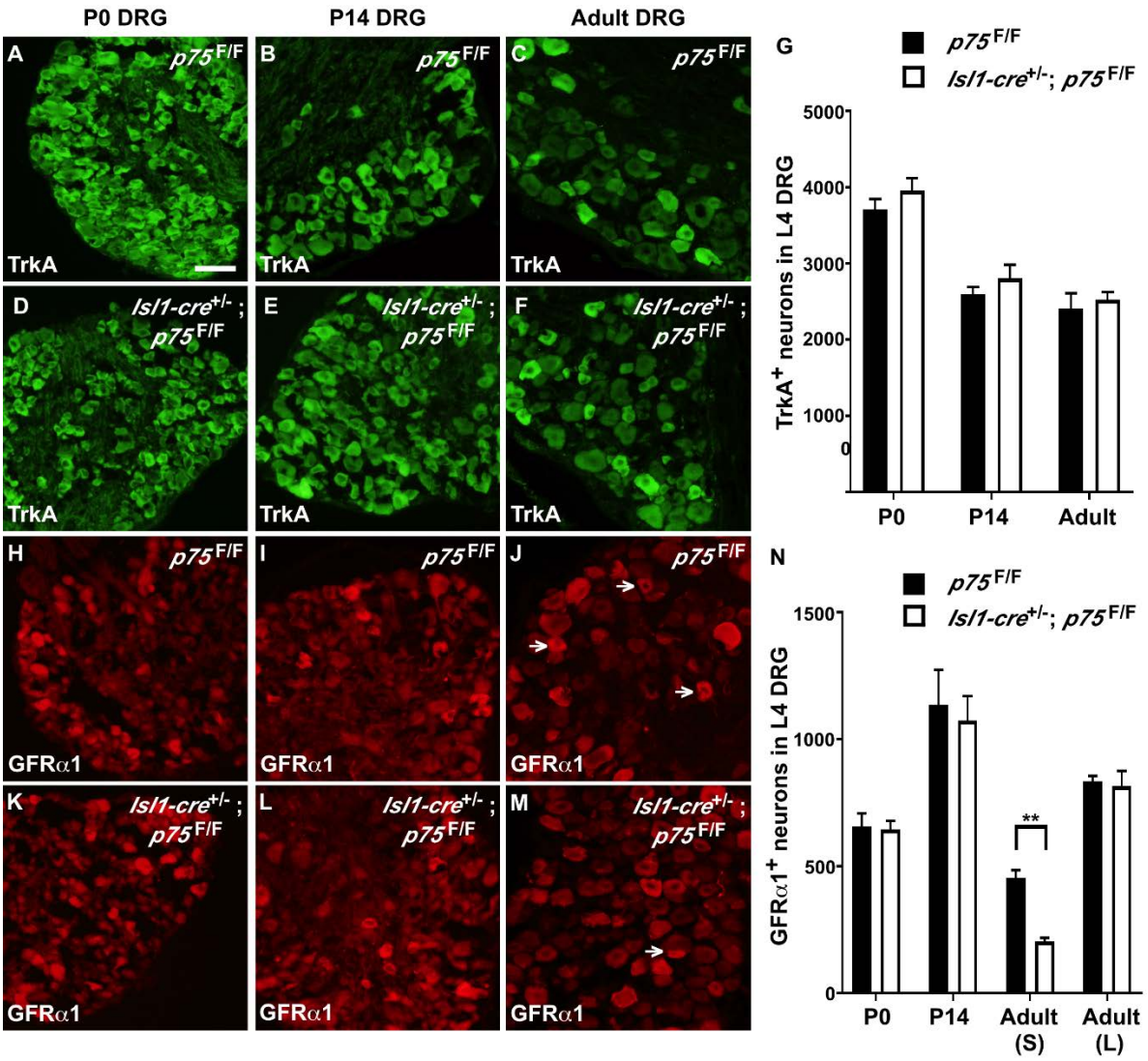

Figure 2.9. Level of TrkA and, GFRα1 expression at P1, p14 and adult DRG

P0, P14, and adult lumbar DRGs from *p75*$^{F/F}$ and *Isl1*-Cre$^{+/-}$; *p75*$^{F/F}$ mice are sectioned and stained with an anti-TrkA and an antiGFRα1 antibody. All images were taken using the same exposure. For TrkA, at P0 (panel A, D), P14 (panel B, E) and adult (panel C, F) stages, no gross differences in immunofluorescence staining were observed between *p75*$^{F/F}$ (panel A, B and C) and *Isl1*-Cre$^{+/-}$; *p75*$^{F/F}$ (panel D, E and F) mice. Quantitation of TrkA+ neurons indicates that there is no difference between *p75*$^{F/F}$ and *Isl1*-Cre$^{+/-}$; *p75*$^{F/F}$ mice for all stages analyzed (panel G). For GFRα1, at P0 (panel H, K), P14 (panel I, L) and adult (panel J, M) stages, no gross difference in immunofluorescence staining was observed between *p75*$^{F/F}$ (panel H, I and J) and *Isl1*-Cre$^{+/-}$; *p75*$^{F/F}$ (panel K, L and M) mice. Quantitation of GFRα1+ neurons indicates that there is no difference between *p75*$^{F/F}$ and *Isl1*-Cre$^{+/-}$; *p75*$^{F/F}$ mice at P0 and P14 ages. In adult DRG there is a significant reduction in small diameter GFRα1+ neurons in *Isl1*-Cre$^{+/-}$; *p75*$^{F/F}$ mice, however, the large diameter GFRa1+ neurons are unchanged (panel N). Scale bar: 100µm. Arrows indicate small diameter GFRa1+ neurons. For panel G and N, value is expressed as mean ± SEM, n=3 for all data points. ** $p<0.01$

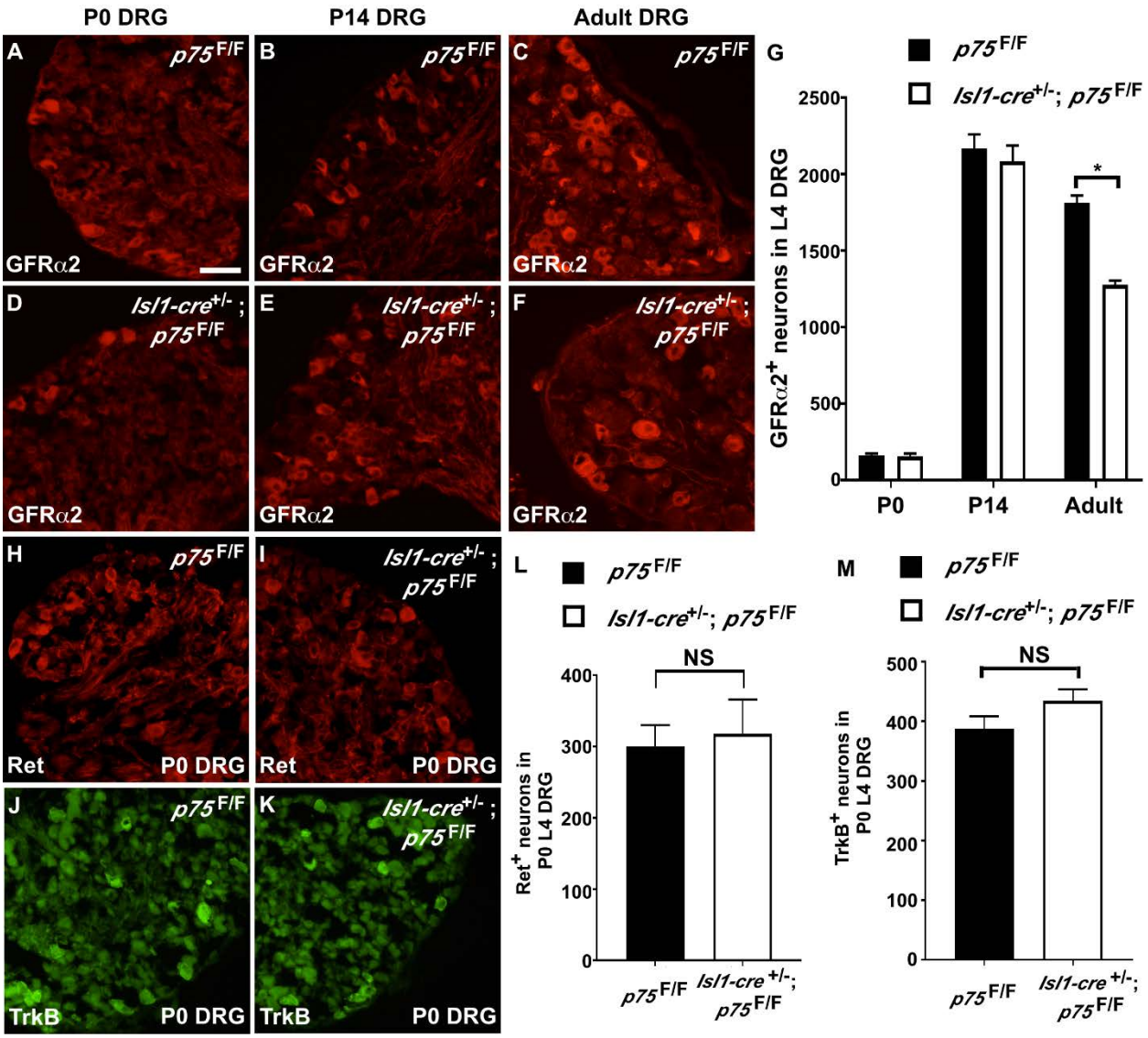

Figure 2.10. Level of GFRα2, Ret and TrkB expression at P0, p14 and adult DRG

P0, P14, and adult lumbar DRGs from *p75*$^{F/F}$ and *Isl1*-Cre$^{+/-}$; *p75*$^{F/F}$ mice are sectioned and stained with an anti-GFRα2 antibody. P0 lumbar DRGs from *p75*$^{F/F}$ and *Isl1*-Cre$^{+/-}$; *p75*$^{F/F}$ mice are sectioned and stained with an anti-Ret or anti-TrkB antibody. All images were taken using the same exposure. For GFRα2, At P0 (panel A, D), P14 (panel B, E) and adult (panel C, F) stages, no gross difference in immunofluorescence staining was observed between *p75*$^{F/F}$ (panel A, B and C) and *Isl1*-Cre$^{+/-}$; *p75*$^{F/F}$ (panel D, E and F) mice. Quantitation of GFRα2+ neurons indicates that, at P0 and P14 ages, there is no difference between *p75*$^{F/F}$ and *Isl1*-Cre$^{+/-}$; *p75*$^{F/F}$ mice. In adult DRG there is a ~30% decrease in the *Isl1*-Cre$^{+/-}$; *p75*$^{F/F}$ mice, which correlates with the loss of IB4+ neurons and the Ret+ /peripherin+ neurons (panel G). For Ret, there is no gross difference in immunofluorescence staining between *p75*$^{F/F}$ (panel H) and *Isl1*-Cre$^{+/-}$; *p75*$^{F/F}$ (panel I) mice at P0. Quantitation of Ret+ neurons indicates there is no difference between *p75*$^{F/F}$

and *Isl1*-Cre$^{+/-}$; *p75*$^{F/F}$ mice at P0 (panel L). For TrkB, there is no gross difference in immunofluorescence staining between *p75*$^{F/F}$ (panel J) and *Isl1*-Cre$^{+/-}$; *p75*$^{F/F}$ (panel K) mice at P0. Quantitation of TrkB+ neurons indicates there is no difference between *p75*$^{F/F}$ and *Isl1*-Cre$^{+/-}$; *p75*$^{F/F}$ mice at P0 (panel M). Scale bar: 100μm. For panel G, L, M, value is expressed as mean ± SEM, n=3 for all data points. * $p < 0.05$. NS, no statistical difference.

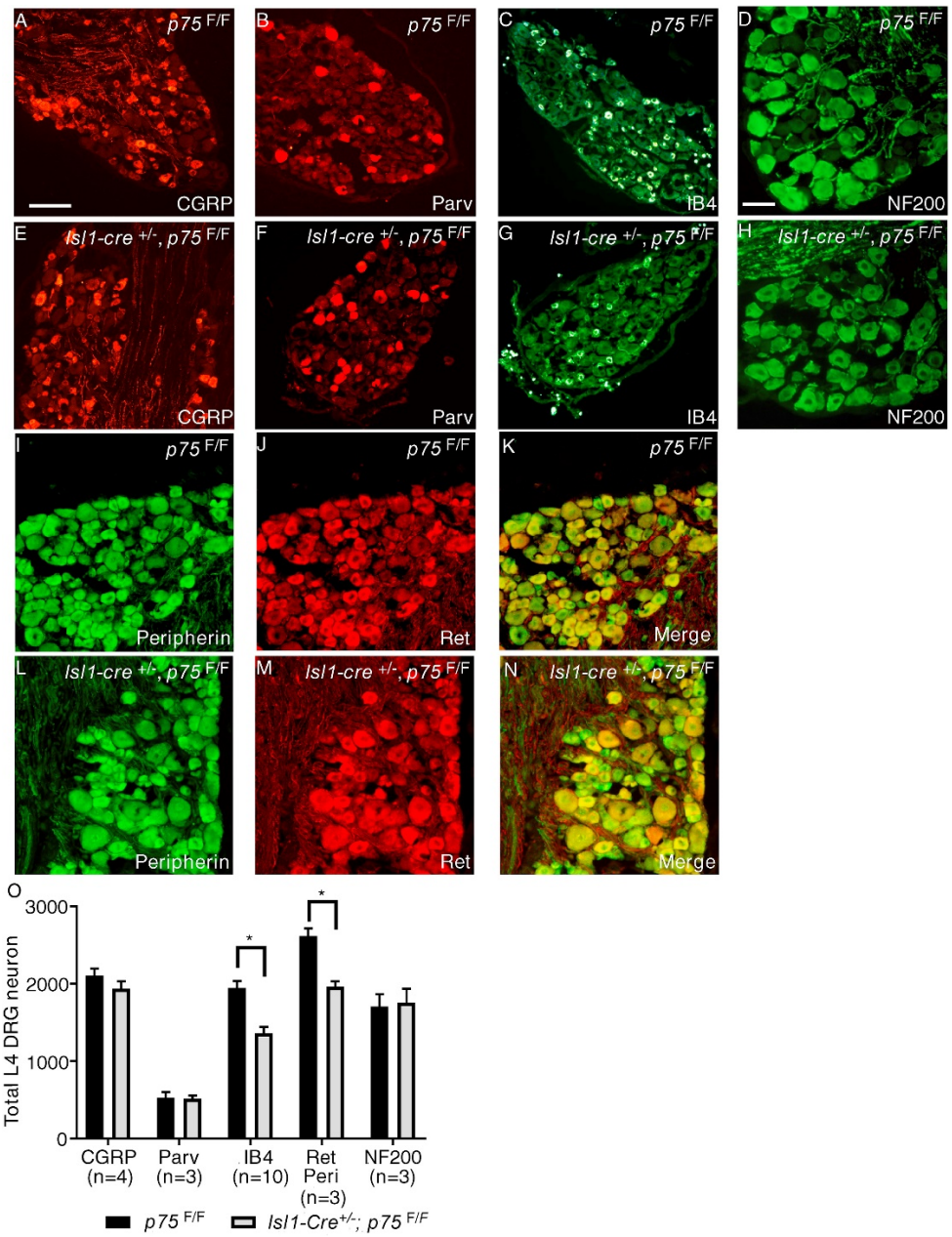

Figure 2.11. IB4^{+} nonpeptidergic nociceptors are selectively lost in *Isl1-Cre*$^{+/-}$; *p75*$^{F/F}$ mice

(A-N) Immunofluorescence staining of adult L4 DRG with anti-CGRP (panel A and E), anti-Parvalbumin (panel B and F), anti-NF200 (panel D and H) antibody, IB4 (panel C and G) or a combination of anti-peripherin (I, L) and anti-Ret (J, M) antibodies from *p75*$^{F/F}$ (panel A-D, I-K) and *Isl1-Cre*$^{+/-}$; *p75*$^{F/F}$ (panel E-H, L-N) mice. Scale bar for A-C, E-G, 200μm (located in panel A), Scale bar for D, H-N 100μm (located in panel D). (O) The quantification of CGRP^{+}, Parvalbumin^{+}, IB4^{+}, Peripherin^{+}/Ret^{+} and NF200^{+} neurons in adult L4 DRGs from *p75*$^{F/F}$ and *Isl1-Cre*$^{+/-}$; *p75*$^{F/F}$ mice. Only the IB4^{+} and Peripherin^{+}/Ret^{+} neurons were significantly reduced in the *Isl1-Cre*$^{+/-}$; *p75*$^{F/F}$ mice.

Values are expressed as mean ± SEM, * $p<0.05$. N indicates the number of animals being counted (each animal provides two DRGs).

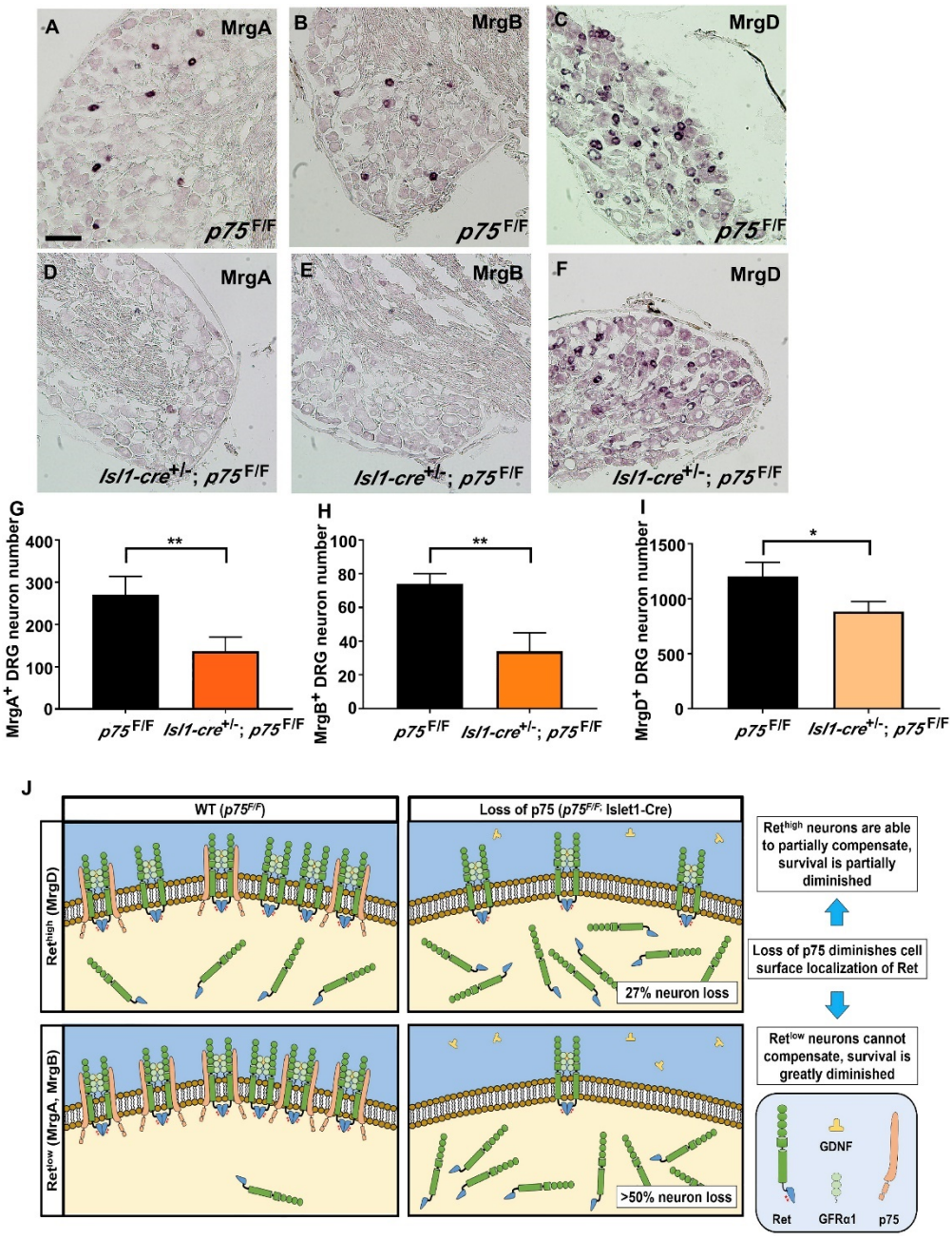

Figure 2.12. Nonpeptidergic neuron deficits in *Isl1-Cre*$^{+/-}$; *p75*$^{F/F}$ mice correlates with level of p75-Ret co-expression

In situ hybridization of adult (6 months old) L4 DRG with MrgA (panel A and D), MrgB (panel B and E) and MrgD (panel C and F) *in situ* probes from *p75*$^{F/F}$ mice (panel A-C) and *Isl1-Cre*$^{+/-}$; *p75*$^{F/F}$ (panel D-F). Scale bar, 100μm. Quantification of MrgA^{+} (panel G), MrgB^{+} (panel H) and MrgD^{+} (panel I) neurons showed that in *Isl1-Cre*$^{+/-}$; *p75*$^{F/F}$ mice, over 50% of MrgA^{+} and MrgB^{+} neurons were lost, while approximately 20% of MrgD^{+} neurons were lost. Importantly, MrgA^{+} and MrgB^{+} neurons were shown to express low level of Ret while MrgD^{+} neurons express high level of Ret. The value is expressed as

mean ± SEM (n=3 for each data point, * $p<0.05$, ** $p<0.01$). (J) The expression of p75 increases the level of Ret on the cell surface in *p75*$^{F/F}$ mice and potentiates GFL-induced Ret phosphorylation and its downstream survival effects. When p75 expression is lost in *Isl1-Cre*$^{+/-}$; *p75*$^{F/F}$ mice, the level of Ret on the cell surface is reduced. For neurons that express high levels of Ret (MrgD^{+}), the high level of Ret expression may compensate for the loss of p75 and results in more modest deficits. In neurons that express low levels of Ret (MrgA^{+} and MrgB^{+}), however, the loss of Ret on the cell surface cannot be compensated for, leading to substantial cell loss.

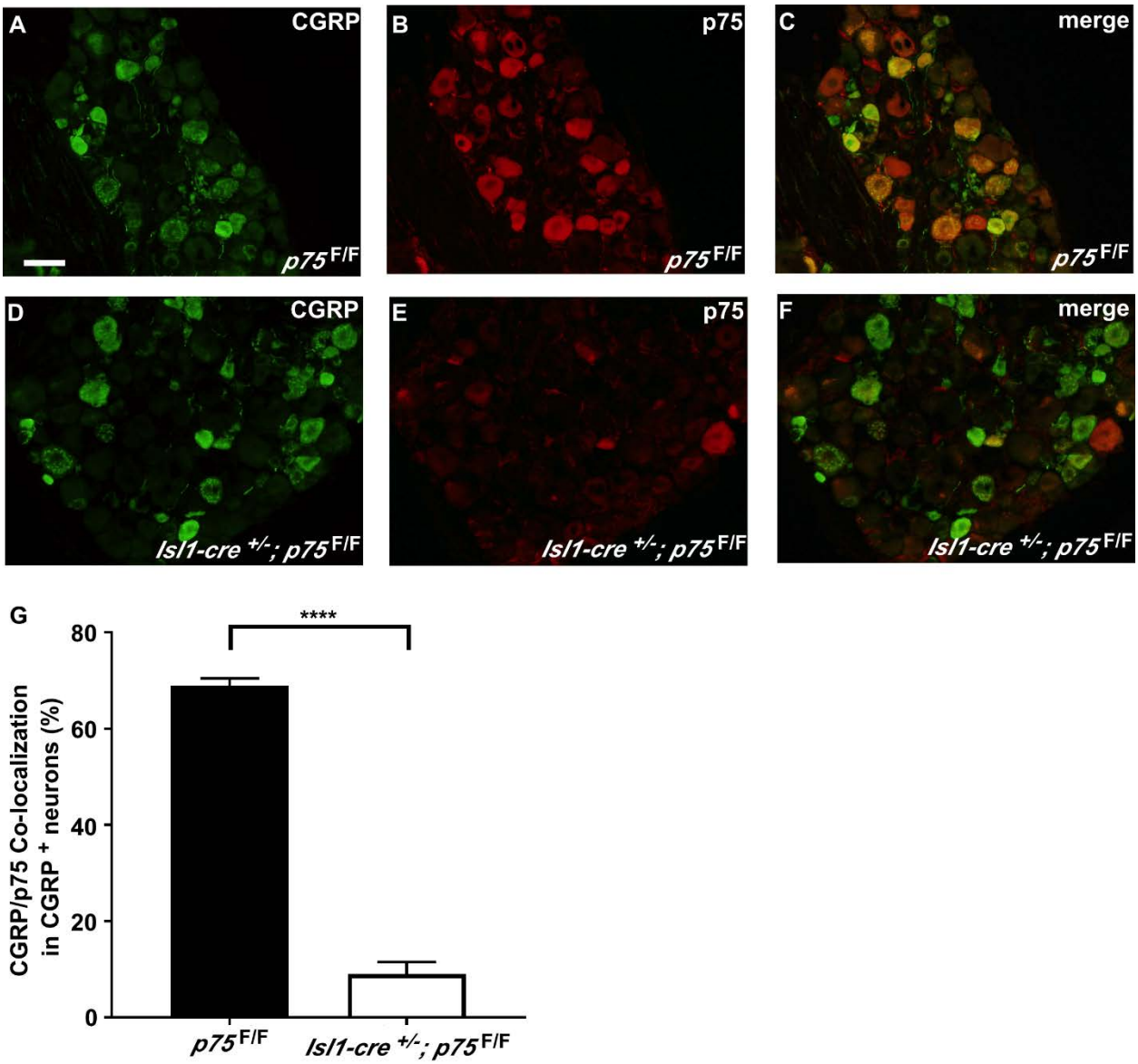

Figure 2.13. p75 is effectively deleted from the CGRP+ neurons in Isl1-Cre$^{+/-}$; *p75*$^{F/F}$ mice

Immunofluorescent staining of adult L4 DRG with anti-CGRP (panel A, D,) or anti-p75 (panel B, E) from *p75*$^{F/F}$ mice (panel A, B, C) and *Isl1*-Cre$^{+/-}$; *p75*$^{F/F}$ mice (Panel D, E, F). Panel C is a merged image of panel A and B; panel F is a merged image of panel D and E. Scale bar: 200μm. G. Quantification of the percentage of p75^{+}/CGRP^{+} dual-labeled neurons. In Isl1-cre$^{+/-}$; p75$^{F/F}$ mice, p75 expression is effectively removed from the vast majority of CGRP^{+} neurons. Value is expressed as mean ± SEM, n=3 for each data point. **** P<0.0001.

Chapter 2 References

Airaksinen, M.S., and Saarma, M. (2002). The GDNF family: signalling, biological functions and therapeutic value. Nat Rev Neurosci *3*, 383-394.

Bentley, C.A., and Lee, K.F. (2000). p75 is important for axon growth and schwann cell migration during development. J Neurosci *20*, 7706-7715.

Bogenmann, E., Thomas, P.S., Li, Q., Kim, J., Yang, L.T., Pierchala, B., and Kaartinen, V. (2011). Generation of mice with a conditional allele for the p75(NTR) neurotrophin receptor gene. Genesis *49*, 862-869.

Bourane, S., Garces, A., Venteo, S., Pattyn, A., Hubert, T., Fichard, A., Puech, S., Boukhaddaoui, H., Baudet, C., Takahashi, S.*, et al.* (2009). Low-threshold mechanoreceptor subtypes selectively express MafA and are specified by Ret signaling. Neuron *64*, 857-870.

Ceni, C., Unsain, N., Zeinieh, M.P., and Barker, P.A. (2014). Neurotrophins in the regulation of cellular survival and death. Handb Exp Pharmacol *220*, 193-221.

Chen, C.L., Broom, D.C., Liu, Y., de Nooij, J.C., Li, Z., Cen, C., Samad, O.A., Jessell, T.M., Woolf, C.J., and Ma, Q. (2006). Runx1 determines nociceptive sensory neuron phenotype and is required for thermal and neuropathic pain. Neuron *49*, 365-377.

Crowley, C., Spencer, S.D., Nishimura, M.C., Chen, K.S., Pitts-Meek, S., Armanini, M.P., Ling, L.H., McMahon, S.B., Shelton, D.L., Levinson, A.D.*, et al.* (1994). Mice lacking nerve growth factor display perinatal loss of sensory and sympathetic neurons yet develop basal forebrain cholinergic neurons. Cell *76*, 1001-1011.

Davies, A.M., Lee, K.F., and Jaenisch, R. (1993). p75-deficient trigeminal sensory neurons have an altered response to NGF but not to other neurotrophins. Neuron *11*, 565-574.

Dong, X., Han, S., Zylka, M.J., Simon, M.I., and Anderson, D.J. (2001). A diverse family of GPCRs expressed in specific subsets of nociceptive sensory neurons. Cell *106*, 619-632.

Ernfors, P., Lee, K.F., Kucera, J., and Jaenisch, R. (1994). Lack of neurotrophin-3 leads to deficiencies in the peripheral nervous system and loss of limb proprioceptive afferents. Cell *77*, 503-512.

Ernsberger, U. (2008). The role of GDNF family ligand signalling in the differentiation of sympathetic and dorsal root ganglion neurons. Cell Tissue Res *333*, 353-371.

Esposito, D., Patel, P., Stephens, R.M., Perez, P., Chao, M.V., Kaplan, D.R., and Hempstead, B.L. (2001). The cytoplasmic and transmembrane domains of the p75 and Trk A receptors regulate high affinity binding to nerve growth factor. J Biol Chem *276*, 32687-32695.

Franck, M.C., Stenqvist, A., Li, L., Hao, J., Usoskin, D., Xu, X., Wiesenfeld-Hallin, Z., and Ernfors, P. (2011). Essential role of Ret for defining non-peptidergic nociceptor phenotypes and functions in the adult mouse. Eur J Neurosci *33*, 1385-1400.

Golden, J.P., Hoshi, M., Nassar, M.A., Enomoto, H., Wood, J.N., Milbrandt, J., Gereau, R.W.t., Johnson, E.M., Jr., and Jain, S. (2010). RET signaling is required for survival and normal function of nonpeptidergic nociceptors. The Journal of neuroscience : the official journal of the Society for Neuroscience *30*, 3983-3994.

Han, L., Ma, C., Liu, Q., Weng, H.J., Cui, Y., Tang, Z., Kim, Y., Nie, H., Qu, L., Patel, K.N.*, et al.* (2013). A subpopulation of nociceptors specifically linked to itch. Nat Neurosci *16*, 174-182.

Hempstead, B.L., Martin-Zanca, D., Kaplan, D.R., Parada, L.F., and Chao, M.V. (1991). High-affinity NGF binding requires coexpression of the trk proto-oncogene and the low-affinity NGF receptor. Nature *350*, 678-683.

Inoue, K., Ito, K., Osato, M., Lee, B., Bae, S.C., and Ito, Y. (2007). The transcription factor Runx3 represses the neurotrophin receptor TrkB during lineage commitment of dorsal root ganglion neurons. J Biol Chem *282*, 24175-24184.

Jones, K.R., Farinas, I., Backus, C., and Reichardt, L.F. (1994). Targeted disruption of the BDNF gene perturbs brain and sensory neuron development but not motor neuron development. Cell *76*, 989-999.

Klein, R., Smeyne, R.J., Wurst, W., Long, L.K., Auerbach, B.A., Joyner, A.L., and Barbacid, M. (1993). Targeted disruption of the trkB neurotrophin receptor gene results in nervous system lesions and neonatal death. Cell *75*, 113-122.

Kramer, I., Sigrist, M., de Nooij, J.C., Taniuchi, I., Jessell, T.M., and Arber, S. (2006). A role for Runx transcription factor signaling in dorsal root ganglion sensory neuron diversification. Neuron *49*, 379-393.

Lee, K.F., Davies, A.M., and Jaenisch, R. (1994). p75-deficient embryonic dorsal root sensory and neonatal sympathetic neurons display a decreased sensitivity to NGF. Development *120*, 1027-1033.

Lee, K.F., Li, E., Huber, L.J., Landis, S.C., Sharpe, A.H., Chao, M.V., and Jaenisch, R. (1992). Targeted mutation of the gene encoding the low affinity NGF receptor p75 leads to deficits in the peripheral sensory nervous system. Cell *69*, 737-749.

Lindfors, P.H., Voikar, V., Rossi, J., and Airaksinen, M.S. (2006). Deficient nonpeptidergic epidermis innervation and reduced inflammatory pain in glial cell line-derived neurotrophic factor family receptor alpha2 knock-out mice. J Neurosci *26*, 1953-1960.

Liu, Q., Sikand, P., Ma, C., Tang, Z., Han, L., Li, Z., Sun, S., LaMotte, R.H., and Dong, X. (2012). Mechanisms of itch evoked by beta-alanine. J Neurosci *32*, 14532-14537.

Liu, Q., Vrontou, S., Rice, F.L., Zylka, M.J., Dong, X., and Anderson, D.J. (2007). Molecular genetic visualization of a rare subset of unmyelinated sensory neurons that may detect gentle touch. Nat Neurosci *10*, 946-948.

Liu, Y., and Ma, Q. (2011). Generation of somatic sensory neuron diversity and implications on sensory coding. Current opinion in neurobiology *21*, 52-60.

Liu, Y., Yang, F.C., Okuda, T., Dong, X., Zylka, M.J., Chen, C.L., Anderson, D.J., Kuner, R., and Ma, Q. (2008). Mechanisms of compartmentalized expression of Mrg class G-protein-coupled sensory receptors. J Neurosci *28*, 125-132.

Luo, W., Enomoto, H., Rice, F.L., Milbrandt, J., and Ginty, D.D. (2009). Molecular identification of rapidly adapting mechanoreceptors and their developmental dependence on ret signaling. Neuron *64*, 841-856.

Luo, W., Wickramasinghe, S.R., Savitt, J.M., Griffin, J.W., Dawson, T.M., and Ginty, D.D. (2007). A hierarchical NGF signaling cascade controls Ret-dependent and Ret-

independent events during development of nonpeptidergic DRG neurons. Neuron *54*, 739-754.

Makkerh, J.P., Ceni, C., Auld, D.S., Vaillancourt, F., Dorval, G., and Barker, P.A. (2005). p75 neurotrophin receptor reduces ligand-induced Trk receptor ubiquitination and delays Trk receptor internalization and degradation. EMBO Rep *6*, 936-941.

Marmigere, F., and Ernfors, P. (2007). Specification and connectivity of neuronal subtypes in the sensory lineage. Nature reviews Neuroscience *8*, 114-127.

Molliver, D.C., Wright, D.E., Leitner, M.L., Parsadanian, A.S., Doster, K., Wen, D., Yan, Q., and Snider, W.D. (1997). IB4-binding DRG neurons switch from NGF to GDNF dependence in early postnatal life. Neuron *19*, 849-861.

Murray, S.S., Bartlett, P.F., and Cheema, S.S. (1999). Differential loss of spinal sensory but not motor neurons in the p75NTR knockout mouse. Neurosci Lett *267*, 45-48.

Ruzankina, Y., Pinzon-Guzman, C., Asare, A., Ong, T., Pontano, L., Cotsarelis, G., Zediak, V.P., Velez, M., Bhandoola, A., and Brown, E.J. (2007). Deletion of the developmentally essential gene ATR in adult mice leads to age-related phenotypes and stem cell loss. Cell stem cell *1*, 113-126.

Scott, A., Hasegawa, H., Sakurai, K., Yaron, A., Cobb, J., and Wang, F. (2011). Transcription factor short stature homeobox 2 is required for proper development of tropomyosin-related kinase B-expressing mechanosensory neurons. J Neurosci *31*, 6741-6749.

Silos-Santiago, I., Molliver, D.C., Ozaki, S., Smeyne, R.J., Fagan, A.M., Barbacid, M., and Snider, W.D. (1995). Non-TrkA-expressing small DRG neurons are lost in TrkA

deficient mice. The Journal of neuroscience : the official journal of the Society for Neuroscience *15*, 5929-5942.

Smeyne, R.J., Klein, R., Schnapp, A., Long, L.K., Bryant, S., Lewin, A., Lira, S.A., and Barbacid, M. (1994). Severe sensory and sympathetic neuropathies in mice carrying a disrupted Trk/NGF receptor gene. Nature *368*, 246-249.

Snider, W.D., and Silos-Santiago, I. (1996). Dorsal root ganglion neurons require functional neurotrophin receptors for survival during development. Philos Trans R Soc Lond B Biol Sci *351*, 395-403.

Srinivas, S., Watanabe, T., Lin, C.S., William, C.M., Tanabe, Y., Jessell, T.M., and Costantini, F. (2001). Cre reporter strains produced by targeted insertion of EYFP and ECFP into the ROSA26 locus. BMC Dev Biol *1*, 4.

Tessarollo, L., Vogel, K.S., Palko, M.E., Reid, S.W., and Parada, L.F. (1994). Targeted mutation in the neurotrophin-3 gene results in loss of muscle sensory neurons. Proc Natl Acad Sci U S A *91*, 11844-11848.

Zylka, M.J., Dong, X., Southwell, A.L., and Anderson, D.J. (2003). Atypical expansion in mice of the sensory neuron-specific Mrg G protein-coupled receptor family. Proc Natl Acad Sci U S A *100*, 10043-10048.

Zylka, M.J., Rice, F.L., and Anderson, D.J. (2005). Topographically distinct epidermal nociceptive circuits revealed by axonal tracers targeted to Mrgprd. Neuron *45*, 17-25.

Lee, K.F., Li, E., Huber, L.J., Landis, S.C., Sharpe, A.H., Chao, M.V., and Jaenisch, R. (1992). Targeted mutation of the gene encoding the low affinity NGF receptor p75 leads to deficits in the peripheral sensory nervous system. Cell *69*, 737-749.

Paul, C.E., Vereker, E., Dickson, K.M., and Barker, P.A. (2004). A pro-apoptotic fragment of the p75 neurotrophin receptor is expressed in p75NTRExonIV null mice. J Neurosci *24*, 1917-1923.

von Schack, D., Casademunt, E., Schweigreiter, R., Meyer, M., Bibel, M., and Dechant, G. (2001). Complete ablation of the neurotrophin receptor p75NTR causes defects both in the nervous and the vascular system. Nat Neurosci *4*, 977-978.

CHAPTER 3: A P75-RET SIGNALING COMPLEX MEDIATES PROGRAMMED CELL DEATH IN DEVELOPING SYMPATHETIC NEURONS

***Summary*:**

Programmed cell death (PCD) is an evolutionarily-conserved process critical in sculpting many organ systems, yet many of the underlying mechanisms remain poorly understood. We investigated the interactions of pro-survival and pro-apoptotic receptors in PCD using the sympathetic nervous system as a model. We demonstrate that Ret, a receptor tyrosine kinase required for the survival of many neuronal populations, is restricted to a subset of degenerating neurons that rapidly undergo apoptosis. Pro-apoptotic conditions induce Ret to associate with the death receptor p75. Genetic deletion of p75 within Ret+ neurons, and deletion of Ret during PCD, inhibits apoptosis both *in vitro* and *in vivo*. Mechanistically, Ret inhibits nerve growth factor (NGF)-mediated survival and downstream signaling that is necessary for sympathetic neuron survival. Additionally, Ret deletion significantly impairs p75 regulated-intramembranous proteolytic (RIP) cleavage, leading to reduced activation of downstream apoptotic effectors. Collectively, these results indicate that Ret acts non-canonically to augment p75-mediated apoptosis.

***Introduction*:**

Apoptosis is a fundamental developmental process during organogenesis. In the nervous system developmental cell death, also known as programmed cell death (PCD), is an evolutionarily conserved process that allows an organism to match the size

of the neuronal population with the size of its target tissue. In the peripheral nervous system there is a widespread overproduction of neurons, with most populations producing twice the number of neurons that are present in adulthood (Oppenheim, 1991). Neurons project to their targets and compete for a limited supply of neurotrophic factors. Neurons that make appropriate or sufficiently extensive connections receive an adequate amount of target-derived neurotrophic factors and survive, while those that do not are eliminated through apoptotic signaling cascades (Levi-Montalcini, 1987; Oppenheim, 1991). Importantly, the mechanisms underlying PCD can be reactivated during nervous system injuries and neurodegenerative diseases (Ibanez and Simi, 2012), underscoring the importance of understanding of these molecular mechanisms in detail.

PCD in the nervous system is perhaps best understood in sympathetic neurons of the superior cervical ganglion (SCG). Perinatally these neurons are wholly dependent on target-derived nerve growth factor (NGF) for their survival (Levi-Montalcini, 1987; Smeyne et al., 1994a). NGF is the founding member of the neurotrophin family, also consisting of brain-derived neurotrophic factor (BDNF), neurotrophin-3 (NT-3), and neurotrophin-4 (NT-4)(Chao, 2003). NGF exerts its pro-survival functions through the receptor tyrosine kinase, TrkA, which is ubiquitously expressed in sympathetic neurons. TrkB and TrkC, the cognate receptors for BDNF/NT-4 and NT-3, respectively, are not expressed in the SCG, and as such, these neurotrophins are dispensable for the survival of developing sympathetic neurons (Bamji et al., 1998).

In addition to the competition for survival factors, evidence also points to the presence of active pro-apoptotic signaling mechanisms through various death receptors

within the TNF superfamily, including the p75 neurotrophin receptor and TNFR1 (Bamji et al., 1998; Barker et al., 2001). p75 is a promiscuous receptor that regulates several cellular functions through its interactions with other co-receptors. p75 can bind to all four neurotrophins (Gentry et al., 2004), and acts collaboratively with sortilin as the high affinity receptor for the proneurotrophins (Nykjaer et al., 2004). In the SCG, p75 has been reported to have both pro-survival and pro-apoptotic functions (Gentry et al., 2004; Kraemer et al., 2014). p75 inhibits ligand-induced TrkA ubiquitination and subsequent internalization and degradation, thereby potentiating NGF-TrkA signaling (Makkerh et al., 2005b). However, in the absence of NGF, or the presence of BDNF or proBDNF, p75 activation triggers apoptosis (Bamji et al., 1998; Kenchappa et al., 2010; Lee et al., 2001). Consistent with these studies, in *p75*$^{-/-}$ mice, the number of sympathetic neurons is greatly increased, and the rate of apoptosis following NGF deprivation is strongly diminished (Bamji et al., 1998; Deppmann et al., 2008). Furthermore, coincident knockout of p75 in *TrkA*$^{-/-}$ sympathetic neurons largely rescues neurons from apoptosis, consistent with a role for p75 in apoptosis following NGF withdrawal (Majdan et al., 2001). These and other studies have led to the proposal that there is competition between neurons during PCD. “Winning” neurons – those that receive adequate amounts of target-derived NGF, and are themselves protected from cell death, upregulate and release pro-apoptotic p75 ligands such as BDNF, which induce apoptosis in nearby unprotected “losing” neurons (Deppmann et al., 2008). Although it remains unclear to what extent NGF withdrawal, pro-apoptotic competition, or a combination of both, ultimately accounts for apoptosis mediated by p75 in the sympathetic nervous system, it is clear that multiple stimuli can induce p75-mediated

apoptosis.

Ret is expressed in the SCG during the period of PCD, but its role has not been examined. Ret signaling has been shown to be critical for survival in a number of neuronal populations including subpopulations of sensory neurons of the dorsal root ganglia (DRG), enteric neurons and spinal γ-motor neurons (Airaksinen and Saarma, 2002; Enomoto et al., 2001; Luo et al., 2009; Luo et al., 2007). Moreover, Ret signaling is required for sympathetic chain ganglia migration, coalescence of the ganglia and early axon pathfinding (Enomoto et al., 2001). These functions result in early and severe morphologic deficits in the SCG prior to the period of PCD in *Ret*$^{-/-}$ mice, limiting investigation of the function of Ret in this process.

In this study we investigated the function of Ret in PCD. We demonstrate that Ret expression is restricted to a subpopulation of apoptotic neurons that are rapidly eliminated. Ret and p75 form a molecular complex induced by pro-apoptotic stimuli, and Ret is required for p75-mediated apoptosis induced by multiple stimuli *in vitro*. Importantly, p75 deletion specifically within Ret-expressing neurons, and Ret deletion specifically during PCD, results in a significant abrogation in programmed cell death *in vivo.* These studies revealed a surprising non-canonical function of Ret in augmenting apoptotic signaling through p75 during PCD *in vivo*.

Results

Ret expression is limited to a subpopulation of neurons that are rapidly eliminated during programmed cell death

Studies analyzing Ret expression in the developing sympathetic nervous system using either a *Ret*$^{GFP/+}$ reporter line or *in situ* hybridization demonstrated that Ret expression is nearly ubiquitous throughout the ganglion by E11.5-E12.5, but then declines significantly by E14.5-E15.5, correlating with its role in sympathetic neuron migration and coalescence of the sympathetic chain ganglia. Curiously, Ret expression then re-emerges by E16.5, corresponding to the onset of PCD (Enomoto et al., 2001; Nishino et al., 1999). While Ret was expressed in many neurons perinatally, very few neurons expressed the GFRα co-receptors, which is surprising given that GFL signaling through Ret requires GFRα receptors. To determine the functional significance of Ret expression during PCD, we performed a tamoxifen (TMX) pulse experiment using a Cre-inducible tomato reporter line (*Rosa26*$^{LSL\text{-}tdTomato}$) crossed to Ret-Cre/ER^{T2} mice (Luo et al., 2009). This experimental strategy (Figure 3.1A) enabled us to permanently mark the population of neurons expressing Ret at E16.5, thereby allowing the determination of the fate of these cells during PCD. Embryos were collected at E17.5, E19.5, and P3. Strikingly, there was a significant 76.4% reduction in the number of Ret+ neurons present at E19.5 compared to E17.5 (Figure 3.1B-3.1C, quantifications in 1E; 952.4 ± 49.1 vs. 224.3 ± 20.0 neurons, $p<0.0001$), with a further loss of neurons by P3 (Figure 3.1D; 13.5 ± 2.3 neurons). These data indicate that the Ret+ neurons present at E16.5 are rapidly eliminated, and the number of Ret+ neurons labeled is strikingly similar to the number of apoptotic SCG neurons reported in previous studies

investigating PCD in the SCG (Aloyz et al., 1998; Majdan et al., 2001). Additionally, we observed many examples of Ret+ neurons appearing atrophic (arrows in 3.1B, 3.1C), a characteristic associated with PCD in sympathetic neurons (Deckwerth and Johnson, 1993).

Given the well-established role of p75 in PCD in the SCG, we sought to determine whether Ret expression coincides with p75 expression during PCD. To this end, SCGs from Ret-Cre/ER^{T2}; *Rosa26*$^{LSL\text{-}tdTomato}$ mice were immunolabeled for p75 and RFP (tomato). As a control for the specificity of p75 immunolabeling, SCGs were taken from *p75*$^{-/-}$ mice at P0 and immunolabeled for p75, which demonstrated a complete lack of staining (Figure 3.2). p75 and RFP co-immunolabeling revealed that p75 is widely expressed throughout the SCG, while Ret expression is restricted to a subpopulation of SCG neurons, all of which express p75 (Figure 3.1B-3.2C). These results indicate that Ret is expressed within a subpopulation of p75-expressing neurons, and that Ret+ neurons undergo apoptosis during the period of PCD.

Ret and p75 associate *in vitro* and *in vivo*

To investigate whether there is a functional interaction between p75 and Ret, we utilized the NIH/3T3 cell line, which does not express Ret9 or Ret51 and expresses only low levels of p75 (Calco et al., 2014). As shown in Figure 3.3A, co-transfection of Ret9 or Ret51 with p75 leads to robust formation of Ret9-p75 and Ret51-p75 receptor complexes, regardless of whether Ret or p75 immunoprecipitation was used. To demonstrate that this interaction is both specific and relevant in neurons *in vivo*, *Ret*$^{fx/fx}$ mice were mated with UBC-Cre/ER^{T2} mice, a TMX inducible Cre line driven by the

ubiquitously-expressed Ubiquitin C promotor (Ruzankina et al., 2007), allowing for temporally controlled deletion of Ret. *Ret*$^{fx/fx}$; UBC-Cre/ER^{T2} mice were administered TMX (0.25 mg/g body weight) from E14.5-E18.5 and euthanized at E19.5 to collect embryos. Spinal cords were then dissected, lysed, and detergent extracted, followed by immunoprecipitation of Ret. Ret deletion was highly efficient, and this led to a corresponding loss in p75 that co-immunoprecipitated with Ret antibodies (Figure 3.3B-D). These findings were further confirmed through proximity ligation assays conducted on NIH/3T3 cells transfected with p75 and Ret51, or p75 and Ret51-HA. As expected, we observed strong co-localization of p75 and HA-tagged Ret when staining using anti-p75 and anti-HA antibodies, but not with untagged Ret (Figure 3.3E). These results indicate that this Ret-p75 interaction is present under physiological conditions *in vitro* and *in vivo*.

Pro-apoptotic p75 ligands enhance the interaction between p75 and Ret

To test the hypothesis that p75-Ret association may be enhanced by pro-apoptotic p75 stimuli including NGF withdrawal, BDNF, and proBDNF, primary sympathetic neurons were generated from E18.5 rat embryos and cultured in the presence of 50 ng/ml NGF. After 2 days, NGF was removed and neurons were rinsed with medium twice, followed by the addition of an anti-NGF (αNGF) blocking antibody for the indicated times. The neurons were then washed, detergent extracted and Ret immunoprecipitations were performed. Although a basal level of association typically existed, blocking NGF signaling led to a striking increase in the interaction between p75 and Ret, which was statistically significant at all time points analyzed following NGF

deprivation (Figure 3.4A, B). BDNF treatment led to a significant increase in p75-Ret association by 12 hours as compared to low NGF ($p < 0.01$), although the extent of this interaction was smaller compared to NGF deprivation (Figure 3.4C, D). Similar to BDNF, stimulation with an uncleavable form of proBDNF (10 ng/ml) led to a striking increase in p75-Ret association by 6 hours, and this increase was sustained for at least 24 hours (Figure 3.4E, F). Despite the robust induction of p75-Ret association following stimulation with proBDNF, we were unable to detect co-immunoprecipitation of the proneurotrophin co-receptor, Sortilin, with Ret, despite reliable detection of sortilin in the immunoprecipitation supernatants (Figure 3.4E). These data suggest a potential sortilin-independent proBDNF induction of p75-Ret complex formation, although it cannot be ruled out that proBDNF cleavage occurs *in vitro*, or that the Ret antibodies used for the immunoprecipitation preclude sortilin co-immunoprecipitation is some manner.

To determine whether pro-apoptotic conditions could induce the formation of this receptor complex *in vivo, Ret*$^{fx/fx}$; UBC-Cre/ER^{T2} mice were used to ensure specificity of immunoprecipitation of the Ret-p75 complex. P0 mice were given tamoxifen (TMX) from P0-P4, followed by injection of vehicle (as a negative control) or a NGF-blocking antibody, as we have done previously (Tsui-Pierchala et al., 2002c). SCGs were then collected, lysed, and subjected to Ret immunoprecipitation and immunoblotting. Ret immunoblotting verified efficient knockdown following TMX administration. Interestingly, we observed that anti-NGF administration led to a significant increase in Ret compared to vehicle-treated mice, with a corresponding increase in co-immunoprecipitating p75 (Figure 3.4G-3.4I). Collectively, these data suggest pro-apoptotic stimuli increase p75-

Ret association, and suggest that Ret is upregulated following exposure to pro-apoptotic stimuli *in vivo.*

p75 enhances TrkA signaling in the presence of NGF, but inhibits canonical GDNF-Ret signaling in sympathetic neurons

Given previous studies indicating that p75 is able to enhance NGF/TrkA signaling in sympathetic and sensory neurons (Lee et al., 1992a), as well as our demonstration of a novel interaction between p75 and Ret, we hypothesized that p75 may be able to modulate canonical Ret signaling. To this end, SCG cultures were generated from P0 $p75^{fx/fx}$; UBC-Cre/ER^{T2} mice (Bogenmann et al., 2011b). Neurons were maintained in the presence of NGF (50 ng/ml) as well as 4-OH-TMX (to induce Cre-mediated recombination; 5 µg/ml) for 5 days. To first assess whether TrkA activation was affected by deletion of p75 as previously reported (Makkerh et al., 2005b), $p75^{fx/fx}$ and $p75^{fx/fx}$; UBC-Cre/ER^{T2} SCG neurons were lysed, detergent extracted, and immunoprecipitated for TrkA. Immunoblotting was performed for pTrkA, TrkA, p75, and actin, and levels of pTrkA/TrkA/Actin were quantified. As displayed in Figure 3.5, p75 deletion was highly effective and led to a significant reduction in pTrkA ($p < 0.05$). These data confirm previous studies indicating that p75 enhances signaling through TrkA in the presence of NGF. To determine whether deletion of p75 altered canonical GFL-Ret signaling, $p75^{fx/fx}$ and $p75^{fx/fx}$; UBC-Cre/ER^{T2} SCG neurons were maintained in NGF (50 ng/ml) and 4-OH-TMX for 5 days. The neurons were then stimulated with GDNF (50 ng/ml) for 15 minutes or 1 hour, followed by detergent extraction and Ret immunoprecipitation. Immunoblotting was performed for phospho-tyrosine, Ret, p75, and actin. Surprisingly,

deletion of p75 led to a striking increase in Ret activation within 1 hour ($p < 0.05$; Figure 3.6A, B). Given that p75 is expressed ubiquitously throughout the SCG, these data indicate that p75 inhibits canonical GFL activation of Ret.

p75 is a mediator of programmed cell death following NGF deprivation.

p75-mediated apoptosis requires the function of a number of downstream signaling effectors, including early binding of TRAF6 and NRIF to full length p75 shortly after activation, an early wave of JNK/c-Jun pathway activation, cleavage of the p75-ECD by the TACE complex, liberation of the p75-ICD by the gamma secretase complex, and a late wave of activation of the JNK/c-Jun pathway, ultimately leading to terminal activation of executioner caspases. These final events lead to morphological and nuclear changes such as DNA fragmentation, chromosome condensation, and nuclear blebbing, all characteristic signs of apoptosis (Kraemer et al., 2014).

To confirm previous studies indicating that p75 is involved in apoptosis in sympathetic neurons, we cultured E18.5-P0 SCG neurons from *p75*$^{-/-}$ mice and *p75*$^{+/+}$ mice (Bogenmann et al., 2011b). These neurons were deprived of NGF (or maintained in NGF, as a control) for 12 hours. Importantly, apoptosis-related nuclear morphological changes (pyknosis) do not begin to become evident until approximately 20 hours following NGF deprivation (Deckwerth and Johnson, 1993). 12 hours following these treatments, neurons were fixed, stained for phospho-c-Jun (p-c-Jun), and the number of neurons with nuclear p-c-Jun accumulation was quantified to assess the extent initiation of apoptosis. Numerous studies investigating PCD in the SCG describe p-c-Jun as one of the earliest molecular events that trigger apoptosis, detectable prior to caspase

activation and nuclear pyknosis (Bamji et al., 1998; Deshmukh and Johnson, 1997; Werth et al., 2000). As demonstrated in 3.7A, there were fewer *p75*$^{-/-}$ neurons displaying phosphorylated c-Jun compared to *p75*$^{+/-}$ controls. As a later indicator of apoptosis, apoptotic neurons were quantified by counting pyknotic nuclei. To this end, sympathetic neurons were deprived of NGF for either 24 or 48 hours. Similar to the p-c-Jun data, *p75*$^{-/-}$ neurons had reduced apoptosis at 24 hours, but not 48 hours, when compared to *p75*$^{+/+}$ neurons (Figure 3.7B). These data are consistent with previous reports indicating that redundant death receptor signaling mechanisms are present and can mediate apoptosis after extended periods of NGF withdrawal in p75-deleted neurons (Deppmann et al., 2008; Kraemer et al., 2014).

Ret is required for programmed cell death in primary sympathetic neurons.

To test the hypothesis that Ret augments p75-mediated apoptosis, primary SCG neurons were produced and transfected with siRNA targeted against Ret, or a non-targeting scrambled siRNA as a control. In addition, for all experiments, a non-targeting siGLO siRNA was included to verify transfection efficiency, which demonstrated that greater than 90% of neurons were transfected. 48 hours following siRNA transfection, neurons were lysed followed by immunoblotting to determine the efficacy of siRNA-mediated knockdown of Ret. Transfection with Ret siRNA, but not scrambled siRNA, was effective in reducing Ret levels by greater than 65% ($p < 0.05$; Figure 3.8A, B). To assess whether Ret is required for p75-mediated apoptosis, 48 hours post transfection, scrambled and Ret-siRNA-transfected neurons were subjected to four conditions for 12 hours: high NGF (100 ng/ml), low NGF (1 ng/ml), BDNF (200 ng/ml) in the presence of

low NGF (1 ng/ml), or αNGF. Neurons were then fixed, and the number of neurons with nuclear p-c-Jun accumulation was assessed (Figure 3.8D-K) and quantified (Figure 3.8C). We observed very few examples of nuclear p-c-Jun accumulation in high NGF (Figure 3.8D, 3.8E) or low NGF-treated conditions (Figure 3.8F, 3.8G), regardless of siRNA or Ret-siRNA transfection. As expected, BDNF and αNGF treatment led to increased nuclear accumulation of p-c-Jun in scrambled siRNA-treated neurons, with NGF deprivation producing more robust effects (Figure 3.8H, 3.8J). In marked contrast, Ret siRNA-treated neurons had significantly reduced p-c-Jun+ nuclei for both treatment groups (3.8I, 3.8K). Quantifications indicated that statistically significant reductions were observed between scrambled siRNA and Ret siRNA neurons treated with BDNF (Figure 3.8C; 46.42% reduction; 31.76 ±1.877 vs. 17.02 ± 1.84 percent; $p < 0.05$) and αNGF (38.24% reduction; 67.95 ± 4.75 vs. 41.97 ± 6.11 percent; $p < 0.0001$). These results demonstrate that Ret is required for p75-mediated apoptotic signaling mediated by both ligand stimulation (BDNF) and trophic factor deprivation (αNGF).

Ret antagonizes NGF-TrkA signaling and survival

While these results indicate that Ret augments early p75-mediated activation of the pro-apoptotic signaling cascade, we sought to determine whether there is a specific threshold of NGF deprivation required to trigger apoptotic p75-Ret signaling by performing a NGF dose response curve. Due to the limited window of transfection efficacy via the siRNA knockdown approach, we utilized a permanent means of deleting Ret by using P0 $Ret^{fx/fx}$ and $Ret^{fx/fx}$; UBC-Cre/ER^{T2} SCG neurons maintained in the

presence of NGF and 4-OH-TMX. Following Cre-mediated deletion of Ret, Ret-WT and Ret-cKO neurons were treated for 24 hours with concentrations of NGF ranging from 0-100 ng/ml. Neuronal apoptosis was then assessed by the presence of pyknotic nuclei. As expected, and consistent with previous 24-hour death assays investigating NGF-mediated survival under similar culture conditions (Putcha et al., 2001), we observed fewer than 50% of Ret-WT neurons were able to survive 24 hours following complete deprivation of NGF (Figure 3.9A), with increasing concentrations of NGF improving survival of these neurons in a dose-dependent manner (Figures 3.9C, 3.9E, 3.9G, 3.9I). In contrast, Ret-cKO neurons had fewer apoptotic profiles with complete NGF deprivation (Figure 3.9B, $p < 0.01$) and 0.1 ng/ml NGF (Figure 3.9D, $p < 0.05$), but had statistically similar numbers of pyknotic nuclei at higher doses (1, 10, 100 ng/ml NGF; Figures 3.9F, 3.9H, 3.9J, 3.9K). Immunoblotting confirmed effective deletion of Ret in *Ret*$^{fx/fx}$; UBC-Cre/ER^{T2} (Ret-cKO) compared to *Ret*$^{fx/fx}$ mice (Ret-WT) (>95%; Figure 3.9L-M). These data suggest that Ret antagonizes NGF signaling through TrkA, and that Ret is required for p75-mediated apoptosis induced by NGF withdrawal in a dose-dependent manner.

To further confirm the role of Ret in p75-mediated apoptosis, BDNF and proBDNF death assays were conducted in several different culture models: (1) *Ret*$^{fx/fx}$; UBC-Cre/ER^{T2} (Ret-cKO) neurons (*Ret*$^{fx/fx}$ as a control), where Ret is deleted as above; (2) *p75*$^{fx/fx}$; *Ret*-Cre/ER^{T2} (p75-RC) neurons (neurons from littermate *p75*$^{fx/fx}$ mice as a control), where p75 is deleted specifically within Ret+ neurons; (3) and *p75*$^{fx/fx}$; UBC-Cre/ER^{T2} (p75-cKO) neurons (neurons from littermate *p75*$^{fx/fx}$ mice as a control), where p75 is deleted in all neurons. Neurons were cultured from the above mice at E18-P0

and maintained for 5 days in the presence of NGF (50 ng/ml) and 4-OH-TMX (5 ug/ml), rinsed, and treated with low NGF (1 ng/ml), or low NGF in the presence of BDNF (200 ng/ml) or proBDNF (10 ng/ml). Neurons were fixed and analyzed for nuclear pyknosis as described above 48 hours after stimulation (Figure 3.9N). Interestingly, both BDNF and proBDNF stimulation led to a substantial increase in apoptosis in control neurons, and this effect was significantly reduced in all cKO models analyzed ($p > 0.0001$; Figure 3.9N).

Deletion of p75 specifically within Ret-expressing neurons impairs programmed cell death *in vitro* and *in vivo*

To determine the extent to which p75 is required for apoptotic signaling initiated by NGF deprivation, P0 $p75^{fx/fx}$ (p75-WT) and $p75^{fx/fx;}$ Ret-Cre/ER^{T2} (p75-RC) neurons were maintained for 5 days in the presence of NGF (50 ng/ml) and 4-OH-TMX (5 ug/ml). Neurons were then rinsed and treated with NGF or deprived of NGF for 12 hours to assess p75-mediated p-c-Jun activation. Neurons were then fixed, stained, and the number of neurons with nuclear p-c-Jun accumulation was quantified (Figure 3.10A, B). While nuclear p-c-Jun was only rarely present in NGF treated neurons for either p75-WT or p75-RC neurons, NGF deprivation led to a substantial increase in the number of p-c-Jun+ nuclei in p75-WT neurons. αNGF treated p75-RC neurons, in contrast, had significantly fewer p-c-Jun+ nuclei (68.6% reduction; 59.45±8.73 vs. 18.70±2.05 percent; $p < 0.0001$).

Given that only a subset of sympathetic neurons express Ret during PCD, and that these *in vitro* data indicate that p75-mediated apoptosis appears to be augmented

by Ret, we hypothesized that deletion of p75 within Ret+ neurons would be sufficient to impair PCD. To test the requirement of p75 in Ret+ neurons during PCD *in vivo*, we utilized *p75*$^{fx/fx}$; Ret-Cre/ER^{T2} mice (or *p75*$^{fx/fx}$ mice as a control; Figure 3.10C). Briefly, mice were given TMX (0.25 mg/g body weight) once per day for 4 days, beginning at E14.5, at which time Ret-dependent SCG migration and coalescence is largely complete (Enomoto et al., 2001). Immunoblotting of the spinal cords from E19.5 mice confirmed the successful deletion of p75 from Ret+ neurons using this TMX dosing regimen (Figure 3.10D, E). SCGs were then stained for cleaved caspase-3, βIII-Tubulin (TuJ1), tyrosine hydroxylase (TH), and DAPI to quantify the number of apoptotic SCG neurons (Figures 3.10F, G). Because caspase-3 is an irreversible executioner caspase, cleaved caspase-3 staining is a highly sensitive marker of neurons undergoing apoptosis. Interestingly, we observed a statistically significant reduction in cleaved caspase-3+ neurons in p75-RC SCGs, compared to the SCGs of p75-WT mice (Figure 3.10G, 50.1% reduction; 96.04 ± 12.84 vs. 48.18 ± 12.77 cc3+ cc3+/mm^3; $p < 0.05$).

Ret is required for p75-mediated apoptosis *in vivo*

To examine whether Ret is directly involved in p75-mediated PCD *in vivo*, we utilized *Ret*$^{fx/fx}$; UBC-Cre/ER^{T2} mice with the TMX dosing strategy described previously (Figure 3.10C) in order to avoid the deleterious effects of Ret deletion during SCG coalescence, while also avoiding perinatal lethality described by other studies involving perturbations of Ret signaling (Uesaka and Enomoto, 2010; Uesaka et al., 2007). SCGs were immunostained for cleaved caspase-3, TH, and DAPI, and the number of cleaved caspase-3+ cells was quantified to compare apoptosis in *Ret*$^{fx/fx}$ (Ret-WT) and *Ret*$^{fx/fx}$;

UBC-Cre/ER^{T2} (Ret-cKO) mice. Ret-cKO mice had significantly fewer cleaved caspase-3+ neurons compared to Ret-WT mice (Figure 3.10H, I; 34.2% reduction; 268.62 vs. 176.85 cc3+/mm^3, $p < 0.05$). Interestingly, this reduction compares similarly to the reduction observed in p75-RC mice. Immunoblotting of spinal cord lysates from Ret-WT and Ret-cKO mice confirmed the efficacy of Ret deletion (Figure 3.10J). To further confirm these findings, total cell counts were performed on SCGs collected from E19.5 Ret-cKO and p75-RC mice administered tamoxifen as described in Figure 3.10C. We observed a significant increase in total cell counts in Ret-cKO (compared to Ret-WT) and p75-RC (compared to p75-WT) SCGs regardless of whether counts were determined using TuJ1 (left side) or TH (right side) as neuronal markers (Figure 3.10K). The magnitude of the increase in neuron numbers was similar in Ret-cKO and p75-RC SCGs (14.51% increase in TuJ1+ counts in Ret-cKO mice compared to 15.55% in p75-RC SCGs; 20.01% increase in TH+ counts in Ret-cKO SCGs compared to 17.79% in p75-RC SCGs). When taken together with the *in vitro* functional assays, these data provide compelling *in vivo* evidence suggesting that Ret augments p75-mediated apoptosis during PCD.

Ret is critical for p75-mediated activation of apoptotic effectors due to inhibition of p75 cleavage.

Having established that Ret augments p75-mediated apoptosis, we examined whether Ret deletion altered p75 enhancement of NGF/TrkA signaling, p75-mediated activation of apoptotic effectors, or both. To this end, primary neurons were cultured from P0 Ret-WT and Ret-cKO mice maintained in NGF and 4-OH-TMX. Neurons were

then maintained in NGF (50 ng/ml), or deprived of NGF for 12 hours, followed by detergent extraction and immunoblotting for Ret. This confirmed that the deletion efficacy using this strategy was greater than 90% for both treatment groups (Figure 3.11A, B). To explore the possibility that Ret deletion results in a reduction of total levels of p75, immunoblotting was performed for p75 (p75 full length; p75-FL; Figure 3.11A, C). NGF-maintained Ret-WT neurons had a significant reduction in p75 following NGF deprivation (Figure 3.11C, $p < 0.05$), likely as a result of regulated intramembrane proteolysis (RIP) cleavage of p75. Interestingly, there was no significant difference in p75 levels in NGF vs. αNGF-treated Ret-cKO neurons (Figure 3.11A, C). To determine directly whether Ret deletion impairs p75 cleavage, thereby impairing downstream apoptotic signaling, Ret-WT and Ret-cKO neurons were treated with NGF or were deprived of NGF for 12 hours in the presence of the degradation pathway inhibitors MG-132 (5 µM) and epoximicin (5 µM). These inhibitors are necessary to prevent the rapid degradation of the p75-CTF generated by RIP cleavage (Kanning et al., 2003). Neurons were then lysed, and p75 cleavage was assessed using an antibody against the p75-CTF, which detects both uncleaved p75 (p75-FL) and the 28 kDa p75-CTF. In this culture system, only the p75-CTF fragment was observed, and we were not able to detect the p75-ICD fragment. Interestingly, deletion of Ret led to a drastic reduction in the amount of p75 cleavage induced by NGF deprivation in Ret-cKO neurons compared to Ret-WT neurons (Figure 3.11D-E). Importantly, the antibody used to detect the p75 cleavage fragments (Promega) has epitopes outside of the CTF as well, thereby likely making binding affinity of the antibody to the p75-FL and p-75-CTF dissimilar. Thus, direct comparison of these p75 fragments is not possible. Finally, to determine whether

this effect was secondary to a reduction in the amount of TACE or Presenilin-1 (PSN-1), immunoblotting was performed and their levels were quantified. As shown in Figure 3.12A-C, no statistically significant differences were observed in TACE or PSN-1 in Ret-cKO neurons as compared to Ret-WT neurons.

To determine whether downstream apoptotic signaling was altered, we performed immunoblotting for p-c-Jun, pJNK, total JNK, and actin in neurons that were either maintained in NGF or deprived of NGF. As expected, NGF deprivation led to a significant activation of p-c-Jun in Ret-WT neurons compared to neurons maintained in NGF. However, in Ret-cKO neurons, this activation of p-c-Jun following NGF deprivation was impaired, and αNGF treated Ret-cKO neurons had significantly lower levels of p-c-Jun compared to Ret-WT neurons (Figure 3.11F, G; $p < 0.01$). Correspondingly, a similar reduction in pJNK/JNK levels was observed as well (Figure 3.11F, H; $p < 0.0001$).

A previous study demonstrated that p75-mediated apoptosis requires interaction with TRAF6 (Kanning et al., 2003). To examine whether TRAF6/p75 association was altered in the absence of Ret, p75 was immunoprecipitated from Ret-WT and Ret-cKO neurons treated with NGF or αNGF, and TRAF6 immunoblotting was performed. No significant differences were observed in TRAF6 association with p75 in any of the conditions examined (Figure 3.12D-E). Taken together, these data suggest that Ret augments apoptotic signaling by facilitating RIP cleavage of p75.

Deletion of Ret prolongs TrkA activation following NGF deprivation by delaying TrkA receptor ubiquitination

Because Ret antagonizes NGF-mediated survival in a dose-dependent manner, we sought to test the hypothesis that Ret antagonizes NGF/TrkA signaling. Ret-WT and Ret-cKO neurons were treated as indicated and immunoblotting was performed for pTrkA, TrkA, and actin (as a loading control). When analyzing the effects of Ret deletion on TrkA signaling, we observed that total levels of TrkA (TrkA/actin) were not affected by either genotype or by the experimental treatment (Figure 3.11I, J). Ret-WT and Ret-cKO neurons maintained in NGF displayed no significant differences in their levels of activated TrkA (pTrkA/TrkA/actin), but Ret-WT neurons had significantly reduced levels of activated TrkA following the removal of NGF (Figure 3.11I, K). Surprisingly, Ret-cKO neurons deprived of NGF for 12 hours did not have a significant reduction in activated TrkA when compared to NGF-maintained neurons (Figure 3.11I, K). Additionally, there was a significantly greater amount of activated TrkA in αNGF-treated Ret-cKO neurons compared to Ret-WT neurons ($p < 0.05$). Based on these findings, we hypothesized that removal of Ret potentiates NGF-TrkA signaling by altering activation-induced TrkA degradation. To test this hypothesis, Ret-WT and Ret-cKO neurons were deprived of NGF overnight, followed by treatment with NGF as indicated. Lysosomal and proteasomal degradative pathways were inhibited by using concanamycin and epoxomycin, respectively, to inhibit the rapid loss of ubiquitinated receptors, explaining why TrkA levels did not change in these experiments. As expected, NGF treatment led to a significant increase in TrkA ubiquitination in Ret-WT neurons by 15 minutes, which was significantly impaired in Ret-cKO neurons ($p > 0.01$). These data indicate that Ret deletion prolongs TrkA signaling following NGF deprivation by potentially delaying TrkA ubiquitination, thereby enhancing NGF-TrkA signaling, ultimately leading to increased

neuronal survival. Collectively, these data suggest that during PCD Ret pushes SCG neurons towards apoptosis both by inhibiting pro-survival signaling through TrkA and enhancing p75-mediated apoptosis.

Discussion

In this study we identified Ret as a novel component of the cell death machinery in sympathetic neurons that acts in concert with p75 during programmed cell death. Ret expression is restricted to neurons that are rapidly eliminated through apoptosis, and pro-apoptotic stimuli induce formation of a Ret-p75 complex. Ret potentiates p75-mediated activation of downstream signaling effectors in response to apoptotic cues, and acts to augment p75-mediated apoptosis in a dose-dependent manner following NGF withdrawal. The removal of p75 specifically within Ret+ neurons is sufficient to diminish PCD, and this is mirrored following deletion of Ret *in vivo*. Ret potentiates apoptosis through two unique mechanisms that are ultimately connected by p75. First, Ret inhibits TrkA activation by promoting receptor ubiquitination, thereby reducing survival signaling. Second, Ret directly enhances RIP cleavage of p75 in response to pro-apoptotic cues, thereby inducing the late activation of the JNK/c-jun pathway that is necessary for downstream activation of pro-apoptotic effectors. Given the functions of Ret in developing neurons to date have been exclusively trophic in nature, these findings raise a number of important future questions.

Ret as a Mediator of p75-Dependent Apoptosis

The *in vitro* and *in vivo* data presented here support the notion that Ret, acting with p75, augments programmed cell death in the developing SCG. Several lines of evidence support this assertion. We demonstrate that knockdown of Ret *in vitro* reduces apoptosis in response to apoptotic cues, and does so in a dose-dependent manner in the case of NGF withdrawal (Figures 3.8 and 3.9). Additionally, and most critically, deletion of p75 specifically within Ret+ neurons is sufficient to diminish apoptotic signaling (Figures 3.9 and 3.10), and deletion of Ret *in vivo* quantitatively duplicates this result (Figure 3.10H, J), suggesting that Ret mediates the majority of p75-dependent apoptosis in SCG neurons. Also lending support to this model, we show that Ret expression in the SCG is limited to a subpopulation of neurons that are rapidly eliminated during the window of PCD (Figure 3.1). While this Ret+ subpopulation of neurons is relatively small when a single TMX pulse is performed (approximately 1,000 neurons), these numbers quantitatively compare with the proportion of SCG neurons undergoing apoptosis at any given time during PCD (Aloyz et al., 1998; Majdan et al., 2001, Wehner et al., 2016). Additionally, our data suggest that *in vivo,* trophic factor withdrawal induces the upregulation of Ret (Figure 3.4G-I). Lastly, it is important to consider that completion of PCD within the SCG occurs over a period of weeks (Deppmann et al., 2008), and thus, the proportion of neurons undergoing apoptosis at any specific age is a snapshot of the overall PCD process.

It remains unclear precisely which pro-apoptotic stimulus chiefly drives programmed cell death through p75, and to what extent p75 accounts for programmed cell death in the SCG. In this study, we observed that deletion of p75 and Ret resulted in substantially impaired apoptosis (Figures 3.8, 3.9 and 3.10), but deletion of neither

receptor fully blocked apoptosis. These data are consistent with previous reports analyzing apoptosis in the SCG in *p75*$^{-/-}$ mice, as well as the *in vivo* data presented here, with p75-RC and Ret-cKO mice having an incomplete loss of cleaved caspase-3+ neurons (Figure 3.10). Furthermore, the deletion of p75 inhibited apoptosis induced by NGF withdrawal at 12 hours and 24 hours, but not by 48 hours (Figure 3.7). Collectively, these data indicate that p75-mediated apoptosis only represents a portion of the PCD occurring in sympathetic neurons, suggesting that other death receptors, or other apoptotic pathways, must play a significant role. Thus, while p75 may represent a critical conduit for sympathetic neurons to undergo PCD, prolonged atrophic or pro-apoptotic conditions may bring forth additional death receptor mechanisms or other pro-apoptotic mediators. Furthermore, our data provide compelling evidence that Ret augments p75-mediated apoptosis. However, it is unclear whether Ret-dependent, and Ret-independent, p75-mediated apoptotic mechanisms may both exist.

Although receptor tyrosine kinases (RTKs) have not been demonstrated to have a role in naturally occurring cell death *in vivo*, previous reports studying pediatric neural tumor cells indicated that TrkA can induce cell death through its interaction with CCM2 (Harel et al., 2009). These findings bear some similarity to those of this study through the indication that TrkA and Ret cannot alone induce apoptosis, but can activate or augment the activity of other pro-apoptotic proteins. The finding that, in developing sympathetic neurons, Ret augments p75-mediated apoptosis implies a highly unusual non-canonical function for Ret. Several neurotrophic factor receptors have been suggested to serve as dependence receptors, whereby in the absence of ligand a pro-apoptotic signal is generated by default. Utilizing transfected cell lines *in vitro*, Bordeaux

et al. reported that Ret expression causes increased apoptosis through a signaling pathway involving caspase cleavage of full length Ret (Bordeaux et al., 2000). Additionally, these investigators found that the addition of GDNF ameliorated apoptosis of cells transfected with Ret, thereby suggesting that Ret acts as a dependence receptor. While these data should be interpreted cautiously due to the exclusive use of transfected cell lines, a method known to cause cellular toxicity, the premise warrants further investigation. Importantly, we did not find evidence of Ret cleavage in response to pro-apoptotic stimuli, nor do we find evidence for a dependence-receptor mechanism of cell death via Ret. Furthermore, in multiple cell lines, transient transfection of Ret does not induce cell death (data not shown). The pro-apoptotic function of Ret described here, supported by both *in vitro* and *in vivo* evidence in neurons, argues for a non-canonical enhancement of p75-mediated apoptosis by Ret reliant exclusively on the presence of apoptotic cues that trigger the activation of p75, and does not involve deprivation of GDNF or other GFLs. Regardless, the investigation of whether this receptor complex serves as a dependence receptor in the absence of GFLs in other neuronal systems represents an interesting future direction.

Context-Dependent Cues Dictate Neuron Survival in Programmed Cell Death

In sympathetic neurons, the functions of p75 can be divided into two main categories: the trophic function of p75 in potentiating NGF/TrkA signaling, and the degenerative functions of p75. Given these opposing functions, a key question that emerges is how p75 can promote both survival and apoptosis. As p75 and TrkA are both ubiquitously expressed throughout the developing SCG, how do individual neurons

determine whether p75 will potentiate TrkA signaling or to actively promote apoptosis? It is possible that Ret acts as one such determinant, whereby upon its expression, p75 is pushed towards a pro-apoptotic signaling role, while also acting to dampen NGF/TrkA pro-survival signaling. To this end, Deppmann et al. (2008) demonstrated that a series of feedback loops regulate PCD in sympathetic neurons: high levels of NGF/TrkA signaling in “winning neurons” reinforces TrkA expression, while also inducing upregulation of pro-apoptotic p75 ligands. These trophically-supported neurons then release these factors to act on neighboring atrophic neurons, which have downregulated TrkA, activating p75 death signaling (Deppmann et al., 2008). In this model, it is likely that Ret is positioned to support this feedback mechanism, whereby expression of Ret antagonizes TrkA activation, expediting its downregulation, while also creating a highly active death receptor complex with p75, ultimately enhancing p75 cleavage and downstream activation by apoptotic effectors.

Based on the co-expression of p75 and Ret in many neuronal populations, we speculate that the proapoptotic p75-Ret receptor complex discovered here may be of physiological significance in other populations, and may have varied functions depending on the cell type. For example, p75 acts to enhance GFL-Ret signaling in subpopulations of DRG sensory neurons, leading to the emergence of nonpeptidergic nociceptors (Chen et al., 2017). Additionally, while Ret has been assumed to function as a pro-survival, pro-growth RTK, this non-canonical function of Ret in augmenting p75-mediated cell death may be of importance in the pathophysiology of nervous system injuries and neurodegenerative diseases.

Acknowledgments

We thank Dr. Vesa Kaartinen for technical expertise in generating p*75*$^{fx/fx}$ mice, Drs. David Ginty and Joseph Savitt for providing *Ret*$^{fx/fx}$ mice, and Drs. Luo and Enomoto for providing Ret-Cre/ER^{T2} mice. Support was provided to C.R.D. through the Rackham Merit Fellowship (University of Michigan), NIDCR T32 DE007057, and NIDCR F30 DE023479. These experiments were supported by NINDS R01 NS089585 awarded to B.A.P. The authors declare no conflict of interest.

Author Contribution

C.R.D. and B.A.P. designed experiments, interpreted data, and wrote the manuscript. C.R.D. performed all *in vitro* experiments with assistance from M.C. and conducted all *in vivo* experiments utilizing Ret-Cre animals with the assistance of E.R.S. N.A.G. performed *in vivo* experiments utilizing UBC-Cre animals. B.A.P. was responsible for the overall direction and communication of the experiments.

Experimental Procedures

Animals

All experiments were carried out in compliance with the guidelines of the Association for Assessment and Accreditation of Laboratory Animal Care International (AAALAC) and were approved by the Institutional Animal Care and Use Committee (IACUC) of the University of Michigan.

Production of Embryos and Tamoxifen Delivery

UBC-Cre/ER^{T2} (Ruzankina et al., 2007), *Ret*$^{fx/fx}$ (Luo et al., 2007), *p75*$^{fx/f}$ and *p75*$^{-/-}$ (Bogenmann et al., 2011b), *Ret*$^{-/-}$ (Schuchardt et al., 1994), *Ret*-Cre/ER^{T2} (Luo et al., 2009), and *Rosa26*$^{LSL\text{-}tdTomato}$ mice (Madisen et al., 2010) have all been previously described, and all mice were maintained in mixed genetic backgrounds, except for *Rosa26*$^{LSL\text{-}tdTomato}$ which was maintained in a C57BL/6J background. For timed matings, noon of the day on which a vaginal plug was detected was considered as E0.5. For the experiments tracing Ret expression, *Rosa26*$^{LSL\text{-}tdTomato}$ mice were crossed to Ret-Cre/ER^{T2} mice and given one intraperitoneal (i.p.) injection of TMX (0.25 mg/g body weight) at E16.5 and euthanized for analysis at E17.5, E19.5, or P3. Additionally, *Ret*$^{fx/fx}$*; UBC*-Cre/ER^{T2} or *p75*$^{fx/fx}$*;* Ret-Cre/ER^{T2} were given i.p. injections of TMX (0.25 mg/g body weight) consecutively for four days beginning at E14.5 and euthanized at E19.5.

In Vivo Administration of NGF Blocking Antibody

Ret$^{fx/fx}$ *or Ret*$^{fx/fx}$; UBC-Cre/ER^{T2} mice were directly administered TMX (0.40 mg/g body weight with maximum volume of 50 µl) via i.p. injection daily for 5 days beginning at P0. At P5, mice were delivered 50 µl of vehicle alone (PBS) or 50 µl of function blocking anti-NGF serum, as described previously (Tsui-Pierchala 2002). Mice received 4 doses of PBS or αNGF once every 12 hours. At P7 the mice were euthanized, and the SCGs were collected and pooled from two mice of identical genotypes per condition. The SCGs were then lysed, detergent extracted, and subjected to Ret immunoprecipitation and immunoblotting.

Detergent Extraction and Immunoprecipitation from Whole Tissues

Spinal cords were harvested separately from P0 *Ret*$^{fx/fx}$*; UBC*-Cre/ER^{T2} mice, and then placed in a 2.0 mL tube with 250 µL IP Buffer lacking NP-40, along with a steel grinding ball (5mm, Qiagen, Valencia, CA). The spinal cords were then mechanically homogenized using the TissueLyzer II (Qiagen). The homogenates were mixed with 250 µL of 2% NP-40-containing IP buffer and incubated for 1 hour at 4°C under gentle agitation. Homogenates were centrifuged for 10 minutes at 16,100xg and subjected to an initial pre-clearing step with protein A and protein G alone at 4°C for 2 hours under gentle agitation, followed by pre-clearing with protein A, protein G, and a species-matched nonspecific control IgG for 2 hours under gentle agitation. Following pre-clearing, immunoprecipitations were performed as described in a following section.

Culture and Transfection of Immortalized Cell Lines and Proximity Ligation Assays

NIH/3T3 cells were maintained in DMEM supplemented with 10% fetal bovine serum (FBS), 2 mM glutamine, and 1% penicillin-streptomycin (Invitrogen, Carlsbad, CA). Cells were plated on 6-well tissue culture plates (Falcon) and allowed to proliferate until an approximate density of 50% confluence was obtained prior to transfection. Transfections were performed using Lipofectamine 2000 according to the manufacturer's instructions (Invitrogen). A total of 5 µg plasmid DNA was added per well, using a plasmid encoding eGFP to keep the total amount of DNA constant between treatments. The plasmid encoding p75 was generously provided by Phil Barker. For proximity ligation assays [PLA], the DuoLink Proximity Ligation Assay (Sigma, Carlsbad, CA) was utilized according to the manufacturer instructions. NIH/3T3 cells were transfected with p75 and Ret51, or p75 and HA-tagged Ret51. Antibodies used for PLA were p75 (Advanced Targeting Systems, 1:500) and HA (Sigma, 1:500), with DuoLink *In Situ* Orange Mouse/Rabbit Kit used for secondary antibody and amplification. DAPI was used for nuclear localization.

Production of Primary Superior Cervical Ganglion Neurons

Superior cervical ganglia (SCGs) were surgically dissected from E19 Sprague-Dawley rats (Charles River, Portage, MI) or P0 $Ret^{fx/fx}$ or $p75^{fx/fx}$ mice, and enzymatically dissociated via incubation in type I collagenase (Worthington) and a 1:1 ratio of HBSS: TrypLE (Invitrogen). Neurons were plated on gas-plasma treated 35 mm^2 dishes (Harrick Plasma; Ithaca, NY) coated with type I collagen (BD Biosciences, San Jose, CA). For all biochemical experiments using rat neurons, cells were plated as mass cultures at a density of 3 ganglia per plate, while experiments using mouse neurons

were plated at a density of two ganglia (one animal) per plate. For death assays, neurons were plated as a droplet at a density of 1 ganglion per plate. Neurons were maintained in minimum essential medium (MEM) containing 50 ng/ml NGF (Harlan), 10% (FBS), anti-mitotic agents aphidicolin (3.3 µg/ml) and 5-fluoro-2-deoxyuridine (20 µM; Sigma, St. Louis, MO), 2 mM glutamine, and 1% penicillin-streptomycin (Invitrogen, Carlsbad, CA). Neurons were maintained at 37°C with 8% CO_2 with medium changes every 3-4 days until experimental treatment. Treatments with growth factors and pharmacological agents were performed as described in the figure legends.

siRNA-Mediated Gene Silencing in Sympathetic Neurons

Neurons (2 DIV) were transfected with small interfering RNA (siRNA) using a scrambled control (siGENOME Non-Targeting siRNA Pool #1, Dharmacon, Lafayette, CO) or *Ret* (ON-TARGETplus SMARTpool, Dharmacon) siRNA at a concentration of 100 nM via i-Fect (Neuromics, Minneapolis, MN) according to the manufacturer's instructions. Transfection efficiency was determined in all experiments by the cotransfection of a fluorescently labeled nontargeting control siRNA (siGLO RISC-free siRNA; Dharmacon). 48 hours post-transfection, at which time expression of siGLO was maximal, neurons were treated as described in the figure legends.

Immunoprecipitations and Quantitative Immunoblotting

Cells were stimulated as indicated in the figure legends. Following stimulation, dishes were placed on ice, gently washed with PBS and lysed with immunoprecipitation buffer (Tris-buffered saline, pH 7.4, 1% Nonidet P-40, 10% glycerol, 500 µM sodium vanadate,

and protease inhibitors) as described previously (Tsui and Pierchala, 2008). Antibodies for α-p75 (5 µl; 07-476, Millipore, Billerica, MA), α-Trk (8 µl; C-14, Santa Cruz), α-Ret51 and/or α-Ret9 (8 µL; C-20 and C-19-G, respectively; Santa Cruz Biotechnology) were added along with protein A and protein G (Invitrogen, Carlsbad, CA) and incubated overnight at 4°C under gentle agitation. Immunoprecipitates were then washed three times with IP buffer and prepared for sodium dodecyl sulfate-polyacrylate gel electrophoresis (SDS-PAGE) by adding 2X sample buffer (tris-buffered saline, pH 6.8, 20% glycerol, 10% β-mercaptoethanol, 0.1% bromophenol blue and 4% SDS) and boiling the samples for 10 minutes.

Samples for western blotting were subjected to SDS-PAGE followed by electroblotting onto polyvinylidene difluoride membranes (Immobilin P; Millipore). Western blot analysis was performed using the following antibodies at the indicated concentrations: α-Ret51 (C-20, Santa Cruz, 1:500-1:1000), α-Ret9 (C19R, Santa Cruz, 1:1000), α-Ret (AF482, R&D, 1:1000), α-phospho-tyrosine (4G10, Millipore, 1:2000-1:3000), α-p75 (Advanced Targeting Systems, 1:1000, or Promega, 1:2000), α-actin (JLA-20, Iowa Hybridoma, 1:2000), pTrkA (9141, 1:1000, Cell Signaling), α-TrkA (C-14, Santa Cruz, 1:1000), α-phospho-c-Jun (9261, Cell Signaling, 1:300), α-phospho-JNK (9251, Cell Signaling, 1:1000), α-JNK (9252, Cell Signaling, 1:1000), α-Sortilin (ab16640, Abcam, 1:1000), TRAF6 (HPA020599, Sigma, 1:1000), α-TACE (sc-6416, Santa Cruz, 1:1000), α-Presenilin-1 (sc-7860, Santa Cruz, 1:1000). Blots were developed using a chemiluminescent substrate (Supersignal, ThermoFisher). For quantifications, scanned images of X-ray films were imported into ImageJ (National Institutes of Health) and processed using the gel analysis tool. Integrated density values

obtained from immunoblots were reported as mean values ± SEM, with arbitrary units on the vertical axis. Values were normalized to the appropriate control: for co-immunoprecipitation studies, values were normalized to the precipitated protein; for phospho-specific signaling effectors, values were normalized to total levels of these effectors; and values were normalized to actin (used as a loading control) for all other samples. All biochemical experiments were performed at least three times with similar results.

Statistics and Data Analysis

All results are expressed as the mean ± s.e.m. All statistical tests were performed using two-tailed parameters with a significance level of $p \leq 0.05$ to test for statistical significance. For all statistical tests involving more than two variables, a two-way ANOVA with multiple comparisons was utilized with a Tukey post-hoc test to adjust for multiple comparisons. A two-tailed student's t-test was utilized for all comparisons between two treatment groups. A two-tailed student's t-test was also utilized to compare each time course treatment group with the corresponding NGF-maintained control for that experiment. The data were originally entered into Excel and imported into GraphPad Prism, which was used for all statistical tests. The presence of asterisks indicates statistical significance. * = $p < 0.05$, ** = $p < 0.01$, *** = $p < 0.001$, **** = $p < 0.0001$. The sample sizes are indicated in the figure legends. No sample sizes of less than 3 independent experiments were utilized. For the SCG counts, when possible, each animal represents the average count of two SCGs to increase statistical accuracy.

Fixation, Sectioning and Immunostaining of Superior Cervical Ganglia

Superior cervical ganglia (SCG) were fixed with 4% paraformaldehyde at 4ºC for 2-3 hours, washed in PBS three times for 10 minutes, and cryoprotected at 4ºC in 1X PBS containing 30% sucrose overnight. Tissues were embedded in OCT (Tissue Tek), frozen and stored at -80ºC until use. SCGs were serially sectioned at 7 µM on a cryostat (CM1950, Leica Biosystems, Germany). Tissue sections were washed with PBS and blocked with 5% normal goat serum in PBS-T (0.1% Triton X-100 in 1X PBS) for 1 hour, followed by incubation with primary antibody (diluted in blocking solution) in a humidified chamber overnight at 4ºC. Sections were washed with PBS-T, and incubated with secondary antibody (1:500) diluted in blocking solution for 2 hours. Sections were washed again with PBS-T and mounted in fluoromount-G with DAPI (Southern Biotech). Images were taken using an inverted fluorescence microscope (Axiovert 200M, Zeiss Microsystems, Germany). Antibodies used include α-cleaved caspase-3 (1:300, Cell Signaling), α-tyrosine hydroxylase (1:1000, Millipore), α-βIII-tubulin [TuJ1] (1:200, Sigma), and α-p75 [NGFr] (1:200, Advanced Targeting Systems). The number of cleaved caspase-3 positive neurons was counted on every third section by an observer naïve to the genotypes of the mice. Area measurements of SCGs were performed in the AxioVision software (Zeiss) using the “Outline” function. For total cell counts, SCGs were serially sectioned at a thickness of 30 µM, stained for TuJ1, TH, and DAPI, and all neurons were quantified using either TuJ1 or TH as a surrogate marker as described in the figure legend.

Figures

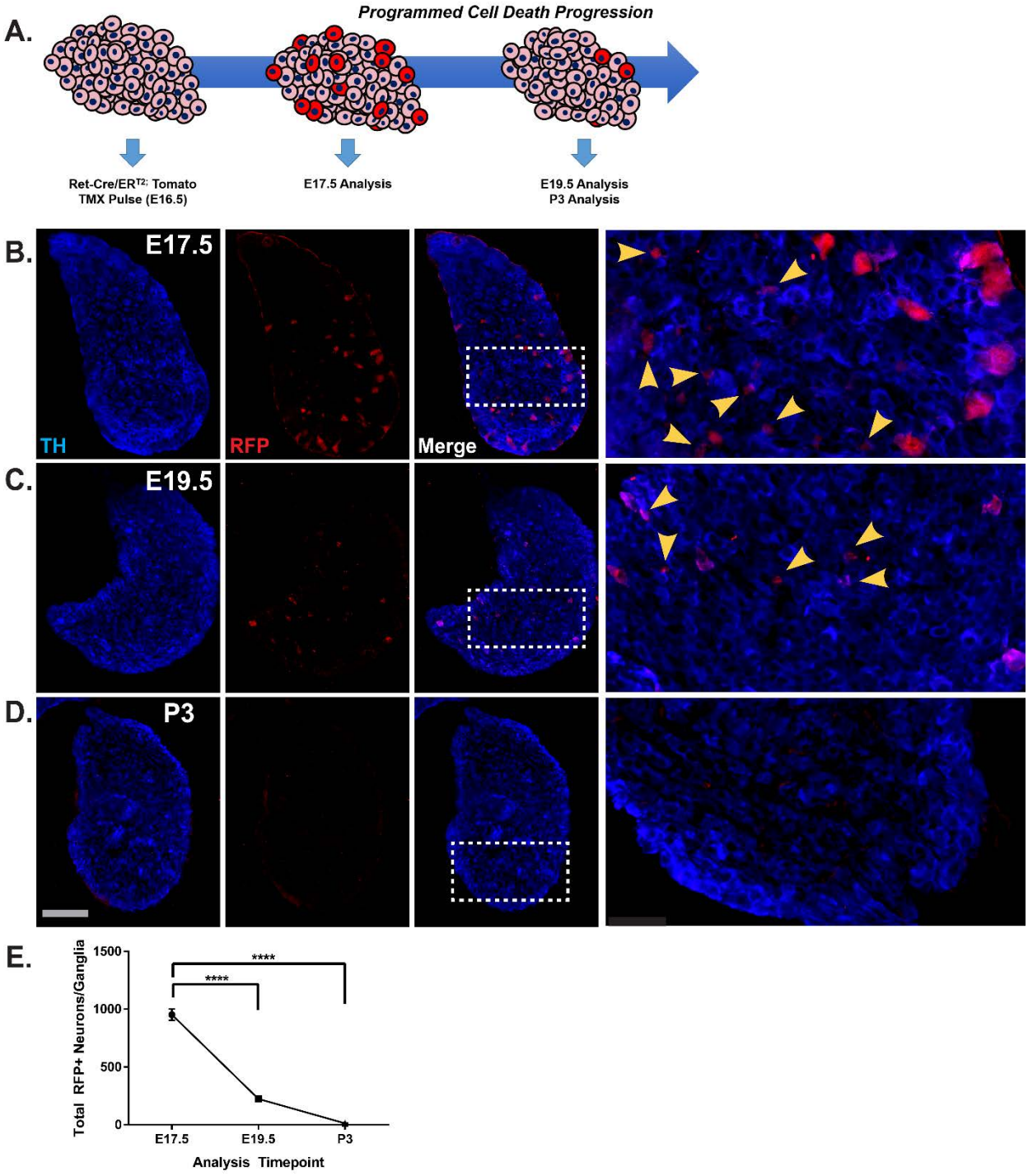
A.
Programmed Cell Death Progression
Ret-Cre/ER^{T2}: Tomato
TMX Pulse (E16.5)
E17.5 Analysis
E19.5 Analysis
P3 Analysis
B.
E17.5
TH
RFP
Merge
C.
E19.5
D.
P3
E.
Total RFP+ Neurons/Ganglia
1500
1000
500
0
****
****
E17.5
E19.5
P3
Analysis Timepoint

Figure 3.1. Ret+ neurons are eliminated during programmed cell death.

(A) Experimental strategy for fate determination of sympathetic neurons expressing Ret at E16.5 throughout the period of programmed cell death. Ret-Cre/ER^{T2}; tomato mice were administered TMX at E16.5, a timepoint by which SCG coalescence and migration is largely complete. Ganglia were then collected at E17.5, E19.5, and P3, and the total number of RFP+ neurons was quantified to ascertain the number of neurons expressing Ret. Immunostaining of SCGs for TH (blue; left-most panel) and RFP (red; indicates Ret expression) was performed at E17.5 (B), E19.5 (C), and P3 (D), with the area indicated in the dotted box magnified in the right-most panel. Yellow arrowheads indicate neurons with atrophic profiles, as indicated by reduced somal diameter, atypical shape, and weak RFP expression. (E) Quantification of total RFP+ neurons per ganglion at each time point. Scale bar, 200 μm.

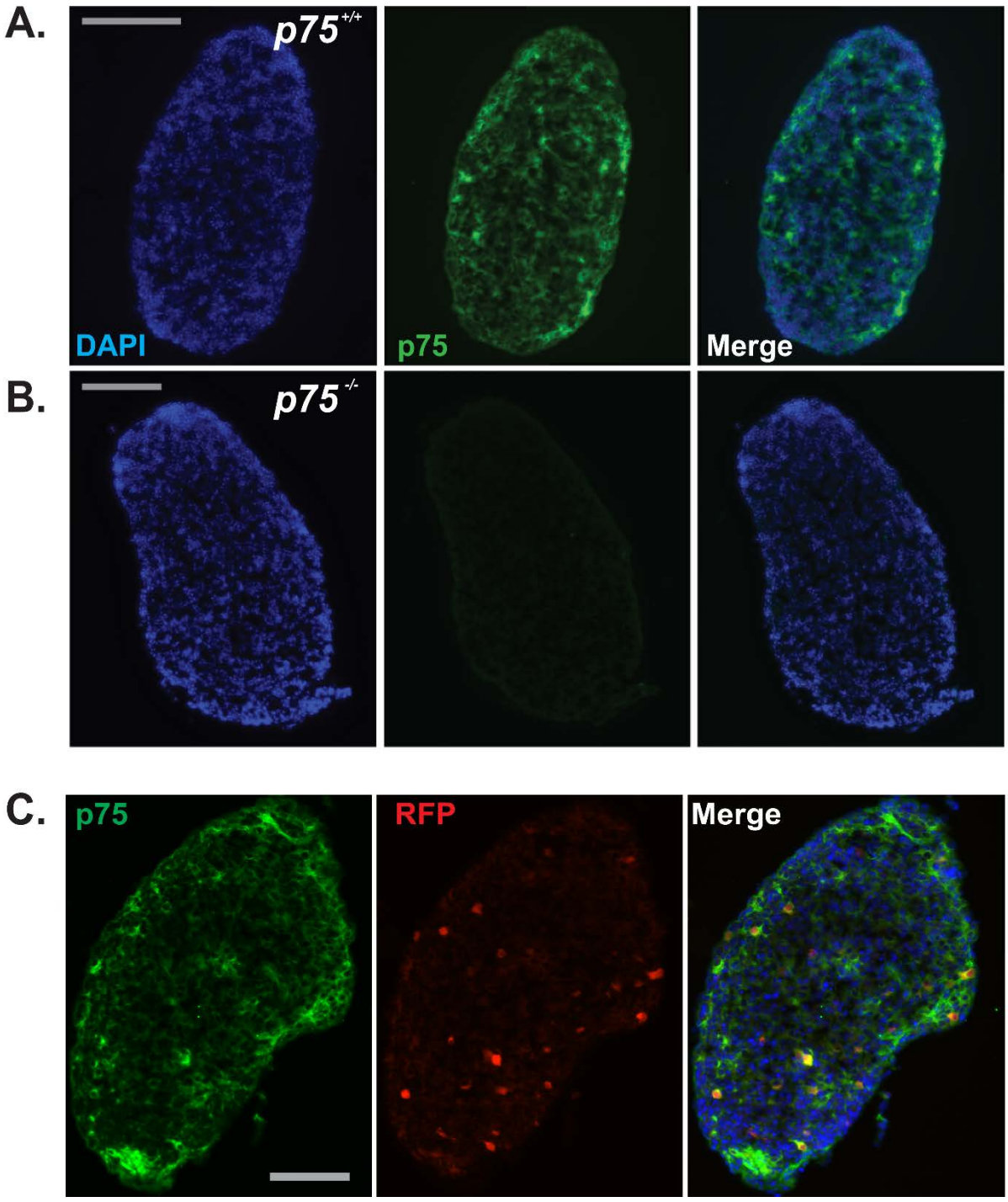

Figure 3.2. Validation of p75 immunostaining.

(A) p75 immunostaining in SCGs taken from *p75*$^{+/+}$ mice. Nuclei are stained with DAPI (blue) and p75 is shown in green. The merged image (panel 3) indicates widespread expression throughout the SCG. **(B)** *p75*$^{-/-}$ SCGs mice lack p75 immunoreactivity. These experiments were performed on animals at P0 (n=3 per genotype). Scale bars: 100 µM.

(C) p75 immunostaining in E18.5 SCGs dissected from *Ret*-Cre/ER^{T2}; tomato mice. Neurons are stained for p75 (green), RFP (labeled Ret+ cells; red), and merged with DAPI to visualize the entire SCG. While p75 staining was observed in most cells throughout the SCG, RFP+ cells were restricted to a subpopulation of highly p75+ neurons. Scale bar: 100 μM. These immunofluorescent labeling experiments were performed at least 3 independent times.

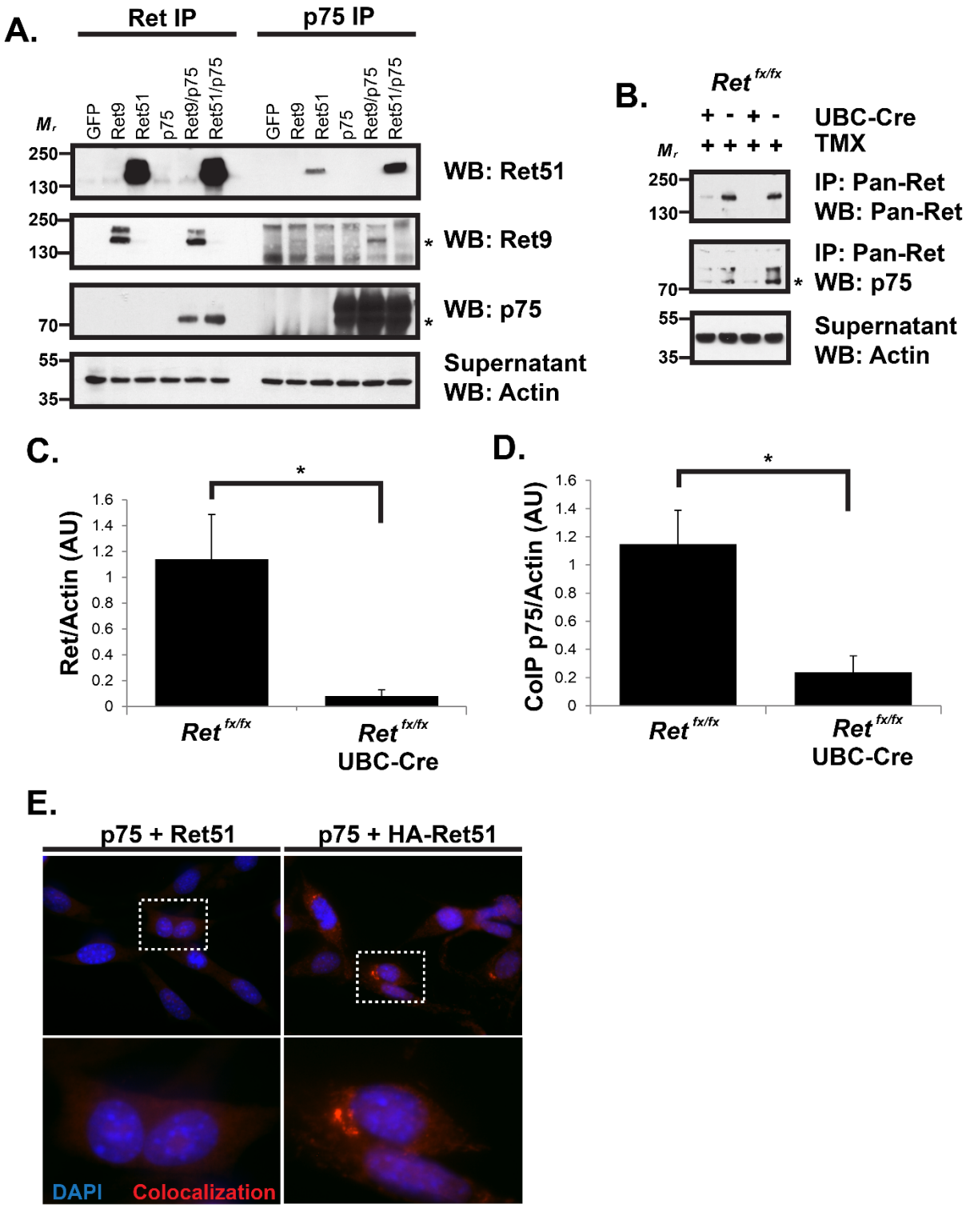
A.
Ret IP
p75 IP
GFP
Ret9
Ret51
p75
Ret9/p75
Ret51/p75
Mr
250
130
70
55
35
WB: Ret51
WB: Ret9
WB: p75
Supernatant
WB: Actin
B.
Ret fx/fx
UBC-Cre
TMX
IP: Pan-Ret
WB: Pan-Ret
IP: Pan-Ret
WB: p75
Supernatant
WB: Actin
C.
Ret/Actin (AU)
Ret fx/fx
Ret fx/fx
UBC-Cre
D.
CoIP p75/Actin (AU)
Ret fx/fx
Ret fx/fx
UBC-Cre
E.
p75 + Ret51
p75 + HA-Ret51
DAPI
Colocalization

Figure 3.3. p75 and Ret interact *in vitro* and *in vivo*.

(A) NIH/3T3 cells were transfected as indicated with GFP, Ret9, Ret51, p75, Ret9/p75, or Ret51/p75 (5 µg total DNA per lane). 36 hours following transfection, cells were lysed and immunoprecipitated for Ret (left 6 lanes) or p75 (right 6 lanes). Immunoprecipitates were run side-by-side to verify validity of protein detection, with immunoblotting for Ret9, Ret51, p75, and actin, as a loading control. These experiments were repeated 5 independent times with similar results. (B) $Ret^{fx/fx}$ mice with or without UBC-Cre/ER^{T2} were administered tamoxifen (TMX) as indicated above the figure. Spinal cords were then lysed, detergent extracted, and subjected to Ret immunoprecipitation followed by immunoblotting for Ret, p75, and actin. (C) Quantification of Ret (normalized to actin) indicated $Ret^{fx/fx}$; UBC-Cre/ER^{T2} mice had significantly reduced levels of Ret ($p < 0.05$; n=6; two-tailed t-test). (D) Quantification of p75 (normalized to actin) indicated that deletion of Ret led to a corresponding loss of co-immunoprecipitating p75 ($p < 0.05$; n=6; two-tailed t-test), indicating that this interaction is specific and occurs *in vivo*. (**E**) NIH/3T3 cells were transfected as indicated (Ret51 and p75 [left] or HA-tagged Ret51 and p75 [right], with higher magnification panels displayed on bottom) followed by brief fixation. DuoLink proximity ligation assays were conducted per manufacturer instructions utilizing α-p75 and α-HA primary antibodies. Red staining indicates the colocalization pattern observed in 3T3 cells transfected with HA-Ret51 and p75 compared to Ret51 and p75 transfected 3T3 cells. These assays were performed three independent times with similar results.

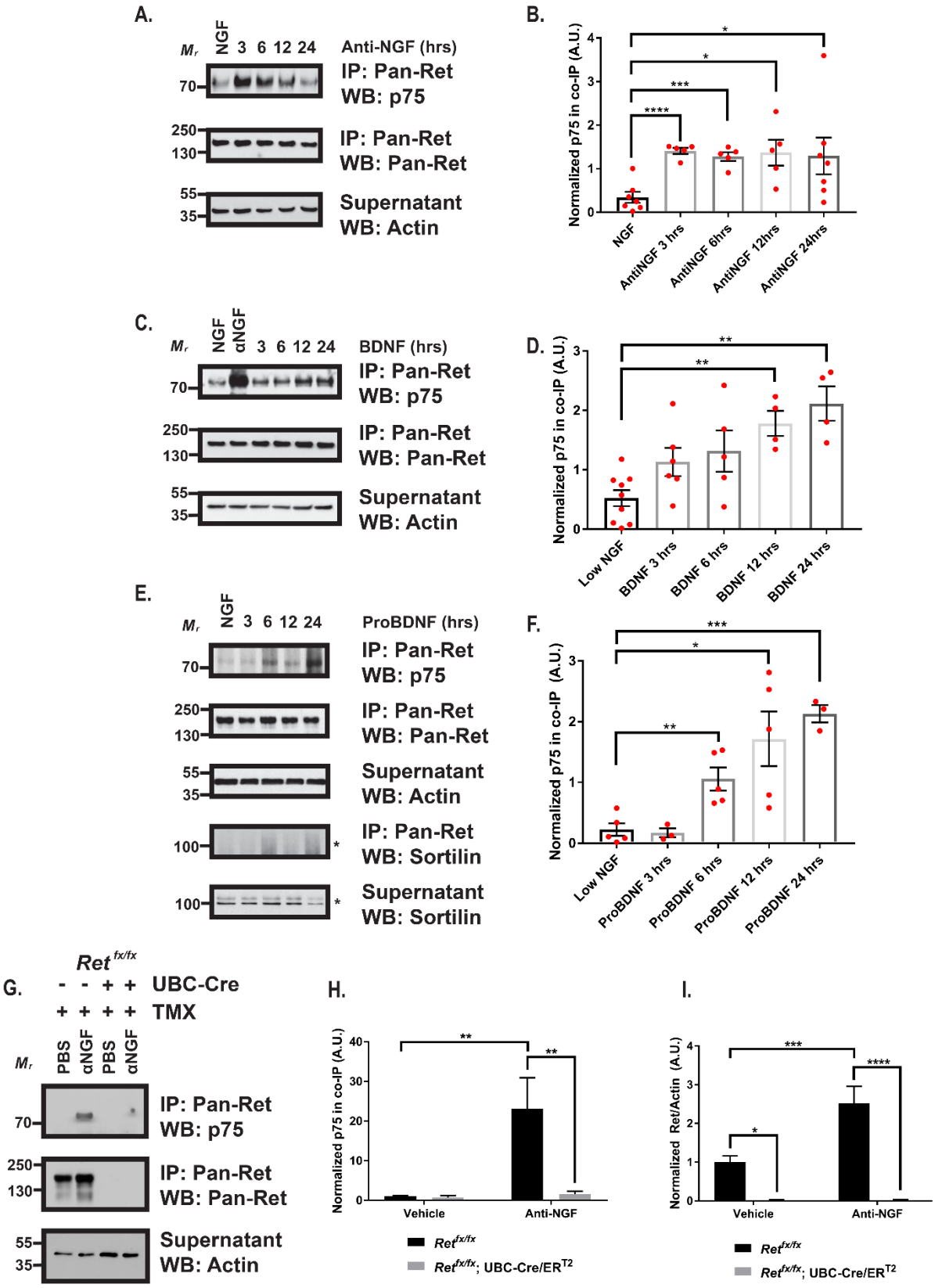
A.
Mr
NGF
3 6 12 24
Anti-NGF (hrs)
70
IP: Pan-Ret
WB: p75
250
130
IP: Pan-Ret
WB: Pan-Ret
55
35
Supernatant
WB: Actin
B.
Normalized p75 in co-IP (A.U.)
NGF
AntiNGF 3 hrs
AntiNGF 6hrs
AntiNGF 12hrs
AntiNGF 24hrs
C.
NGF
αNGF
3 6 12 24
BDNF (hrs)
D.
Low NGF
BDNF 3 hrs
BDNF 6 hrs
BDNF 12 hrs
BDNF 24 hrs
E.
ProBDNF (hrs)
100
IP: Sortilin
Supernatant
F.
ProBDNF 3 hrs
ProBDNF 6 hrs
ProBDNF 12 hrs
ProBDNF 24 hrs
G.
Ret fx/fx
UBC-Cre
TMX
PBS
αNGF
H.
Vehicle
Anti-NGF
Ret fx/fx
Ret fx/fx; UBC-Cre/ER T2
I.
Normalized Ret/Actin (A.U.)

Figure 3.4. Pro-apoptotic stimuli induce p75-Ret complex formation.

(A) Primary sympathetic neurons were cultured in NGF for 2 days, followed by NGF deprivation for 0, 3, 6, 12, or 24 hours as indicated. Ret was immunoprecipitated, followed by immunoblotting for p75, Ret, and actin. (B) Quantifications of panel A. NGF deprivation led to a significant increase in the amount of p75 associated with Ret at all time points analyzed (n=5-7). (C) Primary sympathetic neurons were treated with 200 ng/ml BDNF for 3, 6, 12, and 24 hours followed by immunoprecipitation and immunoblotting as described in A. (D) Quantification of these results indicate that BDNF treatment increases p75-Ret association at 12 hours ($p < 0.01$; n=4) and 24 hours ($p < 0.01$; n=4). (E) Primary sympathetic neurons were treated with 10 ng/ml of a cleavage-resistant recombinant proBDNF (Alomone Labs), followed by immunoprecipitation and immunoblotting as described in A. Sortilin immunoblotting was conducted and detected in supernatants, but not immunoprecipitates. (F) Quantification of these results indicates that proBDNF treatment increases p75-Ret association at 6 hours ($p < 0.01$; n=5), 12 hours ($p < 0.05$, n=5), and 24 hours ($p < 0.001$, n=3). (G) *Ret*$^{fx/fx}$ mice with or without UBC-Cre/ER^{T2} were administered TMX via i.p. injection once per day for 4 days, followed by administration of a blocking antibody against NGF (αNGF), or vehicle as a control, every 12 hours for 2 days. SCGs were then isolated, detergent extracted, and Ret was immunoprecipitated. These immunoprecipitates were immunoblotted for Ret, p75, and actin. (H) Quantification of immunoprecipitated p75 demonstrated that administration of control mice with αNGF led to a significant increase in p75-Ret association ($p < 0.05$; ANOVA; n=7 per genotype/treatment condition). (I) Quantification of Ret demonstrates that TMX delivery was effective at deleting Ret in UBC-Cre/ER^{T2} animals ($p < 0.01$; ANOVA, n=7 per condition). Additionally, a significant increase in Ret was observed in *Ret*$^{fx/fx}$ animals administered αNGF compared to vehicle-treated mice ($p < 0.05$; n=7). For the experiments in A-F, significance was determined using a two-tailed t-test comparing each treatment variable to the 50 ng/ml NGF maintained treatment. All quantifications are normalized to a loading control (actin). Due to variability between experiments, both individual data points from each experiment as well as bar graphs indicating the averages with error bars (mean ± s.e.m.) are displayed for the time course experiments in A-F.

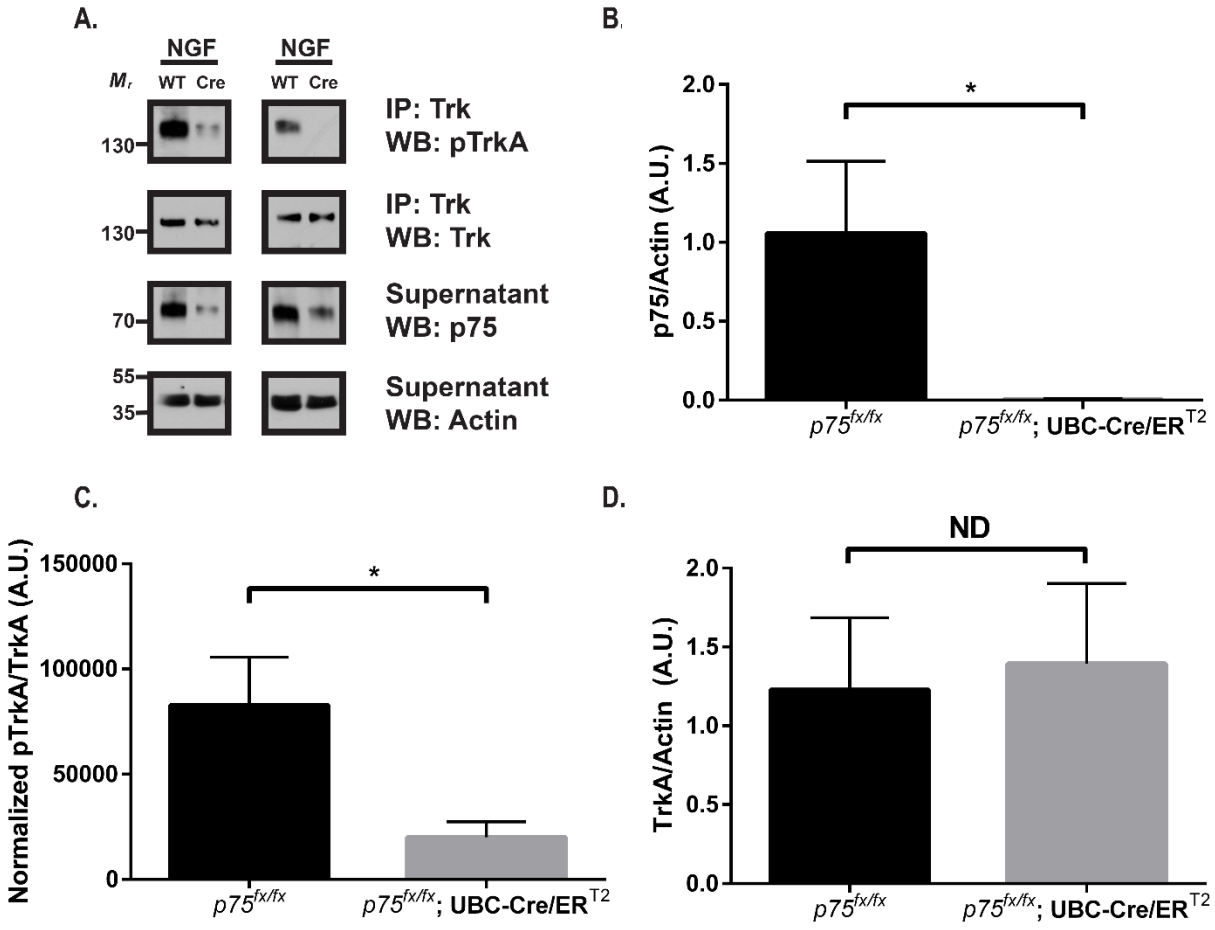

Figure 3.5: p75 potentiates NGF-TrkA signaling in sympathetic neurons.
(A) TrkA immunoprecipitations from *p75$^{fx/fx}$* and *p75$^{fx/fx}$*; UBC-Cre/ER^{T2} primary sympathetic neurons treated with 4-OH-TMX were subjected to western blotting for pTrkA and TrkA to determine the ratio of activated TrkA. Actin immunoblotting of the supernatants was performed as a loading control, while p75 immunoblotting was performed to ensure effective knockdown in p75-cKO mice. Two independent experiments are shown side-by-side. **(B)** Quantification of p75 normalized to actin levels demonstrates efficient knockdown of p75 in *p75$^{fx/fx}$*; UBC-Cre/ER^{T2} neurons (n=3; $p < 0.05$). **(C)** Quantification of the ratio of activated TrkA (pTrkA/TrkA, normalized to actin) indicates that *p75$^{fx/fx}$*; UBC-Cre/ER^{T2} mice have significantly reduced activation of TrkA (n=3; $p < 0.05$). **(D)** Quantification of TrkA levels indicates no difference between genotypes. All experiments display the mean ± s.e.m. (n=3 independent experiments). Two-tailed t-test with a significance level of $p \leq 0.05$ was used to test significance.

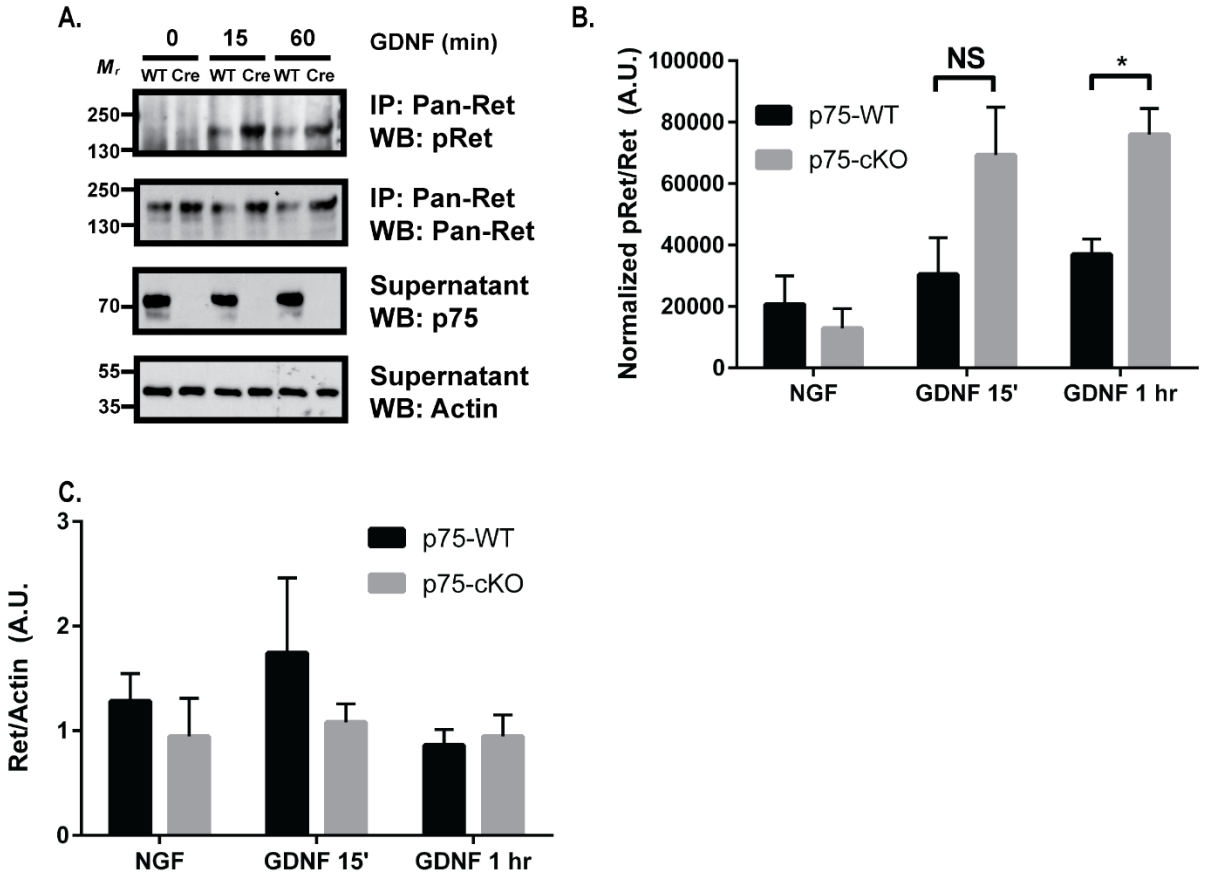

Figure 3.6. p75 inhibits canonical Ret signaling.

(A) *p75*$^{fx/fx}$ (p75-WT) and *p75*$^{fx/fx}$; UBC-Cre/ER^{T2} (p75-cKO) primary sympathetic neurons were treated with 4-OH-TMX and maintained in NGF. Neurons were then treated with medium alone, or with GDNF (50 ng/ml) for 15 minutes or one hour (as indicated in the figure) and subjected to Ret immunoprecipitation followed by immunoblotting for pTyr and Ret to determine the proportion of activated Ret. Actin and p75 immunoblotting of supernatants were performed as a control. **(B)** Quantification of activated Ret (pRet/Ret, normalized to actin) are displayed. GDNF-mediated Ret activation at 1 hour, but not 15 minutes, was significantly enhanced in p75-cKO neurons ($p < 0.05$; Two-way ANOVA). **(C)** Quantification of total Ret levels indicated that deletion of p75 did not significantly alter Ret levels. All experiments display the mean ± s.e.m., with n=4-7 per treatment. Two-way ANOVA with a significance level of $p \leq 0.05$ was used to test significance.

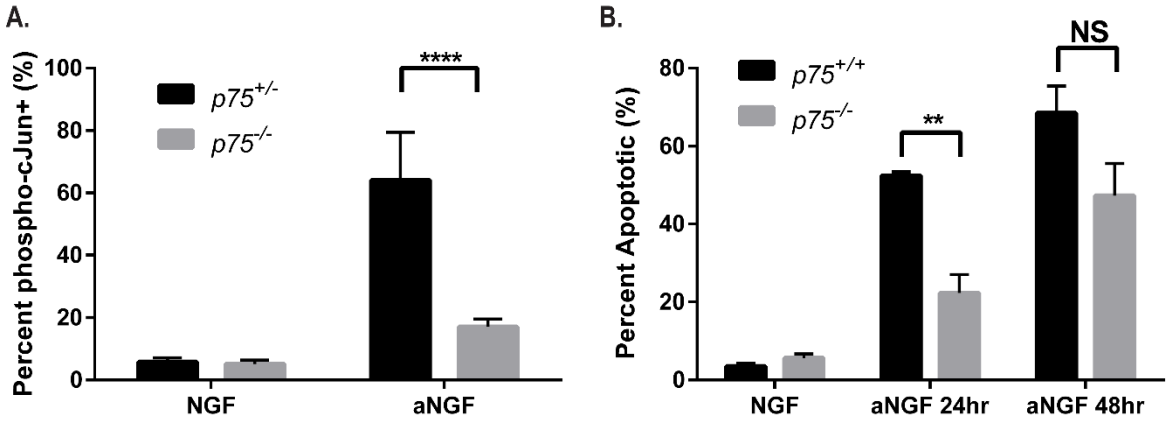

Figure 3.7. p75 promotes sympathetic neuron apoptosis through a p-cJun dependent pathway.

(A) Primary sympathetic neurons were cultured from P0 *p75*$^{+/-}$ and *p75*$^{-/-}$ mice in the presence of NGF. 2 days after plating, neurons were either maintained in high NGF (50 ng/ml) or deprived of NGF and treated with an anti-NGF blocking antibody. 12 hours post-treatment, the percent of neurons with phospho-c-Jun+ (p-cJun) nuclei were quantified. p75$^{-/-}$ neurons had significantly fewer p-cJun+ nuclei compared to *p75*$^{+/-}$ ($p < 0.0001$), suggesting that initiation of apoptosis was impaired in the absence of p75. Significance was tested between all groups using a two-way ANOVA (n=3 *p75*$^{+/-}$ and n=7 *p75*$^{-/-}$). **(B)** *p75*$^{+/-}$ and *p75*$^{-/-}$ neurons were cultured as in panel A and deprived of NGF for 24 or 48 hours, followed by quantification of the number of pyknotic nuclei to ascertain the number of apoptotic neurons. Loss of p75 led to a significant decrease in apoptosis by 24 hours following NGF deprivation ($p < 0.0001$), but no significant differences were observed by 48 hours.

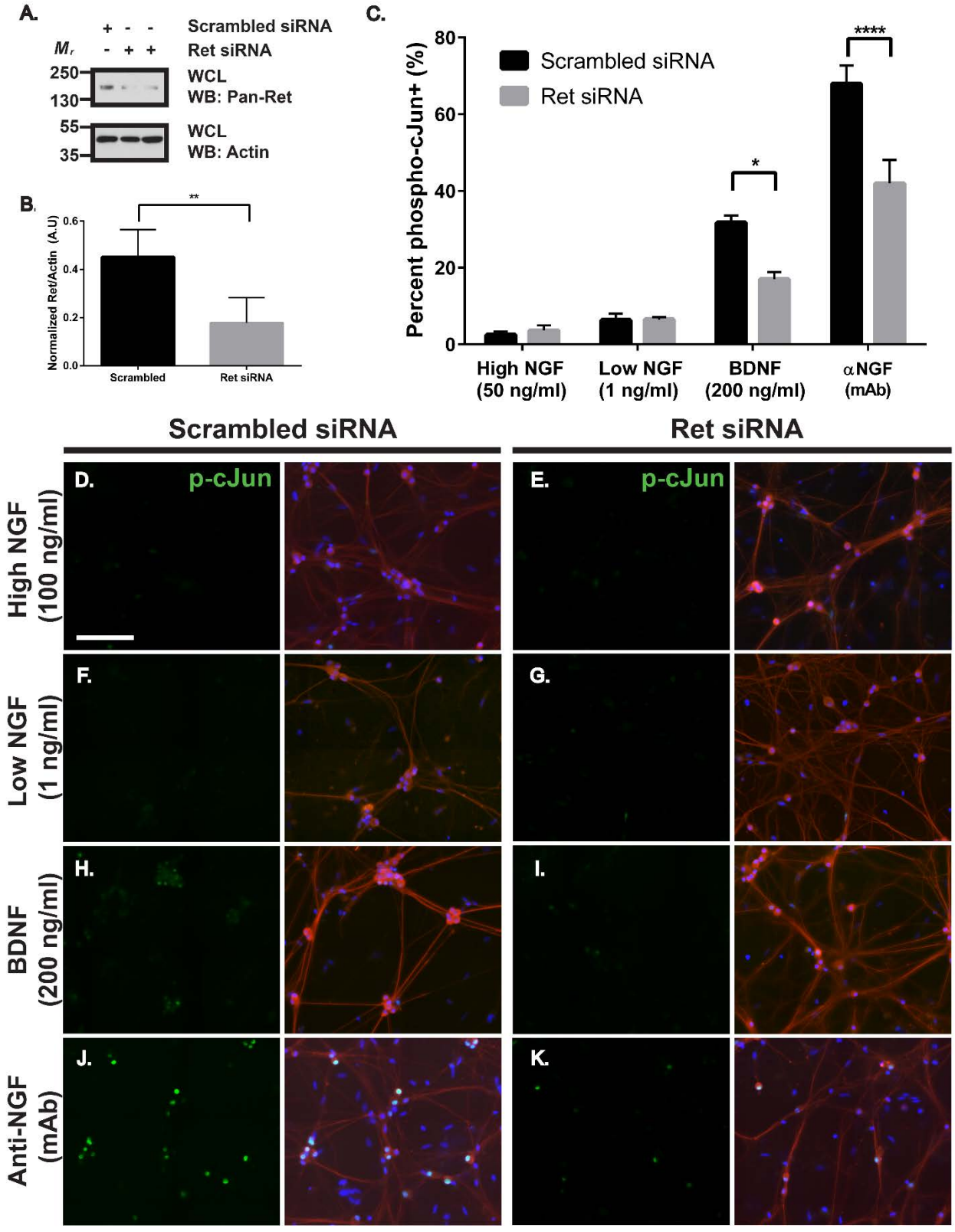
A.
+ - - Scrambled siRNA
M_r - + + Ret siRNA
250
130
WCL
WB: Pan-Ret
55
35
WCL
WB: Actin
B.
**
Normalized Ret/Actin (A.U)
0.6
0.4
0.2
0.0
Scrambled
Ret siRNA
C.
Scrambled siRNA
Ret siRNA
Percent phospho-cJun+ (%)
80
60
40
20
0
*
****
High NGF (50 ng/ml)
Low NGF (1 ng/ml)
BDNF (200 ng/ml)
αNGF (mAb)
Scrambled siRNA
Ret siRNA
High NGF (100 ng/ml)
Low NGF (1 ng/ml)
BDNF (200 ng/ml)
Anti-NGF (mAb)
D. p-cJun
E. p-cJun
F.
G.
H.
I.
J.
K.

Figure 3.8: Ret knockdown blocks p75-mediated p-cJun activation.

(A) Primary E18-P0 rat sympathetic neurons were cultured and transfected with scrambled (left two lanes) or Ret siRNA (right two lanes). 48 hours following transfection, neurons were lysed and immunoblotted for Ret and actin. (B) Quantification of Ret indicates a significant reduction of Ret following siRNA knockdown compared to scrambled control (65%; $p < 0.01$; n=4). (C) Neurons transfected with scrambled or Ret siRNA were treated with high NGF (50 ng/ml), low NGF (1 ng/ml), low NGF (1 ng/ml) with BDNF (200 ng/ml), or αNGF for 12 hours, followed by quantification of the number of p-cJun+ nuclei as described in Supplemental Figure 2. Ret knockdown significantly reduced p-cJun+ nuclei in BDNF ($p < 0.05$) and αNGF ($p < 0.0001$) treated neurons. (D-K) Examples of images of each treatment. TuJ1 (pan-neuronal marker) is displayed in red, nuclei are displayed in blue, and p-cJun is displayed in green. For each treatment, the left-most column displays p-cJun alone. Importantly, rarely were p-cJun+ nuclei observed in NGF-maintained neurons (D-G), while BDNF and αNGF treatment led to significant phosphorylation of cJun (H, J), which was inhibited in Ret siRNA-treated neurons (I, K). Statistical significance was determined using a two-way ANOVA with multiple comparisons, n=4 per condition. Scale bar, 100 μm.

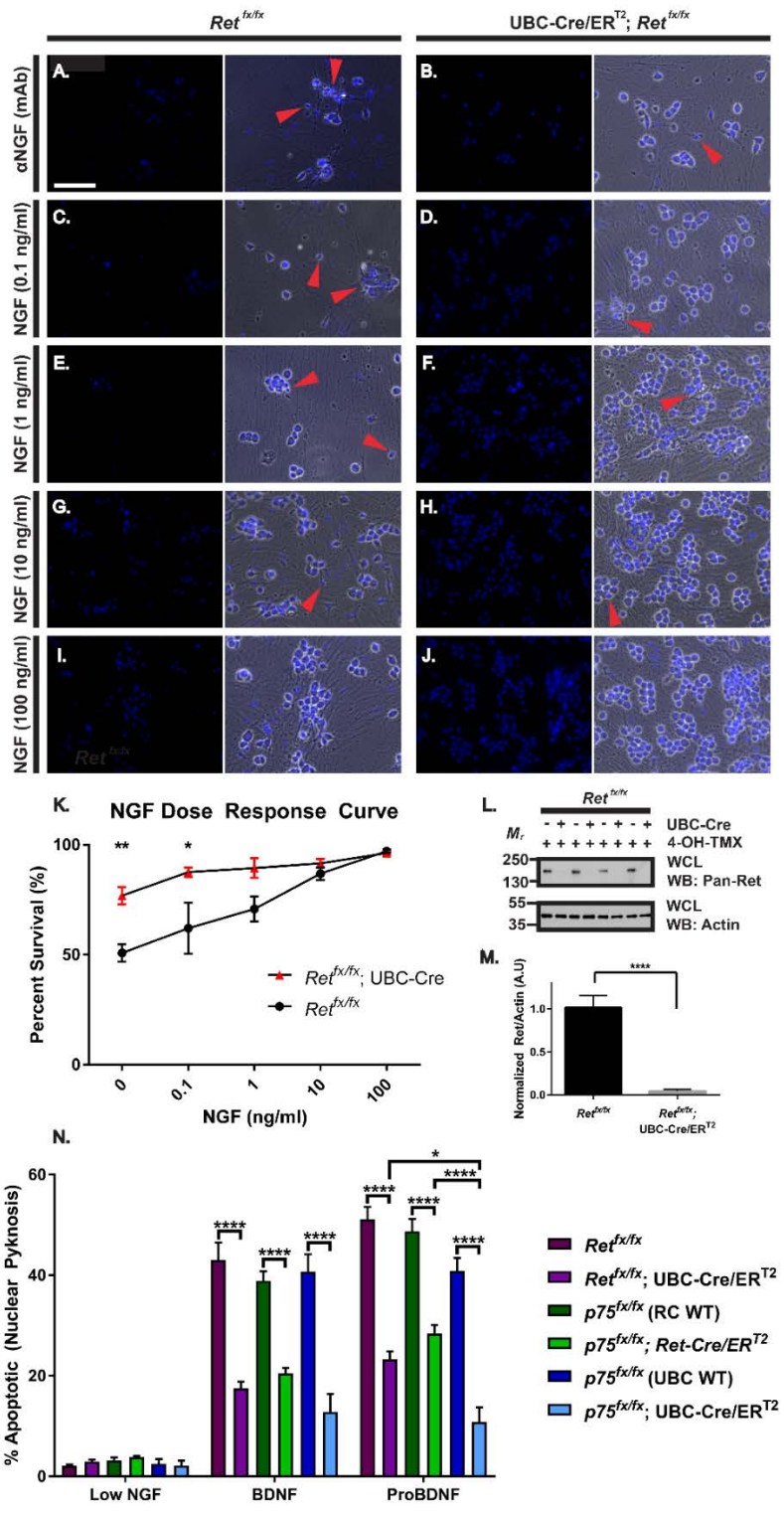

Figure 3.9: Ret deletion enhances NGF-mediated survival.

Ret$^{fx/fx}$ (Ret-WT) and *Ret*$^{fx/fx}$; UBC-Cre/ER^{T2} (Ret-cKO) primary sympathetic neurons were treated with 4-OH-TMX and maintained in NGF. Neurons were then treated for 24 hours with complete NGF deprivation using an anti-NGF blocking antibody (αNGF; panels A, B), 0.1 ng/ml NGF (panels C, D), 1.0 ng/ml NGF (panels E, F), 10 ng/ml NGF (panels G, H), or 100 ng/ml NGF (panels I, J). DAPI alone (left) and DAPI/Phase merged images (right) are displayed. Red arrows indicate apoptotic neurons with pyknotic nuclei. Scale bar represents 100 μM. As expected, increasing concentrations led to a dose-dependent reduction in the number of apoptotic nuclear profiles. (K) Quantification of survival counts. Ret-cKO mice had increased survival in a dose-dependent manner compared to Ret-WT neurons, with significant differences observed with αNGF ($p < 0.01$; n=4 per treatment group) and 0.1 ng/ml ($p < 0.05$; n =3) treatments. Statistical significance was determined using a two-way ANOVA with multiple comparisons, n=3-6 per treatment group. (L) Immunoblot demonstrating the efficacy of Ret knockdown using the 4-OH-TMX system. (M) Quantification of Ret knockdown indicated that greater than 90% of Ret was deleted in Ret-cKO compared to Ret-WT neurons ($p < 0.0001$; two-tailed t-test; n =11-13 per treatment group). (N) Neurons were cultured from animals of the indicated genotypes and maintained as above, followed by treatment with low (1 ng/ml) NGF, or low NGF in the presence of 200 ng/ml BDNF or 10 ng/ml proBDNF. Neurons were fixed after 48 hours, followed by quantification of nuclear pyknosis to ascertain neuronal apoptosis. BDNF and proBDNF induced a significant increase in apoptosis compared to low NGF-maintained neurons, which was significantly reduced in Ret cKO (compared to Ret-WT, n=4 per genotype and treatment group), p75-RC (compared to p75-WT, n=5-6 per genotype and treatment group), and p75-cKO (compared to p75-WT, n=4 per genotype and treatment group) neurons. Quantifications are displayed as the mean percent of apoptotic neurons ± s.e.m. More than 300 neurons were quantified for each treatment. Scale bar, 100 μm.

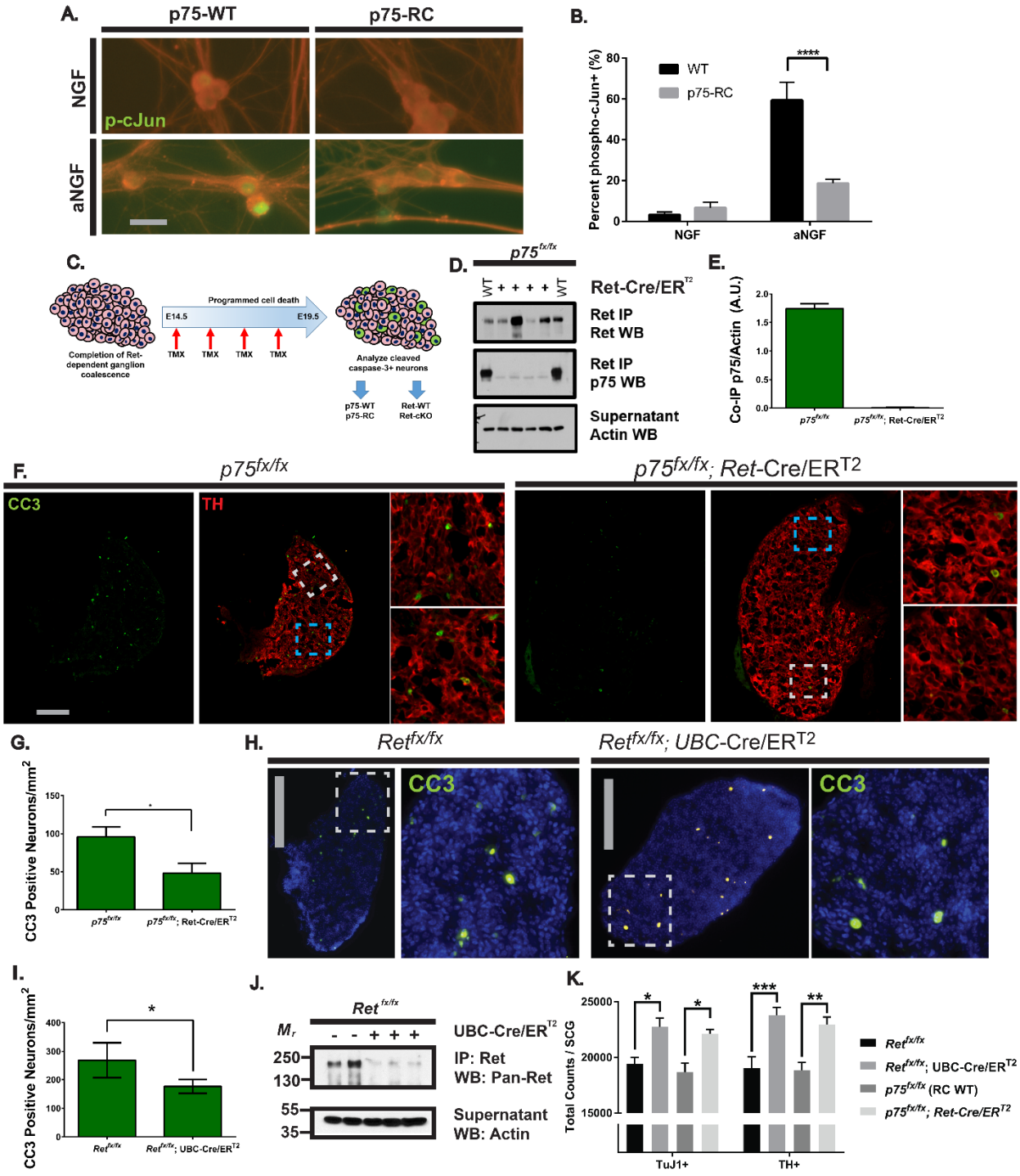

Figure 3.10: Ret collaborates with p75 to mediate sympathetic neuron apoptosis in vivo.

(A) *p75*$^{fx/fx}$ (p75-WT) and *p75*$^{fx/fx}$; *Ret*-Cre/ER^{T2} (p75-RC) primary sympathetic neurons maintained in NGF were treated with 4-OH-TMX to induce recombination. Neurons were then maintained in NGF or deprived of NGF for 24 hours as indicated. Neurons

were stained for TuJ1 (red) or p-c-Jun (green). αNGF application led to robust activation of p-c-Jun in p75-WT neurons, and this activation was significantly abrogated in p75-RC neurons. Scale bar, 25 µm. **(B)** Quantifications of (A) indicate a highly significant difference in NGF deprivation-induced p-cJun activation. **(C)** Experimental strategy for cell autonomous deletion of p75 within Ret+ neurons using *p75*$^{fx/fx}$; *Ret*-Cre/ER^{T2} mice as well as global deletion of Ret utilizing *Ret*$^{fx/fx}$; *UBC*-Cre/ER^{T2} (Ret-cKO) mice. The delivery of TMX between E14.5-E18.5 was employed to avoid the deleterious effects of Ret deletion on early SCG neuron migration and coalescence. Cleaved caspase-3 immunolabeling was conducted to ascertain apoptosis (indicated as green cells). **(D)** Western blot demonstrating efficacy of p75 deletion using the Ret-Cre/ER^{T2} driver and the deletion strategy in (C). **(E)** Quantification of p75 levels immunoprecipitating with Ret normalized to actin. p75-RC mice have significantly reduced p75 compared to p75-WT mice. **(F)** Immunolabeling of TH (red) and cleaved caspase-3 (cc3; green) in p75-WT and p75-RC SCGs. Large panels indicate overall cc3 activity throughout the ganglion, with the two indicated areas shown (upper is white, lower is blue) at larger magnification. Scale bar, 100 □m. **(G)** Quantification of the number of cc3+ neurons normalized to ganglion area indicated that p75-RC mice have significantly reduced apoptosis (two-tailed t-test; $p < 0.05$; n=4 p75-WT and n=7 p75-RC). **(H)** Ret-WT and Ret-cKO SCGs were stained for DAPI and cc3 to ascertain the number of apoptotic neurons. For each genotype, panels on left represent sections of whole ganglia with increased magnification around the selected area displayed to the right. Ret-WT SCGs had fewer cc3+ neurons compared to p75-WT mice (two-tailed t-test; $p < 0.05$; n=5 per genotype), which was quantified in **(I)**. Scale bar, 200 µm. **(J)** Immunoblotting of spinal cords taken from Ret-WT and Ret-cKO mice demonstrate the efficacy of Ret deletion using the experimental paradigm outlined in (C). (**K.**) SCGs were isolated from Ret-WT (n=4), Ret-cKO (n=6), p75-WT (n=3), and p75-cKO (n=5) mice, followed by serial sectioning and quantification of total cell counts using TuJ1 (left 4 bars) or TH (right 4 bars). A significant increase in total neuron numbers was observed in Ret-cKO SCGs compared to Ret-WT controls ($p > 0.05$ for TuJ1; $p > 0.001$ for TH) and in p75-RC SCGs compared to p75-WT controls ($p > 0.001$ for TuJ1; $p > 0.01$ for TH; two-way ANOVA).

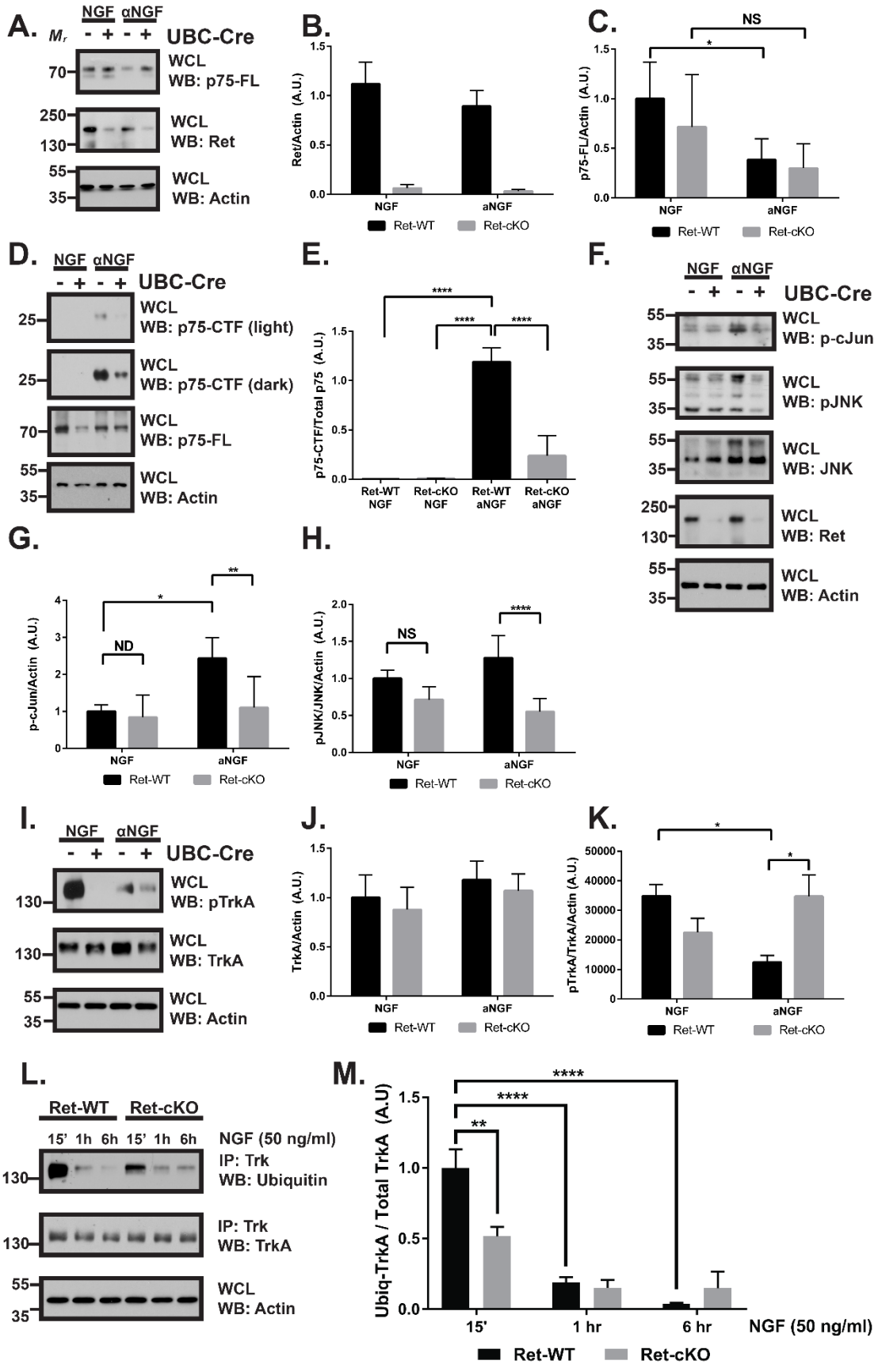
A.
NGF αNGF
- + - + UBC-Cre
Mr
70
WCL
WB: p75-FL
250
130
WCL
WB: Ret
55
35
WCL
WB: Actin
B.
Ret/Actin (A.U.)
1.5
1.0
0.5
0.0
NGF
aNGF
Ret-WT
Ret-cKO
C.
NS
*
p75-FL/Actin (A.U.)
1.5
1.0
0.5
0.0
NGF
aNGF
Ret-WT
Ret-cKO
D.
NGF αNGF
- + - + UBC-Cre
25
WCL
WB: p75-CTF (light)
25
WCL
WB: p75-CTF (dark)
70
WCL
WB: p75-FL
55
35
WCL
WB: Actin
E.
****
****
****
p75-CTF/Total p75 (A.U.)
1.5
1.0
0.5
0.0
Ret-WT NGF
Ret-cKO NGF
Ret-WT aNGF
Ret-cKO aNGF
F.
NGF αNGF
- + - + UBC-Cre
55
35
WCL
WB: p-cJun
55
35
WCL
WB: pJNK
55
35
WCL
WB: JNK
250
130
WCL
WB: Ret
55
35
WCL
WB: Actin
G.
p-cJun/Actin (A.U.)
4
3
2
1
0
*
**
ND
NGF
aNGF
Ret-WT
Ret-cKO
H.
pJNK/JNK/Actin (A.U.)
2.0
1.5
1.0
0.5
0.0
NS
****
NGF
aNGF
Ret-WT
Ret-cKO
I.
NGF αNGF
- + - + UBC-Cre
130
WCL
WB: pTrkA
130
WCL
WB: TrkA
55
35
WCL
WB: Actin
J.
TrkA/Actin (A.U.)
1.5
1.0
0.5
0.0
NGF
aNGF
Ret-WT
Ret-cKO
K.
*
*
pTrkA/TrkA/Actin (A.U.)
50000
40000
30000
20000
10000
0
NGF
aNGF
Ret-WT
Ret-cKO
L.
Ret-WT Ret-cKO
15' 1h 6h 15' 1h 6h
NGF (50 ng/ml)
130
IP: Trk
WB: Ubiquitin
130
IP: Trk
WB: TrkA
55
35
WCL
WB: Actin
M.
****
****
**
Ubiq-TrkA / Total TrkA (A.U)
1.5
1.0
0.5
0.0
15'
1 hr
6 hr
NGF (50 ng/ml)
Ret-WT
Ret-cKO

Figure 3.11: Ret inhibits pro-survival TrkA signaling and augments pro-apoptotic p75 cleavage and downstream signaling.

(A) *Ret*$^{fx/fx}$ (Ret-WT) and *Ret*$^{fx/fx}$; *UBC*-Cre/ER^{T2} (Ret-cKO) primary sympathetic neurons maintained in NGF were treated with 4-OH-TMX to induce recombination. Neurons were then maintained in NGF or deprived of NGF for 12 hours as indicated. Neurons were then lysed, detergent extracted, and immunoblotting was conducted for p75, Ret to verify deletion, and actin. **(B)** Ret-cKO neurons had drastically reduced levels of Ret (>90%) compared to Ret-WT controls, confirming efficacy of deletion (n=6-7 per treatment group) **(C)** Ret-WT neurons deprived of NGF had significantly reduced levels of full length p75 (p75-FL), consistent with NGF deprivation-induced cleavage ($p < 0.05$; n=3). This reduction in p75-FL was not observed in Ret-cKO neurons, indicating Ret is involved in the cleavage of p75. **(D)** Ret-WT and Ret-cKO SCG neurons were generated and treated as indicated in A, with the addition of the degradation inhibitors MG-132 and epoximicin to allow detection of the p75-CTF cleavage product. Samples were immunoblotted for full length p75 (p75-FL) and the C-terminal fragment cleavage product of p75 (p75-CTF), as well as actin. In our culture system, the p75-ICD is not detected. **(E)** Quantification of p75 cleavage (p75-CTF/p75-FL, normalized to actin). As expected, Ret-WT neurons, but not Ret-cKO neurons, had a highly statistically significant increase in p75 cleavage ($p < 0.0001$, n=3). NGF-deprived Ret-cKO neurons also had a highly significant decrease in p75 cleavage compared to NGF-deprived Ret-WT neurons ($p < 0.0001$, n=3). **(F)** Neurons were treated and samples prepared as described in A. Immunoblotting was performed for activated c-Jun (p-c-Jun), activated JNK (pJNK), total JNK, and actin. **(G)** Quantification of p-cJun, normalized to actin. In Ret-WT neurons, but not Ret-cKO neurons, a statistically significant increase was observed in p-c-Jun following NGF deprivation ($p < 0.05$, n=7 per treatment group). Following NGF deprivation, Ret-cKO neurons also displayed a significant decrease in p-c-Jun activation compared to Ret-WT neurons ($p < 0.001$, n=7 per treatment group). **(H)** Quantification of 46 kDa pJNK, normalized to total JNK and actin (pJNK/JNK/Actin). Following NGF deprivation, we observed a statistically significant decrease in activation of pJNK in Ret-cKO neurons compared with Ret-WT neurons ($p < 0.0001$, n=7). **(I)** Neurons were treated and samples prepared as described in A. Immunoblotting was performed for pTrkA, total TrkA, and actin. **(J)** Total levels of TrkA were not altered by deletion of Ret or by NGF deprivation after 12 hours (n=6 per treatment group) **(K)** As expected, deprivation of NGF led to a significant decrease in the proportion of activated TrkA (pTrkA/TrkA, normalized to actin) in Ret-WT neurons ($p < 0.05$, n=6 per treatment group), but not Ret-cKO neurons. Ret-cKO neurons also had a significant increase in the ratio of activated TrkA compared to Ret-WT neurons ($p < 0.05$, n=6 per treatment group). (**L**) Ret-WT or Ret-cKO neurons treated as described in (A) were deprived of NGF overnight to reduce TrkA activation. Neurons were then stimulated with 50 ng/ml NGF for 15 minutes, 1 hour, or 6 hours, following by TrkA immunoprecipitation and immunoblotting for ubiquitin, which is quantified in (**M**). As expected, robust ubiquitination of TrkA was observed in Ret-WT neurons at 15 minutes, as compared to later time points ($p > 0.0001$; n=4 for all treatments). Ret-cKO neurons had significantly reduced TrkA ubiquitination compared to Ret-WT neurons at 15 minutes ($p > 0.01$; n=4), and no significant differences were observed between TrkA-ubiquitination levels at

1 or 6 hours of NGF stimulation for Ret-cKO neurons compared to Ret-WT neurons. Data are represented as the mean ubiquitinated TrkA normalized to total TrkA ± s.e.m.

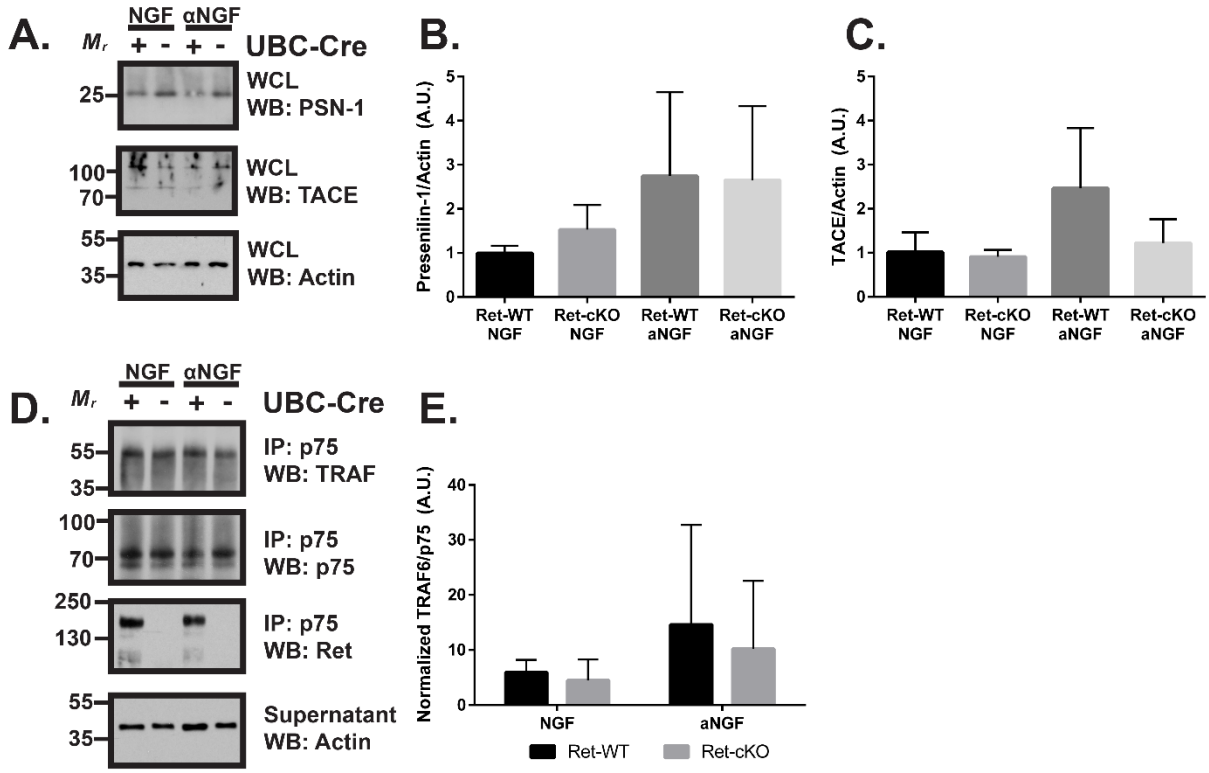

Figure 3.12: Removal of Ret does not alter TRAF6 association with p75 or upregulation of the p75 cleavage enzymes Presenilin-1 and TACE.

(A) *Ret*$^{fx/fx}$ (Ret-WT) and *Ret*$^{fx/fx}$; *UBC*-Cre/ER^{T2} (Ret-cKO) primary SCG neurons maintained in NGF were treated with 4-OH-TMX to induce recombination. Neurons were then maintained in NGF or deprived of NGF for 12 hours as indicated. Neurons were then lysed, detergent extracted, and immunoblotting was performed for TACE and presenilin-1, two enzymes required for regulated intramembrane proteolysis cleavage of p75. **(B)** Quantification of presenilin (PSN-1) normalized to actin and **(C)** TACE normalized to actin. No statistical differences were observed in any of the treatment groups. **(D)** Neurons were treated as described in A. Neurons were then lysed, detergent extracted, and immunoprecipitated for p75 followed by immunoblotting for TRAF6, p75, Ret (to confirm deletion), and actin, as a loading control. **(E)** Quantification of TRAF6 normalized to p75. No statistical differences were observed in any of the treatment groups (n=6-7 per treatment group).

Chapter 3 References

Airaksinen, M.S., and M. Saarma. 2002. The GDNF family: signalling, biological functions and therapeutic value. *Nat. Rev. Neurosci.* 3:383-394.

Aloyz, R.S., S.X. Bamji, C.D. Pozniak, J.G. Toma, J. Atwal, D.R. Kaplan, and F.D. Miller. 1998. p53 is essential for developmental neuron death as regulated by the TrkA and p75 neurotrophin receptors. *The Journal of cell biology*. 143:1691-1703.

Bamji, S.X., M. Majdan, C.D. Pozniak, D.J. Belliveau, R. Aloyz, J. Kohn, C.G. Causing, and F.D. Miller. 1998. The p75 neurotrophin receptor mediates neuronal apoptosis and is essential for naturally occurring sympathetic neuron death. *The Journal of cell biology*. 140:911-923.

Barker, V., G. Middleton, F. Davey, and A.M. Davies. 2001. TNFalpha contributes to the death of NGF-dependent neurons during development. *Nature neuroscience*. 4:1194-1198.

Bogenmann, E., P.S. Thomas, Q. Li, J. Kim, L.T. Yang, B. Pierchala, and V. Kaartinen. 2011. Generation of mice with a conditional allele for the p75(NTR) neurotrophin receptor Gene. *Genesis*.

Bordeaux, M.C., C. Forcet, L. Granger, V. Corset, C. Bidaud, M. Billaud, D.E. Bredesen, P. Edery, and P. Mehlen. 2000. The RET proto-oncogene induces apoptosis: a novel mechanism for Hirschsprung disease. *The EMBO journal*. 19:4056-4063.

Calco, G.N., O.R. Stephens, L.M. Donahue, C.C. Tsui, and B.A. Pierchala. 2014. CD2-associated Protein (CD2AP) Enhances Casitas B-lineage Lymphoma-3/c (Cbl-

3/c)-mediated Ret Isoform-specific Ubiquitination and Degradation via its Amino-terminal SRC Homology 3 (SH3) Domains. *The Journal of biological chemistry*.

Chao, M.V. 2003. Neurotrophins and their receptors: a convergence point for many signalling pathways. *Nature reviews. Neuroscience*. 4:299-309.

Chen, Z., C.R. Donnelly, B. Dominguez, Y. Harada, W. Lin, A.S. Halim, T.G. Bengoechea, B.A. Pierchala, and K.F. Lee. 2017. p75 Is Required for the Establishment of Postnatal Sensory Neuron Diversity by Potentiating Ret Signaling. *Cell reports*. 21:707-720.

de Graaff, E., S. Srinivas, C. Kilkenny, V. D'Agati, B.S. Mankoo, F. Costantini, and V. Pachnis. 2001. Differential activities of the RET tyrosine kinase receptor isoforms during mammalian embryogenesis. *Genes Dev.* 15:2433-2444.

Deckwerth, T.L., and E.M. Johnson, Jr. 1993. Temporal analysis of events associated with programmed cell death (apoptosis) of sympathetic neurons deprived of nerve growth factor. *J. Cell Biol.* 123:1207-1222.

Deppmann, C.D., S. Mihalas, N. Sharma, B.E. Lonze, E. Niebur, and D.D. Ginty. 2008. A model for neuronal competition during development. *Science*. 320:369-373.

Deshmukh, M., and J. Johnson, E.M. 1997. Programmed cell death in neurons: focus on the pathway of nerve growth factor deprivation-induced death of sympathetic neurons. *Molec. Pharm.* 51:897-906.

Enomoto, H., P.A. Crawford, A. Gorodinsky, R.O. Heuckeroth, E.M. Johnson, Jr., and J. Milbrandt. 2001. RET signaling is essential for migration, axonal growth and axon guidance of developing sympathetic neurons. *Development 128, 3963-3974*. 128:3963-3974.

Gentry, J.J., P.A. Barker, and B.D. Carter. 2004. The p75 neurotrophin receptor: multiple interactors and numerous functions. *Progress in brain research*. 146:25-39.

Harel, L., B. Costa, M. Tcherpakov, M. Zapatka, A. Oberthuer, L.M. Hansford, M. Vojvodic, Z. Levy, Z.Y. Chen, F.S. Lee, S. Avigad, I. Yaniv, L. Shi, R. Eils, M. Fischer, B. Brors, D.R. Kaplan, and M. Fainzilber. 2009. CCM2 mediates death signaling by the TrkA receptor tyrosine kinase. *Neuron*. 63:585-591.

Ibanez, C.F., and A. Simi. 2012. p75 neurotrophin receptor signaling in nervous system injury and degeneration: paradox and opportunity. *Trends Neurosci*. 35:431-440.

Kanning, K.C., M. Hudson, P.S. Amieux, J.C. Wiley, M. Bothwell, and L.C. Schecterson. 2003. Proteolytic processing of the p75 neurotrophin receptor and two homologs generates C-terminal fragments with signaling capability. *The Journal of neuroscience : the official journal of the Society for Neuroscience*. 23:5425-5436.

Kenchappa, R.S., C. Tep, Z. Korade, S. Urra, F.C. Bronfman, S.O. Yoon, and B.D. Carter. 2010. p75 neurotrophin receptor-mediated apoptosis in sympathetic neurons involves a biphasic activation of JNK and up-regulation of tumor necrosis factor-alpha-converting enzyme/ADAM17. *The Journal of biological chemistry*. 285:20358-20368.

Kraemer, B.R., S.O. Yoon, and B.D. Carter. 2014. The biological functions and signaling mechanisms of the p75 neurotrophin receptor. *Handbook of experimental pharmacology*. 220:121-164.

Lee, R., P. Kermani, K.K. Teng, and B.L. Hempstead. 2001. Regulation of cell survival by secreted proneurotrophins. *Science*. 294:1945-1948.

Levi-Montalcini, R. 1987. The nerve growth factor 35 years later. *Science*. 237:1154-1162.

Luo, W., H. Enomoto, F.L. Rice, J. Milbrandt, and D.D. Ginty. 2009. Molecular identification of rapidly adapting mechanoreceptors and their developmental dependence on ret signaling. *Neuron*. 64:841-856.

Luo, W., S.R. Wickramasinghe, J.M. Savitt, J.W. Griffin, T.M. Dawson, and D.D. Ginty. 2007. A hierarchical NGF signaling cascade controls Ret-dependent and Ret-independent events during development of nonpeptidergic DRG neurons. *Neuron*. 54:739-754.

Madisen, L., T.A. Zwingman, S.M. Sunkin, S.W. Oh, H.A. Zariwala, H. Gu, L.L. Ng, R.D. Palmiter, M.J. Hawrylycz, A.R. Jones, E.S. Lein, and H. Zeng. 2010. A robust and high-throughput Cre reporting and characterization system for the whole mouse brain. *Nature neuroscience*. 13:133-140.

Majdan, M., G.S. Walsh, R. Aloyz, and F.D. Miller. 2001. TrkA mediates developmental sympathetic neuron survival in vivo by silencing an ongoing p75NTR-mediated death signal. *The Journal of cell biology*. 155:1275-1285.

Makkerh, J.P., C. Ceni, D.S. Auld, F. Vaillancourt, G. Dorval, and P.A. Barker. 2005. p75 neurotrophin receptor reduces ligand-induced Trk receptor ubiquitination and delays Trk receptor internalization and degradation. *EMBO Rep.* 6:936-941.

Nishino, J., K. Mochida, Y. Ohfuji, T. Shimazaki, C. Meno, S. Ohishi, Y. Matsuda, H. Fujii, Y. Saijoh, and H. Hamada. 1999. GFR alpha3, a component of the artemin receptor, is required for migration and survival of the superior cervical ganglion. *Neuron*. 23:725-736.

Nykjaer, A., R. Lee, K.K. Teng, P. Jansen, P. Madsen, M.S. Nielsen, C. Jacobsen, M. Kliemannel, E. Schwarz, T.E. Willnow, B.L. Hempstead, and C.M. Petersen. 2004. Sortilin is essential for proNGF-induced neuronal cell death. *Nature*. 427:843-848.

Oppenheim, R.W. 1991. Cell death during development of the nervous system. *Annu. Rev. Neurosci.* 14:453-501.

Putcha, G.V., K.L. Moulder, J.P. Golden, P. Bouillet, J.A. Adams, A. Strasser, and E.M. Johnson. 2001. Induction of BIM, a proapoptotic BH3-only Bcl-2 family member, is critical for neuronal apoptosis. *Neuron*. 29:615-628.

Ruzankina, Y., C. Pinzon-Guzman, A. Asare, T. Ong, L. Pontano, G. Cotsarelis, V.P. Zediak, M. Velez, A. Bhandoola, and E.J. Brown. 2007. Deletion of the developmentally essential gene ATR in adult mice leads to age-related phenotypes and stem cell loss. *Cell stem cell*. 1:113-126.

Smeyne, R.J., R. Klein, A. Schnapp, L.K. Long, S. Bryant, A. Lewin, S.A. Lira, and M. Barbacid. 1994. Severe sensory and sympathetic neuropathies in mice carrying a disrupted Trk/NGF receptor gene. *Nature*. 368:246-248.

Tsui-Pierchala, B.A., J. Milbrandt, and E.M. Johnson, Jr. 2002. NGF utilizes c-Ret via a novel GFL-independent, inter-RTK signaling mechanism to maintain the trophic status of mature sympathetic neurons. *Neuron*. 33:261-273.

Tsui, C.C., and B.A. Pierchala. 2008. CD2AP and Cbl-3/Cbl-c constitute a critical checkpoint in the regulation of Ret signal transduction. *J. Neurosci.* 28:8789-8800.

Uesaka, T., and H. Enomoto. 2010. Neural precursor death is central to the pathogenesis of intestinal aganglionosis in Ret hypomorphic mice. *The Journal of neuroscience : the official journal of the Society for Neuroscience*. 30:5211-5218.

Uesaka, T., S. Jain, S. Yonemura, Y. Uchiyama, J. Milbrandt, and H. Enomoto. 2007. Conditional ablation of GFRalpha1 in postmigratory enteric neurons triggers unconventional neuronal death in the colon and causes a Hirschsprung's disease phenotype. *Development (Cambridge, England)*. 134:2171-2181.

Werth, J.L., M. Deshmukh, J. Cocabo, J. Johnson, E.M., and S.M. Rothman. 2000. Reversible physiological alterations in sympathetic neurons deprived of NGF but protected from apoptosis by caspase inhibition or Bax deletion. *Exp. Neurol.* 161:203-211.

CHAPTER 4: BIPHASIC FUNCTIONS OF THE GDNF-RET SIGNALING PATHWAY IN CHEMOSENSORY NEURON DEVELOPMENT AND DIVERSIFICATION

***Summary*:**

The development of the taste system relies on the coordinated regulation of cues that direct the simultaneous development of both peripheral taste organs and innervating sensory ganglia, but the underlying mechanisms remain poorly understood. In this study we describe a novel, biphasic function for glial cell line-derived neurotrophic factor (GDNF) in the development and subsequent diversification of chemosensory neurons within the geniculate ganglion (GG). GDNF, acting through the receptor tyrosine kinase, Ret, regulates the expression of the chemosensory fate determinant Phox2b early in GG development. *Ret*$^{-/-}$ mice, but not *Ret*$^{fx/fx}$; *Phox2b*-Cre mice, display a profound loss of Phox2b expression with subsequent chemosensory innervation deficits, indicating that Ret is required for the initial amplification of Phox2b expression, but not its maintenance. Ret expression is extinguished perinatally, but re-emerges postnatally in a subpopulation of large-diameter GG neurons expressing the mechanoreceptor marker NF200 and the GDNF co-receptor GFRα1. Intriguingly, we observed that ablation of these neurons in adult *Ret*-Cre/ER^{T2}; *Rosa26*$^{LSL\text{-}DTA}$ mice caused a specific loss of tactile, but not chemical or thermal, electrophysiological responses. Overall, the GDNF-Ret pathway exerts two critical and distinct functions in the peripheral taste system: embryonic chemosensory cell fate determination and the specification of lingual mechanoreceptors.

***Introduction*:**

Creating the neuronal diversity required to appropriately discriminate different kinds of sensory stimuli, including all aspects of somatosensory, taste, visual, auditory, and olfactory stimuli, is a complex task during vertebrate development. Following neurogenesis, one means of differentiating and specifying unique sensory neuron subpopulations is by selective expression of transcription factors and neurotrophic factor receptors (Liu and Ma, 2011). These signaling pathways regulate the expression of additional transcription factors, ion channels, neurotransmitter receptors, and neuropeptides that define the molecular and functional characteristics of different classes of sensory neurons (Lallemend and Ernfors, 2012). The selective expression of distinct neurotrophic factor receptors is one potential means of delineating functionally distinct populations of somatosensory neurons within the dorsal root ganglion (DRG) and trigeminal ganglion (TG). For example, while TrkB+ large diameter mechanoreceptive neurons afferently innervate Merkel cells and lanceolate endings producing BDNF (Li et al., 2011), TrkA+ small and medium-diameter neurons mediating pain sensation project free nerve endings to the skin where NGF is produced (Chen et al., 2006). Because heterogenous sensory neurons responsive to temperature, touch, and all five taste qualities cohabitate within the peripheral taste ganglia (Boudreau et al., 1971; Lundy and Contreras, 1999; Yokota and Bradley, 2016), this system is well suited to explore the underlying molecular mechanisms regulating sensory neuron diversification and physiology. The geniculate ganglion (GG) houses soma for taste and thermal afferents to lingual taste buds (TBs) in the fungiform papillae, projecting via the

chorda tympani (CT) nerve. Although a major taste ganglion for the anterior tongue, the GG also includes neurons innervating TBs on the soft palate, as well as somatosensory neurons projecting to the external ear (Krimm, 2007). This major ganglion for orofacial sensation is complex and multi-modal, containing soma for taste, touch, and lingual temperature reception (Boudreau et al., 1971; Lundy and Contreras, 1999; Yokota and Bradley, 2016). However, our knowledge of the molecular mechanisms dictating GG chemosensory neuron development and postnatal heterogeneity remain poorly understood, especially compared to primary sensory afferent neurons in the DRG and TG.

Previous studies have focused on the role of the neurotrophins in chemosensory GG development and maintenance, with NT-4 and BDNF emerging as the principal regulators of GG axon guidance (Patel and Krimm, 2012), GG neuron survival (Ma et al., 2009), and CT nerve regeneration (Meng et al., 2017). Despite these advances in our understanding of the development and postnatal maintenance of the peripheral taste system, our knowledge of the roles of other inductive cues involved in sensory neuron specification and diversity remains rudimentary. Additionally, although there is some evidence supporting the presence of molecularly and functionally distinct subpopulations of GG neurons, our knowledge as to the signaling pathways or markers that shape the multi-modal nature of GG neurons is lacking.

Another family of neurotrophic factors, the glial cell line-derived neurotrophic factor (GDNF) family ligands (GFLs), consisting of GDNF, neurturin (NRTN), artemin (ARTN),

and persephin (PSPN), are four homologous growth factors critical for the development of several populations of peripheral neurons, including autonomic neurons (Enomoto et al., 2001), rapidly adapting mechanoreceptors (Luo et al., 2009) and nonpeptidergic nociceptor populations (Luo et al., 2007) within the DRG sensory system. The receptor tyrosine kinase, Ret, conveys the trophic functions of the GFLs (Airaksinen and Saarma, 2002). Importantly, Ret is highly expressed in the GG early in embryonic development (D'Autreaux et al., 2011), and stimulation of early embryonic GG neurons with GDNF promotes axon outgrowth (Rochlin et al., 2000), indicating that the GDNF receptor components are present and poised to exert trophic effects in developing GG sensory neurons.

In this study, we investigated the function of the GDNF-Ret signaling pathway in the development and subsequent postnatal diversification of chemosensory neurons within the GG. To discern the developmental requirement, as well as the molecular and neurophysiological signatures for GG cells and GG/CT afferents, we used expression analyses, genetic models, pharmacologic inhibitors, and neurophysiological approaches. Collectively, we identify a novel, biphasic function for GDNF-Ret signaling in the peripheral taste system, initially acting to promote the chemosensory phenotype of all GG neurons, while acting postnatally to define a unique subpopulation of lingual mechanoreceptors. These data significantly broaden our understanding of the cues responsible for taste neuron development, and bring to light new concepts for understanding GG biology and peripheral sensory circuits of the tongue.

Results

Ret is widely expressed by geniculate chemosensory neurons at E13.5, but expression is extinguished perinatally

A previous study describing the transcriptional profile of GG neurons indicated that a combinatorial expression pattern of $Tlx3^{+}/Islet^{+}/Phox2b^{+}/Phox2a^{+}/Brn3a^{-}$ coincides with a chemosensory neuronal fate, while a $Tlx3^{+}/Islet^{+}/Phox2b^{-}/Phox2a^{-}/Brn3a^{+}$ transcriptional code coincides with somatosensory fate (D'Autreaux et al., 2011). In this study, Phox2b was discovered to serve in sensory neurons as a master regulator commanding a visceral, chemosensory fate, while repressing a somatosensory fate. In this way, the geniculate ganglion exerts a strong polarity between the distal chemosensory neurons innervating the anterior two-thirds of the tongue, and the proximal somatosensory neurons innervating the external ear. Curiously, upon qualitative analysis using *in situ* hybridization, the authors also found strong Ret expression which was correlated with a Phox2b+/Brn3a- chemosensory transcriptional profile as early as E11.5 (D'Autreaux et al., 2011). Importantly, these data suggest that Ret is one of the earliest growth factor receptors expressed by GG neurons, and may be selectively functioning within chemosensory neurons. We quantified the proportion of chemosensory and somatosensory neurons expressing Ret during embryonic development of the GG. For these purposes, chemosensory neurons were defined as TuJ1+ neurons expressing Phox2b, while somatosensory neurons were those lacking Phox2b expression. To validate the use of Phox2b as a specific marker of chemosensory neurons (Dauger et al., 2003b), we conducted immunolabeling of

Phox2b, RFP (detects the tdTomato protein), and TuJ1 (a pan-neuronal marker) in GG and TG from P0 *Rosa26*$^{LSL\text{-}tdTomato/+}$*; Phox2b-Cre*$^{tg/+}$ mice. The TG, known to be Phox2b-/Brn3a+, was analyzed as a negative control (Fode et al., 1998). For the specificity of RFP immunolabeling, *Rosa26*$^{LSL\text{-}tdTomato/+}$*; Phox2b-Cre*$^{+/+}$ mice were also analyzed. We observed that 98.84% of neurons immunoreactive for Phox2b were also RFP+, indicating a high reliability of this Phox2b antibody in labeling chemosensory neurons (98.84 ± 0.11%; Figure 4.1A). Further validating the use of Phox2b as a marker of chemosensory neurons, we found that 0.03% of TG neurons exhibited labeling for Phox2b, and in all cases, these neurons were RFP+ (Figure 4.1B). The majority of RFP+ immunolabeling in the TG was restricted to axons, likely due to labeling of trigeminal motor axons passing through the ganglion. These data confirm the high fidelity of Phox2b immunolabeling of chemosensory neurons and validate the use of the *Phox2b-Cre*$^{tg/+}$ line.

To determine the spatiotemporal expression pattern of Ret in the GG, we performed a tamoxifen (TMX) pulse labeling experiment using a Cre-inducible tomato reporter line (*Rosa26*$^{LSL\text{-}tdTomato}$) crossed to Ret-Cre/ER^{T2} mice (Luo et al., 2009). Importantly, we used this reporter strategy to avoid limitations in specificity occasionally observed with Ret immunostaining. Two time periods were analyzed (outlined in Figure 4.2A): 4 daily TMX injections from E9.5-E12.5, with analysis performed at E13.5; or 4 daily TMX injections from E14.5-E17.5, with analysis conducted at E18.5. Notably, analysis of these early and late embryonic timepoints allowed an examination into Ret expression during periods corresponding with transcriptional diversification and target innervation, respectively (Krimm, 2007; Mistretta and Liu, 2006). Ganglia were

immunolabeled for TuJ1, Phox2b, and RFP, and total numbers of chemosensory (Figure 4.2B) and somatosensory (Figure 4.2C) neurons expressing Ret were quantified. Coinciding with previous studies, we found that the majority of chemosensory neurons were Ret+ at E13.5 (69.41 ± 4.35%), but expression was greatly reduced by E18.5 (3.38 ± 0.42%; Figure 4.2B-F). Additionally, very few somatosensory neurons expressed Ret at either timepoint analyzed (Figure 4.2B-F).

Given that Ret is highly expressed by chemosensory GG neurons prior to lingual innervation, we hypothesized that the Ret ligand GDNF is present locally, acting on Ret+ chemosensory neurons. To test this hypothesis, we used a TMX pulse labeling experiment using *Rosa26*$^{LSL\text{-}tdTomato}$; *GDNF*-IRES-Cre/ER^{T2} (*GDNF*$^{Cre/+}$) mice (Cebrian et al., 2014), and analyzed the previously described timepoints (Figure 4.2A). Ganglia were collected from E13.5 and E18.5 labeled mice and immunolabeling was again performed for TuJ1, Phox2b, and RFP (to label GDNF+ cells). Surprisingly, GDNF expression was restricted to GG neurons themselves, rather than the surrounding tissues (Figure 4.3). Similar to the Ret expression quantifications, we observed that many chemosensory neurons express GDNF at E13.5 (27.14 ± 0.85%), but expression is virtually lost by E18.5 (4.31 ± 0.22%; Figure 4.3A, C). Additionally, few somatosensory neurons express GDNF at E13.5 (0.43 ± 0.06%) or E18.5 (8.62 ± 1.45%; Figure 4.3B, 4.3C). Collectively, these data suggest that a GDNF-Ret paracrine signaling pathway exists in chemosensory GG neurons early in development.

Ret is required for expression of the chemosensory fate determinant Phox2b, but not Brn3a or TrkB

Sensory neuron diversification relies on differential transcriptional activities that induce and maintain expression of required growth factor receptors, and these receptors in turn serve activator or repressor functions (Lallemend and Ernfors, 2012). The expression of Ret within the E9.5-E12.5 developmental window, but not within E14.5-E17.5, suggests an early role in chemosensory fate determination. It is during this embryonic period that GG neurons begin their initial transcriptional fate acquisition (D'Autreaux et al., 2011) and initial axon outgrowth, but they do not reach their final targets until at least one day later (Krimm, 2007). Given this timeline, we hypothesized that Ret is unlikely to be involved in target innervation, but rather, may play a role in early transcriptional diversification. Therefore, we analyzed total GG neuron numbers and the proportion of Phox2b+ neurons in *Ret*$^{-/-}$ mice or *Ret*$^{+/+}$ mice, as a control (Schuchardt et al., 1994) (Figure 4.4A-C). Strikingly, although no difference was observed in the total number of neurons (*Ret*$^{+/+}$: 767.63 ± 29.35 neurons vs. *Ret*$^{-/-}$: 761.35 ± 35.33 neurons; p = 0.9014; Figure 4.4A, 4.4B), we observed a significant reduction in the proportion of neurons with detectable Phox2b immunolabeling (*Ret*$^{+/+}$: 73.78 ± 2.17% vs. *Ret*$^{-/-}$: 44.00 ± 5.84%; a 40.4% reduction; p = 0.0015). There was also a substantially reduced intensity of Phox2b in neurons that retained a positive signal (Figure 4.4D). To determine whether this loss of Phox2b expression was coupled with a change in the proportion of neurons expressing the somatosensory transcriptional fate determinant Brn3a (Huang et al., 2001), or the broadly expressed TrkB receptor involved in GG survival (Patel and Krimm, 2010), we examined TuJ1, Brn3a, and TrkB expression, followed by quantification of the proportion of each subgroup. There was no change in the proportion of neurons expressing Brn3a (*Ret*$^{+/+}$: 32.67 ± 2.37% vs. *Ret*$^{-/-}$: 30.60 ± 6.57%;

p = 0.7587; Figure 4.4F, 4.4G). Likewise, there was no change in the proportion of neurons expressing TrkB (Figure 4.4E, 4.4G), which was expressed widely in both chemosensory and somatosensory GG neurons alike (*Ret*$^{+/+}$: 97.06 ± 0.49% vs. *Ret*$^{-/-}$: 98.08 ± 0.31%; p = 0.1161). To validate our immunostaining for TrkB, we also immunostained for TuJ1, Islet1 (a pan-sensory neuron marker), and GFP on P0 TGs isolated from *TrkB*$^{GFP/+}$ or *TrkB*$^{GFP/GFP}$ mice. TrkB labeling overlapped nearly completely with GFP in *TrkB*$^{GFP/+}$ mice, which retain one functional copy of TrkB protein, but no TrkB immunolabeling was observed in *TrkB*$^{GFP/GFP}$ knockout mice (Li et al., 2011), despite the presence of GFP+ neurons (Figure 4.5).

Ret is required for the amplification of Phox2b

Two possibilities can explain the loss of Phox2b expression in Ret knockout mice at E18.5: (1) Ret is required for the initiation of Phox2b expression within the chemosensory GG population; or (2) Ret is required for the amplification of Phox2b expression within chemosensory GG neurons. To distinguish between these two, we crossed Ret conditional knockout mice (*Ret*$^{fx/fx}$)(Luo et al., 2007) with *Phox2b*-Cre$^{tg/+}$ mice (Ret-cKO). *Ret*$^{fx/fx}$; *Phox2b*-Cre$^{+/+}$ (Ret-WT) mice were analyzed as a control. These mice will only undergo recombination following the initiation of Phox2b expression, thereby testing whether Ret is needed for the initiation of Phox2b. Tissues were immunostained for Phox2b and TuJ1 and total neuron numbers and the proportion of Phox2b+ GG neurons were quantified. Interestingly, there was no difference in total neuron numbers (Figure 4.6A-B; Ret-WT: 723.60 ± 13.47 vs. Ret-cKO: 789.15 ± 25.43; p = 0.0712) or in the proportion of Phox2b+ neurons (Figures 4.6A-C; Ret-WT: 65.07 ±

1.02% vs. Ret-cKO: 61.39 ± 2.98%; p = 0.3503), indicating that Ret is dispensable for Phox2b maintenance. To further explore this hypothesis, we crossed Ret conditional knockout mice with conventional germline knockout mice to generate *Ret*$^{fx/-}$ mice (and *Ret*$^{fx/+}$ mice as a control). The Ret conditional knockout mice were created to harbor a single nucleotide missense mutation (V805A) in the tyrosine kinase domain, which is functionally silent but makes Ret in these mice susceptible to a highly selective chemical inhibition of kinase activity with the pharmacologic inhibitor 1NM-PP1 (Chen et al., 2005a). Ret signaling *in vivo* generally functions via a positive feedback loop, where Ret activation promotes further Ret expression, and blocking Ret activation therefore impairs Ret expression (Luo et al., 2007; Tsui-Pierchala et al., 2002c). We used this system as a reversible means of reducing Ret levels and activity during a defined developmental time window.

To verify that daily systemic administration of 1NM-PP1 was effective in reducing total Ret levels, pregnant dams were injected daily with 1NM-PP1 from E14.5-E17.5, and spinal cords were isolated from E18.5 *Ret*$^{fx/+}$ and *Ret*$^{fx-}$ embryos, followed by quantitative immunoblotting for Ret and actin (as a loading control, Figure 4.7A). This is an especially strict confirmation of Ret knockdown, as 1NM-PP1 must pass through the blood brain barrier to achieve adequate inhibition of spinal cord neurons, in contrast to the GG in the periphery. Importantly, we observed that administration of 1NM-PP1 to *Ret*$^{fx/-}$ mice led to a substantial reduction in total Ret levels, as predicted (*Ret*$^{fx/+}$: 1.00 ± 0.19 arbitrary units (a.u) vs. 0.23 ± 0.05 a.u.; 77% reduction; p = 0.0048; Figure 4.7B). Having demonstrated that this technique is effective in knocking down Ret in a

temporally controlled manner, we administered 1NM-PP1 to *Ret*$^{fx/-}$ and *Ret*$^{fx/+}$ mice from E9.5-E12.5, with analysis at E18.5, and from E13.5-E17.5, with analysis at E18.5. Interestingly, when compared to GGs collected from *Ret*$^{fx/+}$ mice, *Ret*$^{fx/-}$ animals administered 1NM-PP1 from E9.5-E12.5 again had no change in total neuron numbers (*Ret*$^{fx/+}$: 710.25 ± 20.67 vs. *Ret*$^{fx/-}$: 659.60 ± 26.30; p = 0.2056; Figure 4.7C, 4.7D), but displayed a 29.9% reduction in the proportion of Phox2b+ neurons (*Ret*$^{fx/+}$*:* 65.92 ± 4.54% vs. *Ret*$^{fx/-}$*:* 46.24 ± 2.74%; p = 0.0041; Figure 4.7C, 4.7D). This was in contrast to the cohort of mice administered TMX from E14.5-E17.5, in which no changes were observed in total neuron numbers (*Ret*$^{fx/+}$: 698.44 ± 35.74 vs. *Ret*$^{fx/-}$: 676.18 ± 23.46; p = 0.6167; Figure 4.7E) or in the proportion of Phox2b+ neurons (*Ret*$^{fx/+}$: 63.78 ± 3.70% vs. *Ret*$^{fx/-}$: 61.56 ± 2.01%; p = 0.6118; Figure 4.7F). These data indicate that Ret is required for the early amplification of Phox2b expression in chemosensory neurons, but is dispensable for its maintenance, concordant with the observed spatiotemporal expression pattern of Ret. Additionally, the data demonstrate that an early disruption of Ret signaling, between E9.5-E12.5, is sufficient to irreversibly impair Phox2b expression. Lastly, Ret is not required for the survival of GG neurons, and appears to specifically regulate chemosensory cell fate determination.

Loss of Ret results in fungiform papilla chemosensory innervation deficits

Germline *Phox2b*$^{LacZ/LacZ}$ knockout mice have normal total GG neuron numbers (D'Autreaux et al., 2011). In these mice, however, chemosensory neurons transitioned to a molecular profile consistent with a somatosensory neuronal fate (Brn3a+, Runx1+, Drg11+), accompanied by a conversion to somatosensory axonal projection patterns.

Although loss of Ret only leads to a partial disruption in Phox2b expression in chemosensory neurons, we hypothesized that chemosensory innervation of fungiform papillae would also be disrupted. Anterior tongues were collected from E18.5 *Ret*$^{+/+}$ and *Ret*$^{-/-}$ mice, and stained for TuJ1, P2X3 (a selective marker of chemosensory nerve fibers)(Ishida et al., 2009), and K8 (to label early taste buds). When analyzing the entire papilla, no difference was observed in the amount of K8+ immunolabeling (Figure 4.8A, 4.8B; $p = 0.5367$) or in the density of TuJ1+ immunolabeling (Figure 4.8A, $p = 0.3629$) between *Ret*$^{+/+}$ and *Ret*$^{-/-}$ mice. Interestingly, we observed a highly significant reduction in P2X3-labeled nerve fibers within the total fungiform papillae area (Figure 4.8A, 4.8C; 29.0% reduction; $p < 0.0001$). Correspondingly, we observed a substantial reduction in P2X3-labeled fibers when restricting analysis to the K8+ taste bud region (Figure 4.8D; 38.9% reduction; $p < 0.0001$), despite a small but significant increase in total TuJ1+ immunolabeling within the taste bud area ($p = 0.0199$). Collectively, these data indicate that loss of Ret leads to subsequent loss of chemosensory differentiation, ultimately leading to deficits in the axon terminal expression of the neurotransmitter receptor P2X3.

Ret reemerges in a unique subpopulation of chemosensory neurons postnatally

Building on the demonstrated embryonic role for GDNF-Ret signaling in prenatal chemosensory cell fate determination, we determined whether Ret expression remains extinguished postnatally. Using *Rosa26*$^{LSL\text{-}tdTomato}$; *Ret*-Cre/ER^{T2} mice we examined Ret expression within the first week of postnatal life, a time during which the peripheral taste system is still maturing, and in adulthood, when complete maturation is reached. TMX

was administered daily to P3-P7 or P60-P64 mice with analysis commencing one day following the last TMX administration (postnatal day 8 and 65, respectively). Surprisingly, given that Ret expression was nearly completely lost by late embryonic development (E18.5 timepoint from Figure 4.2B re-graphed in Figure 4.9C), we observed an upregulation of Ret within a subpopulation of chemosensory GG neurons at P8 (14.53 ± 0.64%; Figure 4.9A-C), which was further increased by P65 (20.11 ± 2.72%; Figure 4.9B-C).

The low abundance of Ret+ chemosensory GG neurons is reminiscent of subpopulations within the DRG and TG, where distinct subpopulations of neurons can be defined by their expression of neurotrophic factor receptors, somal diameter, and molecular properties, all of which influence their sensory properties (Liu and Ma, 2011). Within the GG chemosensory population, there is evidence that these neurons are heterogeneous in terms of size, electrical properties, and neurochemical signature (Al-Hadlaq et al., 2003; Boudreau et al., 1971; Fei and Krimm, 2013; Grigaliunas et al., 2002; Kitamura et al., 1982; Lundy and Contreras, 1999; Yokota and Bradley, 2016). To further characterize the Ret+ population within the GG and determine whether these neurons represent a distinct subpopulation, we analyzed the somal diameter of Ret+ chemosensory neurons (RFP+/Phox2b+) compared to Ret+ somatosensory neurons (RFP+/Phox2b-), which represent 82.28% and 17.72% of the total Ret+ neurons in the GG, respectively (Figure 4.10A). The Ret+ chemosensory neurons, on average, were significantly larger than Ret+/Phox2b- neurons (Figure 4.10B, C; 22.34 ± 0.23 μm vs. 20.51 ± 0.43 μm; $p = 0.0005$), and 23.22% of Ret+ chemosensory GG neurons have somal diameters greater than 27 μm, compared to 10.53% of Ret+ somatosensory

neurons. Interestingly, 66.59% of neurons expressed Ret, but not TrkB (Ret+/TrkB-), whereas 33.41% of neurons expressed both receptors (Ret+/TrkB+; Figure 4.10D, 4.10E; yellow arrows). The Ret+/TrkB- neurons were typically larger than Ret+/TrkB+ neurons ($p < 0.0058$; 23.81 ± 0.26 µm for Ret+/TrkB- compared to 22.65 ± 0.33 µm for Ret+/TrkB+) and also Ret-/TrkB+ neurons ($p = 0.0001$; 19.28 ± 0.15 µm for Ret-/TrkB+). Ret+/TrkB+ neurons were also significantly larger than the Ret-/TrkB+ neurons ($p < 0.0001$). These data argue for the existence of at least three distinct subpopulations of neurons within the GG based on morphological properties of the cells as well as neurotrophic factor receptor expression.

Ret signaling defines a subpopulation of large-diameter neurofilament heavy chain-enriched (NF200+) low threshold mechanoreceptors within the DRG (Bourane et al., 2009; Luo et al., 2009). Given that GG Ret+ neurons were of larger diameter, we examined whether Ret+ GG neurons expressed NF200. Additionally, we analyzed which GFRα co-receptors were expressed within GG neurons. Interestingly, we observed GFRα1 immunoreactivity within Ret+/NF200+ GG neurons (Figure 4.9D), but were unable to detect either GFRα2+ or GFRα3+ GG neurons (Figure 4.11A), despite the presence of strong immunoreactivity for both co-receptors within the TG (Figure 4.11B), as has been previously reported (Heuckeroth et al., 1999; Naveilhan et al., 1998). Additionally, to further characterize the NF200+ population of neurons, we analyzed adult *Rosa26*$^{LSL\text{-}tdTomato/+}$*; Phox2b-Cre*$^{tg/+}$ GGs. As expected, Brn3a and Phox2b immunolabeling were almost mutually exclusive with only rare examples of double-labeled neurons (green arrows, Figure 4.11C). Although examples of Brn3a/NF200+ neurons (yellow arrows) were observed, Phox2b/NF200+ neurons (blue

arrows) were much more abundant, indicating that a large population of transcriptionally chemosensory neurons express the mechanoreceptor marker NF200 (Figure 4.11C). To validate the postnatal increase in expression, lysates were prepared from P0 or adult GG and quantitative immunoblotting was performed (Figure 4.11D). As expected, we observed a statistically significant increase in normalized Ret expression in adult mice compared to P0 (Figure 4.11E), further substantiating the postnatal increase in Ret expression. Collectively, these data indicate that Ret expression re-emerges postnatally within large diameter chemosensory neurons expressing Ret, GFRα1 and NF200, and thus, molecularly define a unique subpopulation of lingual GG sensory neurons that are likely to be mechanoreceptors.

Examination of Ret+ nerve fibers within fungiform papillae

To investigate whether Ret-expressing chemosensory GG neurons project into TBs, we immunostained anterior tongues dissected from TMX-labeled adult *Rosa26*$^{LSL\text{-}tdTomato}$; *Ret*-Cre/ER^{T2} mice for TuJ1 (green), RFP (Ret; red), and K8 (blue). Fungiform papillae were imaged in their entirety, and we documented anterior, middle, and posterior locations on the tongue. To determine the projection pattern of Ret+ nerve fibers, maximum projection images were utilized, along with the original composite z-stack to assess whether nerve fibers were terminating within the K8+ taste bud area. RFP+ nerve fibers (red) terminating within the K8+ area were classified as intragemmal, while those terminating outside the K8+ area were classified as extragemmal. There was variability in the extent of innervation of fungiform papillae, although 94.89% of all FP had either a combination of extragemmal and intragemmal (Figure 4.12A) Ret+ nerve

fibers or exclusively extragemmal nerve fibers (Figure 4.12B). To quantify the extent of Ret+ innervation within each category (extragemmal and intragemmal), we further divided each group into three categories: (1) no innervation; (2) less than 3 nerve branches; and (3) greater than 3 nerve branches. When analyzing extragemmal Ret+ fibers, we observed that 85.2% of FP were extensively innervated by Ret+ fibers (> 3 branches), 13.1% of FP were moderately innervated by Ret+ fibers (1-3 branches), and 1.7% of FP had no extragemmal Ret+ fibers (Figure 4.12C), although in all three of these cases no nerve fibers were observed. When analyzing intragemmal Ret+ fibers (those within the K8+ region), we observed 13.1% of FP had >3 branches, 31.8% had 1-3 branches, and 56.25% had no intragemmal Ret+ nerve fibers (Figure 4.12D). To determine whether the location of FP on the dorsal tongue influenced innervation density or pattern, when normalizing for the total number of FP counted within each region (tip vs. middle vs. posterior tongue), we observed no changes in the distribution of either extragemmal or intragemmal nerve fibers (Figure 4.13A, 4.13B). Additionally, in 7.96% of FP, we observed elongated Ret+ TRCs which extended the full length of the taste bud (Figure 4.13C), and in all instances these were present on the anterior-most tip of the tongue.

GDNF is expressed within fungiform papillae, but not geniculate ganglion neurons

Based on the expression of GFRα1 within GG neurons, and the complete lack of GFRα2 and GFRα3, the expression pattern of GDNF was examined. We used *Rosa26*$^{LSL\text{-}tdTomato}$; *GDNF*-IRES-Cre/ER^{T2} mice, and these adult mice were administered

TMX on 5 successive days, euthanized, and GG and anterior tongues were collected. Tongues were immunostained for TuJ1, RFP (GDNF), and K8 or E-Cadherin (E-Cad), a marker of cells within the lingual epithelium. Importantly, GDNF was expressed predominantly within the basal epithelium layer, both in the fungiform papilla walls as well as the cells within and around the taste bud (Figure 4.12E). No GDNF+ nerve fibers were observed, indicating a lack of GDNF expression by GG neurons themselves. Correspondingly, analysis of the GG confirmed this result, as no examples of GDNF+ neurons were observed within the GG, although GDNF+ satellite cells within the facial nerve were occasionally seen (Figure 4.14E).

Differences in the innervation patterns have been reported between extragemmal nerve fibers originating from the Phox2b^{-}/Brn3a^{+} TG, somatosensory in nature, and intragemmal nerve fibers originating from the Phox2b^{+}/Brn3a^{-} GG, chemosensory in nature (Dauger et al., 2003b; Zaidi and Whitehead, 2006). We further examined this model using adult *Rosa26*$^{LSL\text{-}tdTomato/+}$*; Phox2b-Cre*$^{tg/+}$ mice to selectively label and trace GG/CT chemosensory afferent fibers within FP. To our surprise, when analyzing FP, we observed that 31.8% of FP analyzed had > 3 nerve fibers outside the K8+ region (Figure 4.14A), 18.5% of FP had 1-3 nerve fibers outside the K8+ region (Figure 4.14B), and 49.7% of FP had no extragemmal nerve fibers (Figure 4.14C; quantifications provided in Figure 4.12D). Confirming previous studies, all papillae analyzed (151/151) had intragemmal labeling. These data suggest that some Phox2b+ GG neurons may project extragemmally, to an area adjacent to the K8+ taste bud region. Thus, while analysis of intragemmal nerve fibers is a strong predictor of chemosensory innervation

origin, analysis of extragemmal innervation may represent a mixture of somatosensory TG afferents and Phox2b+/chemosensory GG/CT afferents. However, we cannot rule out the potential contribution of Phox2b+ sympathetic nerve fibers to the FP. Although only 43.75% of Ret+ nerve fibers project intragemmally, a proportion of the observed extragemmal nerve fiber labeling (98.30% of all FP) may also be of chemosensory origin.

Ablation of Ret+ geniculate neurons results in a loss of tactile, but not chemical or cold responses

We next sought to determine whether Ret+ GG neurons underlie a particular lingual sensory modality. *Ret*-Cre/ER^{T2} mice were crossed with a transgenic *Rosa26*$^{LSL\text{-}DTA/LSL\text{-}DTA}$ line (abbreviated *DTA*$^{+/+}$), whereupon TMX administration leads to ablation of all Ret+ cells, thereby eliminating all GG neurons expressing Ret (Figure 4.15A). These DTA mice have been previously characterized, and show very rapid loss of cells following Cre induction (Wu et al., 2006). TMX was administered to adult *Ret*$^{Cre/+}$*; DTA*$^{+/+}$ (Ret-ablated) mice or *Ret*$^{+/+}$*; DTA*$^{+/+}$ (wildtype) mice, as a control, for three days, followed by whole nerve recording from the CT nerve. In all mice, efficacy of Ret+ neuron ablation was confirmed histologically following electrophysiological recordings by analyzing total Phox2b+ neurons. Ret-ablated mice had fewer Phox2b+ neurons compared to WT mice (WT: 384.5 ± 15.6 neurons vs. Ret-ablated: 336.6 ± 27.8 neurons; a 12.5% reduction; n=9 and n=14, respectively; representative image shown in Figure 4.15B), although some variability was observed. Given our data indicating that approximately 20% of adult neurons express Ret, and most of these (82.28%) neurons

are chemosensory, we reasoned that our ablation efficacy was similar to the expected value (16.5%). Additionally, other phenotypic effects in Ret-ablated mice were observed that indicated a reliable ablation of Ret+ cells, such as an enlarged gastrointestinal tract, indicative of a Hirschsprung's-like phenotype. Interestingly, when focusing our analysis on the mice verified to have strong deletion meeting the inclusion criteria (see methods), we observed no differences in chemical responses (Figure 4.16A, Figure 4.15C) or cold responses (Figure 4.16B, Figure 4.15D) in any of the Ret-ablated mice compared to WT controls. In stark contrast, we observed a complete loss of tactile responses in 4/7 Ret-ablated mice, despite the presence of spontaneous nerve activity. Additionally, we observed a substantially weakened tactile response in 1/7 Ret-ablated mouse, and no change in tactile responses in 2 Ret-ablated mice (Figure 4.16C, Figure 4.15E). Because responses to tactile stimuli are rapidly adapting, and not sustained, we present raw responses rather than summated recordings for tactile stimulation. These data indicate that the Ret-expressing GG neurons projecting via the chorda tympani nerve to FPs are a population of functionally-unique mechanoreceptors, although we cannot rule out that they may be multimodal in function.

Discussion

Ret specifies chemosensory cell fate acquisition

The coexistence of distinct chemosensory and somatosensory neurons within the same ganglion, each with unique transcriptional codes and subsequent peripheral and central projection patterns, makes the GG is an interesting model in which to study sensory neuron specification. Our analysis of mice with germline Ret deletion (Figure 4.4A-C),

conditional deletion of Ret following Phox2b expression (Figure 4.6A-C), and temporal pharmacologic inhibition of Ret (Figure 4.7C-G) support the notion that Ret is required for Phox2b amplification, but not its initiation or maintenance. Interestingly, Ret deletion did not impact neuronal survival and we observed no significant change in the expression pattern of the neurotrophic factor receptor TrkB (Figure 4.4D, 4.4F), the neurotrophic signaling pathway supporting GG neurons during axon guidance and target-dependent survival (Ma et al., 2009). Additionally, the loss of Ret impaired chemosensory innervation of developing taste buds within the fungiform papillae (Figure 4.8A-F), arguing that loss of chemosensory cell fate leads to a subsequent impairment in peripheral projections of GG neurons. However, whether this reflects a complete loss of these nerve fibers, or simply a loss of the chemosensory-specific neurotransmitter receptor P2X3 used to label these fibers, is unknown.

A previous study analyzing *Phox2b*$^{LacZ/LacZ}$ knockout mice demonstrated that loss of Phox2b in chemosensory GG neurons results in acquisition of Brn3a expression (D'Autreaux et al., 2011). Despite loss of Phox2b expression, we did not see an increase in the proportion of geniculate neurons expressing the determinant Brn3a (Figure 4.4F, G). Although our data support the notion that Ret promotes Phox2b expression within chemosensory neurons, and its removal results in a substantial loss of Phox2b, Ret deletion is not synonymous with the complete knockout of Phox2b. These results may reflect the partial nature of the Ret knockout phenotype, as only a 30-40% reduction in the proportion of chemosensory neurons expressing Phox2b was observed (depending on the experimental model analyzed). In addition, many more

neurons had a qualitative reduction Phox2b expression, with some residual expression remaining. Two previous studies investigating the interrelationship of Brn3a with Ret in the DRG (Zou et al., 2012) and the TG (Huang et al., 1999) demonstrated that Brn3a and Ret are spatially segregated in their expression patterns, and that Ret+ neurons are spared in Brn3a knockout mice. For these reasons, it is perhaps not surprising that Ret deletion does not impact Brn3a. Likely, the residual low level of Phox2b expression is sufficient to inhibit Brn3a expression within these neurons, suggesting that the role of Ret in this process is to amplify the expression of Phox2b, but Ret signaling itself does not directly influence Brn3a expression. Building on the aforementioned studies, and based on our results, we propose a model in which (1) Phox2b induces Ret expression in chemosensory neurons; (2) Ret, acting as part of a positive feedback loop, amplifies the expression of Phox2b during the early embryonic window prior to target innervation; (3) Phox2b represses Brn3a expression. Thus, there is a critical window in which the interaction between Ret and Phox2b is required for the acquisition of the appropriate transcriptional fate.

Ret specifies a distinct subpopulation of chemosensory neurons postnatally

Based on experiments analyzing Ret reporter mice, approximately 20% of GG neurons express Ret in adult mice. These findings bear some similarity to other sensory neuron populations wherein there are subpopulations of neurons with differential neurotrophic factor receptor expression that can be delineated based on molecular, physical, and functional characteristics (Lallemend and Ernfors, 2012). Most Ret+ GG neurons were chemosensory as defined by Phox2b expression (82.28%; Figure 4.10A), with

approximately a 2:1 ratio of neurons lacking TrkB (Ret+/TrkB-) compared to neurons expressing both receptors (Ret+/TrkB+; Figure 4.10D-E). These neurons were large in diameter, when compared to neurons positive for only TrkB (Figure 4.10), and expressed the mechanoreceptor marker NF200 (Figure 4.10D). Additionally, when analyzing GFRα co-receptors present within the GG, which are required for downstream Ret signaling, only GFRα1 was detectable (Figure 4.10D, 4.11). Correspondingly, we observed many Ret+ nerve fibers, both intragemmal and extragemmal in nature (Figure 4.12), as well as many GDNF+ cells within the fungiform papillae, including those within and immediately surrounding the taste bud region (Figure 4.12E). Finally, electrophysiological recordings of mice in which Ret+ neurons were ablated indicate that these Ret+ neurons function as a unique subpopulation of GG/CT afferent mechanoreceptive neurons (Figure 4.16).

While several studies have begun to expand our knowledge of the heterogeneity within the GG (Boudreau et al., 1971; Fei and Krimm, 2013; Finger et al., 2005; Lundy and Contreras, 1999; Yokota and Bradley, 2016), our understanding of the cellular basis defining the multi-modality of orofacial chemosensory neurons remains quite rudimentary in comparison to TG and DRG somatosensory neurons, where as many as 11 molecularly distinct subpopulations have been described (Usoskin et al., 2015). This is the first study demonstrating the existence of a molecularly, morphologically, and functionally distinct lingual GG neuron subtype. Given that Ret+ neurons are chemosensory (Phox2b+) in molecular profile, but have physiological and morphological properties of mechanoreceptors, they represent a unique population dissimilar from

pinna-projecting somatosensory neurons within the GG, lingually-projecting chemosensory neurons within the GG, as well as Ret+ mechanoreceptors in the TG and DRG. As such, the specific nomenclature for these transcriptionally chemosensory, but functionally somatosensory, neurons is a subject for debate. Interestingly, mice administered pharmacologic purinergic receptor inhibitors (Vandenbeuch et al., 2015) as well as P2X2/P2X3 double knockout mice (Finger et al., 2005) lose chemical, but not tactile responses. Furthermore, loss of the fungiform TBs following pharmacologic inhibition of the sonic hedgehog pathway disrupts chemical, but not tactile, chorda tympani responses (Kumari et al., 2015), suggesting that the taste bud itself is not required for the mechanical responses. Thus, it remains unknown what the gating mechanisms are for these mechanical responses, as well as what pre-synaptic lingual sensory end-organs are responsible for communicating with these fibers. Further defining the receptive fields and adaptation properties of these neurons remains an important future direction, as does the identification of the physiological significance of these neurons.

Experimental Procedures

Production of Embryos, Tamoxifen Delivery, and 1NM-PP1 Administration

Ret$^{fx/fx}$ (Luo et al. 2007), *Ret*$^{-/-}$ (Schuchardt et al., 1994), *Ret*-Cre/ER^{T2} (Luo et al. 2009), *Rosa26*$^{LSL\text{-}TdTomato}$ (Madisen et al., 2010), *Phox2b*-Cre$^{tg/+}$ (Rossi et al., 2011), *GDNF*-IRES-Cre/ER^{T2} (Cebrian et al., 2014), and *Rosa26*$^{LSL\text{-}DTA}$ (Wu et al., 2006) mice have all been previously described. All mice were maintained in mixed genetic backgrounds and all comparisons were made using littermates. For timed mating experiments, noon of the day on which a vaginal plug was detected was considered E0.5. For the experiments tracing Ret or GDNF expression, tamoxifen (TMX; T5648, Sigma Aldrich, St. Louis, MO) was dissolved in corn oil and administered via intraperitoneal injection at a dose of 0.25 mg/g body weight, at timepoints described in the figure legends, with Cre-negative littermate controls analyzed in all experiments. For the experiments utilizing the pharmacologic inhibitor 1NM-PP1 (catalog #529581, EMD Millipore, Temecula, CA), pregnant dams were given i.p. injections daily (16.6 ng/g body weight, as previously described)(Chen et al., 2005a) at the indicated timepoints, and 1NM-PP1 was also maintained in the drinking water at a concentration of (1 mM) to maintain chemical inhibition. All experiments were carried out in compliance with the guidelines of the Association for Assessment and Accreditation of Laboratory Animal Care International (AAALAC) and were approved by the Institutional Animal Care and Use Committee (IACUC) of the University of Michigan.

Neuron Counts, Somal Diameter Measurements, and Innervation Classification

The average somal diameter of GG neurons was observed to be 22.02 ± 0.20 µm, and for this reason we performed cell counts on 20 µm serial sections of the entire GG. For experiments analyzing TGs from *Rosa26*$^{LSL\text{-}tdTomato/+}$*; Phox2b-Cre*$^{tg/+}$ mice, counts were performed on 3 sections per ganglion, approximately 200 µm apart. Somal diameters were measured at the widest aspect of each neuron using the TuJ1 channel. For innervation classifications, maximum projections as well as the original composite z-stack images were utilized to assess whether nerve fibers were terminating within the K8+ taste bud area. Nerve fibers terminating within the K8+ area were classified as intragemmal, while those terminating outside the K8+ area were classified as extragemmal. Greater than 3 nerve fibers was chosen as an arbitrary cutoff point to subcategorize FP into those having extensive (>3 fibers) or slight-moderate (1-3 fibers) innervation density. Detailed description of the protocol used for Fiji quantification of fungiform papilla innervation and Phox2b expression are expanded in the Supplemental Information.

Statistics and Data Analysis

All results are expressed as the mean ± s.e.m. All statistical tests were performed using two-tailed parameters with a significance level of $p \leq 0.05$ to test for statistical significance. A two-tailed student's t-test was utilized for all comparisons between two treatment groups. Comparisons between more than two treatment groups were performed with one-way ANOVA. The data were originally entered into Excel and imported into GraphPad Prism, which was used for all statistical tests and graph production. The presence of asterisks indicates statistical significance. * = $p < 0.05$, ** =

$p < 0.01$, *** = $p < 0.001$, **** = $p < 0.0001$. The sample sizes are indicated in the results and figure legends. No sample sizes of less than 3 independent experiments were utilized. For all GG counts, when possible, each animal represents the average count of two GGs to increase statistical accuracy. For all pooled analyses of FP, statistical tests were performed on both the pooled data and the individualized animal data to ensure that no differences in outcome were obtained.

Chorda Tympani Nerve Recordings

Mice were anesthetized with a ketamine-xylazine mixture (80-100 mg/kg ketamine, 5-10 mg/kg xylazine delivered i.p.) and maintained with ketamine (80-100 mg/kg) as needed. The CT was exposed by a lateral approach, dissected, cut centrally, and placed on a recording electrode. An indifferent electrode was placed in nearby tissue. Amplified neural activity was observed in an oscilloscope and passed through an analog-to-digital converter and recorded using the Spike2 program (Cambridge Electronic Design). The amplified signal was also passed through an integrator circuit with 0.5 sec time constant. Tactile stimuli consisted of stroking the anterior tongue quadrant five times over a period of 5s, while thermal stimuli consisted of application of 4°C water. The indicated chemical stimuli were dissolved in distilled water at room temperature, and 3-5 mL was applied to the tongue using a syringe. Chemicals remained on the tongue for 20s, followed by a distilled water rinse for 30s. NaCl and NH_4Cl were applied throughout the nerve recording to monitor stability and changes from baseline. The initial increase in integrated recordings at onset and rinse of chemicals from the tongue includes the stimulus artifact, seen when a chemical or rinse contacts the tongue (Yokota and

Bradley, 2016), and the initial high frequency transient response can be useful for measuring response latency or assessing temporal aspects of the summated response. Neither integrated onset or offset is related to the somatosensory response. The tactile responses observed were to a moving, light stroking stimulus only.

Fixation, Sectioning, and Immunostaining

GG and TG were collected and fixed overnight in 4% paraformaldehyde at 4°C, while tongues were dissected within the mandible and fixed for 2-3 hours, dissected free from the mandible, and fixed for another 2-3 hours at room temperature. Tissues were cryopreserved, embedded in OCT (Tissue Tek, VWR, Radnor, PA) and stored at -80°C until sectioning. GGs and TGs were sectioned at a thickness of 20 µm on a cryostat (CM1950, Leica Biosystems, Germany), except for one cohort of animals where sections were produced at 40 µm. In all cases, sections were collected serially. Tongues were sectioned at a thickness of 20 µm for Ret and GDNF expression tracing experiments, while 50 µm sections were produced and collected serially for the analysis of Ret knockout mice to avoid double counting FPs. For immunostaining, sections were first rehydrated in PBS for 30 minutes at room temperature, following by blocking in 10% normal donkey serum (Jackson ImmunoResearch, West Grove, PA), 0.25-0.5% bovine serum albumin (Sigma, Billerica, MA), and mouse-on-mouse blocking reagent (1 drop per 1.5 ml blocking solution; Vector Laboratories, Burlingame, CA) in 0.3% triton X-100/PBS (PBS-X). Following blocking, the following primary antibodies were diluted in 0.3% PBS-X and incubated on the sections overnight at 4°C (48 hours at 4°C for 50 µm

tongue sections) in a humidified chamber: α-RFP (1:200-1:500; 600-401-379; Rockland, Limerick, PA), α-Phox2b (1:200-1:500; AF4940; R&D, Minneapolis, MN), α-TuJ1 (βIII-Tubulin; 1:200; T8578; Sigma), α-TrkB (1:250-1:400, AF1494, R&D), α-Brn3a/Pou4f1 (1:25; MAB1585; Millipore), α-P2X3 (1:200-1:400; AB5895, Millipore), α-GFRα1 (1:50; AF560; R&D), α-GFRα2 (1:100; AF429; R&D), α-GFRα3 (1:100; AF2645; R&D), α-NF200 (1:200-1:500; NFH, Aves Labs Inc., Tigard, OR combined with 1:500; ab8135; Abcam, Cambridge, MA), α-Islet1 (1:200; 39-4D5-s; Developmental Studies Hybridoma Bank, Iowa City, IA), α-cytokeratin-8 (TROMA-I; 1:50 [supernatant], DSHB), and α-E-Cadherin (1:1000-1:2000; AF748; R&D). Slides were washed 3-4 times with 0.3% PBS-X, and secondary antibodies against the intended species were added at a concentration of 1:200 (GG and TGs) or 1:400 (tongues) (all raised in donkey; CF488, CF543, or CF633 from Biotium Biosciences, Fremont, CA). After secondary antibody incubation, slides were washed with 0.3% PBS-X 3 times, followed by washes in PBS. Slides were coverslipped with DAPI Fluoromount-G (Southern Biotech, Birmingham, AL) and stored in darkness until imaging. All imaging was performed on a Leica SP5 confocal microscope using the LAS-AF software (Leica Microsystems, Wetzlar, Germany). Images were taken at 20X or 63X magnification with high resolution (2048x2048) and a z-step size of 1 µm (tongues) or 2.0 µm (GG and TGs). For tongues, every FP (identified using DAPI) was imaged in its entirety (15-25 optical sections). For GGs and TGs, every section containing neurons (identified using TuJ1 channel) was imaged. Maximum projection and Median noise reduction (pixel width of 5 Kernels; LAS Software, Leica Biosystems, Buffalo Grove, IL) was applied to all files to generate a single composite image for all subsequent analyses.

Fiji Quantification of Fungiform Papilla Innervation and Phox2b Expression

All FP from 50 µm sections produced from E18.5 *Ret*$^{+/+}$ and *Ret*$^{-/-}$ anterior tongues were imaged in their entirety. During both image capture and analysis, the experimenters were naïve to the experimental conditions. All imaging of individual papillae took place at 63x magnification. Following image collection and processing, images were imported into ImageJ using the Fiji image processing package (Schindelin et al., 2012). Quantifications were performed in two ways: quantification of the P2X3+ and TuJ1+ pixels within the K8+ region, or quantification of the K8+, P2X3+, and TuJ1+ pixels within the entire fungiform papilla. The K8+ region was defined by setting the threshold to 1, and outlining all positive pixels, while the basal epithelium defining the fungiform papilla trench was used to delineate the entire fungiform papillae. Once the borders surrounding the full fungiform papilla or K8+ region were determined, the channels are split, converted to greyscale, and thresholds are set for each channel to minimize inclusion of background quantification. To control for variability in threshold setting, all quantifications were performed by two independent investigators (naïve to experimental conditions) and averaged together. Quantifications with greater than 10% variability between were omitted from inclusion. For the experiments analyzing residual Phox2b expression in Ret germline knockout mice, GGs were collected, sectioned, and imaged as described above. Channels were separated, converted to greyscale, and individual neurons were sampled by an observer naïve to experimental conditions. The data are reported as the mean pixel count per GG neuron ± s.e.m.

Tissue Lysis and Quantitative Immunoblotting

Spinal cords were harvested from 1NM-PP1-treated *Ret*$^{fx/+}$ and *Ret*$^{fx/-}$ mice at E18.5 (Figure 3) and GG from P0 and adult C57BL/6J mice (Jackson Laboratory, Strain #000664) were placed in a 2.0 mL tube with 250 µL lysis buffer (pH 7.4 Tris-buffered saline, 10% glycerol, 500 µm sodium vanadate, and complete protease inhibitors) lacking detergent, along with a steel grinding ball (5mm, Qiagen, Valencia, CA). For the experiments utilizing GGs, ganglia were collected bilaterally along with the facial nerve, and 3 animals were pooled for each tube to increase protein yields. Tissues were then mechanically homogenized using the TissueLyzer II (Qiagen) at a frequency of 20 Hz for 5 minutes. The homogenates were mixed with equal volume of lysis buffer containing 2% Nonidet P-40 (NP-40), and incubated for 1 hour at 4°C under gentle agitation. Homogenates were then centrifuged for 10 minutes at 16,100xg twice to remove insoluble material. Samples were then prepared for sodium dodecyl sulfate-polyacrylate gel electrophoresis (SDS-PAGE) by adding 2X sample buffer (pH 6.8 tris-buffered saline, 20% glycerol, 10% β-mercaptoethanol, 0.05% bromophenol blue, and 4% SDS) and boiling the samples. Samples for western blotting were subjected to SDS-PAGE followed by electroblotting onto polyvinylidene difluoride membranes (Immobilon P, Millipore). Western blot analysis was performed using the following antibodies at the indicated concentrations: α-Ret (AF482, R&D, 1:1000) and α-actin (JLA-20, Iowa Hybridoma, 1:2000). For quantifications, scanned images of x-ray films were imported into ImageJ (National Institutes of Health, Bethesda, MD) and processed using the gel analysis toolkit. Integrated density values were reported as the mean ± s.e.m in arbitrary units (a.u.) on the vertical axis. Total Ret levels were normalized to actin as a loading

control. 1NM-PP1 experiments were performed on n=7 *Ret*$^{fx/+}$ and n=10 *Ret*$^{fx/-}$ mice from 3 separate litters. Experiments comparing P0 vs. adult expression of Ret in the GG were performed on 5 (P0) or 6 (adult) separate lysates.

Verification of Diphtheria Toxin Ablation

Ret+ neuron ablation was verified in TMX-treated *Ret*-Cre/ER^{T2}; *Rosa26*$^{LSL\text{-}DTA/LSL\text{-}DTA}$ mice by serially sectioning GG of *Ret*$^{+/+}$*; DTA*$^{+/+}$ and *Ret*$^{Cre/+}$*; DTA*$^{+/+}$ mice and performing Phox2b counts. Ret-ablated mice having full electrophysiological traces and demonstrating a loss of Phox2b+ neurons greater than one statistical deviation from the mean of the control group (a number chosen based on the adult expression data) were subsequently included in the analysis, while those not meeting these criteria were excluded.

Acknowledgements

We thank Dr. Archana Kumari, Alan Halim, Esther Suh, and Tommy Vu for technical assistance. We thank Dr. Wenqin Liu and Dr. Hideki Enomoto for providing *Ret*-Cre/ER^{T2} mice and Dr. David Ginty and Dr. Joseph Savitt for providing *Ret*$^{fx/fx}$ mice. We thank Robin Krimm for providing *TrkB*$^{GFP/GFP}$ tissues and for technical expertise. Support was provided to CRD through NIDCR T32 DE007057 and NIDCR F30 DE023479. These experiments were supported by NINDS R01 NS089585 and NIDCD R01 DC015799 awarded to BAP and NIDCD R01 DC014428 to CMM and RMB. The authors declare no conflicts of interest.

Author Contributions

CRD and BAP designed experiments, interpreted data, and wrote the manuscript, with assistance from all authors. CRD designed and performed the experiments with assistance from AAS. The electrophysiological experiments were performed by CRD, CMM, and RMB. BAP was responsible for the overall direction and communication of the experiments.

***Figures*:**

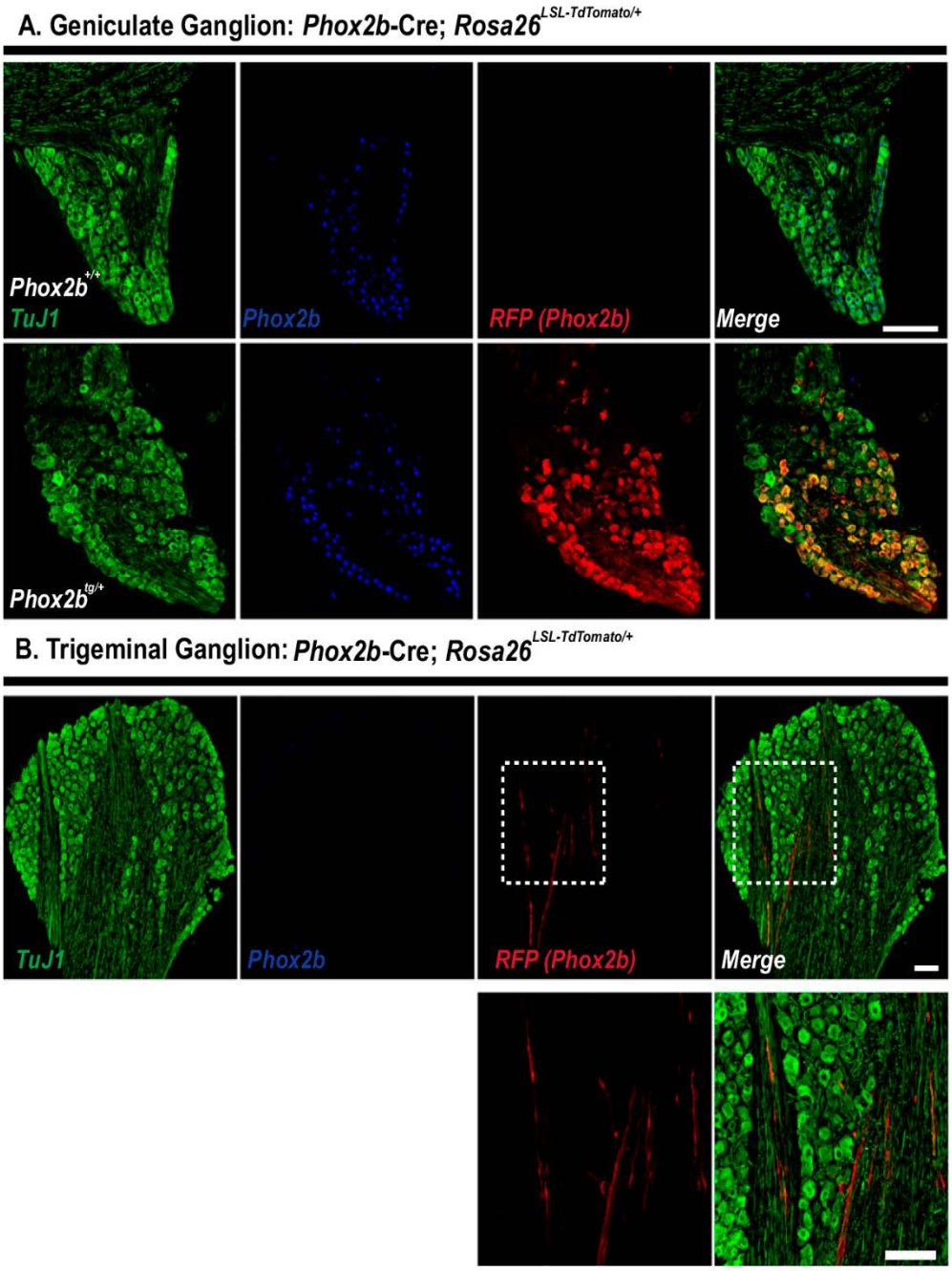

Figure 4.1. Characterization of *Phox2b*-Cre$^{tg/+}$ mice and Phox2b immunostaining.
(A) GGs were collected from P0 *Phox2b*-Cre$^{+/+}$; *Rosa26*$^{LSL\text{-}TdTomato/+}$ (upper panels) or *Phox2b*-Cre$^{tg/+}$; *Rosa26*$^{LSL\text{-}TdTomato/+}$ (lower panels) and stained for TuJ1 (green), Phox2b (blue), RFP (indicates Ret; red), with the merged image displayed in the right most panels. Nearly complete overlap (98.84 ± 0.11%) was observed of Phox2b-immunoreactivity and RFP staining, indicating high reliability of Phox2b immunostaining. (B) TGs from the mice *Phox2b*-Cre$^{tg/+}$; *Rosa26*$^{LSL\text{-}TdTomato/+}$ had a nearly complete

absence of Phox2b immunoreactivity (blue) and a corresponding absence of RFP labeling, further validating Phox2b immunostaining and the *Phox2b*-Cre$^{tg/+}$ reporter. Similar results were observed in GG from n = 4 separate mice. Scale bar represents 100 µM.

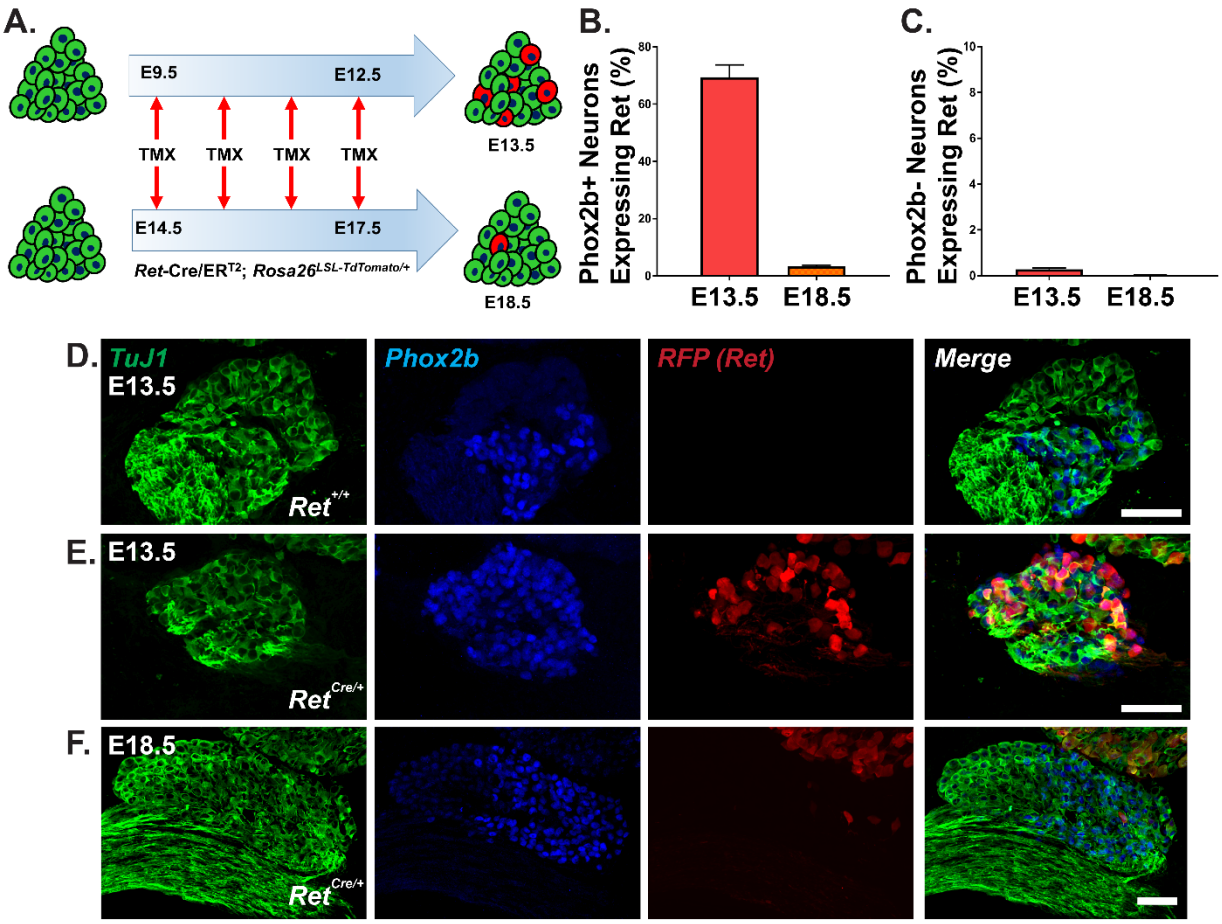

Figure 4.2. Ret is highly expressed in chemosensory geniculate neurons early in development.

(A) Experimental strategy for tracing Ret expression in embryonic geniculate ganglia. Tamoxifen (TMX) was administered to Ret-Cre/ER^{T2}; *Rosa26*$^{LSL-TdTomato/+}$ reporter mice at E9.5-E12.5 with E13.5 analysis (upper) and E14.5-E17.5 with E18.5 analysis (lower). (B) Quantification of the proportion of chemosensory (Phox2b+) neurons expressing Ret demonstrates widespread expression within chemosensory neurons (E13.5; n=3), but Ret expression is extinguished perinatally (E18.5; n=4). (C) Quantification of the proportion of somatosensory (Phox2b-) neurons expressing Ret. (D-F) Immunofluorescence with TuJ1 (green), Phox2b (blue), and RFP (indicating Ret; red) with merged images on the right. (D) Staining in a *Ret*$^{+/+}$ littermate demonstrates specificity of RFP antibody. (E) Ret was widely expressed in chemosensory neurons at the E13.5 analysis timepoint, but (F) largely absent upon analysis at E18.5. Note that the TG in the upper right hand corner of the image has many Ret+ neurons at this age. Scale bar represents 50 µm.

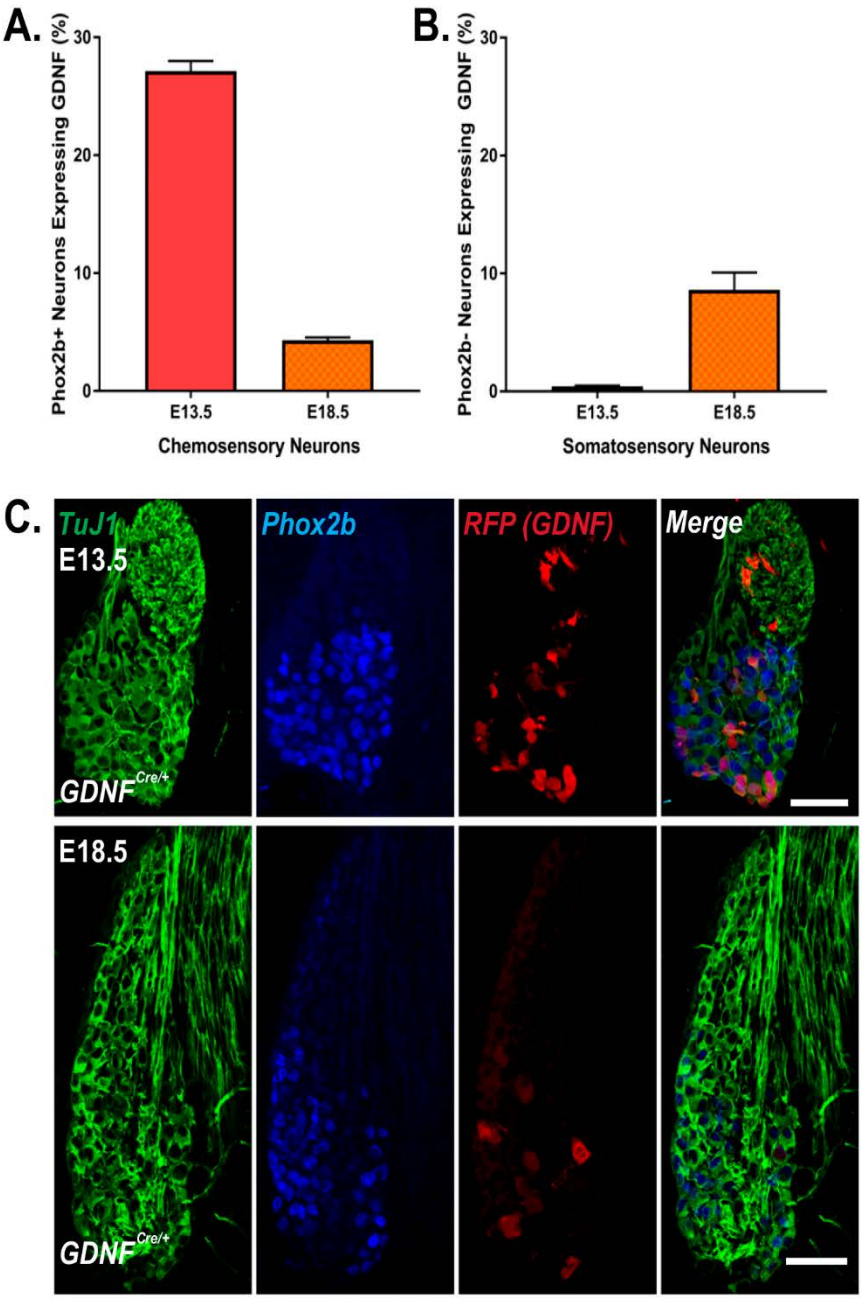

Figure 4.3. Validation of TrkB immunostaining.

Ganglia from P0 heterozygous *TrkB*$^{GFP/+}$ (one functional copy of TrkB protein; left column) or homozygous *TrkB*$^{GFP/GFP}$ (no TrkB protein produced; right column) mice were sectioned and immunostained for Islet1 (pan sensory marker; red), GFP (indicating cells normally expressing TrkB; green), and TrkB (labeling actual TrkB protein; blue). Trigeminal ganglia were imaged. Nearly complete overlap of GFP and TrkB staining was observed in *TrkB*$^{GFP/+}$ neurons, while no TrkB staining was observed in *TrkB*$^{GFP/GFP}$ ganglia, despite the remaining presence of TrkB+ large-diameter

neurons. These data provide evidence for reliable TrkB immunostaining using this antibody and immunostaining method. Similar results were observed from n = 3 separate TGs. Scale bar represents 50 μM.

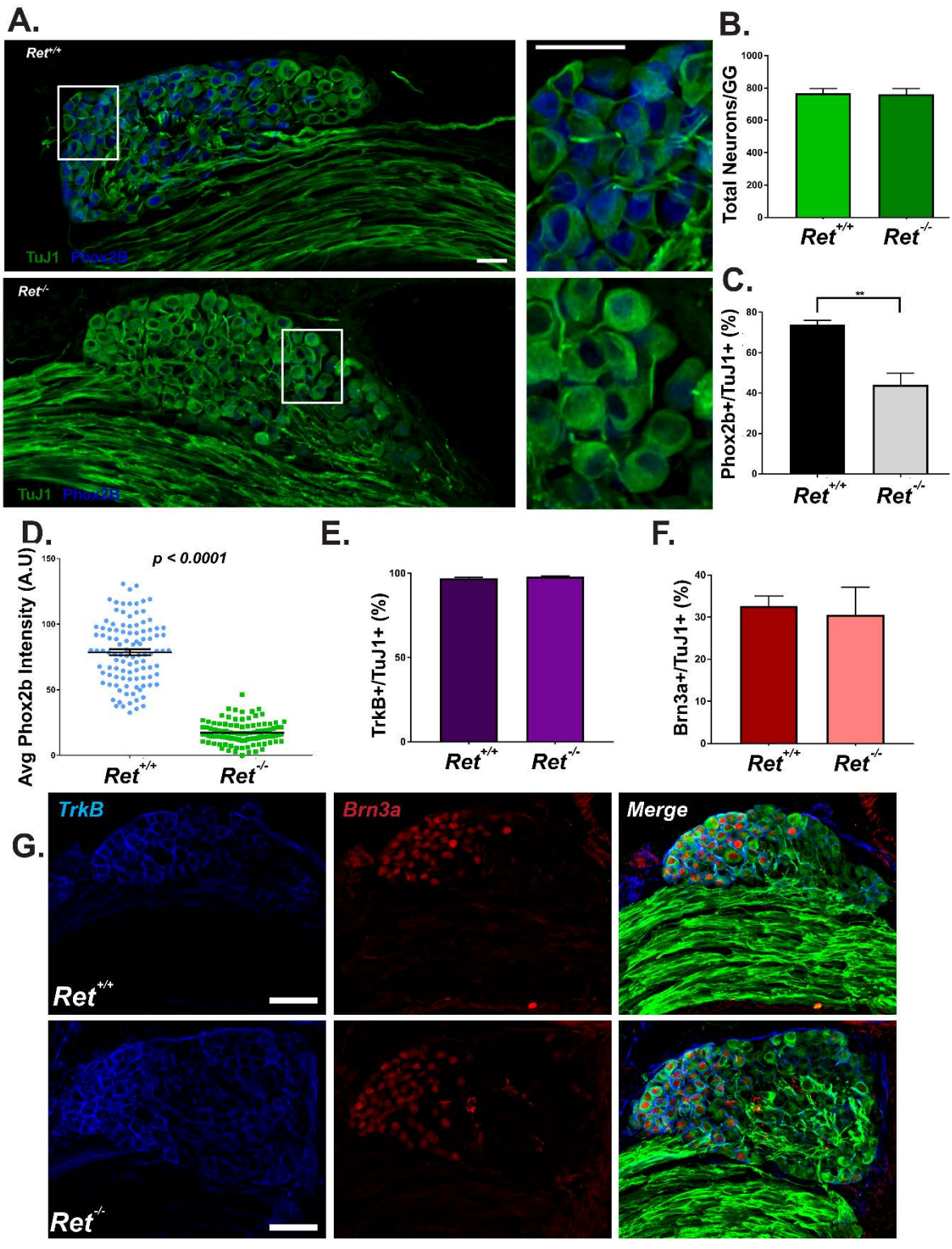
A.
Ret+/+
TuJ1 Phox2B
Ret-/-
TuJ1 Phox2B
B.
Total Neurons/GG
1000
800
600
400
200
0
Ret+/+
Ret-/-
C.
**
Phox2b+/TuJ1+ (%)
80
60
40
20
0
Ret+/+
Ret-/-
D.
p < 0.0001
Avg Phox2b Intensity (A.U)
150
100
50
0
Ret+/+
Ret-/-
E.
TrkB+/TuJ1+ (%)
100
50
0
Ret+/+
Ret-/-
F.
Brn3a+/TuJ1+ (%)
40
30
20
10
0
Ret+/+
Ret-/-
G.
TrkB
Brn3a
Merge
Ret+/+
Ret-/-

Figure 4.4. Ret is required for the expression of the chemosensory fate determinant Phox2b, but is dispensable for chemosensory neuron survival.

(A) GGs were taken from E18.5 *Ret*$^{+/+}$ and *Ret*$^{-/-}$ mice and immunostained for TuJ1 and Phox2b. The left panel displays the entire ganglion, and the area bordered by the white box is magnified on the right. *Ret*$^{-/-}$ mice had substantially fewer Phox2b+ neurons, and those with residual expression appeared reduced in Phox2b staining intensity. (B) The total number of GG neurons was assessed by counting TuJ1+ neurons. No difference was observed in total numbers of *Ret*$^{+/+}$ GGs (n=6) compared to *Ret*$^{-/-}$ GGs (n=9; p = 0.9014). (C) Quantification of the proportion of neurons expressing Phox2b. *Ret*$^{-/-}$ GGs had a reduction in Phox2b+ neurons compared to *Ret*$^{+/+}$ GGs (40.1% reduction; p = 0.0015). (D) The intensity of Phox2b expression was quantified in *Ret*$^{+/+}$ and *Ret*$^{-/-}$ GG. *Ret*$^{-/-}$ GGs had significantly lower Phox2b immunolabeling ($p < 0.0001$) compared to *Ret*$^{+/+}$ GGs. (E) Immunostaining was performed on *Ret*$^{+/+}$ and *Ret*$^{-/-}$ GGs for the somatosensory transcription factor Brn3a and the BDNF receptor TrkB. (E) No differences were observed in TrkB expression (p = 0.1161, n=7 *Ret*$^{+/+}$ and n=6 *Ret*$^{-/-}$ mice). (F) No differences were observed in Brn3a expression (p = 0.7587; n=7 *Ret*$^{+/+}$ and n=6 *Ret*$^{-/-}$ mice). (G) Representative immunolabeling for TuJ1 (green), Brn3a (red), and TrkB (blue). The merged image demonstrates TrkB is widely expressed throughout the ganglion, while Brn3a expression is expressed in a polarized manner. (Scale bars represent 100 µm. Statistical significance for each comparison was determined with a two-tailed t-test.

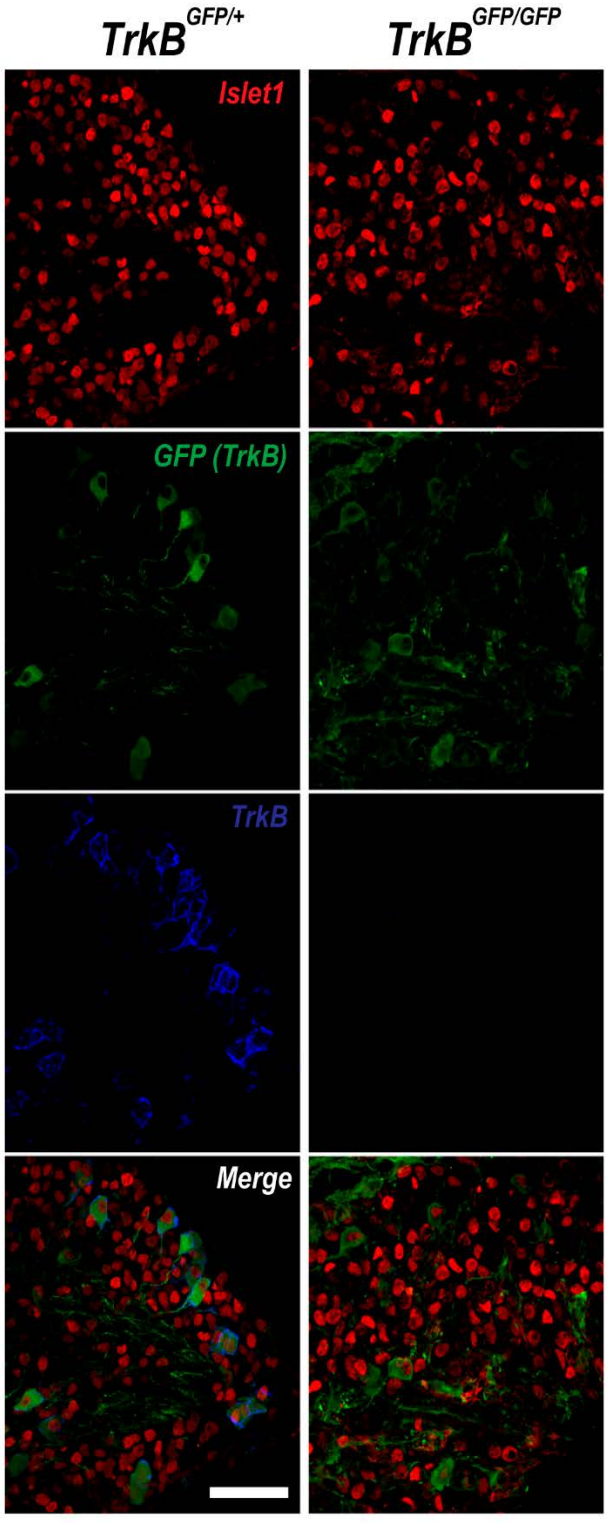
TrkB GFP/+
TrkB GFP/GFP
Islet1
GFP (TrkB)
TrkB
Merge

Figure 4.5. Characterization of Ret+ adult geniculate ganglion neurons.
(A) Classification of Phox2b expression in *Ret*-Cre/ER^{T2}; *Rosa26*$^{LSL\text{-}TdTomato/+}$ reporter mice given TMX as described in figure 5. 82.28% of all Ret+ neurons counted from n = 5 mice were chemosensory (Phox2b+). (B) Histogram displaying the distribution of somal diameters, measured at the widest aspect of each RFP+ (Ret-expressing) neuron, in RFP+ chemosensory (Phox2b+) and somatosensory (Phox2b-) GG neurons. A trend was observed for RFP+/Phox2b+ neurons to be larger in diameter compared to RFP+/Phox2b- neurons ($p = 0.0005$). (C) Graphical representation of the somal diameter of RFP+/Phox2b- (blue dots) and RFP+/Phox2b+ neurons (orange dots) with the mean somal diameter indicated by the black line. Many more chemosensory Ret+ neurons were >30 µM in somal diameter. Two-tailed t-test indicated that the RFP+/Phox2b+ neurons were significantly larger than RFP+/Phox2b- neurons ($p = 0.0005$). (D) Characterization of overlap in Ret expression with TrkB protein expression in *Ret*-Cre/ER^{T2}; *Rosa26*$^{LSL\text{-}TdTomato/+}$ reporter GGs administered TMX as described in Figure 5. Ret expression was observed to be more restricted compared to TrkB. Examples of RFP+/TrkB+ and RFP+/TrkB- (yellow arrow) neurons could be observed. Scale bar represents 50 µM. (E) Classification of overlap in RFP and TrkB expression (n = 4). Approximately 2/3 of neurons expressed Ret but not TrkB, while 1/3 of neurons expressed both receptors. (F) Histogram displaying the distribution of somal diameters in Ret-/TrkB+ (dark blue bars), Ret+/TrkB+ (light blue bars) and Ret+/TrkB- (red bars) GG neurons. As in B, somal diameter of Ret+/TrkB- neurons was shifted to the right (larger) compared to Ret+/TrkB+ and Ret-/TrkB+ neurons. (G) Graphical representation of the somal diameter of Ret-/TrkB+ (dark blue dots), Ret+/TrkB+ (light blue dots) and Ret+/TrkB- (red dots) with mean indicated by the black bars. A statistically significant increase in somal diameter was observed (one-way ANOVA) between all groups, with Ret+/TrkB- being significantly larger than Ret+/TrkB+ ($p = 0.0058$) and Ret-/TrkB+ ($p < 0.0001$) neurons. Ret+/TrkB+ neurons were also found to be significantly larger than Ret-/TrkB+ neurons ($p < 0.0001$).

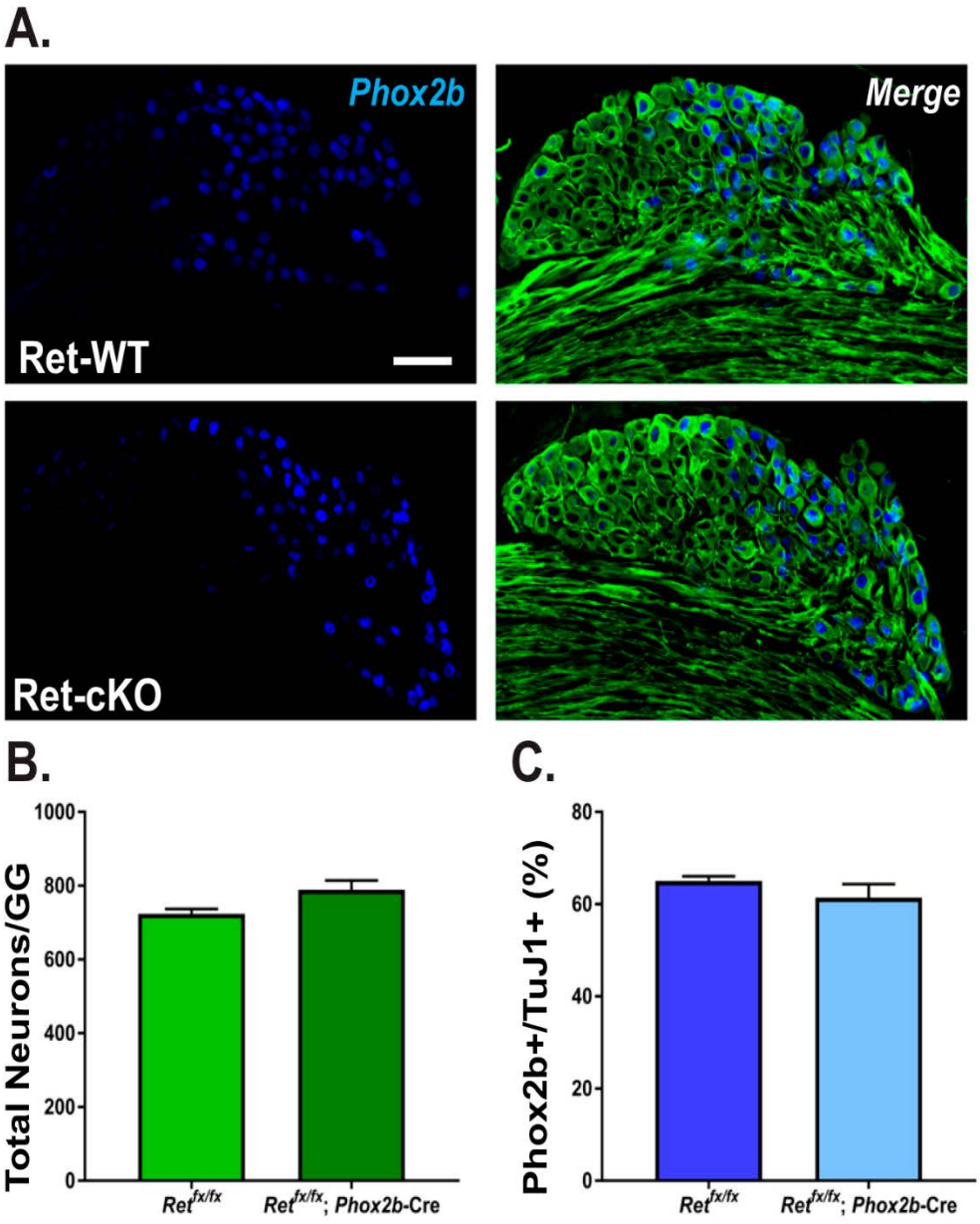

Figure 4.6. Expression profile of GFRα2, GFRα3, and NF200 in the geniculate ganglion.

(A) GGs taken from adult *Ret*-Cre/ER^{T2}; *Rosa26*$^{LSL\text{-}TdTomato/+}$ reporter mice administered TMX were immunostained for TuJ1 (green), RFP (Ret; red), and GFRα2 (blue; upper) or GFRα3 (blue; lower), with the merged image displayed on the right. Although some GFRα2+ nerve fibers could be visualized within the nearby facial nerve, no neuronal staining was observed for either co-receptor within the GG. (B) To confirm that the GFRα2 and GFRα3 immunostaining procedure was working, we analyzed TGs taken from the mice described above. Clear examples of GFRα2+ (upper) and GFRα3+ (lower) TG neurons were observed, most of which co-expressed Ret. Similar results

were obtained in n=3 individual mice with similar results. Collectively, these data indicate that GFRα2 and GFRα3 are not present within GGs, providing further evidence for a GDNF-GFRα1-Ret signaling axis in adult GGs. (D) GGs were collected from adult *Rosa26*$^{LSL\text{-}tdTomato/+}$*; Phox2b-Cre*$^{tg/+}$ mice and stained for NF200 (green), Brn3a (blue), and Phox2b (RFP; red) to ascertain the transcriptional profile of NF200+ GG neurons. We observed almost complete segregation of Brn3a and Phox2b expression (lower left panel merged), as expected based on previous literature. Rare examples of Brn3a+/Phox2b+ neurons were observed (green arrows). While some examples of Brn3a+/NF200+ neurons were observed (lower middle panel; yellow arrows), many more examples of Phox2b+/NF200+ neurons were observed (lower right panel; blue arrows). Scale bar represents 50 μM.

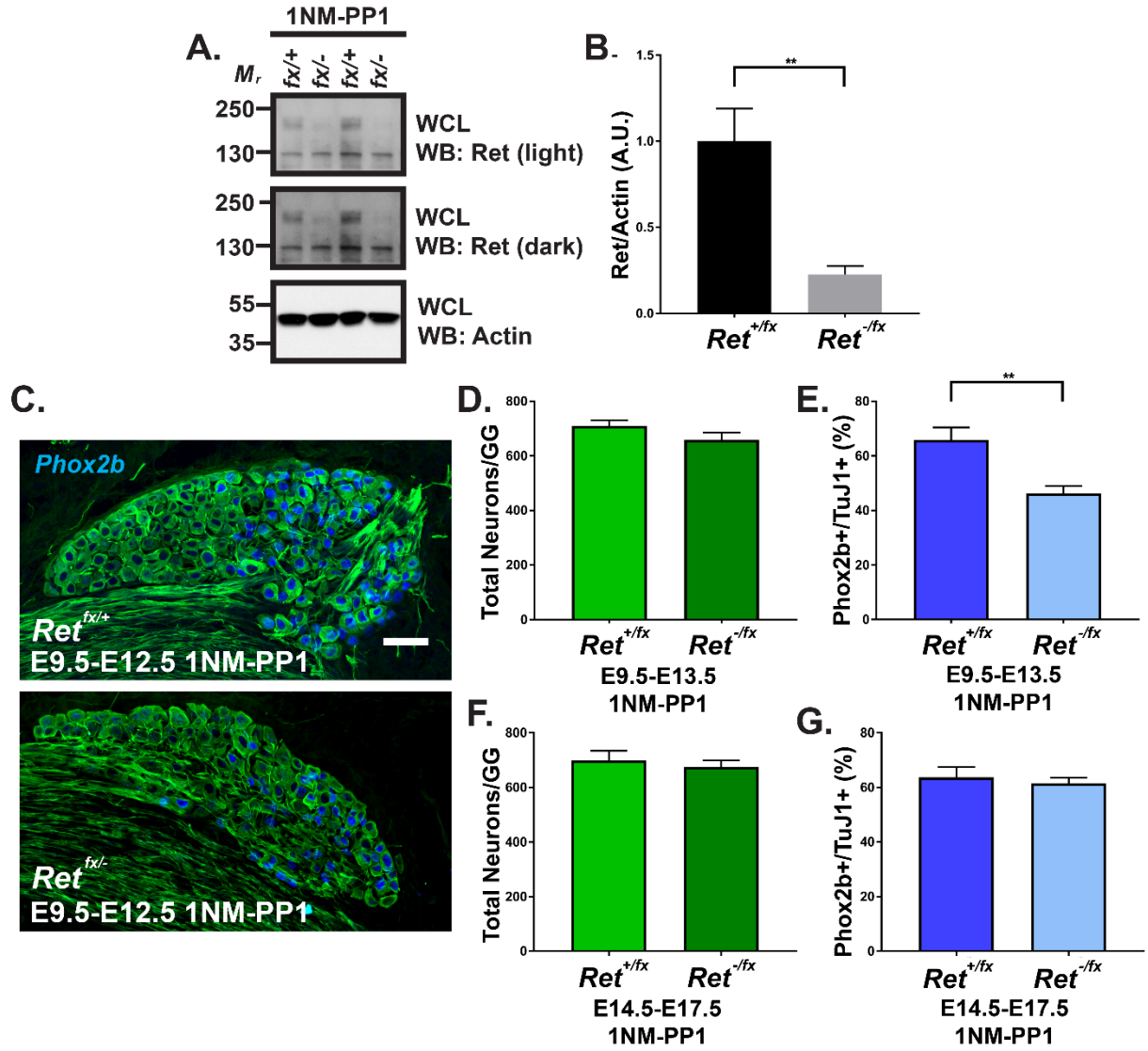

Figure 4.7. Ret is required for the amplification of Phox2b early in development.
(A) The selective Ret inhibitor, 1NM-PP1 was administered to mice of the indicated genotypes at E14.5 until E18.5. Spinal cords were collected, homogenized, and detergent extracted, followed by immunoblotting for Ret, or actin (as a loading control). (B) Quantification of total Ret levels (normalized to actin). We observed a reduction of approximately 77% of total Ret levels following 1NM-PP1 administration in *Ret*$^{fx/-}$ mice (n=7) compared to *Ret*$^{fx/+}$ mice (n=10; p = 0.0048). (C) *Ret*$^{fx/+}$ and *Ret*$^{fx/-}$ mice were administered 1NM-PP1 via daily from E9.5-E12.5. Mice were euthanized on E13.5 and GGs were immunostained for TuJ1 and Phox2b. Similar to the results observed in Ret germline knockout mice, *Ret*$^{fx/-}$ mice had substantially fewer Phox2b+ neurons with no apparent change in total neuron number. Total neurons (D) and the proportion of Phox2b+ neurons (E) were quantified. No difference was observed in total neuron

numbers (p = 0.2056; n = 4-6). *Ret*$^{fx/-}$ had a reduction in the proportion of Phox2b+ neurons compared to *Ret*$^{fx/+}$ (p = 0.0041; n = 4-6). (F) *Ret*$^{fx/+}$ and *Ret*$^{fx/-}$ mice were administered 1NM-PP1 as described in C from E14.5 to E17.5. GGs were again immunostained for TuJ1 and Phox2b. No significant differences were observed between genotypes in the total number of neurons (p = 0.6167; n = 5 for each) or (G) the proportion of Phox2b+ neurons (0.6118; n = 5 for each). Scale bar represents 100 µm.

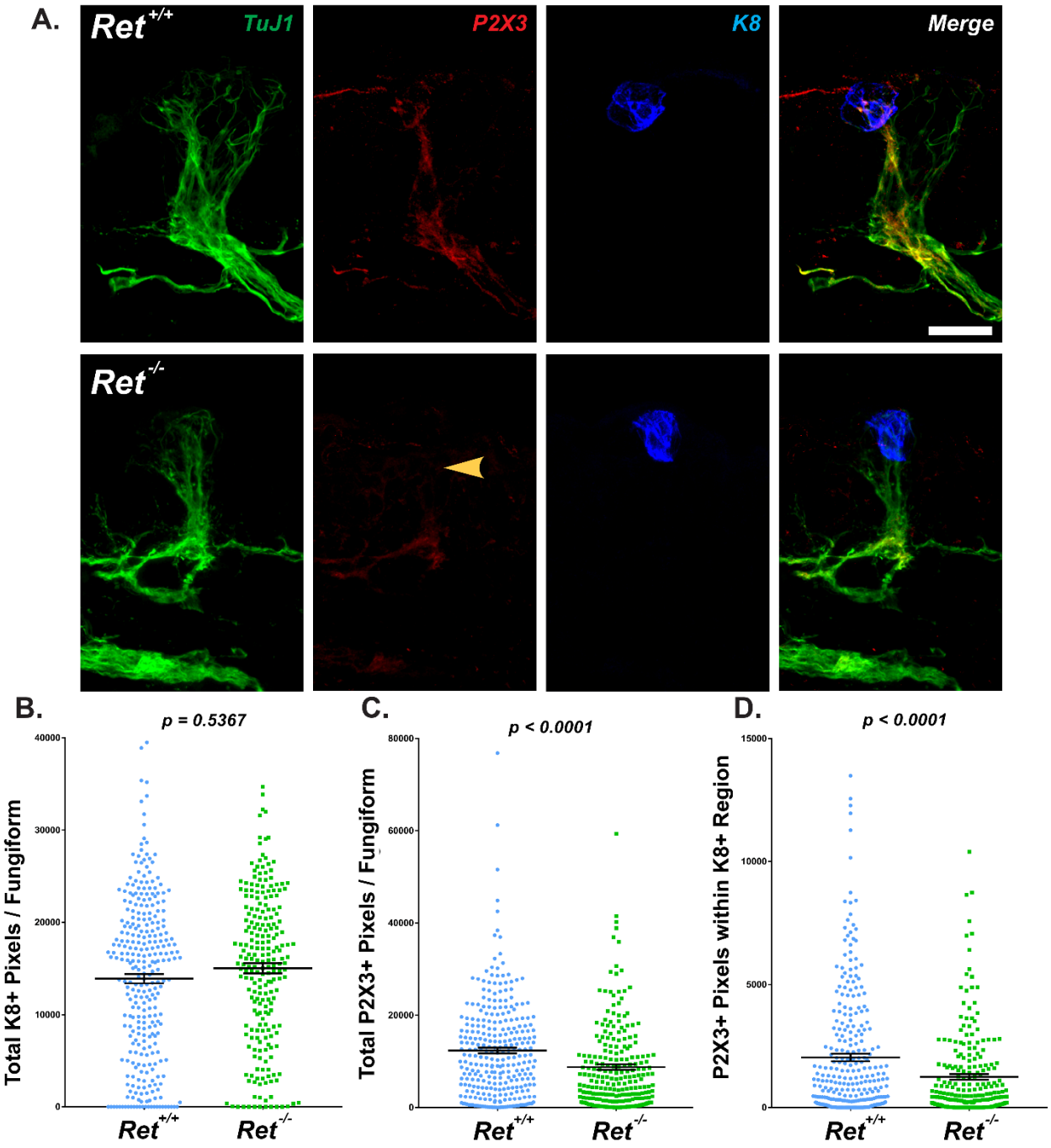

Figure 4.8. Loss of Ret results in deficits in fungiform papilla chemosensory innervation.

(A) Tongues were collected from E18.5 *Ret*$^{+/+}$ and *Ret*$^{-/-}$ mice, serially sectioned at 50 µm, and immunostained for TuJ1 (green), P2X3 (red), K8 (blue) and merged. Many more examples of FP lacking apically projecting P2X3+ fibers were observed in *Ret*$^{-/-}$ compared to *Ret*$^{+/+}$ tongues (yellow arrow). (B) All fungiform papillae from n = 4 mice

were imaged (n = 300 *Ret*$^{+/+}$ FP and n = 230 *Ret*$^{-/-}$ FP) and quantified as described in the Methods. When analyzing the entire papilla, no differences were observed in the number of K8+ pixels per FP ($p = 0.5367$). (C) A highly significant reduction in P2X3+ pixels was observed in *Ret*$^{-/-}$ mice ($p < 0.0001$). When analyzing only the nerve fibers present within the K8+ region, (F) P2X3+ pixels were substantially reduced ($p < 0.0001$). The graphs in B-D display the individual data points (colored circle and squares), while the mean ± s.e.m. is indicated by the black line. Scale bar represents 25 µm.

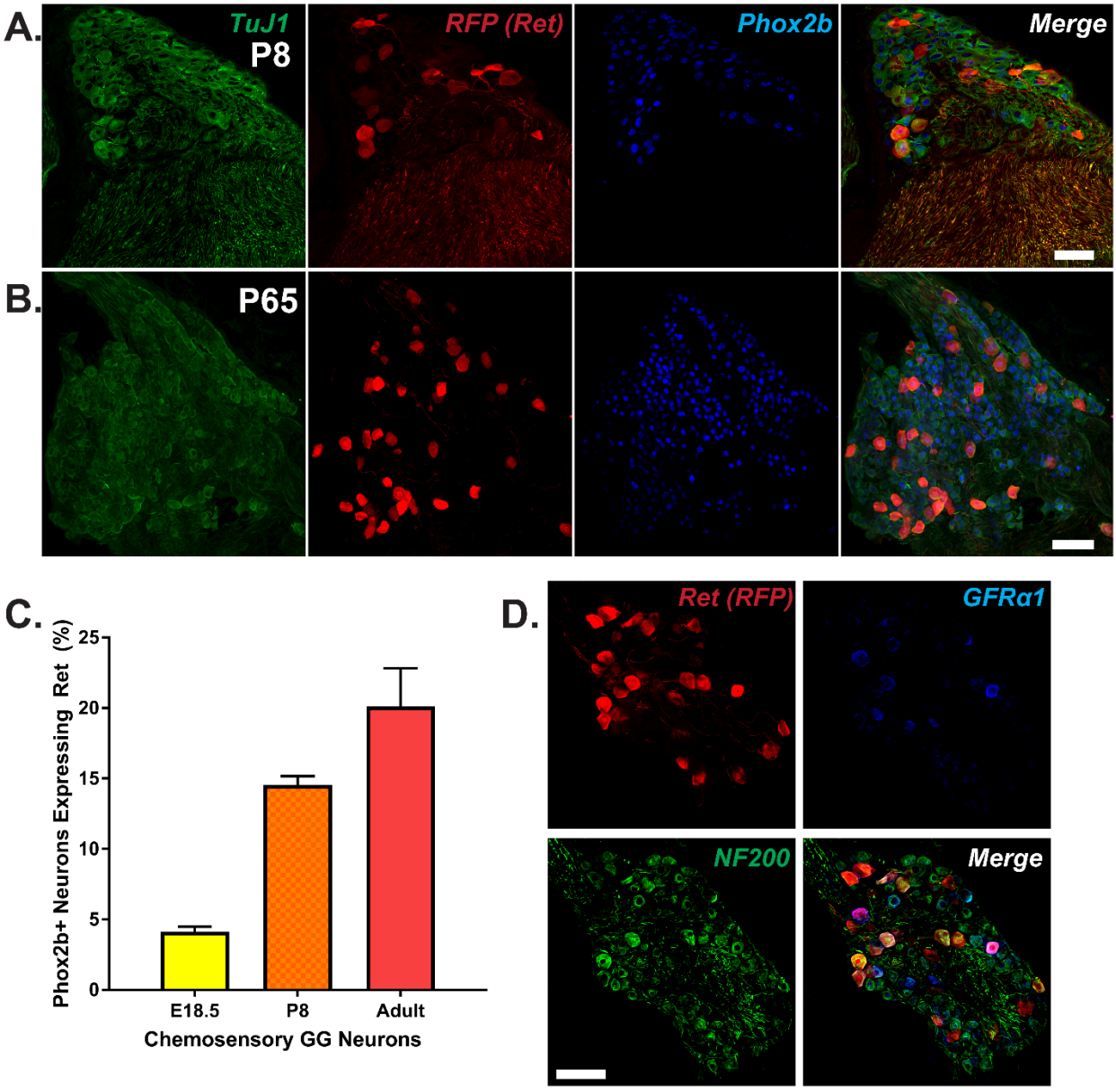

Figure 4.9. Ret is expressed postnatally in a subpopulation of GFRα1/NF200+ chemosensory neurons.

(A) Ret-Cre/ER^{T2}; *Rosa26*$^{LSL\text{-}TdTomato/+}$ mice were administered TMX at P3-P7 and analyzed at P8 or (B) P60-P64 and analyzed at P65. GGs were stained for TuJ1 (green), RFP (indicating Ret, red), and Phox2b (blue). (C) Quantification of Ret expression at E18.5 (re-graphed from figure 1B), P8, and P65 indicated that a substantial number of chemosensory neurons upregulate Ret postnatally. (D) Adult GGs from TMX-labeled Ret-Cre/ER^{T2}; *Rosa26*$^{LSL\text{-}TdTomato/+}$ were immunostained for RFP (red), GFRα1 (blue) and the mechanoreceptor marker neurofilament heavy chain (NF200). Many neurons demonstrated overlapping expression of all Ret, GFRα1, and

NF200 (representative image from n=4 individual experiments). Scale bars represent 50 µm.

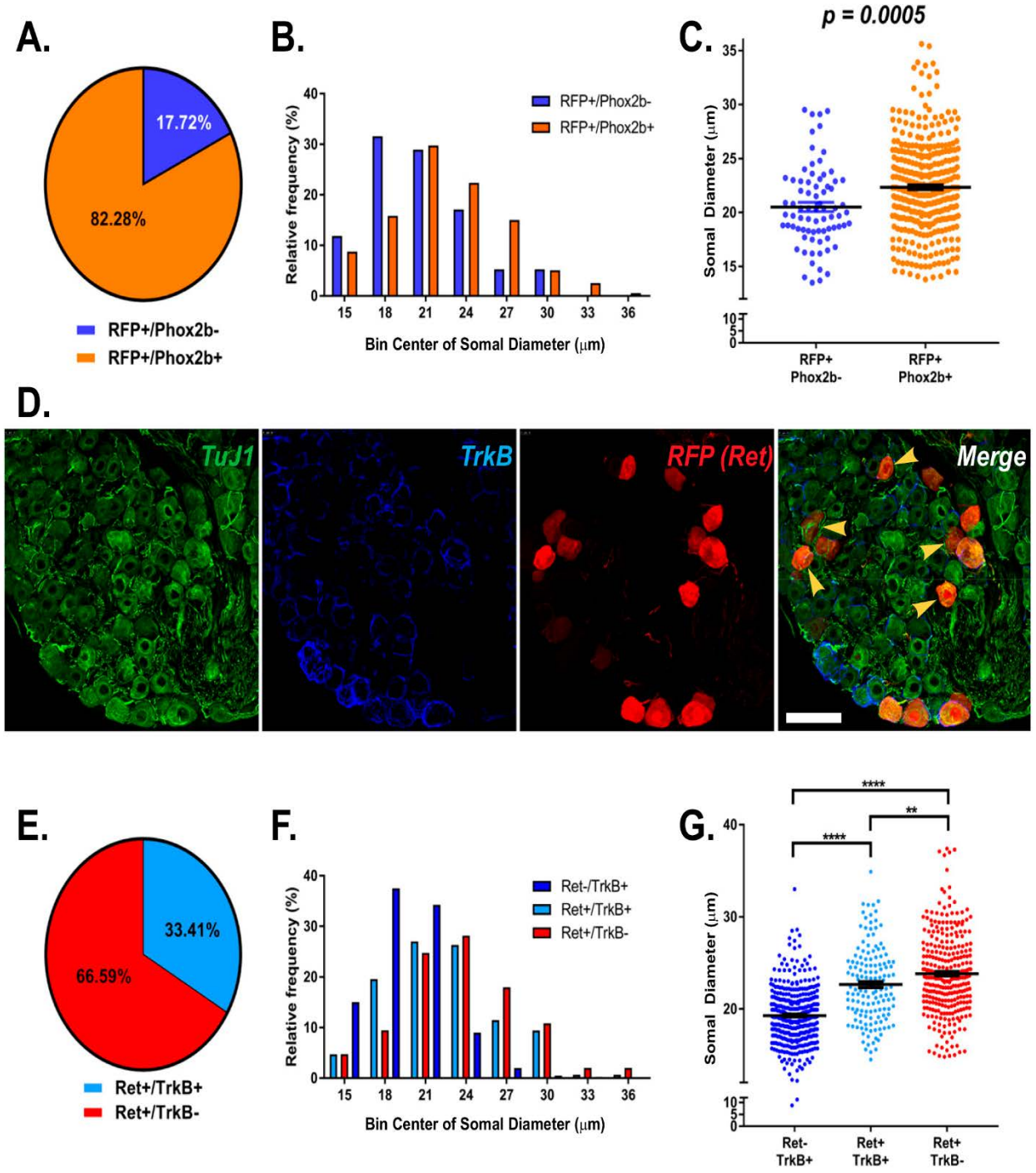

Figure 4.10. Characterization of Ret expression in fungiform papillae.

(A) To determine whether any regional differences in Ret expression exist, we analyzed FP from adult *Ret*-Cre/ER^{T2}; *Rosa26*$^{LSL\text{-}TdTomato/+}$ reporter tongues labeled with TMX as described in figure 5. To control for the increased density of FP on the tip of the anterior tongue compared to the middle and posterior aspect of the anterior tongue, the number

within each group was divided by the total number of FP within that region to yield a percentage of all FP counted (n=5 individual mice). Regardless of regional localization, a similar distribution pattern was observed for extragemmal fibers (>3 fibers/tip: 81.65%; >3 fibers/middle: 83.78%; >3 fibers/posterior 90.00%; 1-3 fibers/tip: 15.59%; 1-3 fibers/middle: 10.81%; 1-3 fibers/posterior: 10.00%; no fibers/tip: 2.75%; no fibers/middle: 5.41%; no fibers/posterior: 0.00%). (B) Similarly, intragemmal fibers were classified to identify potential regional differences as described in A. No differences in distribution pattern were observed (>3 fibers/tip: 11.01%; >3 fibers/middle: 10.81%; >3 fibers/posterior 16.67%; 1-3 fibers/tip: 30.28%; 1-3 fibers/middle: 32.43%; 1-3 fibers/posterior: 36.67%; no fibers/tip: 58.72%; no fibers/middle: 56.76%; no fibers/posterior: 46.67%). A small increase overall was seen in intragemmal Ret+ fibers in the posterior region when discounting innervation density categories (53.54% Ret+ intragemmal fibers in posterior vs. 43.24% and 41.29% Ret+ intragemmal fibers in middle and tip of the anterior tongue, respectively). (C) A small number of Ret+ taste receptor cells (TRC) were observed (8% of FP overall; always present in tip of the tongue). These Ret+ TRCs were generally of an elongated morphology, spanning apically to basally within the taste bud. Scale bar represents 25 μM.

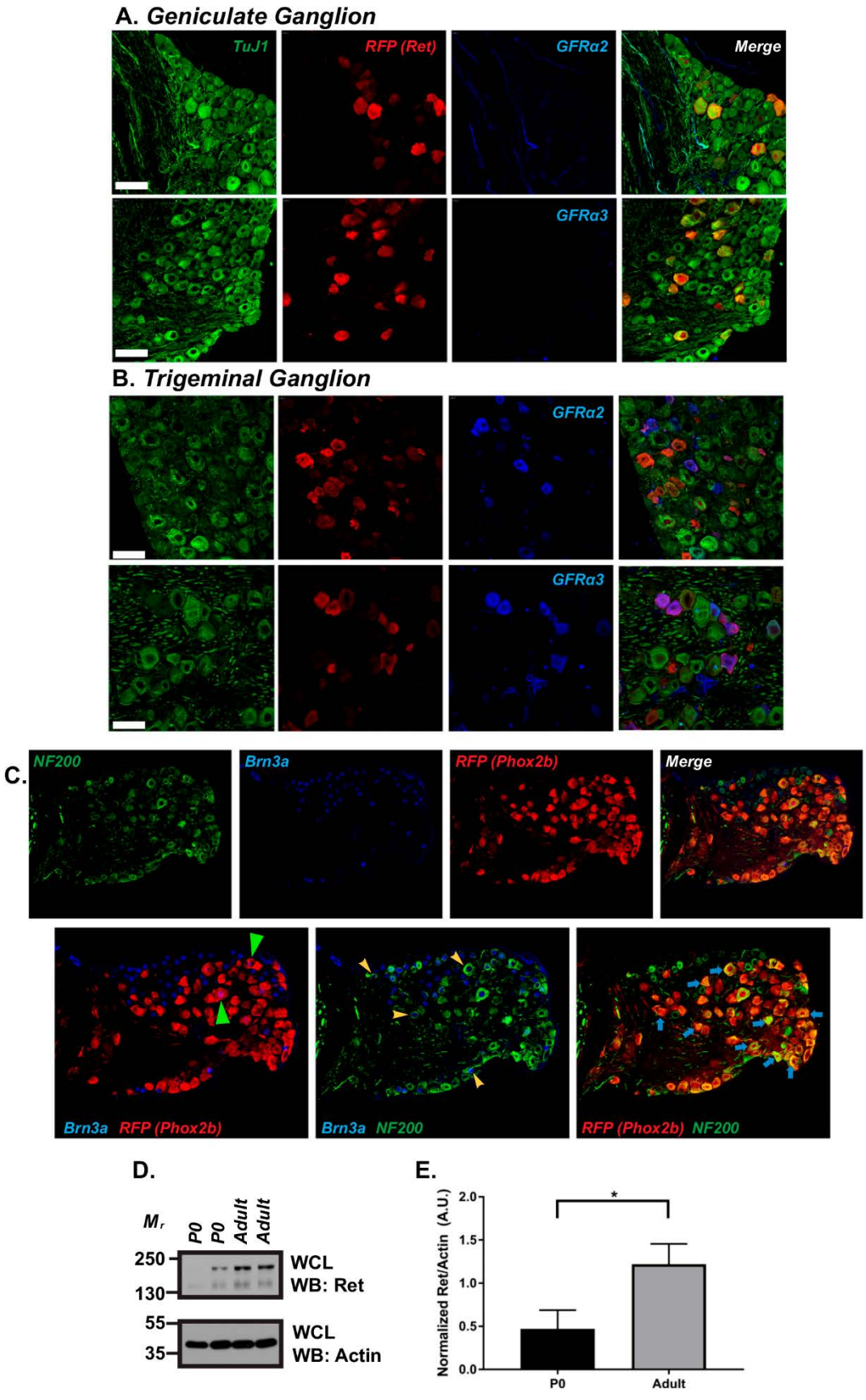
A. Geniculate Ganglion
TuJ1
RFP (Ret)
GFRα2
Merge
GFRα3
B. Trigeminal Ganglion
GFRα2
GFRα3
C.
NF200
Brn3a
RFP (Phox2b)
Merge
Brn3a RFP (Phox2b)
Brn3a NF200
RFP (Phox2b) NF200
D.
Mr
P0
P0
Adult
Adult
250
130
WCL
WB: Ret
55
35
WCL
WB: Actin
E.
Normalized Ret/Actin (A.U.)
2.0
1.5
1.0
0.5
0.0
*
P0
Adult

Figure 4.11. Expression profile of GFRα2, GFRα3, and NF200 in the geniculate ganglion.

(A) GGs taken from adult *Ret*-Cre/ER^{T2}; *Rosa26*$^{LSL\text{-}TdTomato/+}$ reporter mice administered TMX were immunostained for TuJ1 (green), RFP (Ret; red), and GFRα2 (blue; upper) or GFRα3 (blue; lower), with the merged image displayed on the right. Although some GFRα2+ nerve fibers could be visualized within the nearby facial nerve, no neuronal staining was observed for either co-receptor within the GG. (B) To confirm that the GFRα2 and GFRα3 immunostaining procedure was working, we analyzed TGs taken from the mice described above. Clear examples of GFRα2+ (upper) and GFRα3+ (lower) TG neurons were observed, most of which co-expressed Ret. Similar results were obtained in n=3 individual mice with similar results. Collectively, these data indicate that GFRα2 and GFRα3 are not present within GGs, providing further evidence for a GDNF-GFRα1-Ret signaling axis in adult GGs. (D) GGs were collected from adult *Rosa26*$^{LSL\text{-}tdTomato/+}$*; Phox2b-Cre*$^{tg/+}$ mice and stained for NF200 (green), Brn3a (blue), and Phox2b (RFP; red) to ascertain the transcriptional profile of NF200+ GG neurons. We observed almost complete segregation of Brn3a and Phox2b expression (lower left panel merged), as expected based on previous literature. Rare examples of Brn3a+/Phox2b+ neurons were observed (green arrows). While some examples of Brn3a+/NF200+ neurons were observed (lower middle panel; yellow arrows), many more examples of Phox2b+/NF200+ neurons were observed (lower right panel; blue arrows). Scale bar represents 50 μM.

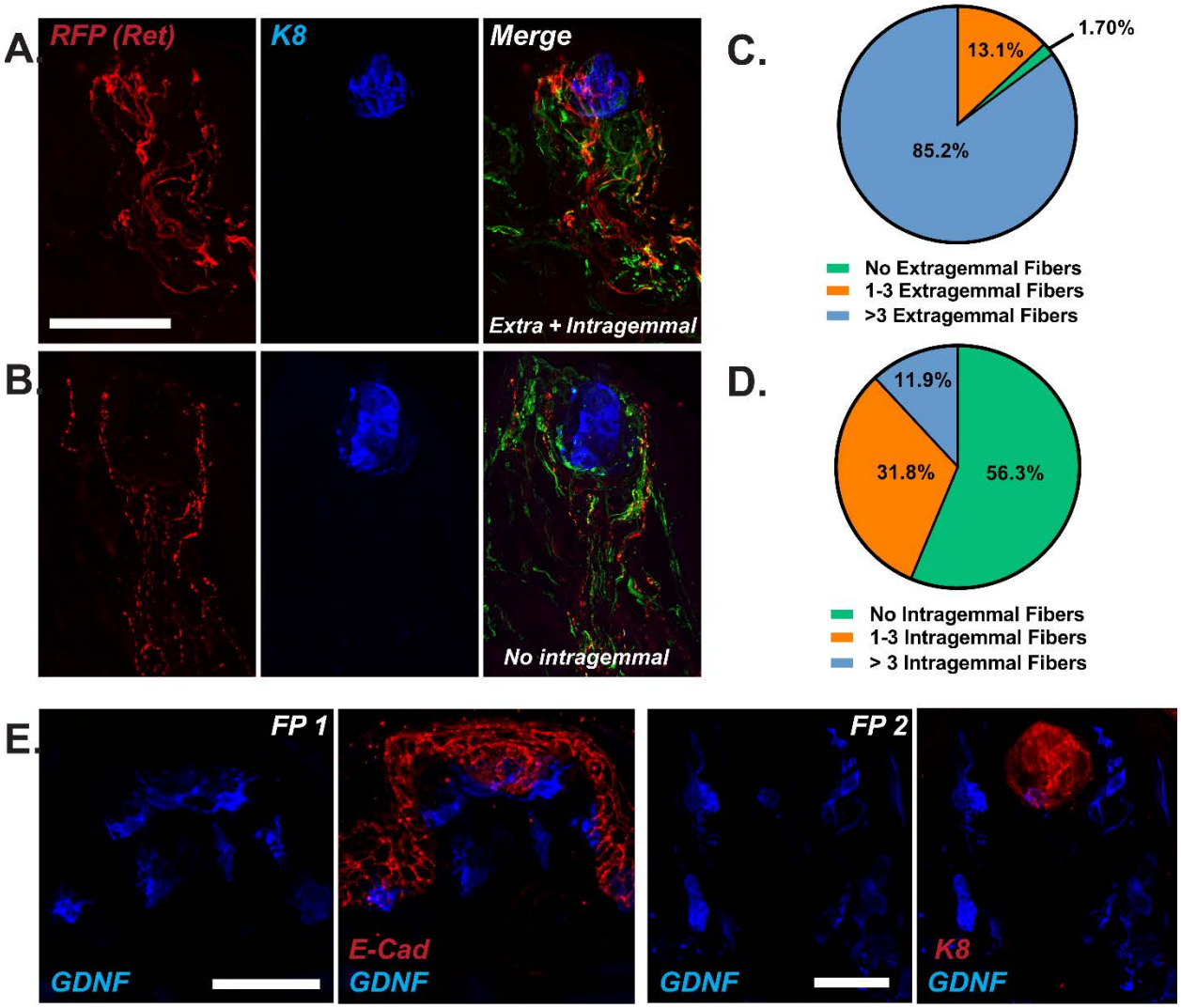

Figure 4.12. Distribution pattern of Ret+ nerve fibers and GDNF+ cells within fungiform papillae.

(A) Whole tongues from adult Ret-Cre/ER^{T2}; *Rosa26*$^{LSL\text{-}TdTomato/+}$ mice were immunostained for RFP (indicates Ret, red), K8 (blue) and TuJ1 (green; present in merged image). 176 FP from n=5 individual mice were imaged and the pattern of Ret expression was categorized as intragemmal (within the K8+ region) or extragemmal (outside of the K8+ region). Panel A shows an example of a FP with extensive (> 3 fibers) intragemmal and extragemmal innervation by Ret+ fibers. (B) Example of a FP with extensive (>3 fibers) extragemmal labeling but no intragemmal Ret+ fibers. (C) Quantification of the innervation density of Ret+ extragemmal fibers indicates that the vast majority of FP have extragemmal fibers present (98.3%), most of which (85.2%) have greater than 3 fibers. (D) Quantification of the innervation density of intragemmal Ret+ fibers demonstrates that many FP (43.7%) have an intragemmal projection pattern. (E) 5 daily doses of TMX was administered to adult *GDNF*-IRES-Cre/ER^{T2};

Rosa26$^{LSL\text{-}TdTomato/+}$ via i.p. injection. Tongues were then fixed, preserved, serially sectioned, and immunostained for RFP (indicating GDNF; blue) and E-Cadherin (red; left panel, FP 1) or K8 (red; right panel, FP 2). All FP were imaged from n=4 individual mice. We observed a variable pattern of expression of GDNF within the TB region (ranging from 0-2 cells generally present within the basal aspect of the TB, but strong labeling of GDNF in the perigemmal space immediately surrounding the TB. In addition, GDNF+ cells were observed in the E-Cad+ trenches at the base of the FP. On occasion, GDNF+ cells were observed in the mesenchymal core of the FP. Scale bar represents 50 μm. In all cases Cre-negative littermate controls were always utilized to control for RFP immunostaining specificity.

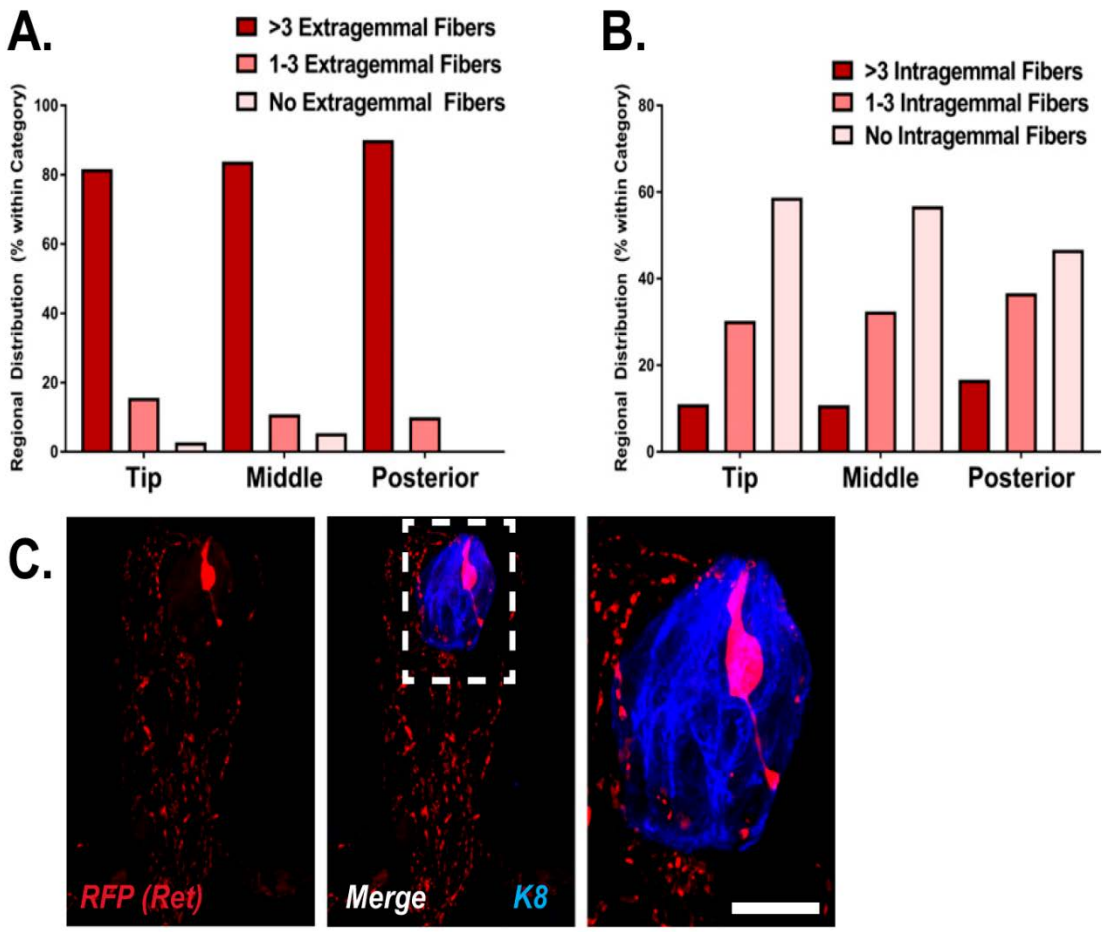

Figure 4.13. Characterization of Ret expression in fungiform papillae.
(A) To determine whether any regional differences in Ret expression exist, we analyzed FP from adult *Ret*-Cre/ER^{T2}; *Rosa26*$^{LSL\text{-}TdTomato/+}$ reporter tongues labeled with TMX as described in figure 5. To control for the increased density of FP on the tip of the anterior tongue compared to the middle and posterior aspect of the anterior tongue, the number within each group was divided by the total number of FP within that region to yield a percentage of all FP counted (n=5 individual mice). Regardless of regional localization, a similar distribution pattern was observed for extragemmal fibers (>3 fibers/tip: 81.65%; >3 fibers/middle: 83.78%; >3 fibers/posterior 90.00%; 1-3 fibers/tip: 15.59%; 1-3 fibers/middle: 10.81%; 1-3 fibers/posterior: 10.00%; no fibers/tip: 2.75%; no fibers/middle: 5.41%; no fibers/posterior: 0.00%). (B) Similarly, intragemmal fibers were classified to identify potential regional differences as described in A. No differences in distribution pattern were observed (>3 fibers/tip: 11.01%; >3 fibers/middle: 10.81%; >3 fibers/posterior 16.67%; 1-3 fibers/tip: 30.28%; 1-3 fibers/middle: 32.43%; 1-3 fibers/posterior: 36.67%; no fibers/tip: 58.72%; no fibers/middle: 56.76%; no fibers/posterior: 46.67%). A small increase overall was seen in intragemmal Ret+ fibers in the posterior region when discounting innervation density categories (53.54% Ret+ intragemmal fibers in posterior vs. 43.24% and 41.29% Ret+ intragemmal fibers in

middle and tip of the anterior tongue, respectively). (C) A small number of Ret+ taste receptor cells (TRC) were observed (8% of FP overall; always present in tip of the tongue). These Ret+ TRCs were generally of an elongated morphology, spanning apically to basally within the taste bud. Scale bar represents 25 μM.

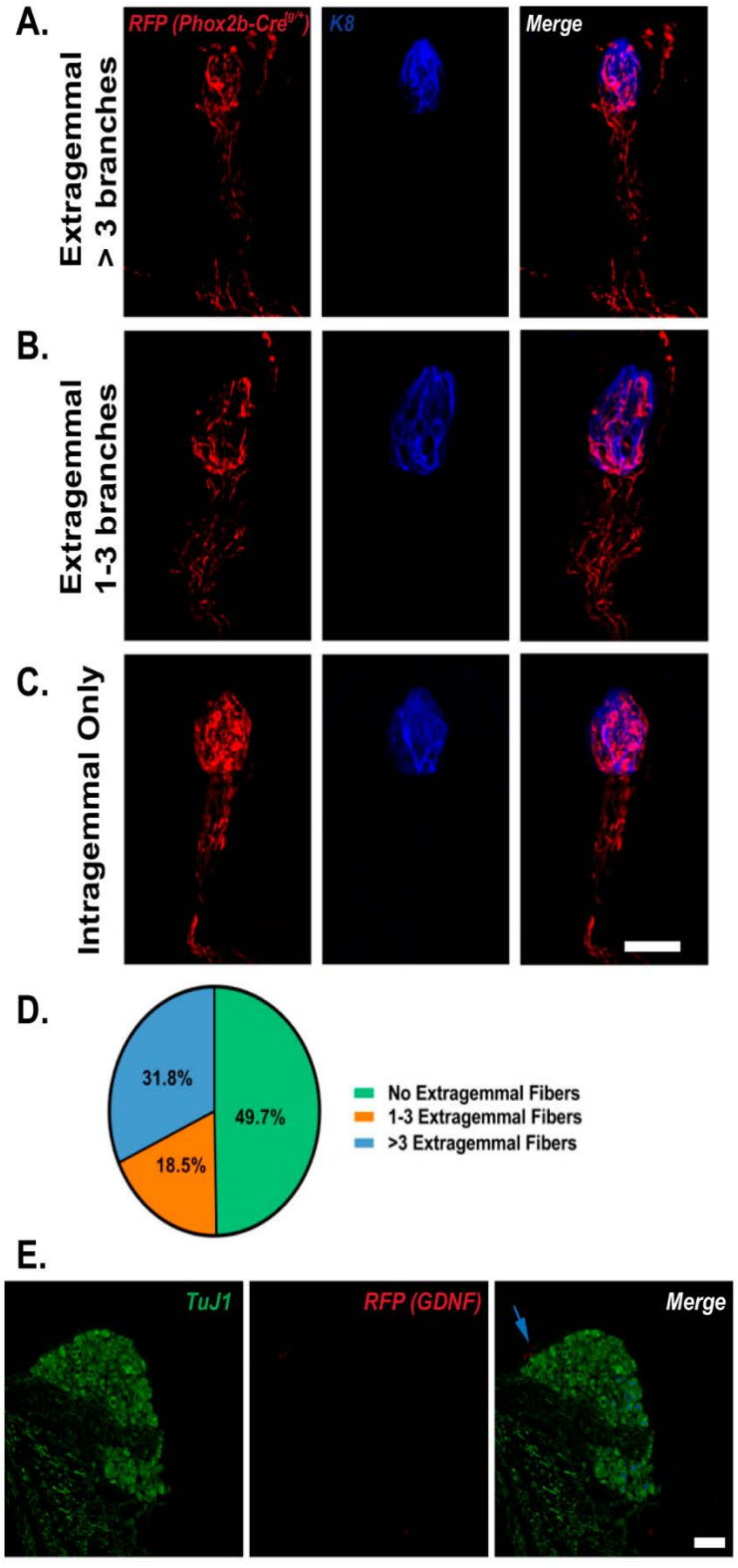
A.
Extragemmal
> 3 branches
RFP (Phox2b-Cre^tg/+)
K8
Merge
B.
Extragemmal
1-3 branches
C.
Intragemmal Only
D.
31.8%
49.7%
18.5%
No Extragemmal Fibers
1-3 Extragemmal Fibers
>3 Extragemmal Fibers
E.
TuJ1
RFP (GDNF)
Merge

Figure 4.14. Many chemosensory nerves terminate outside the taste bud region.
To ascertain whether all chemosensory GG neurons projected to the taste bud region proper, tongues were collected from adult *Phox2b*-Cre$^{tg/+}$; *Rosa26*$^{LSL\text{-}TdTomato/+}$ and stained for K8 (blue) and RFP (chemosensory axons; red), with the merged image displayed. 151 fungiform papillae from n = 5 individual mice were serially imaged and categorized as having (A) >3 extragemmal branches, (B) 1-3 extragemmal branches (≤ 3), or (C) no extragemmal branches (intragemmal only). All FP analyzed had intragemmal labeling (A-C). All FP had intragemmal labeling of FP. (D) A Pie chart is used to graphically describe the proportion of FP within each category. Surprisingly, we observed 50.3% of FP had extragemmal labeling in total (31.8% with >3 fibers; 18.5% with 1-3 fibers), while the remaining 49.7% had no extragemmal labeling. These data may suggest that a substantial portion of FP have chemosensory axons projecting outside the K8+ region. Scale bar represents 25 µM. (E) GGs were taken from n=4 adult *GDNF*-IRES-Cre/ER^{T2}; *Rosa26*$^{LSL\text{-}TdTomato/+}$ mice and stained for TuJ1 (green), RFP (indicating GDNF, red), and Phox2b (blue) to ascertain whether GDNF is expressed by GG neurons. No instances of GDNF+ neurons were observed. On occasion, GDNF+ satellite cells within the facial nerve were labeled (blue arrow). Scale bar represent 50 µm.

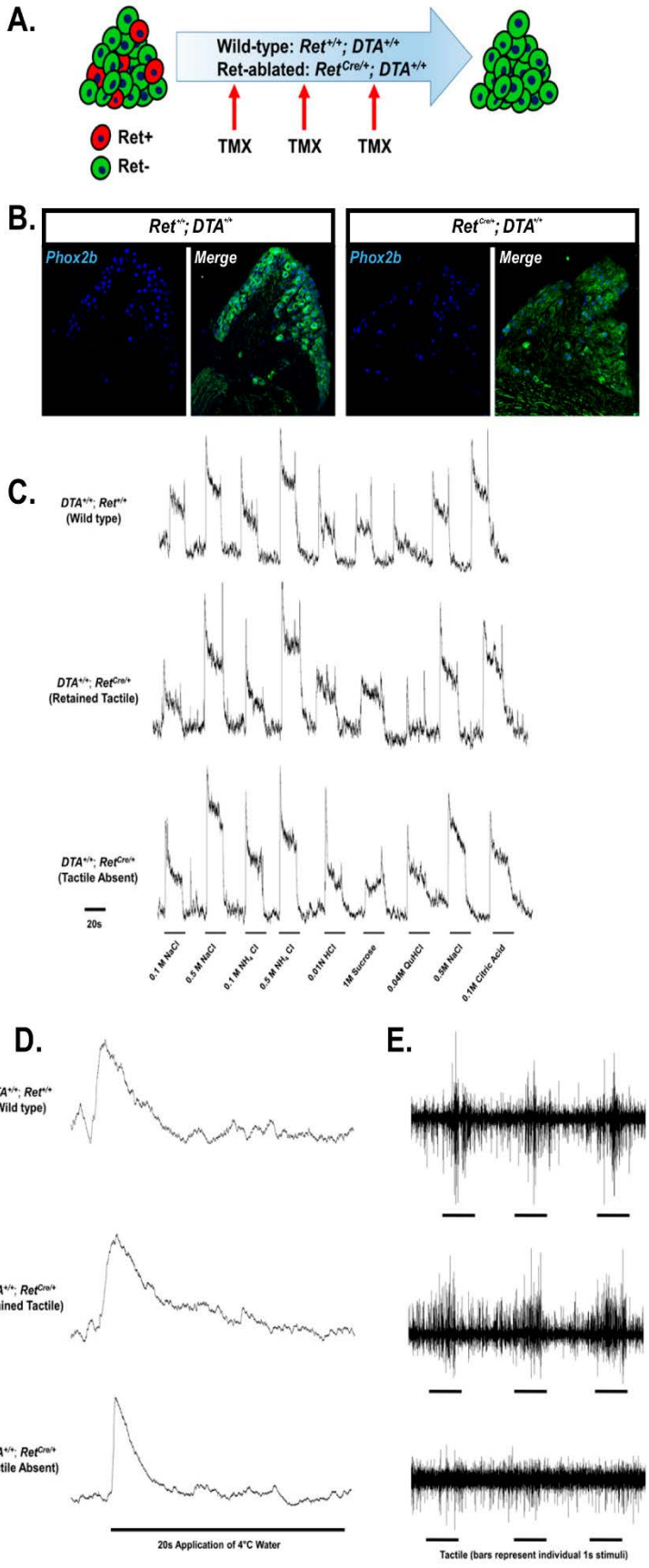
A.
Wild-type: Ret+/+; DTA+/+
Ret-ablated: RetCre/+; DTA+/+
TMX
TMX
TMX
Ret+
Ret-
B.
Ret+/+; DTA+/+
RetCre/+; DTA+/+
Phox2b
Merge
Phox2b
Merge
C.
DTA+/+; Ret+/+
(Wild type)
DTA+/+; RetCre/+
(Retained Tactile)
DTA+/+; RetCre/+
(Tactile Absent)
20s
0.1 M NaCl
0.5 M NaCl
0.1 M NH4 Cl
0.5 M NH4 Cl
0.01N HCl
1M Sucrose
0.04M QuHCl
0.5M NaCl
0.1M Citric Acid
D.
DTA+/+; Ret+/+
(Wild type)
DTA+/+; RetCre/+
(Retained Tactile)
DTA+/+; RetCre/+
(Tactile Absent)
20s Application of 4°C Water
E.
Tactile (bars represent individual 1s stimuli)

Figure 4.15. DTA deletion and additional electrophysiological traces from wildtype and Ret-ablated mice.

(A) Schematic demonstrating the ablation of Ret+ neurons *in vivo* prior to electrophysiological recordings. TMX was administered daily for 3 days, and mice were subsequently utilized for whole nerve recordings from the chorda tympani. (B) GGs from $Ret^{+/+}$; $DTA^{+/+}$ (WT) and $Ret^{Cre/+}$; $DTA^{+/+}$ (Ret-ablated) mice were serially sectioned, immunostained for Phox2b (blue) and TuJ1 (green, overlaid in merge). Ret-ablated mice had fewer total numbers of Phox2b+ GG neurons, indicating reliable deletion. Scale bar represents 100 µm. (C-E) Representative chorda tympani integrated nerve responses to various taste stimuli (C), 4°C water (D), or raw responses to tactile stimuli (E) are displayed. For each panel, the WT animal is displayed in the top trace, while the middle trace represents the electrophysiological responses of a Ret-ablated mouse meeting the inclusion criteria, yet retaining tactile responses (n = 2). The bottom trace is an additional representative trace from a Ret-ablated mouse with a complete loss of tactile responses (n = 4 complete loss, n = 1 partial loss).

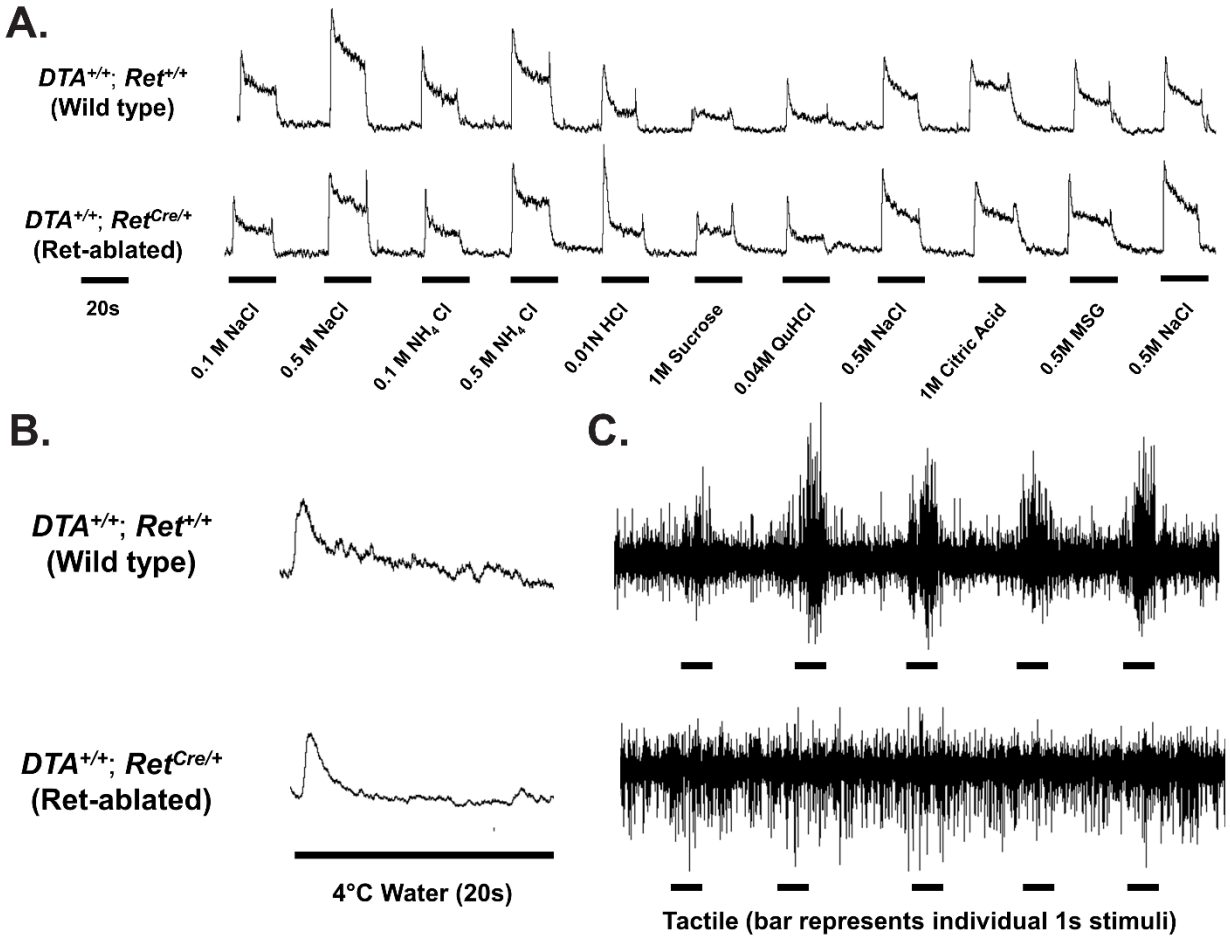

Figure 4.16. Ablation of Ret+ neurons results in deficits in tactile, but not chemical or thermal responses.

Chorda tympani integrated nerve responses to (A) taste stimuli and (B) cold stimuli are unaffected in *Ret$^{Cre/+}$; DTA$^{+/+}$* mice (Ret-ablated; lower trace) compared to control animals. (C) A representative trace demonstrating the loss of chorda tympani responses to tactile stimulation (upper: WT; lower: Ret-ablated). Of the 7 *Ret$^{Cre/+}$; DTA$^{+/+}$* mice tested, 4 had loss of tactile responses, 1 had substantially weakened responses, and two had a residual response (additional traces displayed in Supplementary Figure 9). Despite the loss of tactile responses, spontaneous neural activity remains intact in Ret-ablated nerves. Because responses to tactile stimuli are not sustained, tactile responses are not integrated but presented as whole nerve recordings.

Chapter 4 References

Airaksinen, M.S., and M. Saarma. 2002. The GDNF family: signalling, biological functions and therapeutic value. *Nat. Rev. Neurosci.* 3:383-394.

Al-Hadlaq, S.M., R.M. Bradley, D.K. MacCallum, and C.M. Mistretta. 2003. Embryonic geniculate ganglion neurons in culture have neurotrophin-specific electrophysiological properties. *Neuroscience*. 118:145-159.

Aloyz, R.S., S.X. Bamji, C.D. Pozniak, J.G. Toma, J. Atwal, D.R. Kaplan, and F.D. Miller. 1998. p53 is essential for developmental neuron death as regulated by the TrkA and p75 neurotrophin receptors. *The Journal of cell biology*. 143:1691-1703.

Anastasia, A., P.A. Barker, M.V. Chao, and B.L. Hempstead. 2015. Detection of p75NTR Trimers: Implications for Receptor Stoichiometry and Activation. *The Journal of neuroscience : the official journal of the Society for Neuroscience*. 35:11911-11920.

Anders, J., S. Kjar, and C.F. Ibanez. 2001. Molecular modeling of the extracellular domain of the RET receptor tyrosine kinase reveals multiple cadherin-like domains and a calcium-binding site. *The Journal of biological chemistry*. 276:35808-35817.

Ball, D.W. 2011. Management of medullary thyroid cancer. *Minerva Endocrinol.* 36:87-98.

Baloh, R.H., M.G. Tansey, J.P. Golden, D.J. Creedon, R.O. Heuckeroth, C.L. Keck, D.B. Zimonjic, N.C. Popescu, E.M. Johnson, Jr., and J. Milbrandt. 1997. TrnR2, a

novel receptor that mediates neurturin and GDNF signaling through Ret. *Neuron*. 18:793-802.

Baloh, R.H., M.G. Tansey, P.A. Lampe, T.J. Fahrner, H. Enomoto, K.S. Simburger, M.L. Leitner, T. Araki, E.M. Johnson, Jr., and J. Milbrandt. 1998. Artemin, a novel member of the GDNF ligand family, supports peripheral and central neurons and signals through the GFRalpha3-RET receptor complex. *Neuron*. 21:1291-1302.

Bamji, S.X., M. Majdan, C.D. Pozniak, D.J. Belliveau, R. Aloyz, J. Kohn, C.G. Causing, and F.D. Miller. 1998. The p75 neurotrophin receptor mediates neuronal apoptosis and is essential for naturally occurring sympathetic neuron death. *The Journal of cell biology*. 140:911-923.

Barak, S., S. Ahmadiantehrani, V. Kharazia, and D. Ron. 2011. Positive autoregulation of GDNF levels in the ventral tegmental area mediates long-lasting inhibition of excessive alcohol consumption. *Translational psychiatry*. 1.

Barker, P.A., and E.M. Shooter. 1994. Disruption of NGF binding to the low affinity neurotrophin receptor p75LNTR reduces NGF binding to TrkA on PC12 cells.

Barker, V., G. Middleton, F. Davey, and A.M. Davies. 2001. TNFalpha contributes to the death of NGF-dependent neurons during development. *Nature neuroscience*. 4:1194-1198.

Bartus, R.T., and E.M. Johnson, Jr. 2017. Clinical tests of neurotrophic factors for human neurodegenerative diseases, part 2: Where do we stand and where must we go next? *Neurobiology of disease*. 97:169-178.

Battaini, F. 2001. Protein kinase C isoforms as therapeutic targets in nervous system disease states. *Pharm. Res.* 44:353-361.

Beattie, E.C., C.L. Howe, A. Wilde, F.M. Brodsky, and W.C. Mobley. 2000. NGF signals through TrkA to increase clathrin at the plasma membrane and enhance clathrin-mediated membrane trafficking. *J. Neurosci.* 20:7325-7333.

Bentley, C.A., and K.F. Lee. 2000. p75 is important for axon growth and schwann cell migration during development. *J Neurosci*. 20:7706-7715.

Bertrand, M.J., R.S. Kenchappa, D. Andrieu, M. Leclercq-Smekens, H.N. Nguyen, B.D. Carter, F. Muscatelli, P.A. Barker, and O. De Backer. 2008. NRAGE, a p75NTR adaptor protein, is required for developmental apoptosis in vivo. *Cell Death Differ*. 15:1921-1929.

Bespalov, M.M., Y.A. Sidorova, S. Tumova, A. Ahonen-Bishopp, A.C. Magalhaes, E. Kulesskiy, M. Paveliev, C. Rivera, H. Rauvala, and M. Saarma. 2011. Heparan sulfate proteoglycan syndecan-3 is a novel receptor for GDNF, neurturin, and artemin. *The Journal of cell biology*. 192:153-169.

Bogenmann, E., P.S. Thomas, Q. Li, J. Kim, L.T. Yang, B. Pierchala, and V. Kaartinen. 2011a. Generation of mice with a conditional allele for the p75(NTR) neurotrophin receptor gene. *Genesis*. 49:862-869.

Bogenmann, E., P.S. Thomas, Q. Li, J. Kim, L.T. Yang, B. Pierchala, and V. Kaartinen. 2011b. Generation of mice with a conditional allele for the p75(NTR) neurotrophin receptor Gene. *Genesis*.

Bordeaux, M.C., C. Forcet, L. Granger, V. Corset, C. Bidaud, M. Billaud, D.E. Bredesen, P. Edery, and P. Mehlen. 2000. The RET proto-oncogene induces apoptosis: a novel mechanism for Hirschsprung disease. *The EMBO journal*. 19:4056-4063.

Boudreau, J.C., B.E. Bradley, P.R. Bierer, S. Kruger, and C. Tsuchitani. 1971. Single unit recordings from the geniculate ganglion of the facial nerve of the cat. *Experimental brain research*. 13:461-488.

Bourane, S., A. Garces, S. Venteo, A. Pattyn, T. Hubert, A. Fichard, S. Puech, H. Boukhaddaoui, C. Baudet, S. Takahashi, J. Valmier, and P. Carroll. 2009. Low-threshold mechanoreceptor subtypes selectively express MafA and are specified by Ret signaling. *Neuron*. 64:857-870.

Brown, D.A., and E. London. 1998. Functions of lipid rafts in biological membranes. *Annu Rev Cell Dev Biol*. 14:111-136.

Buj-Bello, A., J. Adu, L.G. Pinon, A. Horton, J. Thompson, A. Rosenthal, M. Chinchetru, V.L. Buchman, and A.M. Davies. 1997. Neurturin responsiveness requires a GPI-linked receptor and the Ret receptor tyrosine kinase. *Nature*. 387:721-724.

Buj-Bello, A., V.L. Buchman, A. Horton, A. Rosenthal, and A.M. Davies. 1995. GDNF is an age-specific survival factor for sensory and autonomic neurons. *Neuron*. 15:821-828.

Cabrera, J.R., L. Sanchez-Pulido, A.M. Rojas, A. Valencia, S. Manes, J.R. Naranjo, and B. Mellstrom. 2006. Gas1 is related to the glial cell-derived neurotrophic factor family receptors alpha and regulates Ret signaling. *J. Biol. Chem*. 281:14330-14339.

Cacalano, G., I. Farinas, L.C. Wang, K. Hagler, A. Forgie, M. Moore, M. Armanini, H. Phillips, A.M. Ryan, L.F. Reichardt, M. Hynes, A. Davies, and A. Rosenthal. 1998. GFRalpha1 is an essential receptor component for GDNF in the developing nervous system and kidney. *Neuron*. 21:53-62.

Calco, G.N., O.R. Stephens, L.M. Donahue, C.C. Tsui, and B.A. Pierchala. 2014. CD2-associated Protein (CD2AP) Enhances Casitas B-lineage Lymphoma-3/c (Cbl-3/c)-mediated Ret Isoform-specific Ubiquitination and Degradation via its Amino-terminal SRC Homology 3 (SH3) Domains. *The Journal of biological chemistry*.

Cebrian, C., N. Asai, V. D'Agati, and F. Costantini. 2014. The number of fetal nephron progenitor cells limits ureteric branching and adult nephron endowment. *Cell reports*. 7:127-137.

Ceni, C., N. Unsain, M.P. Zeinieh, and P.A. Barker. 2014. Neurotrophins in the regulation of cellular survival and death. *Handb Exp Pharmacol*. 220:193-221.

Ceyhan, G.O., K.H. Schafer, A.G. Kerscher, U. Rauch, I.E. Demir, M. Kadihasanoglu, C. Bohm, M.W. Muller, M.W. Buchler, N.A. Giese, M. Erkan, and H. Friess. 2010. Nerve growth factor and artemin are paracrine mediators of pancreatic neuropathy in pancreatic adenocarcinoma. *Annals of surgery*. 251:923-931.

Chao, M.V. 1994. The p75 Neurotrophin Receptor. *J. Neuroboil.* 25:1373-1385.

Chao, M.V. 2003. Neurotrophins and their receptors: a convergence point for many signalling pathways. *Nature reviews. Neuroscience*. 4:299-309.

Charalampopoulos, I., A. Vicario, I. Pediaditakis, A. Gravanis, A. Simi, and C.F. Ibanez. 2012. Genetic dissection of neurotrophin signaling through the p75 neurotrophin receptor. *Cell reports*. 2:1563-1570.

Chen, C.L., D.C. Broom, Y. Liu, J.C. de Nooij, Z. Li, C. Cen, O.A. Samad, T.M. Jessell, C.J. Woolf, and Q. Ma. 2006. Runx1 determines nociceptive sensory neuron phenotype and is required for thermal and neuropathic pain. *Neuron*. 49:365-377.

Chen, K.S., M.C. Nishimura, M.P. Armanini, C. Crowley, S.D. Spencer, and H.S. Phillips. 1997. Disruption of a single allele of the nerve growth factor gene results in atrophy of basal forebrain cholinergic neurons and memory deficits. *The Journal of neuroscience : the official journal of the Society for Neuroscience*. 17:7288-7296.

Chen, X., H. Ye, R. Kuruvilla, N. Ramanan, K.W. Scangos, C. Zhang, N.M. Johnson, P.M. England, K.M. Shokat, and D.D. Ginty. 2005a. A chemical-genetic approach to studying neurotrophin signaling. *Neuron*. 46:13-21.

Chen, Z., C.R. Donnelly, B. Dominguez, Y. Harada, W. Lin, A.S. Halim, T.G. Bengoechea, B.A. Pierchala, and K.F. Lee. 2017. p75 Is Required for the Establishment of Postnatal Sensory Neuron Diversity by Potentiating Ret Signaling. *Cell reports*. 21:707-720.

Chen, Z.Y., A. Ieraci, M. Tanowitz, and F.S. Lee. 2005b. A novel endocytic recycling signal distinguishes biological responses of Trk neurotrophin receptors. *Molecular biology of the cell*. 16:5761-5772.

Cohen, S., and R. Levi-Montalcini. 1956. A nerve growth stimulating factor isolated from snake venom. *Proc. Natl. Acad. Sci.* 42:571-574.

Creedon, D.J., M.G. Tansey, R.H. Baloh, P.A. Osborne, P.A. Lampe, T.J. Fahrner, R.O. Heuckeroth, J. Milbrandt, and E.M. Johnson, Jr. 1997. Neurturin shares receptors and signal transduction pathways with glial cell line-derived neurotrophic factor in sympathetic neurons. *Proceedings of the National Academy of Sciences of the United States of America*. 94:7018-7023.

Crowder, R.J., and R.S. Freeman. 1998. Phosphatidylinositol 3-kinase and Akt protein kinase are necessary and sufficient for the survival of Nerve Growth Factor-dependent sympathetic neurons. *J. Neurosci.* 18:2933-2943.

Crowley, C., S.D. Spencer, M.C. Nishimura, K.S. Chen, S. Pitts-Meek, M.P. Armanini, L.H. Ling, S.B. McMahon, D.L. Shelton, A.D. Levinson, and et al. 1994. Mice lacking nerve growth factor display perinatal loss of sensory and sympathetic neurons yet develop basal forebrain cholinergic neurons. *Cell*. 76:1001-1011.

Curtis, R., K.M. Adryan, J.L. Stark, J.S. Park, D.L. Compton, G. Weskamp, L.J. Huber, M.V. Chao, R. Jaenisch, K.-F. Lee, R.M. Lindsay, and P.S. DiStefano. 1995. Differential role of the low affinity neurotrophin receptor (p75) in retrograde axonal transport of the neurotrophins. *Neuron*. 14:1201-1211.

D'Autreaux, F., E. Coppola, M.-R. Hirsch, C. Birchmeier, and J.-F. Brunet. 2011. Homeoprotein Phox2b commands a somatic-to-visceral switch in cranial sensory pathways. *PNAS*. 108:20018-20023.

Datta, S.R., H. Dudek, X. Tao, S. Masters, H. Fu, Y. Gotoh, and M.E. Greenberg. 1997. Akt phosphorylation of BAD couples survival signals to the cell-intrinsic death machinery. *Cell*. 91:231-241.

Dauger, S., A. Pattyn, F. Lofaso, C. Gaultier, C. Goridis, J. Gallego, and J.F. Brunet. 2003. Phox2b controls the development of peripheral chemoreceptors and afferent visceral pathways. *Development (Cambridge, England)*. 130:6635-6642.

Davies, A.M., K.F. Lee, and R. Jaenisch. 1993. p75-deficient trigeminal sensory neurons have an altered response to NGF but not to other neurotrophins. *Neuron*. 11:565-574.

Deckwerth, T.L., and E.M. Johnson, Jr. 1993. Temporal analysis of events associated with programmed cell death (apoptosis) of sympathetic neurons deprived of nerve growth factor. *J. Cell Biol.* 123:1207-1222.

Deppmann, C.D., S. Mihalas, N. Sharma, B.E. Lonze, E. Niebur, and D.D. Ginty. 2008. A model for neuronal competition during development. *Science (New York, N.Y.)*. 320:369-373.

Deshmukh, M., and J. Johnson, E.M. 1997. Programmed cell death in neurons: focus on the pathway of nerve growth factor deprivation-induced death of sympathetic neurons. *Molec. Pharm.* 51:897-906.

Dong, X., S. Han, M.J. Zylka, M.I. Simon, and D.J. Anderson. 2001. A diverse family of GPCRs expressed in specific subsets of nociceptive sensory neurons. *Cell*. 106:619-632.

Donnelly, C.R., A.A. Shah, C.M. Mistretta, R.M. Bradley, and B.A. Pierchala. 2018. Biphasic functions for the GDNF-Ret signaling pathway in chemosensory neuron development and diversification. *Proceedings of the National Academy of Sciences of the United States of America*. 115:E516-e525.

Dudek, H., S.A. Datta, T.F. Franke, M.J. Birnbaum, R. Yao, G.M. Cooper, R.A. Segal, D.R. Kaplan, and M.E. Greenberg. 1997. Regulation of neuronal survival by the serine-threonine protein kinase Akt. *Science (New York, N.Y.)*. 275:628-830.

Durbec, P., C.V. Marcos-Gutierrez, C. Kilkenny, M. Grigoriou, K. Wartiowaara, P. Suvanto, D. Smith, B. Ponder, F. Costantini, M. Saarma, and et al. 1996. GDNF signalling through the Ret receptor tyrosine kinase [see comments]. *Nature*. 381:789-793.

Ehlers, M.D., D.R. Kaplan, D.L. Price, and V.E. Koliatsos. 1995. NGF-stimulated retrograde transport of TrkA in the Mammalian Nervous System. *J. Cell Bio.* 130:149-156.

Eide, F.F., D.H. Lowenstein, and L.F. Reichardt. 1993. Neurotrophins and their receptors- current concepts and implications for neurologic diseases. *Exp. Neurol.* 121:200-214.

Emmerson, P.J., F. Wang, Y. Du, Q. Liu, R.T. Pickard, M.D. Gonciarz, T. Coskun, M.J. Hamang, D.K. Sindelar, K.K. Ballman, L.A. Foltz, A. Muppidi, J. Alsina-Fernandez, G.C. Barnard, J.X. Tang, X. Liu, X. Mao, R. Siegel, J.H. Sloan, P.J. Mitchell, B.B. Zhang, R.E. Gimeno, B. Shan, and X. Wu. 2017. The metabolic effects of GDF15 are mediated by the orphan receptor GFRAL. *Nature medicine*. 23:1215-1219.

Encinas, M., R.J. Crowder, J. Milbrandt, and E.M. Johnson, Jr. 2004. Tyrosine 981, a novel Ret autophosphorylation site, binds c-Src to mediate neuronal survival. *J. Biol. Chem.* 279:18262-18269.

Eng, C. 1996. Seminars in medicine of the Beth Israel Hospital, Boston. The RET proto-oncogene in multiple endocrine neoplasia type 2 and Hirschsprung's disease. *N Engl J Med*. 335:943-951.

Enokido, Y., F. de Sauvage, J.A. Hongo, N. Ninkina, A. Rosenthal, V.L. Buchman, and A.M. Davies. 1998. GFR alpha-4 and the tyrosine kinase Ret form a functional receptor complex for persephin. *Curr Biol*. 8:1019-1022.

Enomoto, H., P.A. Crawford, A. Gorodinsky, R.O. Heuckeroth, E.M. Johnson, Jr., and J. Milbrandt. 2001. RET signaling is essential for migration, axonal growth and axon

guidance of developing sympathetic neurons. *Development 128, 3963-3974*. 128:3963-3974.

Enomoto, H., R.O. Heuckeroth, J.P. Golden, E.M. Johnson, Jr., and J. Milbrandt. 2000. Development of cranial parasympathetic ganglia requires sequential actions of GDNF and neurturin. *Development (Cambridge, England)*. 127:4877-4889.

Enomoto, H., I. Hughes, J. Golden, R.H. Baloh, S. Yonemura, R.O. Heuckeroth, E.M.J. Johnson, and J. Milbrandt. 2004. GFRalpha1 expression in cells lacking RET is dispensable for organogenesis and nerve regeneration. *Neuron*. 44:623-636.

Ernfors, P., K.F. Lee, J. Kucera, and R. Jaenisch. 1994. Lack of neurotrophin-3 leads to deficiencies in the peripheral nervous system and loss of limb proprioceptive afferents. *Cell*. 77:503-512.

Ernsberger, U. 2008. The role of GDNF family ligand signalling in the differentiation of sympathetic and dorsal root ganglion neurons. *Cell Tissue Res*. 333:353-371.

Esposito, D., P. Patel, R.M. Stephens, P. Perez, M.V. Chao, D.R. Kaplan, and B.L. Hempstead. 2001. The cytoplasmic and transmembrane domains of the p75 and Trk A receptors regulate high affinity binding to nerve growth factor. *J Biol Chem*. 276:32687-32695.

Fei, D., and R.F. Krimm. 2013. Taste neurons consist of both a large TrkB-receptor-dependent and a small TrkB-receptor-independent subpopulation. *PLoS One*. 8:e83460.

Finger, T.E., V. Danilova, J. Barrows, D.L. Bartel, A.J. Vigers, L. Stone, G. Hellekant, and S.C. Kinnamon. 2005. ATP signaling is crucial for communication from taste buds to gustatory nerves. *Science (New York, N.Y.)*. 310:1495-1499.

Fode, C., G. Gradwohl, X. Morin, A. Dierich, M. LeMeur, C. Goridis, and F. Guillemot. 1998. The bHLH protein NEUROGENIN 2 is a determination factor for epibranchial placode-derived sensory neurons. *Neuron*. 20:483-494.

Fontana, X., M. Hristova, C. Da Costa, S. Patodia, L. Thei, M. Makwana, B. Spencer-Dene, M. Latouche, R. Mirsky, K.R. Jessen, R. Klein, G. Raivich, and A. Behrens. 2012. c-Jun in Schwann cells promotes axonal regeneration and motoneuron survival via paracrine signaling. *The Journal of cell biology*. 198:127-141.

Frade, J.M., and Y.A. Barde. 1999. Genetic evidence for cell death mediated by nerve growth factor and the neurotrophin receptor p75 in the developing mouse retina and spinal cord. *Development (Cambridge, England)*. 126:683-690.

Frade, J.M., A. Rodriguez-Tebar, and Y.-A. Barde. 1996. Induction of cell death by endogenous nerve growth factor through its p75 receptor. *Nature*. 383:166-168.

Franck, M.C., A. Stenqvist, L. Li, J. Hao, D. Usoskin, X. Xu, Z. Wiesenfeld-Hallin, and P. Ernfors. 2011. Essential role of Ret for defining non-peptidergic nociceptor phenotypes and functions in the adult mouse. *Eur J Neurosci*. 33:1385-1400.

Franke, T.F., D.R. Kaplan, and L.C. Cantley. 1997. PI3K: Downstream AKTion blocks apoptosis. *Cell*. 88:435-437.

Gardell, L.R., R. Wang, C. Ehrenfels, M.H. Ossipov, A.J. Rossomando, S. Miller, C. Buckley, A.K. Cai, A. Tse, S.F. Foley, B. Gong, L. Walus, P. Carmillo, D. Worley, C. Huang, T. Engber, B. Pepinsky, R.L. Cate, T.W. Vanderah, J. Lai, D.W. Sah, and F. Porreca. 2003. Multiple actions of systemic artemin in experimental neuropathy. *Nature medicine*. 9:1383-1389.

Gatto, G., I. Dudanova, P. Suetterlin, A.M. Davies, U. Drescher, J.L. Bixby, and R. Klein. Protein tyrosine phosphatase receptor type O inhibits trigeminal axon growth and branching by repressing TrkB and Ret signaling. *The Journal of neuroscience : the official journal of the Society for Neuroscience*. 33:5399-5410.

Geetha, T., R.S. Kenchappa, M.W. Wooten, and B.D. Carter. 2005. TRAF6-mediated ubiquitination regulates nuclear translocation of NRIF, the p75 receptor interactor. *The EMBO journal*. 24:3859-3868.

Gentry, J.J., P.A. Barker, and B.D. Carter. 2004. The p75 neurotrophin receptor: multiple interactors and numerous functions. *Progress in brain research*. 146:25-39.

Gill, S.S., N.K. Patel, G.R. Hotton, K. O'Sullivan, R. McCarter, M. Bunnage, D.J. Brooks, C.N. Svendsen, and P. Heywood. 2003. Direct brain infusion of glial cell line-derived neurotrophic factor in Parkinson disease. *Nat. Medicine*.

Ginty, D.D., and R.A. Segal. 2002. Retrograde neurotrophin signaling: Trk-ing along the axon. *Current opinion in neurobiology*. 12:268-274.

Golden, J.P., R.H. Baloh, P.T. Kotzbauer, P.A. Lampe, P.A. Osborne, J. Milbrandt, and E.M. Johnson, Jr. 1998. Expression of neurturin, GDNF, and their receptors in the adult mouse CNS. *The Journal of comparative neurology*. 398:139-150.

Golden, J.P., J.A. DeMaro, P.A. Osborne, J. Milbrandt, and E.M. Johnson, Jr. 1999. Expression of neurturin, GDNF, and GDNF family-receptor mRNA in the developing and mature mouse. *Experimental neurology*. 158:504-528.

Golden, J.P., M. Hoshi, M.A. Nassar, H. Enomoto, J.N. Wood, J. Milbrandt, R.W.t. Gereau, E.M. Johnson, Jr., and S. Jain. 2010. RET signaling is required for

survival and normal function of nonpeptidergic nociceptors. *The Journal of neuroscience : the official journal of the Society for Neuroscience*. 30:3983-3994.

Gould, T.W., S. Yonemura, R.W. Oppenheim, S. Ohmori, and H. Enomoto. 2008. The neurotrophic effects of glial cell line-derived neurotrophic factor on spinal motoneurons are restricted to fusimotor subtypes. *j. Neurosci.* 28:2131-2146.

Greene, L.A., Kaplan, D. R. 1995. Early events in neurotrophin signalling via Trk and p75. *Curr. Opin. Neurobiol.* 5:579-587.

Grigaliunas, A., R.M. Bradley, D.K. MacCallum, and C.M. Mistretta. 2002. Distinctive neurophysiological properties of embryonic trigeminal and geniculate neurons in culture. *Journal of neurophysiology*. 88:2058-2074.

Grimes, M.L., J. Zhou, E.C. Beattle, E.C. Yuen, D.E. Hall, J.S. Valletta, K.S. Topp, J.H. LaVail, N.W. Bunnett, and W.C. Mobley. 1996. Endocytosis of activated TrkA: evidence that nerve growth factor induces formation of signaling endosomes. *Journal of neuroscience*. 16 (24):7950-7964.

Grimm, J., M. Sachs, S. Britsch, S. Di Cesare, T. Schwarz-Romond, K. Alitalo, and W. Birchmeier. 2001. Novel p62dok family members, dok-4 and dok-5, are substrates of the c-Ret receptor tyrosine kinase and mediate neuronal differentiation. *J. Cell Biol.* 154:345-354.

Gupta, V.K., Y. You, A. Klistorner, and S.L. Graham. 2013. TrkB receptor signalling: implications in neurodegenerative, psychiatric and proliferative disorders. *Int. J. Mol. Sci.* 14:10122-10142.

Hamburger, V. 1934. The effets wing bud extirpation on the development of the central nervous system in chick embryos. *J. Exp. Zool.* 68:449-494.

Hamburger, V., and R. Levi-Montalcini. 1949. Proliferation, differentiation and degeneration in the spinal ganglia of the chick embryo under normal and experimental conditions. *J. Exp. Zool.* 111:457-501.

Han, L., C. Ma, Q. Liu, H.J. Weng, Y. Cui, Z. Tang, Y. Kim, H. Nie, L. Qu, K.N. Patel, Z. Li, B. McNeil, S. He, Y. Guan, B. Xiao, R.H. Lamotte, and X. Dong. 2013. A subpopulation of nociceptors specifically linked to itch. *Nat Neurosci*. 16:174-182.

Hantzopoulos, P.A., C. Suri, D.J. Glass, M.P. Goldfarb, and G.D. Yancopoulos. 1994. The low affinity NGF receptor, p75, can collaborate with each of the trks to potentiate functional responses to the neurotrophins. *Neuron*. 13:187-201.

Harel, L., B. Costa, M. Tcherpakov, M. Zapatka, A. Oberthuer, L.M. Hansford, M. Vojvodic, Z. Levy, Z.Y. Chen, F.S. Lee, S. Avigad, I. Yaniv, L. Shi, R. Eils, M. Fischer, B. Brors, D.R. Kaplan, and M. Fainzilber. 2009. CCM2 mediates death signaling by the TrkA receptor tyrosine kinase. *Neuron*. 63:585-591.

He, X.L., and K.C. Garcia. 2004. Structure of nerve growth factor complexed with the shared neurotrophin receptor p75. *Science (New York, N.Y.)*. 304:870-875.

Hemmings, B.A. 1997. Akt signaling: linking membrane events to life and death decisions. *Science (New York, N.Y.)*. 275:628-630.

Hempstead, B.L., D. Martin-Zanca, D.R. Kaplan, L.F. Parada, and M.V. Chao. 1991. High-affinity NGF binding requires coexpression of the trk proto-oncogene and the low-affinity NGF receptor. *Nature*. 350:678-683.

Heuckeroth, R.O., H. Enomoto, J.R. Grider, J.P. Golden, J.A. Hanke, A. Jackman, D.C. Molliver, M.E. Bardgett, W.D. Snider, E.M. Johnson, Jr., and J. Milbrandt. 1999. Gene targeting reveals a critical role for neurturin in the development and

maintenance of enteric, sensory, and parasympathetic neurons [see comments]. *Neuron*. 22:253-263.

Hibbert, A.P., B.M. Kramer, F.D. Miller, and D.R. Kaplan. 2006. The localization, trafficking and retrograde transport of BDNF bound to p75NTR in sympathetic neurons. *Mol Cell Neurosci*. 32:387-402.

Hohn, A., J. Leibrock, K. Bailey, and Y.-A. Barde. 1990. Identification and characterization of a novel member of the nerve growth factor/brain derived neurotrophic factor family. *Nature*. 344:339-341.

Horger, B.A., M.C. Nishimura, M.P. Armanini, L.C. Wang, K.T. Poulsen, C. Rosenblad, D. Kirik, B. Moffat, L. Simmons, J. Johnson, E.M., J. Milbrandt, A. Rosenthal, A. Bjorklund, R.A. Vandlen, M.A. Hynes, and H.S. Phillips. 1998. Neurturin exerts potent actions on survival and function of midbrain dopaminergic neurons. *J. Neurosci.* 18:4929-4937.

Hsu, J.Y., S. Crawley, M. Chen, D.A. Ayupova, D.A. Lindhout, J. Higbee, A. Kutach, W. Joo, Z. Gao, D. Fu, C. To, K. Mondal, B. Li, A. Kekatpure, M. Wang, T. Laird, G. Horner, J. Chan, M. McEntee, M. Lopez, D. Lakshminarasimhan, A. White, S.P. Wang, J. Yao, J. Yie, H. Matern, M. Solloway, R. Haldankar, T. Parsons, J. Tang, W.D. Shen, Y. Alice Chen, H. Tian, and B.B. Allan. 2017. Non-homeostatic body weight regulation through a brainstem-restricted receptor for GDF15. *Nature*. 550:255-259.

Huang, E.J., W. Liu, B. Fritzsch, L.M. Bianchi, L.F. Reichardt, and M. Xiang. 2001. Brn3a is a transcriptional regulator of soma size, target field innervation and axon

pathfinding of inner ear sensory neurons. *Development (Cambridge, England)*. 128:2421-2432.

Huang, E.J., K. Zang, A. Schmidt, A. Saulys, M. Xiang, and L.F. Reichardt. 1999. POU domain factor Brn-3a controls the differentiation and survival of trigeminal neurons by regulating Trk receptor expression. *Development (Cambridge, England)*. 126:2869-2882.

Ibanez, C.F. 2013. Structure and physiology of the RET receptor tyrosine kinase. *Cold Spring Harbor perspectives in biology*. 5.

Ibanez, C.F., and A. Simi. 2012. p75 neurotrophin receptor signaling in nervous system injury and degeneration: paradox and opportunity. *Trends Neurosci*. 35:431-440.

Inoue, K., K. Ito, M. Osato, B. Lee, S.C. Bae, and Y. Ito. 2007. The transcription factor Runx3 represses the neurotrophin receptor TrkB during lineage commitment of dorsal root ganglion neurons. *J Biol Chem*. 282:24175-24184.

Ishida, Y., S. Ugawa, T. Ueda, T. Yamada, Y. Shibata, A. Hondoh, K. Inoue, Y. Yu, and S. Shimada. 2009. P2X(2)- and P2X(3)-positive fibers in fungiform papillae originate from the chorda tympani but not the trigeminal nerve in rats and mice. *The Journal of comparative neurology*. 514:131-144.

Ishiguro, Y., T. Iwashita, H. Murakami, N. Asai, K.-I. Iida, H. Goto, T. Hayakawa, and M. Takahashi. 1999. The role of amino acids surrounding tyrosine 1062 in Ret in specific binding of the Shc phosphotyrosine-binding domain. *Endocrinology*. 140:3992-3998.

Ito, T., X. Deng, B.K. Carr, and W.S. May. 1997. Bcl-2 phosphorylation required for anti-apoptosis function. *J. Biol. Chem.* 272:11671-11673.

Ivanchuk, S.M., C. Eng, W.K. Cavenee, and L.M. Mulligan. 1997. The expression of RET and its multiple splice forms in developing human kidney. *Oncogene*. 14:1811-1818.

Iwamoto, T., M. Taniguchi, N. Asai, K. Ohkusu, I. Nakashima, and M. Takahashi. 1993. cDNA cloning of mouse ret proto-oncogene and its sequence similarity to the cadherin superfamily. *Oncogene*. 8:1087-1091.

Jain, S., M. Encinas, E.M. Johnson, Jr., and J. Milbrandt. 2006. Critical and distinct roles for key RET tyrosine docking sites in renal development. *Genes Dev.* 20:321-333.

Jain, S., C.K. Naughton, M. Yang, A. Strickland, K. Vij, M. Encinas, J. Golden, A. Gupta, R. Heuckeroth, E.M. Johnson, Jr., and J. Milbrandt. 2004. Mice expressing a dominant-negative Ret mutation phenocopy human Hirschsprung disease and delineate a direct role of Ret in spermatogenesis. *Development (Cambridge, England)*. 131:5503-5513.

Jing, S., D. Wen, Y. Yu, P.L. Holst, Y. Luo, M. Fang, R. Tamir, L. Antonio, Z. Hu, R. Cupples, J.C. Louis, S. Hu, B.W. Altrock, and G.M. Fox. 1996. GDNF-induced activation of the ret protein tyrosine kinase is mediated by GDNFR-alpha, a novel receptor for GDNF. *Cell*. 85:1113-1124.

Jones, K.R., I. Farinas, C. Backus, and L.F. Reichardt. 1994. Targeted disruption of the BDNF gene perturbs brain and sensory neuron development but not motor neuron development. *Cell*. 76:989-999.

Kanning, K.C., M. Hudson, P.S. Amieux, J.C. Wiley, M. Bothwell, and L.C. Schecterson. 2003. Proteolytic processing of the p75 neurotrophin receptor and two homologs

generates C-terminal fragments with signaling capability. *The Journal of neuroscience : the official journal of the Society for Neuroscience*. 23:5425-5436.

Kaplan, D.R., and R.M. Stephens. 1994. Neurotrophin signal transduction by the trk receptor. *J. Neurobiol.* 25:1404-1417.

Kenchappa, R.S., C. Tep, Z. Korade, S. Urra, F.C. Bronfman, S.O. Yoon, and B.D. Carter. 2010. p75 neurotrophin receptor-mediated apoptosis in sympathetic neurons involves a biphasic activation of JNK and up-regulation of tumor necrosis factor-alpha-converting enzyme/ADAM17. *The Journal of biological chemistry*. 285:20358-20368.

Kenchappa, R.S., N. Zampieri, M.V. Chao, P.A. Barker, H.K. Teng, B.L. Hempstead, and B.D. Carter. 2006. Ligand-dependent cleavage of the P75 neurotrophin receptor is necessary for NRIF nuclear translocation and apoptosis in sympathetic neurons. *Neuron*. 50:219-232.

Kennedy, S.G., A.J. Wagner, S.D. Conzen, J. Jordan, A. Bellacosa, P.M. Tsichlis, and N. hay. 1997. The PI-3 kinase/AKT signaling pathway delivers an anti-apoptotic signal. *Genes & Development*. 11:701-713.

Kirkham, M., and R.G. Parton. 2005. Clathrin-independent endocytosis: new insights into caveolae and non-caveolar lipid raft carriers. *Biochim. Biophys. Acta*. 1746:349-363.

Kitamura, K., R.S. Kimura, and H.F. Schuknecht. 1982. The ultrastructure of the geniculate ganglion. *Acta oto-laryngologica*. 93:175-186.

Kjaer, S., and C.F. Ibanez. 2003. Identification of a surface for binding to the GDNF-GFR alpha 1 complex in the first cadherin-like domain of RET. *The Journal of biological chemistry*. 278:47898-47904.

Klein, R. 1994. Role for neurotrophins in mouse neuronal development. *FASEB*. 8:738-744.

Klein, R., D. Martin-Zanca, M. Barbacid, and L.F. Parada. 1990. Expression of the tyrosine kinase receptor gene trkB is confined to the murine embryonic and adult nervous system. *Development (Cambridge, England)*. 109:845-850.

Klein, R., I. Silos-Santiago, R.J. Smeyne, S.A. Lira, R. Brambilla, S. Bryant, L. Zhang, W.D. Snider, and M. Barbacid. 1994. Disruption of the neurotrophin-3 receptor gene trkC eliminates Ia muscle afferents and results in abnormal movements. *Nature*. 368:249-251.

Klein, R., R.J. Smeyne, W. Wurst, L.K. Long, B.A. Auerbach, A.L. Joyner, and M. Barbacid. 1993a. Targeted disruption of the trkB neurotrophin receptor gene results in nervous system lesions and neonatal death. *Cell*. 75:113-122.

Klein, R., R.J. Smeyne, W. Wurst, L.K. Long, B.A. Auerbach, A.L. Joyner, and M. Barbacid. 1993b. Targeted disruption of the trkB neurotrophin receptor gene results in nervous system lesions and neonatal death. *Cell*. 75:113-122.

Knowles, P.P., J. Murray-Rust, S. Kjaer, R.P. Scott, S. Hanrahan, M. Santoro, C.F. Ibanez, and N.Q. McDonald. 2006. Structure and chemical inhibition of the RET tyrosine kinase domain. *The Journal of biological chemistry*. 281:33577-33587.

Kopra, J.J., A. Panhelainen, S. Af Bjerken, L.L. Porokuokka, K. Varendi, S. Olfat, H. Montonen, T.P. Piepponen, M. Saarma, and J.O. Andressoo. 2017. Dampened

Amphetamine-Stimulated Behavior and Altered Dopamine Transporter Function in the Absence of Brain GDNF. *The Journal of neuroscience : the official journal of the Society for Neuroscience*. 37:1581-1590.

Kordower, J.H. 2003. In vivo gene delivery of glial cell line--derived neurotrophic factor for Parkinson's disease. *Ann. Neurol.* 53:S120-S132.

Kotzbauer, P.T., P.A. Lampe, R.O. Heuckeroth, J.P. Golden, D.J. Creedon, E.M. Johnson, Jr., and J. Milbrandt. 1996. Neurturin, a relative of glial-cell-line-derived neurotrophic factor. *Nature*. 384:467-470.

Kraemer, B.R., S.O. Yoon, and B.D. Carter. 2014. The biological functions and signaling mechanisms of the p75 neurotrophin receptor. *Handbook of experimental pharmacology*. 220:121-164.

Kramer, E.R., L. Aron, G.M.J. Ramakers, S. Seitz, X. Zhuang, K. Beyer, M.P. Smidt, and R. Klein. 2007. Absence of Ret signaling in mice causes progressive and late degeneration of the nigrostriatal system. *PLOS Biology*. 5:e39.

Kramer, I., M. Sigrist, J.C. de Nooij, I. Taniuchi, T.M. Jessell, and S. Arber. 2006. A role for Runx transcription factor signaling in dorsal root ganglion sensory neuron diversification. *Neuron*. 49:379-393.

Krimm, R.F. 2007. Factors that regulate embryonic gustatory development. *BMC Neuro.* 8:S4.

Kumar, A., J. Kopra, K. Varendi, L.L. Porokuokka, A. Panhelainen, S. Kuure, P. Marshall, N. Karalija, M.A. Harma, C. Vilenius, K. Lillevali, T. Tekko, J. Mijatovic, N. Pulkkinen, M. Jakobson, M. Jakobson, R. Ola, E. Palm, M. Lindahl, I. Stromberg, V. Voikar, T.P. Piepponen, M. Saarma, and J.O. Andressoo. 2015.

GDNF Overexpression from the Native Locus Reveals its Role in the Nigrostriatal Dopaminergic System Function. *PLoS genetics*. 11:e1005710.

Kumari, A., A.N. Ermilov, B.L. Allen, R.M. Bradley, A.A. Dlugosz, and C.M. Mistretta. 2015. Hedgehog pathway blockade with the cancer drug LDE225 disrupts taste organs and taste sensation. *J. Neurophysiol.* 113:1034-1040.

Kurokawa, K., T. Iwashita, H. Murakami, H. Hayashi, K. Kawai, and M. Takahashi. 2001. Identification of SNT/FRS2 docking site on RET receptor tyrosine kinase and its role for signal transduction. *Oncogene*. 20:1929-1938.

Kuruvilla, R., L.S. Zweifel, N.O. Glebova, B.E. Lonze, G. Valdez, H. Ye, and D.D. Ginty. 2004. A neurotrophin signaling cascade coordinates sympathetic neuron development through differential control of TrkA trafficking and retrograde signaling. *Cell*. 118:243-255.

Lallemend, F., and P. Ernfors. 2012. Molecular interactions underlying the specification of sensory neurons. *Trends Neurosci*. 35:373-381.

Lamballe, F., P. Tapley, and M. Barbacid. 1993. trkC encodes multiple neurotrophin-3 receptors with distinct biological properties and substrate specificities. *EMBO*. 12:3083-3094.

Le Hir, H., N. Charlet-Berguerand, V. de Franciscis, and C. Thermes. 2002. 5'-End RET splicing: absence of variants in normal tissues and intron retention in pheochromocytomas. *Oncology*. 63:84-91.

Lee, K.-F., E. Li, J. Huber, S.C. Landis, A.H. Sharpe, M.V. Chao, and R. Jaenisch. 1992a. Targeted mutation of the gene encoding the low affinity NGF receptor p75 leads to deficits in the peripheral sensory nervous system. *Cell*. 69:737-749.

Lee, K.F., A.M. Davies, and R. Jaenisch. 1994. p75-deficient embryonic dorsal root sensory and neonatal sympathetic neurons display a decreased sensitivity to NGF. *Development*. 120:1027-1033.

Lee, K.F., E. Li, L.J. Huber, S.C. Landis, A.H. Sharpe, M.V. Chao, and R. Jaenisch. 1992b. Targeted mutation of the gene encoding the low affinity NGF receptor p75 leads to deficits in the peripheral sensory nervous system. *Cell*. 69:737-749.

Lee, R., P. Kermani, K.K. Teng, and B.L. Hempstead. 2001. Regulation of cell survival by secreted proneurotrophins. *Science (New York, N.Y.)*. 294:1945-1948.

Leibrock L., Lottspeich F., Hohn A., Hofer M., Hengerer B., Masiakowski P., Thoenen H., and a.B. Y-A. 1989. Molecular cloning and expression of brain-derived neurotrophic factor. *Nature*. 341:149-152.

Levi-Montalcini, R. 1987. The nerve growth factor 35 years later. *Science (New York, N.Y.)*. 237:1154-1162.

Levi-Montalcini, R., and P.U. Angeletti. 1968. Nerve growth factor. *Physiol Rev*. 48:534-569.

Levi-Montalcini, R., and V. Hamburger. 1951. Selective growth-stimulating effets of mouse sarcoma on the sensory and sympathetic nervous system of the chick embryo. *J. Exp. Zool.* 116:321-361.

Levi-Montalcini, R., and V. Hamburger. 1953. A diffusible agent of mouse saroma, producing hyperplasia of sympathetic ganglia and hyperneurotization of viscera in the chick embryo. *J. Exp. Zool.* 1123:233-287.

Li, L., M. Rutlin, V.E. Abraira, C. Cassidy, L. Kus, S. Gong, M.P. Jankowski, W. Luo, N. Heintz, H.R. Koerber, C.J. Woodbury, and D.D. Ginty. 2011. The functional

organization of cutaneous low-threshold mechanosensory neurons. *Cell*. 147:1615-1627.

Lin, L.F., D.H. Doherty, J.D. Lile, S. Bektesh, and F. Collins. 1993. GDNF: a glial cell line-derived neurotrophic factor for midbrain dopaminergic neurons. *Science (New York, N.Y.)*. 260:1130-1132.

Lindfors, P.H., V. Voikar, J. Rossi, and M.S. Airaksinen. 2006. Deficient nonpeptidergic epidermis innervation and reduced inflammatory pain in glial cell line-derived neurotrophic factor family receptor alpha2 knock-out mice. *J Neurosci*. 26:1953-1960.

Liu, Q., P. Sikand, C. Ma, Z. Tang, L. Han, Z. Li, S. Sun, R.H. LaMotte, and X. Dong. 2012. Mechanisms of itch evoked by beta-alanine. *J Neurosci*. 32:14532-14537.

Liu, Q., S. Vrontou, F.L. Rice, M.J. Zylka, X. Dong, and D.J. Anderson. 2007. Molecular genetic visualization of a rare subset of unmyelinated sensory neurons that may detect gentle touch. *Nat Neurosci*. 10:946-948.

Liu, Y., and Q. Ma. 2011. Generation of somatic sensory neuron diversity and implications on sensory coding. *Current opinion in neurobiology*. 21:52-60.

Liu, Y., F.C. Yang, T. Okuda, X. Dong, M.J. Zylka, C.L. Chen, D.J. Anderson, R. Kuner, and Q. Ma. 2008. Mechanisms of compartmentalized expression of Mrg class G-protein-coupled sensory receptors. *J Neurosci*. 28:125-132.

Lo, D.C. 1992. Signal transduction and regulation of neurotrophins. *Curr. Opin. Neurobiol.* 2:336-340.

Lorenzo, M.J., C. Eng, L.M. Mulligan, T.J. Stonehouse, C.S. Healey, B.A. Ponder, and D.P. Smith. 1995. Multiple mRNA isoforms of the human RET proto-oncogene generated by alternate splicing. *Oncogene*. 10:1377-1383.

Lundy, R.F., Jr., and R.J. Contreras. 1999. Gustatory neuron types in rat geniculate ganglion. *Journal of neurophysiology*. 82:2970-2988.

Luo, W., H. Enomoto, F.L. Rice, J. Milbrandt, and D.D. Ginty. 2009. Molecular identification of rapidly adapting mechanoreceptors and their developmental dependence on ret signaling. *Neuron*. 64:841-856.

Luo, W., S.R. Wickramasinghe, J.M. Savitt, J.W. Griffin, T.M. Dawson, and D.D. Ginty. 2007. A hierarchical NGF signaling cascade controls Ret-dependent and Ret-independent events during development of nonpeptidergic DRG neurons. *Neuron*. 54:739-754.

Ma, L., G.F. Lopez, and R.F. Krimm. 2009. Epithelial-derived brain-derived neurotrophic factor is required for gustatory neuron targeting during a critical developmental period. *The Journal of neuroscience : the official journal of the Society for Neuroscience*. 29:3354-3364.

Madisen, L., T.A. Zwingman, S.M. Sunkin, S.W. Oh, H.A. Zariwala, H. Gu, L.L. Ng, R.D. Palmiter, M.J. Hawrylycz, A.R. Jones, E.S. Lein, and H. Zeng. 2010. A robust and high-throughput Cre reporting and characterization system for the whole mouse brain. *Nature neuroscience*. 13:133-140.

Maisonpierre P. C., Belluscio L., Squinto S., Ip N., Furth M. E., Lindsay R. M., and G.D. and Yancopoulos. 1990. Neurotrophin-3: a neurotrophic factor related to NGF and BDNF. *Science (New York, N.Y.)*. 247:1446-1451.

Majdan, M., G.S. Walsh, R. Aloyz, and F.D. Miller. 2001. TrkA mediates developmental sympathetic neuron survival in vivo by silencing an ongoing p75NTR-mediated death signal. *The Journal of cell biology*. 155:1275-1285.

Makkerh, J.P., C. Ceni, D.S. Auld, F. Vaillancourt, G. Dorval, and P.A. Barker. 2005a. p75 neurotrophin receptor reduces ligand-induced Trk receptor ubiquitination and delays Trk receptor internalization and degradation. *EMBO Rep.* 6:936-941.

Makkerh, J.P., C. Ceni, D.S. Auld, F. Vaillancourt, G. Dorval, and P.A. Barker. 2005b. p75 neurotrophin receptor reduces ligand-induced Trk receptor ubiquitination and delays Trk receptor internalization and degradation. *EMBO Rep*. 6:936-941.

Marks, W.J., Jr., T.L. Baumann, and R.T. Bartus. 2016. Long-Term Safety of Patients with Parkinson's Disease Receiving rAAV2-Neurturin (CERE-120) Gene Transfer. *Human gene therapy*. 27:522-527.

Marmigere, F., and P. Ernfors. 2007. Specification and connectivity of neuronal subtypes in the sensory lineage. *Nature reviews. Neuroscience*. 8:114-127.

Mauffray, M., O. Domingues, F. Hentges, J. Zimmer, D. Hanau, and T. Michel. 2015. Neurturin influences inflammatory responses and airway remodeling in different mouse asthma models. *Journal of immunology (Baltimore, Md. : 1950)*. 194:1423-1433.

Melillo, R.M., M. Santoro, S.H. Ong, M. Billaud, F. A., Y.R. Hadari, J. Schlessinger, and I. Lax. 2001. Docking protein FRS2 links the protein tyrosine kinase RET and its oncogenic forms with the mitogen-activated protein kinase signaling cascade. *Mol. Cell. Biol.* 21:4177-4187.

Meng, L., T. Huang, C. Sun, D.L. Hill, and R. Krimm. 2017. BDNF is required for taste axon regeneration following unilateral chorda tympani nerve section. *Experimental neurology*. 293:27-42.

Meng, X., M. Lindahl, M.E. Hyvonen, M. Parvinen, D.G. de Rooij, M.W. Hess, A. Raatikainen-Ahokas, K. Sainio, H. Rauvala, M. Lakso, J.G. Pichel, H. Westphal, M. Saarma, and H. Sariola. 2000. Regulation of cell fate decision of undifferentiated spermatogonia by GDNF. *Science (New York, N.Y.)*. 287:1489-1493.

Milbrandt, J., F.J. de Sauvage, T.J. Fahrner, R.H. Baloh, M.L. Leitner, M.G. Tansey, P.A. Lampe, R.O. Heuckeroth, P.T. Kotzbauer, K.S. Simburger, J.P. Golden, J.A. Davies, R. Vejsada, A.C. Kato, M. Hynes, D. Sherman, M. Nishimura, L.C. Wang, R. Vandlen, B. Moffat, R.D. Klein, K. Poulsen, C. Gray, A. Garces, E.M. Johnson, Jr., and et al. 1998. Persephin, a novel neurotrophic factor related to GDNF and neurturin. *Neuron*. 20:245-253.

Mistretta, C.M., and H.X. Liu. 2006. Development of fungiform papillae: patterned lingual gustatory organs. *Arch. Histol. Cytol.* 69:199-208.

Molliver, D.C., D.E. Wright, M.L. Leitner, A.S. Parsadanian, K. Doster, D. Wen, Q. Yan, and W.D. Snider. 1997a. IB4-binding DRG neurons switch from NGF to GDNF dependence in early postnatal life. *Neuron*. 19:849-861.

Molliver, D.C., D.E. Wright, M.L. Leitner, A.S. Parsadanian, K. Doster, D. Wen, Q. Yan, and W.D. Snider. 1997b. IB4-binding DRG neurons switch from NGF to GDNF dependence in early postnatal life. *Neuron*. 19:849-861.

Moore, M.W., R.D. Klein, I. Farinas, H. Sauer, M. Armanini, H. Phillips, L.F. Reichardt, A.M. Ryan, K. Carver-Moore, and A. Rosenthal. 1996. Renal and neuronal abnormalities in mice lacking GDNF. *Nature*. 382:76-79.

Mullican, S.E., X. Lin-Schmidt, C.N. Chin, J.A. Chavez, J.L. Furman, A.A. Armstrong, S.C. Beck, V.J. South, T.Q. Dinh, T.D. Cash-Mason, C.R. Cavanaugh, S. Nelson, C. Huang, M.J. Hunter, and S.M. Rangwala. 2017. GFRAL is the receptor for GDF15 and the ligand promotes weight loss in mice and nonhuman primates. *Nature medicine*. 23:1150-1157.

Murray, S.S., P.F. Bartlett, and S.S. Cheema. 1999. Differential loss of spinal sensory but not motor neurons in the p75NTR knockout mouse. *Neurosci Lett*. 267:45-48.

Nakamura, T., R. Sanokawa, Y. Sasaki, D. Ayusawa, M. Oishi, and M. Nozomu. 1996. N-Shc: a neural-specific adapter molecule that mediates signaling from neurotrophin/Trk to Ras/MAPK pathway. *Oncogene*. 13:1111-1121.

Naveilhan, P., C. Baudet, A. Mikaels, L. Shen, H. Westphal, and P. Ernfors. 1998. Expression and regulation of GFRalpha3, a glial cell line-derived neurotrophic factor family receptor. *Proceedings of the National Academy of Sciences of the United States of America*. 95:1295-1300.

Nichols, B.J., and J. Lippincott-Schwartz. 2001. Endocytosis without clathrin coats. *Trends Cell Biol.* 11:406-412.

Nikolaev, A., T. McLaughlin, D.D. O'Leary, and M. Tessier-Lavigne. 2009. APP binds DR6 to trigger axon pruning and neuron death via distinct caspases. *Nature*. 457:981-989.

Nishino, J., K. Mochida, Y. Ohfuji, T. Shimazaki, C. Meno, S. Ohishi, Y. Matsuda, H. Fujii, Y. Saijoh, and H. Hamada. 1999. GFR alpha3, a component of the artemin receptor, is required for migration and survival of the superior cervical ganglion. *Neuron*. 23:725-736.

Nykjaer, A., R. Lee, K.K. Teng, P. Jansen, P. Madsen, M.S. Nielsen, C. Jacobsen, M. Kliemannel, E. Schwarz, T.E. Willnow, B.L. Hempstead, and C.M. Petersen. 2004. Sortilin is essential for proNGF-induced neuronal cell death. *Nature*. 427:843-848.

Obermeier, A., R.A. Bradshaw, K. Seedorf, A. Choidas, J. Schlessinger, and A. Ullrich. 1994. Neuronal differentiation signals are controlled by nerve growth factor receptor/Trk binding sites for SHC and PLC gamma. *EMBO J.* 13:1585-1590.

Oppenheim, R.W. 1991. Cell death during development of the nervous system. *Annu. Rev. Neurosci.* 14:453-501.

Pan, Z.W., and J.C. Li. 2012. Advances in molecular genetics of Hirschsprung's disease. *Anat. Rec.* 295:1628-1638.

Paratcha, G., F. Ledda, L. Baars, M. Coulpier, V. Besset, J. Anders, R. Scott, and F. Ibanez. 2001. Released GFRa1 potentiates downstream signaling, neuronal survival, and differentiation via a novel mechanism of recruitment of c-Ret to lipid rafts. *Neuron*. 29:171-184.

Paratcha, G., F. Ledda, and C.F. Ibanez. 2003. The neural cell adhesion molecule NCAM is an alternative signaling receptor for GDNF family ligands. *Cell*. 113:867-879.

Parkash, V., and A. Goldman. 2009. Comparison of GFL-GFRalpha complexes: further evidence relating GFL bend angle to RET signalling. *Acta crystallographica. Section F, Structural biology and crystallization communications*. 65:551-558.

Patel, A.V., and R.F. Krimm. 2010. BDNF is required for the survival of differentiated geniculate ganglion neurons. *Developmental biology*. 340:419-429.

Patel, A.V., and R.F. Krimm. 2012. Neurotrophin-4 regulates the survival of gustatory neurons earlier in development using a different mechanism than brain-derived neurotrophic factor. *Developmental biology*. 365:50-60.

Paul, C.E., E. Vereker, K.M. Dickson, and P.A. Barker. 2004. A pro-apoptotic fragment of the p75 neurotrophin receptor is expressed in p75NTRExonIV null mice. *J Neurosci*. 24:1917-1923.

Pereira, D.B., and M.V. Chao. 2007. The tyrosine kinase Fyn determines the localization of TrkB receptors in lipid rafts. *The Journal of neuroscience : the official journal of the Society for Neuroscience*. 27:4859-4869.

Pezet, S., and S.B. McMahon. 2006. Neurotrophins: mediators and modulators of pain. *Annu Rev Neurosci*. 29:507-538.

Pichel, J.G., L. Shen, H.Z. Sheng, A.C. Granholm, J. Drago, A. Grinberg, E.J. Lee, S.P. Huang, M. Saarma, B.J. Hoffer, H. Sariola, and H. Westphal. 1996. Defects in enteric innervation and kidney development in mice lacking GDNF. *Nature*. 382:73-76.

Pierchala, B.A., J. Milbrandt, and E.M. Johnson, Jr. 2006. Glial cell line-derived neurotrophic factor-dependent recruitment of Ret into lipid rafts enhances

signaling by partitioning Ret from proteasome-dependent degradation. *J. Neurosci.* 26:2777-2787.

Pozas, E., and C.F. Ibanez. 2005. GDNF and GFRalpha1 promote differentiation and tangential migration of cortical GABAergic neurons. *Neuron*. 45:701-713.

Putcha, G.V., M. Deshmukh, and J. Johnson, E.M. 1999. Bax translocation is a critical event in neuronal apoptosis: regulation by neuroprotectants, BCL-2, and caspases. *J. Neurosci.* 19:7476-7485.

Putcha, G.V., K.L. Moulder, J.P. Golden, P. Bouillet, J.A. Adams, A. Strasser, and E.M. Johnson. 2001. Induction of BIM, a proapoptotic BH3-only Bcl-2 family member, is critical for neuronal apoptosis. *Neuron*. 29:615-628.

Ramaswamy, S., J.L. McBride, I. Han, E.M. Berry-Kravis, L. Zhou, C.D. Herzog, M. Gasmi, R.T. Bartus, and J.H. Kordower. 2009. Intrastriatal CERE-120 (AAV-Neurturin) protects striatal and cortical neurons and delays motor deficits in a transgenic mouse model of Huntington's disease. *Neurobiology of disease*. 34:40-50.

Riccio, A., B. Pierchala, C. Ciarallo, and D. Ginty. 1997. An NGF-TrkA-Mediated retrograde signal to transcription factor CREB in sympathetic neurons. *Science (New York, N.Y.)*. 227:1097-1100.

Richardson, D.S., A.Z. Lai, and L.M. Mulligan. 2006. RET ligand-induced internalization and its consequences for downstream signaling. *Oncogene*. 25:3206-3211.

Richardson, D.S., D.M. Rodrigues, B.D. Hyndman, M.J.F. Crupi, A.C. Nicolescu, and L.M. Mulligan. 2012. Alternative splicing results in RET isoforms with distinct trafficking properties. *Mol. Biol. Cell*. 23:3838-3850.

Rochlin, M.W., R. O'Connor, R.J. Giger, J. Verhaagen, and A.I. Farbman. 2000. Comparison of neurotrophin and repellent sensitivities of early embryonic geniculate and trigeminal axons. *The Journal of comparative neurology*. 422:579-593.

Rossi, J., N. Balthasar, D. Olson, M. Scott, E. Berglund, C.E. Lee, M.J. Choi, D. Lauzon, B.B. Lowell, and J.K. Elmquist. 2011. Melanocortin-4 receptors expressed by cholinergic neurons regulate energy balance and glucose homeostasis. *Cell metabolism*. 13:195-204.

Ruzankina, Y., C. Pinzon-Guzman, A. Asare, T. Ong, L. Pontano, G. Cotsarelis, V.P. Zediak, M. Velez, A. Bhandoola, and E.J. Brown. 2007. Deletion of the developmentally essential gene ATR in adult mice leads to age-related phenotypes and stem cell loss. *Cell stem cell*. 1:113-126.

Sakai, K., K.M. Sanders, M.R. Youssef, K.M. Yanushefski, L.E. Jensen, G. Yosipovitch, and T. Akiyama. 2017. Role of neurturin in spontaneous itch and increased nonpeptidergic intraepidermal fiber density in a mouse model of psoriasis. *Pain*. 158:2196-2202.

Salvatore, D., M.V. Barone, G. Salvatore, R.M. Melillo, G. Chiappetta, A. Mineo, G. Fenzi, G. Vecchio, A. Fusco, and M. Santoro. 2000. Tyrosines 1015 and 1062 are *in vivo* autophosphorylation sites in Ret and Ret-derived oncoproteins. *J. Clin. Endo. Metab.* 85:3898-3907.

Sanchez, M.P., I. Silos-Santiago, J. Frisen, B. He, S.A. Lira, and M. Barbacid. 1996. Renal agenesis and the absence of enteric neurons in mice lacking GDNF. *Nature*. 382:70-73.

Santoro, M., R. Rosati, M. Grieco, M.T. Berlingieri, G.L. D'Amato, V. de Franciscis, and A. Fusco. 1990. The ret proto-oncogene is consistently expressed in human pheochromocytomas and thyroid medullary carcinomas. *Oncogene*. 5:1595-1598.

Sasselli, V., V. Pachnis, and A.J. Burns. 2012. The enteric nervous system. *Developmental biology*. 366:64-73.

Schindelin, J., I. Arganda-Carreras, E. Frise, V. Kaynig, M. Longair, T. Pietzsch, S. Preibisch, C. Rueden, S. Saalfeld, B. Schmid, J.Y. Tinevez, D.J. White, V. Hartenstein, K. Eliceiri, P. Tomancak, and A. Cardona. 2012. Fiji: an open-source platform for biological-image analysis. *Nature methods*. 9:676-682.

Schuchardt, A., V. D'Agati, L. Larsson-Blomberg, F. Constantini, and V. Pachnis. 1994. Defects in the kidney and enteric nervous system of mice lacking the tyrosine kinase receptor Ret. *Nature*. 367:380-383.

Schuchardt, A., V. D'Agati, V. Pachnis, and F. Costantini. 1996. Renal agenesis and hypodysplasia in ret-k^- mutant mice result from defects in ureteric bud development. *Development (Cambridge, England)*. 122.

Scott, A., H. Hasegawa, K. Sakurai, A. Yaron, J. Cobb, and F. Wang. 2011. Transcription factor short stature homeobox 2 is required for proper development of tropomyosin-related kinase B-expressing mechanosensory neurons. *J Neurosci*. 31:6741-6749.

Sidorova, Y.A., K. Matlik, M. Paveliev, M. Lindahl, E. Piranen, J. Milbrandt, U. Arumae, M. Saarma, and M.M. Bespalov. 2010. Persephin signaling through GFRalpha1:

the potential for the treatment of Parkinson's disease. *Mol Cell Neurosci*. 44:223-232.

Silos-Santiago, I., D.C. Molliver, S. Ozaki, R.J. Smeyne, A.M. Fagan, M. Barbacid, and W.D. Snider. 1995. Non-TrkA-expressing small DRG neurons are lost in TrkA deficient mice. *The Journal of neuroscience : the official journal of the Society for Neuroscience*. 15:5929-5942.

Smeyne, R.J., R. Klein, A. Schnapp, L.K. Long, S. Bryant, A. Lewin, S.A. Lira, and M. Barbacid. 1994a. Severe sensory and sympathetic neuropathies in mice carrying a disrupted Trk/NGF receptor gene. *Nature*. 368:246-249.

Smeyne, R.J., R. Klein, A. Schnapp, L.K. Long, S. Bryant, A. Lewin, S.A. Lira, and M. Barbacid. 1994b. Severe sensory and sympathetic neuropathies in mice carrying a disrupted Trk/NGF receptor gene. *Nature*. 368:246-248.

Snider, W.D. 1994. Functions of the Neurotrophins during Nervous System Development: what the knockouts are teaching us. *Cell*. 77:627-638.

Snider, W.D., and I. Silos-Santiago. 1996. Dorsal root ganglion neurons require functional neurotrophin receptors for survival during development. *Philos Trans R Soc Lond B Biol Sci*. 351:395-403.

Spencer, A., L. Yu, V. Guili, F. Reynaud, Y. Ding, J. Ma, J. Jullien, D. Koubi, E. Gauthier, D. Cluet, J. Falk, V. Castellani, C. Yuan, and B.B. Rudkin. 2017. Nerve Growth Factor Signaling from Membrane Microdomains to the Nucleus: Differential Regulation by Caveolins. *International journal of molecular sciences*. 18.

Srinivas, S., T. Watanabe, C.S. Lin, C.M. William, Y. Tanabe, T.M. Jessell, and F. Costantini. 2001. Cre reporter strains produced by targeted insertion of EYFP and ECFP into the ROSA26 locus. *BMC Dev Biol*. 1:4.

Stephens, R.M., D.M. Loeb, T.D. Copeland, T. Pawson, L.A. Greene, and D.R. Kaplan. 1994. Trk receptors use redundant signal transduction pathways involving SHC and PLC-gamma 1 to mediate NGF responses. *Neuron*. 12:691-705.

Tahira, T., Y. Ishizaka, F. Itoh, T. Sugimura, and M. Nagao. 1990. Characterization of ret proto-oncogene mRNAs encoding two isoforms of the protein product in a human neuroblastoma cell line. *Oncogene*. 5:97-102.

Tansey, M.G., R.H. Baloh, J. Milbrandt, and E.M. Johnson, Jr. 2000. GFRa-mediated localization of RET to lipid rafts is required for effective downstream signaling, differentiation, and neuronal survival. *Neuron*. 25:611-623.

Taraviras, S., C.V. Marcos-Gutierrez, P. Durbec, H. Jani, M. Grigoriou, M. Sukumaran, L.C. Wang, M. Hynes, G. Raisman, and V. Pachnis. 1999. Signalling by the RET receptor tyrosine kinase and its role in the development of the mammalian enteric nervous system. *Development (Cambridge, England)*. 126:2785-2797.

Tatsumi, N., R. Miki, K. Katsu, and Y. Yokouchi. 2007. Neurturin-GFRalpha2 signaling controls liver bud migration along the ductus venosus in the chick embryo. *Developmental biology*. 307:14-28.

Tessarollo, L., P. Tsoulfas, M.J. Donovan, M.E. Palko, J. Blair-Flynn, B.L. Hempstead, and L.F. Parada. 1997. Targeted deletion of all isoforms of the trkC gene suggests the use of alternate receptors by its ligand neurotrophin-3 in neuronal

development and implicates trkC in normal cardiogenesis. *Proceedings of the National Academy of Sciences of the United States of America*. 94:14776-14781.

Tessarollo, L., P. Tsoulfas, D. Martin-Zanca, D.J. Gilbert, N.A. Jenkins, N.G. Copeland, and L. Parada. 1993. trkC, a receptor for neurtophin-3, is widely expressed in the developing nervous system and in non-neuronal tissues. *Development (Cambridge, England)*. 118:463-475.

Tessarollo, L., K.S. Vogel, M.E. Palko, S.W. Reid, and L.F. Parada. 1994. Targeted mutation in the neurotrophin-3 gene results in loss of muscle sensory neurons. *Proc Natl Acad Sci U S A*. 91:11844-11848.

Tomac, A., E. Lindqvist, L.F. Lin, S.O. Ogren, D. Young, B.J. Hoffer, and L. Olson. 1995. Protection and repair of the nigrostriatal dopaminergic system by GDNF in vivo. *Nature*. 373:335-339.

Tomac, A.C., A.D. Agulnick, N. Haughey, C.F. Chang, Y. Zhang, C. Backman, M. Morales, M.P. Mattson, Y. Wang, H. Westphal, and B.J. Hoffer. 2002. Effects of cerebral ischemia in mice deficient in Persephin. *Proc. Natl. Acad. Sci. USA*. 99:9521-9526.

Trupp, M., E. Arenas, M. Fainzilber, A.S. Nilsson, B.A. Sieber, M. Grigoriou, C. Kilkenny, E. Salazar-Grueso, V. Pachnis, and U. Arumae. 1996. Functional receptor for GDNF encoded by the c-ret proto-oncogene. *Nature*. 381:785-789.

Trupp, M., N. Belluardo, H. Funakoshi, and C.F. Ibanez. 1997. Complementary and overlapping expression of glial cell line-derived neurotrophic factor (GDNF), c-ret proto-oncogene, and GDNF receptor- alpha indicates multiple mechanisms of

trophic actions in the adult rat CNS. *The Journal of neuroscience : the official journal of the Society for Neuroscience*. 17:3554-3567.

Tsui-Pierchala, B.A., R.C. Ahrens, R.J. Crowder, J. Milbrandt, and J. Johnson, E.M. 2002a. The long and short isoforms of Ret function as independent signaling complexes. *J. Biol. Chem.* 277:34618-34625.

Tsui-Pierchala, B.A., M. Encinas, J. Milbrandt, and J. Johnson, E.M. 2002b. Lipid rafts in neuronal signaling and function. *TINS*. 25:412-417.

Tsui-Pierchala, B.A., and D.D. Ginty. 1999. Characterization of an NGF-P-TrkA retrograde-signaling complex and age-dependent regulation of TrkA phosphorylation in sympathetic neurons. *J. Neurosci.* 19:8207-8218.

Tsui-Pierchala, B.A., J. Milbrandt, and E.M. Johnson, Jr. 2002c. NGF utilizes c-Ret via a novel GFL-independent, inter-RTK signaling mechanism to maintain the trophic status of mature sympathetic neurons. *Neuron*. 33:261-273.

Tsui, C.C., N.A. Gabreski, S.J. Hein, and B.A. Pierchala. 2015. Lipid rafts are physiologic membrane microdomains necessary for the morphogenic and developmental functions of glial cell line-derived neurotrophic factor in vivo. *J. Neurosci.* 35:13233-13243.

Tsui, C.C., and B.A. Pierchala. 2008. CD2AP and Cbl-3/Cbl-c constitute a critical checkpoint in the regulation of Ret signal transduction. *J. Neurosci.* 28:8789-8800.

Tsui, C.C., and B.A. Pierchala. 2010. The differential axonal degradation of Ret accounts for cell-type-specific function of glial cell line-derived neurotrophic factor

as a retrograde survival factor. *The Journal of neuroscience : the official journal of the Society for Neuroscience*. 30:5149-5158.

Uesaka, T., and H. Enomoto. 2010. Neural precursor death is central to the pathogenesis of intestinal aganglionosis in Ret hypomorphic mice. *The Journal of neuroscience : the official journal of the Society for Neuroscience*. 30:5211-5218.

Uesaka, T., S. Jain, S. Yonemura, Y. Uchiyama, J. Milbrandt, and H. Enomoto. 2007. Conditional ablation of GFRalpha1 in postmigratory enteric neurons triggers unconventional neuronal death in the colon and causes a Hirschsprung's disease phenotype. *Development (Cambridge, England)*. 134:2171-2181.

Usoskin, D., A. Furlan, S. Islam, H. Abdo, P. Lonnerberg, D. Lou, J. Hjerling-Leffler, J. Haeggstrom, O. Kharchenko, P.V. Kharchenko, S. Linnarsson, and P. Ernfors. 2015. Unbiased classification of sensory neuron types by large-scale single-cell RNA sequencing. *Nature neuroscience*. 18:145-153.

Vandenbeuch, A., E.D. Larson, C.B. Anderson, S.A. Smith, A.P. Ford, T.E. Finger, and S.C. Kinnamon. 2015. Postsynaptic P2X3-containing receptors in gustatory nerve fibres mediate responses to all taste qualities in mice. *The Journal of physiology*. 593:1113-1125.

Vilar, M., I. Charalampopoulos, R.S. Kenchappa, A. Reversi, J.M. Klos-Applequist, E. Karaca, A. Simi, C. Spuch, S. Choi, W.J. Friedman, J. Ericson, G. Schiavo, B.D. Carter, and C.F. Ibanez. 2009a. Ligand-independent signaling by disulfide-crosslinked dimers of the p75 neurotrophin receptor. *J Cell Sci*. 122:3351-3357.

Vilar, M., I. Charalampopoulos, R.S. Kenchappa, A. Simi, E. Karaca, A. Reversi, S. Choi, M. Bothwell, I. Mingarro, W.J. Friedman, G. Schiavo, P.I. Bastiaens, P.J.

Verveer, B.D. Carter, and C.F. Ibanez. 2009b. Activation of the p75 neurotrophin receptor through conformational rearrangement of disulphide-linked receptor dimers. *Neuron*. 62:72-83.

Volosin, M., W. Song, R.D. Almeida, D.R. Kaplan, B.L. Hempstead, and W.J. Friedman. 2006. Interaction of survival and death signaling in basal forebrain neurons: roles of neurotrophins and proneurotrophins. *The Journal of neuroscience : the official journal of the Society for Neuroscience*. 26:7756-7766.

Volosin, M., C. Trotter, A. Cragnolini, R.S. Kenchappa, M. Light, B.L. Hempstead, B.D. Carter, and W.J. Friedman. 2008. Induction of proneurotrophins and activation of p75NTR-mediated apoptosis via neurotrophin receptor-interacting factor in hippocampal neurons after seizures. *The Journal of neuroscience : the official journal of the Society for Neuroscience*. 28:9870-9879.

von Schack, D., E. Casademunt, R. Schweigreiter, M. Meyer, M. Bibel, and G. Dechant. 2001. Complete ablation of the neurotrophin receptor p75NTR causes defects both in the nervous and the vascular system. *Nat Neurosci*. 4:977-978.

Warren Olanow, C., R.T. Bartus, T.L. Baumann, S. Factor, N. Boulis, M. Stacy, D.A. Turner, W. Marks, P. Larson, P.A. Starr, J. Jankovic, R. Simpson, R. Watts, B. Guthrie, K. Poston, J.M. Henderson, M. Stern, G. Baltuch, C.G. Goetz, C. Herzog, J.H. Kordower, R. Alterman, A.M. Lozano, and A.E. Lang. 2015. Gene delivery of neurturin to putamen and substantia nigra in Parkinson disease: A double-blind, randomized, controlled trial. *Annals of neurology*. 78:248-257.

Wehner, A.B., H. Abdesselem, T.L. Dickendesher, F. Imai, Y. Yoshida, R.J. Giger, and B.A. Pierchala. 2016a. Semaphorin 3A is a retrograde cell death signal in

developing sympathetic neurons. *Development (Cambridge, England)*. 143:1560-1570.

Wehner, A.B., A.M. Milen, R.L. Albin, and B.A. Pierchala. 2016b. The p75 neurotrophin receptor augments survival signaling in the striatum of pre-symptomatic Q175(WT/HD) mice. *Neuroscience*. 324:297-306.

Werth, J.L., M. Deshmukh, J. Cocabo, J. Johnson, E.M., and S.M. Rothman. 2000. Reversible physiological alterations in sympathetic neurons deprived of NGF but protected from apoptosis by caspase inhibition or Bax deletion. *Exp. Neurol.* 161:203-211.

Wu, S., Y. Wu, and M.R. Capecchi. 2006. Motoneurons and oligodendrocytes are sequentially generated from neural stem cells but do not appear to share common lineage-restricted progenitors in vivo. *Development (Cambridge, England)*. 133:581-590.

Yang, L., C.C. Chang, Z. Sun, D. Madsen, H. Zhu, S.B. Padkjaer, X. Wu, T. Huang, K. Hultman, S.J. Paulsen, J. Wang, A. Bugge, J.B. Frantzen, P. Norgaard, J.F. Jeppesen, Z. Yang, A. Secher, H. Chen, X. Li, L.M. John, B. Shan, Z. He, X. Gao, J. Su, K.T. Hansen, W. Yang, and S.B. Jorgensen. 2017. GFRAL is the receptor for GDF15 and is required for the anti-obesity effects of the ligand. *Nature medicine*. 23:1158-1166.

Ye, H., R. Kuruvilla, L.S. Zweifel, and D.D. Ginty. 2003. Evidence in support of signaling endosome-based retrograde survival of sympathetic neurons. *Neuron*. 39:57-68.

Yokota, Y., and R.M. Bradley. 2016. Receptive field size, chemical and thermal responses, and fiber conduction velocity of rat chorda tympani geniculate ganglion neurons. *Journal of neurophysiology*. 115:3062-3072.

Yuen, E.C., Y. Li, R.E. Mischel, C.L. Howe, D.M. Holtzman, and W.C. Mobley. 1996. Neurotrophins and the Neurotrophic Factor Hypothesis. *Neural Notes*. 1:3-7.

Zaidi, F.N., and M.C. Whitehead. 2006. Discrete innervation of murine taste buds by peripheral taste neurons. *The Journal of neuroscience : the official journal of the Society for Neuroscience*. 26:8243-8253.

Zou, M., S. Li, W.H. Klein, and M. Xiang. 2012. Brn3a/Pou4f1 regulates dorsal root ganglion sensory neuron specification and axonal projection into the spinal cord. *Developmental biology*. 364:114-127.

Zylka, M.J., X. Dong, A.L. Southwell, and D.J. Anderson. 2003. Atypical expansion in mice of the sensory neuron-specific Mrg G protein-coupled receptor family. *Proc Natl Acad Sci U S A*. 100:10043-10048.

Zylka, M.J., F.L. Rice, and D.J. Anderson. 2005. Topographically distinct epidermal nociceptive circuits revealed by axonal tracers targeted to Mrgprd. *Neuron*. 45:17-25.

CHAPTER 5: CONCLUSION AND FUTURE DIRECTIONS

A Key Role for p75 in Augmenting GFL-Ret Signal Transduction

Our demonstration of the important role of p75 in augmenting Ret signaling in nonpeptidergic nociceptors in Chapter 2 of this thesis generates several intriguing questions. Given that p75- and Ret-deficient mice overtly share few phenotypic similarities with one another, wherein p75-null mice are viable, while Ret-null mice die at birth (Lee et al., 1992; Trupp et al., 1996), it is clear that p75 is not required for Ret signal transduction in all cell types. Even among Ret+ sensory neurons, no loss of Ret-dependent low threshold mechanoreceptors was observed in our study. Given these observations, what makes Ret+ nociceptors uniquely depend on p75? The investigation of this receptor complex in both sensory and sympathetic neurons led to the discovery of important differences in neurotrophic factor signaling between these two populations. In the same experiments performed in parallel in both neuron populations, p75 was required for GFL activation in sensory, but not sympathetic neurons. Even Ret^{high} $MrgD^{+}$ nociceptors are lost in the absence of p75, indicating that it's not simply a function of Ret levels that dictate the requirement for p75.

One possibility is that redundancies exist in the mechanisms underlying Ret trafficking. SorLA, a member of the sortilin-related receptor family, was recently shown to target Ret for endocytosis, preventing its degradation and thereby potentiating signaling in midbrain neurons (Glerup et al., 2013). Thus, it is possible, and perhaps likely, to suggest that differential expression of cell type-specific regulators of Ret trafficking may underlie the differential requirement for p75 in augmenting Ret signaling

in various tissues. To determine which cell types in particular require p75 for GFL/Ret-mediated signal transduction, the generation of a transgenic model such as *Ret*$^{fx/fx}$; *p75*-Cre mice would facilitate this investigation. Additionally, enhanced understanding of the structural basis underlying the interaction between p75 and Ret, and the subsequent creation of mutant animals that prevent the interaction between them would be key in understanding the cell type-specific requirement for p75. Finally, given that p75 potentiates GFL-Ret signal transduction, and that overactive Ret signaling has been implicated in numerous cancers including human pheochromocytoma and papillary thyroid carcinoma, whether mutations in p75 can also lead to overactivated Ret signaling leading to human disease is an intriguing question. In concordance with this idea, p75 was shown to be overexpressed in human papillary thyroid carcinoma samples, while p75 was not observed in normal thyroid tissue (Rocha et al., 2006). Further studies investigating the functional consequences for p75 potentiation of Ret signaling is therefore an important future direction.

Non Cell-Autonomous Functions for p75 in Sensory Neuron Development During Embryogenesis

Perhaps a more surprising finding than the role for p75 in augmenting GFL signaling is the observation that sensory neuron-specific deletion of p75 did not phenocopy p75 germline null mice (Chapter 2). As one of the first knockout strains to be produced, and at the time when p75 was already understood to be a major regulator for neurotrophin signaling, the most overt phenotype observed in p75-null mice were hindpaw clubbing resulting from sensory abnormalities. Subsequent studies discovered that in sensory

neurons *in vitro*, p75 enhanced NGF binding to TrkA, shifting the dose response to enhance the TrkA signaling and NGF-mediated survival (Barker and Shooter, 1994; Davies et al., 1993; Hantzopoulos et al., 1994). For this reason, the function of p75 in DRG sensory neurons was assumed to be restricted to potentiating the function of NGF/TrkA signaling. Surprisingly, our data suggest that p75 is dispensable for NGF-mediated survival, as the survival of peptidergic nociceptors is unaffected despite less than 10% of p75 remaining following *Islet1*-Cre-mediated deletion of p75.

In lieu of these findings, why do germline p75-null mice lose approximately 50% of sensory neurons by birth, when the function of p75 in sensory neurons appears to be dispensable during embryonic development? We posit that the most likely explanation for these findings is an early embryonic function for p75 in Schwann cells. It has been shown previously that deficits in Schwann cell development caused by loss of ErbB2 results in a severe loss of sensory and motor neurons by E11.5, along with a severe reduction in neurite extension and target innervation (Morris et al., 1999; Woldeyesus et al., 1999). In support of this model, p75 is known to be highly expressed in Schwann cells, and Bentley and Lee (2000) demonstrated that p75-deficient mice mimic the phenotype observed in *ErbB2*$^{-/-}$ mice, albeit less severely (Bentley and Lee, 2000). Specifically, although neuron counts were not performed, the authors observed that peripheral axon outgrowth was stunted beginning at E11.5 in *p75*$^{-/-}$ mice, along with a loss of the Schwann cell marker S100β. Additionally, using *in vitro* functional assays, the authors found that the migration of Schwann cells cultured from p75-deficient DRGs was severely diminished, suggesting p75 is an important regulator of Schwann cell migration. In future studies, the comparison of p75 conditional knockouts using various

Schwann cell-specific Cre lines to allow for the elimination of p75 function during several distinct developmental windows using mouse lines such as Wnt1-Cre, P0-Cre, and ErbB2-Cre. Experiments such as these will be vital for our understanding of the embryonic function of p75 in sensory neuron development.

Ret as a Novel Regulator of Cell Death

To date, a small number of studies have suggested that Ret acts as a dependence receptor to promote apoptosis. To arrive at this conclusion, Ret was overexpressed in heterologous cell lines, and the extent of apoptosis subsequently quantified in the presence or absence of GDNF (Bordeaux et al., 2000). Importantly, we find no evidence of a dependence receptor model of Ret signal transduction. As noted in the introduction, there are several tissues in which Ret is not co-expressed with the GFRα co-receptors (Golden et al., 1998; Nosrat et al., 1997), and many tumor populations in which Ret is upregulated in the absence of its co-receptors, yet these populations are not eliminated (Santoro et al., 1990). Whether Ret can serve as a dependence receptor in a physiological system remains to be demonstrated, but in the studies reported here, we find no evidence of this phenomenon.

No studies to date have demonstrated a role for receptor tyrosine kinases in cell death during normal organismal development. However, TrkA activation has been shown to induce apoptosis in pediatric neuroblastoma tumor cells. Interestingly, TrkA does not mediate these effects through a direct mechanism, but instead interacts with CCM2 (Malcavernin) through its PTB domain to mediate these effects. CCM2, in turn, has a Karet domain which is essential for the pro-apoptotic effects, although the

mechanism underlying these interactions is unclear (Harel et al., 2009). These findings bear some similarity to our discovery that Ret promotes developmental cell death in sympathetic neurons indirectly through its ability to augment the function of p75, which itself promotes apoptosis through the interaction with cell death pathways. Similar to the studies performed to identify the structural basis of the interaction of TrkA with CCM2, determining the precise means by which Ret and p75 physically associate remains an important future direction, which could lead to the development of new tools to investigate this developmental function of Ret.

Dual Functions of a Novel p75-Ret Receptor Complex

In a recent study by Lin et al. (2015), a genetic approach was undertaken using alanine-scanning mutagenesis to dissect how p75 is able to interact with many different co-receptors to promote different signaling pathways capable of promoting survival, apoptosis, or growth cone collapse. In this study, the authors found that pro-apoptotic and pro-survival pathways mapped to different regions of the p75 death domain, with pro-apoptotic regions inducing JNK activation while pro-survival regions promoted activation of NF-κB (Charalampopoulos et al., 2012). Interestingly, in this thesis we discover the existence of a p75-Ret receptor complex that can promote both survival and apoptotic signaling pathways, depending on which ligand promotes the assembly of the complex. Given the structure-function analysis performed above, it would be interesting to identify how p75 and Ret physically associate, and whether the ligand promoting the assembly of the receptor complex would change how these two receptors interact.

Although these studies took advantage of the developmental dependence of sensory neurons on Ret signaling for survival, as well as the well-characterized role for p75 in developmental cell death in sympathetic neurons, we have identified a receptor complex with dual functions, the output of which depends on which ligand activates the assembly of the complex, and thus, which receptor becomes activated (Figure 5.1). it would be interesting to investigate how this receptor complex may function if both signaling pathways were activated simultaneously. For example, while sympathetic neurons were utilized to investigate the role for Ret in p75-mediated apoptosis due to its well characterized pro-apoptotic roles in developmental cell death in this system, p75 also mediates apoptosis of other neuronal populations including sensory and cerebellar neurons. In these systems, it is tempting to suggest that p75 may serve as a "coincidence detector" – acting as an integrator for both neurotrophic factor and competition factor signals to ultimately trigger survival and apoptosis. One might posit that under these conditions, maximal concentrations of GFLs would silence BDNF-mediated apoptosis, thereby promoting survival, and that maximal concentrations of BDNF with sub-threshold levels of GFLs would promote apoptosis.

Ret as a Novel Regulator for Phox2b Expression

In chapter 4, we investigate the roles of GDNF-Ret signaling in chemosensory neuron development and function. During embryogenesis, like other placodally-derived cranial sensory ganglia, the geniculate ganglion begins as a homogenous placode of Neurogenin2-positive cells (Krimm, 2007). Through a series of differentiation steps, two anatomically and functionally-distinct groups of neurons develop: a proximal

somatosensory population, innervating the external ear, and a distal chemosensory population, innervating taste buds on the soft palate and the anterior two-thirds of the dorsal tongue. In our study, we demonstrated that Ret expression leads to the initial amplification of Phox2b expression in chemosensory neurons of the geniculate ganglion. While Ret knockout mice have a substantial reduction in Phox2b expression, no phenotype was observed when Ret was deleted after Phox2b expression had been initiated, using both a pharmacologic and conditional genetic approach. While these data provide the novel insight that Ret is upstream of Phox2b, the question that remains is what governs the expression of Ret? And spatiotemporally, why is Ret expression restricted to distal neurons that are destined to be lingually-projecting chemosensory neurons?

While little is known regarding Ret initiation in chemosensory neurons, a considerable breadth of literature is available regarding transcriptional regulation of Ret in autonomic and enteric neuron populations. There are several reports suggesting that Phox2b expression promotes the expression of Ret, as *Phox2b*$^{-/-}$ mice lose Ret expression in all autonomic ganglia (D'Autreaux et al., 2011; Dauger et al., 2003; Pattyn et al., 1999). Interestingly, while the authors conclude from these findings that Phox2b is upstream of Ret, they do not directly demonstrate that Ret expression depends on Phox2b expression. Given that many phenotypic changes occur in the autonomic ganglia of *Phox2b*$^{-/-}$ mice, including a loss of the biosynthetic machinery for adrenergic neurotransmitters and a change of in several additional autonomic transcription factors, it is possible that the loss of Ret is secondary to the loss of another regulator. Additionally, the experiments conducted so far do not rule out the possibility that Ret

initiates Phox2b expression, which in turn acts to further promote the expression of Ret, thereby serving as a positive feedback loop. It is interesting to consider that Phox2b and Ret-deficient mice share several characteristics, including loss of autonomic and enteric ganglia, reduction in several cranial sensory ganglia, and an association with Hirschsprung's Disease in human patients with loss of function mutations in either gene (Pattyn et al., 1999; Sasselli et al., 2012). To understand whether Phox2b globally specifies Ret expression, or vice versa, a broad phenotypic analysis of *Ret*$^{fx/fx}$; *Phox2b*-Cre and *Ret*-Cre; P*hox2b*$^{fx/fx}$ mice should be undertaken, with special attention given to autonomic, enteric, and cranial sensory ganglia. Interestingly, our creation of *Ret*$^{fx/fx}$; *Phox2b*-Cre mice allowed us the observation that these mice are viable, fertile, and have normal life expectancy (data not shown), indicating that in other populations Ret is also likely to be dispensable for maintenance of Phox2b.

Heterogeneity Within the Geniculate Ganglion

In this thesis, we demonstrate the existence of a unique subpopulation of chemosensory GG neurons, which are molecularly, morphologically, and functionally distinct. Given the complex sensory modalities that exist within the geniculate ganglion, the absence of literature to date that describes the cellular basis for the observed heterogeneity in GG neuron function is surprising. While the DRG sensory system has been described to possess at least six molecularly and functionally distinct subpopulations (Chiu et al., 2014), and perhaps as many as eleven subpopulations (Usoskin et al., 2015), much less is known regarding GG subpopulations. In a recent study by Dvoryanchikov et al. (2017), single cell RNA sequencing of 96 GG neurons

was undertaken with subsequent hierarchical clustering and principal component analysis to determine whether distinct subpopulations could be categorized based on transcriptome analysis (Dvoryanchikov et al., 2017). In this study, the authors were able to identify three subclusters of neurons, each possessing unique transcription factors and neurotransmitter receptor profiles indicative of individual subpopulations of neurons. Although this study significantly advanced our understanding of cellular heterogeneity within the GG, it seems likely that additional subpopulations exist that remain to be identified. Studies undertaken in the DRG sensory neurons that identifed six and eleven subpopulations involved single cell sequencing on 334 (Chiu et al., 2014) and 622 (Usoskin et al., 2015) neurons, respectively, allowing enhanced depth of sequencing and greater representation of rare groups of neurons. This approach is hindered by the cost and time associated with single cell RNA sequencing. Interestingly, Macosko et al. (2015) describe a new approach, Drop-Seq, which partially subverts this limitation. In this strategy, cells are separated into nanoliter-sized droplets, and the RNA from each cell is subsequently tagged with a unique barcode, allowing the RNAs from thousands of individual cells to be collected and sequenced together while retaining the ability to identify the cellular origins of each transcript. This approach allowed the authors to perform an unparalleled single cell sequencing of 44,408 mouse retinal cells, leading to the identification of at least 39 transcriptionally-distinct cell populations (Macosko et al., 2015). It seems likely that further studies utilizing powerful single cell transcriptomics of GG neurons such as Drop-Seq based approaches will allow for the identification of many additional populations, which will pave the way for investigators to identify functionally distinct gustatory neurons and address questions related to taste coding.

Within the three subclusters of neurons observed by Dvoryanchikov et al. (2017), a small cluster of neurons expressing both gustatory and mechanosensory-related genes was described, in part corroborating our identification and the description of a chemosensory mechanoreceptor. Interestingly, the neurons within this small cluster were demonstrated to express *Ret* as well as *Gfrα2*. Although our study identifies these neurons as expressing GFRα1 rather than GFRα2, it is likely that this subcluster is the population identified in our study. As a future direction, it would be interesting to identify how the central projections of these neurons differ from other gustatory GG neurons. It is also interesting to consider, in the future, the evolutionary origins and functional significance of these neurons. Given that mechanoreceptors within the trigeminal ganglion abundantly innervate the tongue, providing the majority of lingual mechanosensation, the physiological significance of this small population of gustatory mechanoreceptors is unclear. As these neurons possess both gustatory and mechanosensory qualities, it is tempting to speculate that they may be involved in the detection of food texture, integrating the physical and chemical properties of food. Interestingly, even in the fruit fly *Drosophila melanogaster*, there is a clear preference for food with a specific hardness or viscosity, and this preference has been demonstrated to be mediated by a unique population of multidendritic neurons that innervates the base of taste hairs (Zhang et al., 2016). Corroborating these findings in mammalian systems will depend on the development of behavioral assays that are able to adequately control for variations in the chemical properties of taste while allowing for the manipulation of the physical properties of food. One approach that could be undertaken would be to develop behavioral food texture assays utilizing P2X2/P2X3

double knockout animals, which lack the ability to respond to chemical tastants but retain somatosensory responses (Finger et al., 2005), which may allow for the determination of whether these neurons play a role in food texture decisions.

Concluding Remarks:

The work completed in this thesis project details several examples of novel neurotrophic factor signaling mechanisms and physiological functions regulating neuron development during organogenesis. These studies also provided, with clarity, specific examples of crosstalk between neurotrophic factor signaling pathways in neuron differentiation, survival, and apoptosis. Collectively, broadening our understanding of neurotrophic factor signaling mechanisms during development and in postnatal neuron maintenance will enhance our understanding of peripheral neuron development, and improve our ability to design novel therapeutics utilizing these factors to treat nervous system injuries and neurodegenerative diseases.

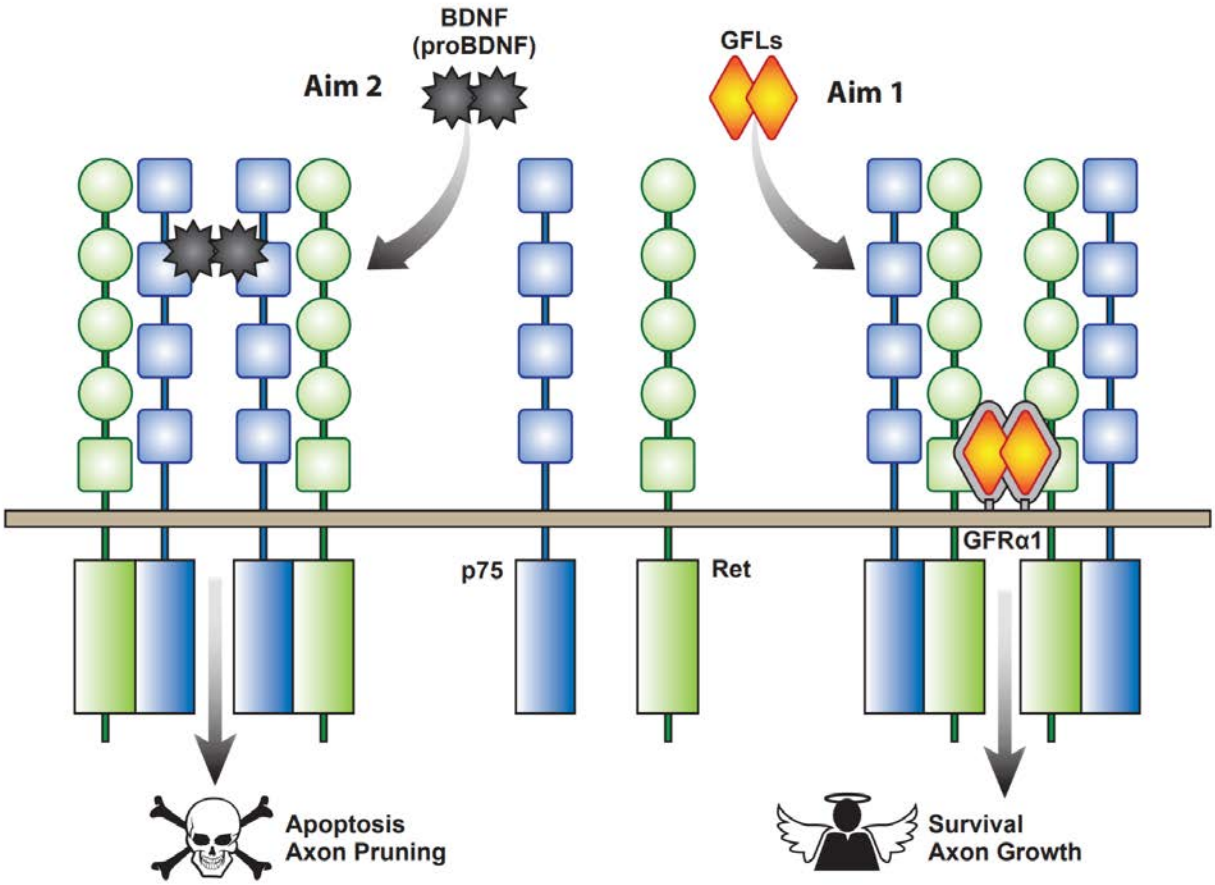

Figure 5.1. Dual functions of a p75-Ret receptor complex.

Both GFLs and BDNF can promote the interaction between p75 and Ret. GFL-mediated activation of p75-Ret receptor formation leads to downstream survival and growth response through Ret-mediated pathways, while proBDNF and BDNF (or NGF deprivation) induce p75-mediated apoptosis. We posit axon pruning may also depend on this receptor complex.

***Chapter 5 References*:**

Barker, P.A., and E.M. Shooter. 1994. Disruption of NGF binding to the low affinity neurotrophin receptor p75LNTR reduces NGF binding to TrkA on PC12 cells.

Bentley, C.A., and K.F. Lee. 2000. p75 is important for axon growth and schwann cell migration during development. *The Journal of neuroscience : the official journal of the Society for Neuroscience*. 20:7706-7715.

Bordeaux, M.C., C. Forcet, L. Granger, V. Corset, C. Bidaud, M. Billaud, D.E. Bredesen, P. Edery, and P. Mehlen. 2000. The RET proto-oncogene induces apoptosis: a novel mechanism for Hirschsprung disease. *The EMBO journal*. 19:4056-4063.

Charalampopoulos, I., A. Vicario, I. Pediaditakis, A. Gravanis, A. Simi, and C.F. Ibanez. 2012. Genetic dissection of neurotrophin signaling through the p75 neurotrophin receptor. *Cell reports*. 2:1563-1570.

Chiu, I.M., L.B. Barrett, E.K. Williams, D.E. Strochlic, S. Lee, A.D. Weyer, S. Lou, G.S. Bryman, D.P. Roberson, N. Ghasemlou, C. Piccoli, E. Ahat, V. Wang, E.J. Cobos, C.L. Stucky, Q. Ma, S.D. Liberles, and C.J. Woolf. 2014. Transcriptional profiling at whole population and single cell levels reveals somatosensory neuron molecular diversity. *eLife*. 3.

D'Autreaux, F., E. Coppola, M.-R. Hirsch, C. Birchmeier, and J.-F. Brunet. 2011. Homeoprotein Phox2b commands a somatic-to-visceral switch in cranial sensory pathways. *PNAS*. 108:20018-20023.

Dauger, S., A. Pattyn, F. Lofaso, C. Gaultier, C. Goridis, J. Gallego, and J.-F. Brunet. 2003. Phox2b controls the development of peripheral chemoreceptors and afferent visceral pathways. *Development (Cambridge, England)*. 130:6635-6642.

Davies, A.M., K.-F. Lee, and R. Jaenisch. 1993. p75-deficient trigeminal sensory neurons have an altered response to NGF but not to other neurotrophins. *Neuron*. 11:565-574.

Dvoryanchikov, G., D. Hernandez, J.K. Roebber, D.L. Hill, S.D. Roper, and N. Chaudhari. 2017. Transcriptomes and neurotransmitter profiles of classes of gustatory and somatosensory neurons in the geniculate ganglion. *Nature communications*. 8:760.

Finger, T.E., V. Danilova, J. Barrows, D.L. Bartel, A.J. Vigers, L. Stone, G. Hellekant, and S.C. Kinnamon. 2005. ATP signaling is crucial for communication from taste buds to gustatory nerves. *Science (New York, N.Y.)*. 310:1495-1499.

Glerup, S., M. Lume, D. Olsen, J.R. Nyengaard, C.B. Vaegter, C. Gustafsen, E.I. Christensen, M. Kjolby, A. Hay-Schmidt, D. Bender, P. Madsen, M. Saarma, A. Nykjaer, and C.M. Petersen. 2013. SorLA controls neurotrophic activity by sorting of GDNF and its receptors GFRalpha1 and RET. *Cell reports*. 3:186-199.

Golden, J.P., R.H. Baloh, P.T. Kotzbauer, P.A. Lampe, P.A. Osborne, J. Milbrandt, and E.M. Johnson, Jr. 1998. Expression of neurturin, GDNF, and their receptors in the adult mouse CNS. *The Journal of comparative neurology*. 398:139-150.

Hantzopoulos, P.A., C. Suri, D.J. Glass, M.P. Goldfarb, and G.D. Yancopoulos. 1994. The low affinity NGF receptor, p75, can collaborate with each of the trks to potentiate functional responses to the neurotrophins. *Neuron*. 13:187-201.

Harel, L., B. Costa, M. Tcherpakov, M. Zapatka, A. Oberthuer, L.M. Hansford, M. Vojvodic, Z. Levy, Z.Y. Chen, F.S. Lee, S. Avigad, I. Yaniv, L. Shi, R. Eils, M.

Fischer, B. Brors, D.R. Kaplan, and M. Fainzilber. 2009. CCM2 mediates death signaling by the TrkA receptor tyrosine kinase. *Neuron*. 63:585-591.

Krimm, R.F. 2007. Factors that regulate embryonic gustatory development. *BMC Neuro.* 8:S4.

Lee, K.-F., E. Li, J. Huber, S.C. Landis, A.H. Sharpe, M.V. Chao, and R. Jaenisch. 1992. Targeted mutation of the gene encoding the low affinity NGF receptor p75 leads to deficits in the peripheral sensory nervous system. *Cell*. 69:737-749.

Macosko, E.Z., A. Basu, R. Satija, J. Nemesh, K. Shekhar, M. Goldman, I. Tirosh, A.R. Bialas, N. Kamitaki, E.M. Martersteck, J.J. Trombetta, D.A. Weitz, J.R. Sanes, A.K. Shalek, A. Regev, and S.A. McCarroll. 2015. Highly Parallel Genome-wide Expression Profiling of Individual Cells Using Nanoliter Droplets. *Cell*. 161:1202-1214.

Morris, J.K., W. Lin, C. Hauser, Y. Marchuk, D. Getman, and K.F. Lee. 1999. Rescue of the cardiac defect in ErbB2 mutant mice reveals essential roles of ErbB2 in peripheral nervous system development. *Neuron*. 23:273-283.

Nosrat, C.A., A. Tomac, B.J. Hoffer, and L. Olson. 1997. Cellular and developmental patterns of expression of Ret and glial cell line-derived neurotrophic factor receptor alpha mRNAs. *Exp. Brain Res.* 115:410-422.

Pattyn, A., X. Morin, H. Cremer, C. Goridis, and J.F. Brunet. 1999. The homeobox gene Phox2b is essential for the development of autonomic neural crest derivatives. *Nature*. 399:366-370.

Rocha, A.S., B. Risberg, J. Magalhaes, V. Trovisco, I.V. de Castro, P. Lazarovici, P. Soares, B. Davidson, and M. Sobrinho-Simoes. 2006. The p75 neurotrophin

receptor is widely expressed in conventional papillary thyroid carcinoma. *Human pathology*. 37:562-568.

Santoro, M., R. Rosati, M. Grieco, M.T. Berlingieri, G.L. D'Amato, V. de Franciscis, and A. Fusco. 1990. The ret proto-oncogene is consistently expressed in human pheochromocytomas and thyroid medullary carcinomas. *Oncogene*. 5:1595-1598.

Sasselli, V., V. Pachnis, and A.J. Burns. 2012. The enteric nervous system. *Developmental biology*. 366:64-73.

Trupp, M., E. Arenas, M. Fainzilber, A.S. Nilsson, B.A. Sieber, M. Grigoriou, C. Kilkenny, E. Salazar-Grueso, V. Pachnis, and U. Arumae. 1996. Functional receptor for GDNF encoded by the c-ret proto-oncogene. *Nature*. 381:785-789.

Usoskin, D., A. Furlan, S. Islam, H. Abdo, P. Lonnerberg, D. Lou, J. Hjerling-Leffler, J. Haeggstrom, O. Kharchenko, P.V. Kharchenko, S. Linnarsson, and P. Ernfors. 2015. Unbiased classification of sensory neuron types by large-scale single-cell RNA sequencing. *Nature neuroscience*. 18:145-153.

Woldeyesus, M.T., S. Britsch, D. Riethmacher, L. Xu, E. Sonnenberg-Riethmacher, F. Abou-Rebyeh, R. Harvey, P. Caroni, and C. Birchmeier. 1999. Peripheral nervous system defects in erbB2 mutants following genetic rescue of heart development. *Genes & development*. 13:2538-2548.

Zhang, Y.V., T.J. Aikin, Z. Li, and C. Montell. 2016. The Basis of Food Texture Sensation in Drosophila. *Neuron*. 91:863-877.